AD_____

Award Number: DAMD17-97-1-7082

TITLE: Novel Mechanisms of Mammary Oncogenesis by Human Adenovirus Type 9

PRINCIPAL INVESTIGATOR: Ronald Javier, Ph.D.

CONTRACTING ORGANIZATION: Baylor College of Medicine
Houston, Texas 77030

REPORT DATE: July 2001

TYPE OF REPORT: Final

PREPARED FOR: U.S. Army Medical Research and Materiel Command
Fort Detrick, Maryland 21702-5012

DISTRIBUTION STATEMENT: Approved for Public Release;
Distribution Unlimited

REPORT DOCUMENTATION PAGE

Form Approved
OMB No. 074-0188

1. AGENCY USE ONLY (Leave blank)	2. REPORT DATE	3. REPORT TYPE AND DATES COVERED
	July 2001	Final (14 Jun 97 - 13 Jun 01)

4. TITLE AND SUBTITLE
Novel Mechanisms of Mammary Oncogenesis by Human Adenovirus Type 9

5. FUNDING NUMBERS
DAMD17-97-1-7082

6. AUTHOR(S)
Ronald Javier, Ph.D.

7. PERFORMING ORGANIZATION NAME(S) AND ADDRESS(ES)
Baylor College of Medicine
Houston, Texas 77030
E-Mail: rjavier@bcm.tmc.edu

8. PERFORMING ORGANIZATION REPORT NUMBER

9. SPONSORING / MONITORING AGENCY NAME(S) AND ADDRESS(ES)
U.S. Army Medical Research and Materiel Command
Fort Detrick, Maryland 21702-5012

10. SPONSORING / MONITORING AGENCY REPORT NUMBER

11. SUPPLEMENTARY NOTES
Report contains color photos

12a. DISTRIBUTION / AVAILABILITY STATEMENT
Approved for Public Release; Distribution Unlimited

12b. DISTRIBUTION CODE

13. ABSTRACT *(Maximum 200 Words)*

The purpose of this proposal was to elucidate novel mechanisms of breast cancer development. Toward this goal, transformation by the E4-ORF1 oncoprotein of Ad9, a virus that generates exclusively estrogen-dependent mammary tumors in rats, was linked to its ability to bind and sequester the cellular PDZ-proteins MUPP1, MAGI-1, DLG, and ZO-2 in cells. Moreover, over-expression of ZO-2, a candidate tumor suppressor protein associated with breast cancer, inhibited Ad9 E4-ORF1-induced transformation. Transformation by Ad9 E4-ORF1 was likewise linked to its ability to activate cellular phosphoinositide 3-kinase (PI 3-K), and this activity depended on interactions of Ad9 E4-ORF1 with its cellular PDZ-protein targets. Additionally, we showed that MAGI-1 forms a complex with the tumor suppressor protein PTEN, a lipid phosphatase that antagonizes PI 3-K, and that MAGI-1 and PTEN synergize to block Ad9 E4-ORF1-induced PI 3-K stimulation. Coupled with the fact that Ad9 E4-ORF1 could activate PI 3-K signaling in PTEN-null cells, our findings suggest that Ad9 E4-ORF1-induced PI 3-K pathway activation involves both PTEN-dependent and -independent mechanisms. We postulate that Ad9 E4-ORF1-associated PDZ proteins may function, in part, to antagonize PI 3-K signaling and, consequently, that inactivation of these cellular factors or their associated pathways may contribute to the development of breast malignancies.

14. SUBJECT TERMS
Breast Cancer, Ad9 E4-ORF1, MUPP1, MAGI-1, DLG, ZO-2, PI 3-K

15. NUMBER OF PAGES
122

16. PRICE CODE

17. SECURITY CLASSIFICATION OF REPORT	18. SECURITY CLASSIFICATION OF THIS PAGE	19. SECURITY CLASSIFICATION OF ABSTRACT	20. LIMITATION OF ABSTRACT
Unclassified	Unclassified	Unclassified	Unlimited

Table of Contents

INTRODUCTION

One of my research career goals is to decipher a novel cellular pathway which, when perturbed, leads to the development of breast cancer. The proposed research of this Career Development Award focused on the unique viral oncogenic determinant encoded by human adenovirus type 9 (Ad9), a virus that elicits exclusively mammary tumors in rats. Following infection of newborn rats with Ad9, female animals develop estrogen-dependent mammary tumors (primarily fibroadenomas) within multiple mammary glands after a three-month latency period, whereas no tumors of any type form in infected male rats. In contrast to other adenoviruses, the tumorigenic determinant of Ad9 is the E4 region-encoded open reading frame 1 (Ad9 E4-ORF1) oncoprotein. Our results obtained to date suggest that the oncogenic functions of Ad9 E4-ORF1 are intimately linked to its abilities both to bind a specific group of cellular PDZ proteins and to activate the phosphoinositide 3-kinase (PI 3-K) signaling pathway in cells. The fact that Ad9 E4-ORF1 mutants unable to complex with cellular PDZ proteins fail to activate the PI 3-K pathway suggests an intriguing novel association between these cellular factors and this important signaling cascade. Therefore, studies of this model system may reveal a completely new route for breast cancer development. The main goal of this project was to elucidate a detailed molecular model of Ad9 E4-ORF1 oncoprotein function. The two objectives of the proposed work were: **(1) To identify the Ad9 E4-ORF1-associated cellular proteins and (2) To reveal the mechanism whereby Ad9 E4-ORF1 activates the PI 3-K signaling pathway in cells** (*approved revised objective*)**.**

BODY

TECHNICAL OBJECTIVE 1: Identify the Ad9 E4-ORF1-associated cellular proteins.

Task 1: *Fractionate Ad9 E4-ORF1-expressing and non-expressing cells into cytoplasms, nuclei, and membranes; protein blot fractions with a radiolabelled GST-Ad9 E4-ORF1 fusion protein probe to determine subcellular location of Ad9 E4-ORF1-associated cellular proteins.*

Task 2: *Obtain commercially-available lamba phage cDNA expression libraries; construct lamba phage cDNA expression libraries.*

Task 3: *Screen lambda expression libraries with radiolabelled GST-Ad9 E4-ORF1 fusion protein probe; rescreen positive plaques with transformation-defective GST-Ad9 E4-ORF1 fusion protein probes. Sequence cDNA inserts of phage that react with wild-type but not mutant Ad9 E4-ORF1 proteins.*

Task 4: *Prepare GST and GST-Ad9 E4-ORF1 fusion protein columns for large-scale purification of cellular proteins. Obtain commercially-available HeLa cell pellets and prepare cell lysates. Pass cell lysates through GST column and then GST-Ad9 E4-ORF1 column. Isolate Ad9 E4-ORF1-associated cellular proteins as bands on a protein gel. Have proteins microsequenced.*

Task 5: *Characterize cellular proteins isolated from lambda phage expression library screening and purification; show that proteins are genuine Ad9 E4-ORF1-associated cellular proteins. Determine functional significance of Ad9 E4-ORF1-associated cellular proteins binding to the Ad9 E4-ORF1 oncoprotein.*

Results that demonstrate our successful accomplishment of the above *Tasks* of *Technical Objective 1* have been reported in three published papers and one submitted manuscript (see *Appendices*, **Papers 1, 4, 5 and 7**). In these four papers, we utilized the approaches described in *Tasks 1-4*, or alternatively tested known proteins having appropriate sizes, to identify the four major Ad9 E4-ORF1-associated cellular proteins as the PDZ proteins MUPP1, MAGI-1, ZO-2 and DLG. For *Task 5*, roles for these PDZ proteins in Ad9 E4-ORF1-induced transformation were suggested by the fact that transformation-defective but not transformation-competent Ad9 E4-ORF1 mutants failed to bind these cellular factors in cells. In addition, over-expression of ZO-2 blocked Ad9 E4-ORF1-mediated focus formation in CREF cells. While these types of polypeptide generally act as adaptors in cell signaling, the specific functions of the Ad9 E4-ORF1-associated PDZ proteins are not yet known. Nevertheless, it seems pertinent that mammalian DLG is a functional homolog of the *Drosophila* dlg tumor suppressor protein and that DLG over-expression blocks progression of mammalian cells from G0/G1 to S phase of the cell cycle. Recent findings likewise suggest that ZO-2 is a tumor suppressor protein, as its expression was reportedly lost or significantly decreased in the majority of examined human breast adenocarcinomas, as well as in certain other human malignancies. Additionally, ZO-2 has been shown to form a complex with ZO-1, which is also a suspected tumor suppressor protein implicated in breast cancer. Significantly, in Paper 7, our findings indicate that ZO-2 binds to

tumorigenic Ad9 E4-ORF1 but not to non-tumorigenic adenovirus E4-ORF1 proteins. From these observations, we hypothesize that DLG and ZO-2, and perhaps MUPP1 and MAGI-1, function to suppress the neoplastic growth of cells and that Ad9 E4-ORF1 inactivates these PDZ proteins in cells. Consistent with this idea, in Papers 4, 5 and 7, we demonstrated that Ad9 E4-ORF1 aberrantly sequesters these cellular factors in the cytoplasm of cells. Related to these findings, we also reported results showing that E6 oncoproteins from high-risk human papillomaviruses, agents associated with the vast majority of human cervical carcinomas, likewise bind MUPP1, MAGI-1 and DLG and target these cellular factors for degradation (see *Appendices*, **Papers 3, 4, and 5**).

We published two additional studies highly relevant to the work of this proposal (see *Appendices*, **Papers 2 and 6**). In Paper 2, we showed that Ad9 E1-region transforming functions are dispensable for Ad9 to generate mammary tumors in animals. This report is the first demonstration of a tumorigenic adenovirus in which these well-known gene functions have no role in tumorigenesis. In Paper 6, we published results indicating that, in addition to representing the major oncogenic determinant of Ad9, the Ad9 E4-ORF1 oncoprotein directly contributes to the ability of Ad9 to target tumorigenesis specifically to the mammary glands of rats. The latter finding interestingly suggests that mammary cells are particularly sensitive to oncogenic transformation induced by perturbation of Ad9 E4-ORF1-associated PDZ-protein function. This intriguing idea may indicate that these cellular factors play a prominent role in regulating the growth and differentiation of mammary cells.

TECHNICAL OBJECTIVE 2: Reveal the mechanism whereby Ad9 E4-ORF1 activates the phosphoinositide 3-kinase (PI 3-K)/protein kinase B (PKB) signaling pathway in cells (*Approved revised objective*).

While carrying out the studies of this proposal, we discovered that Ad9 E4-ORF1 activates PKB of the PI 3-K signaling cascade in cells (Fig. 1). Other findings with Ad9 E4-ORF1 proteins having mutations within C-terminal Region III (the PDZ domain-binding motif) or Regions I and II (unknown functions) indicated that interactions of Ad9 E4-ORF1 with its PDZ protein targets are necessary, although not sufficient, for both the transforming and tumorigenic properties of this viral oncoprotein (Fig. 2).

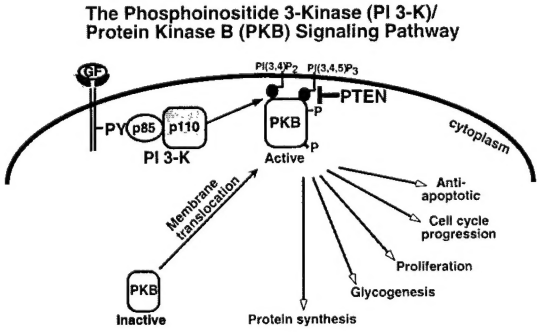

Fig. 1. Illustration of the PI 3-K/PKB signaling cascade. In this model, PI 3-K associates with an activated growth factor receptor at the membrane, where it phosphorylates lipid substrates to generate D3-phosphoinositides. After translocation to the membrane by binding to these D3-phosphoinositide second messengers, PKB is subsequently activated by protein kinases such as PDK1 (not shown). Activated PKB regulates a variety of cellular processes, including apoptosis and cell cycle progression. The PTEN tumor suppressor protein antagonizes this signaling pathway by dephosphorylating the D3 phosphate of D3-phosphoinositides.

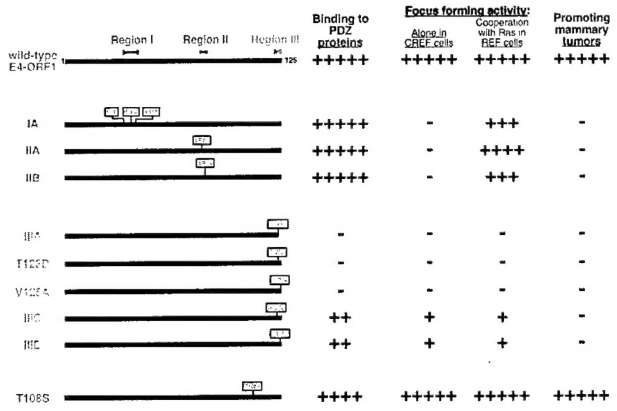

Fig. 2. Protein binding and transforming properties of mutant Ad9 E4-ORF1 proteins. The relative capacities of mutant Ad9 E4-ORF1 proteins (i) to bind the four E4-ORF1-associated cellular PDZ proteins, (ii) to induce transformed foci on CREF fibroblasts or primary rat embryo fibroblasts (REFs), or (iii) to promote Ad9-induced rat mammary tumors compared to the wild-type Ad9 E4-ORF1 protein are indicated. The transformation-proficient T108S E4-ORF1 mutant was included as a control in these assays. The facts that transformation-defective Region I and II mutants retain wild-type binding to PDZ proteins whereas the Region III mutants either fail or show reduced binding to these cellular factors suggest that these interactions are necessary but not sufficient for transformation by the Ad9 E4-ORF1 oncoprotein.

We initially showed that Ad9 E4-ORF1 specifically activated PKB kinase activity but not ERK2 kinase activity in COS7 cells (Fig. 3).

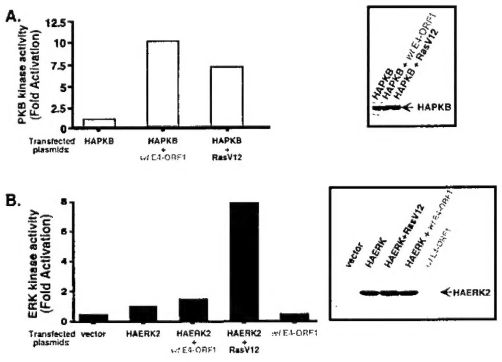

Fig. 3. Ad9 E4-ORF1 specifically activates PKB in COS7 cells. (A) COS7 cells on 60 mm dishes were lipofected with 1.6 μg of pSG5-HAPKB plasmid and 6.4 μg of either empty GW1 plasmid (vector) or a GW1 plasmid expressing wild-type E4-ORF1 or activated RasV12. Cells serum-starved for 16 h were harvested at 48 h post-transfection. Cell proteins (200 μg) in lysis buffer were first immunoprecipitated with α-HA antibodies and then subjected to an *in vitro* PKB kinase assay using H2B as substrate (*left panel*). The right panel shows that similar amounts of HAPKB protein were used in these *in vitro* kinase assays. **(B)** COS7 cells were lipofected with pCEP-HAERK2 plasmid and either wild-type E4-ORF1 or activated RasV12 plasmid and then harvested as described in (A) above. Cell proteins (200 μg) in lysis buffer were first immunoprecipitated with α-HA antibodies and then subjected to an *in vitro* ERK2 kinase assay using MBP as substrate (*left panel*). The right panel shows that similar amounts of HAERK2 protein were used in these *in vitro* kinase assays.

We performed similar assays in CREF fibroblast lines stably expressing wild-type or mutant Ad9 E4-ORF1 proteins. The results showed that wild-type Ad9 E4-ORF1, but not transformation-defective mutant Ad9 E4-ORF1 proteins, activates PKB in these lines (Fig. 4). Similar results were obtained in transient expression assays with these Ad9 E4-ORF1 proteins in CREF cells (Fig. 5). These findings significantly demonstrate that the tranforming potential Ad9 E4-ORF1 is intimately linked to its ability to activate PKB in cells.

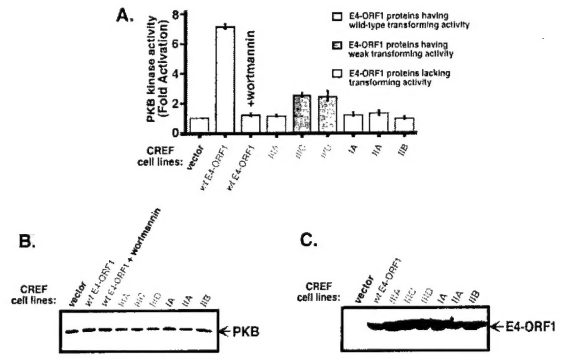

Fig. 4. Impaired PKB activation by Ad9 E4-ORF1 mutants in stable CREF lines. (A) Normal CREF cells or CREF cells stably expressing wild-type or mutant E4-ORF1 were serum-starved for 16 h. Cell proteins (1 mg) in lysis buffer were first immunoprecipitated with PKB antibodies (Upstate) and then subjected to an *in vitro* PKB kinase assay using histone 2B (H2B) as substrate. Phosphorylated H2B was detected by autoradiography and quantified with a phosphorimager. **(B)** Similar amounts of PKB protein were utilized in the *in vitro* kinase assays shown in (A) above. **(C)** The different CREF cell lines express similar amounts of E4-ORF1 protein.

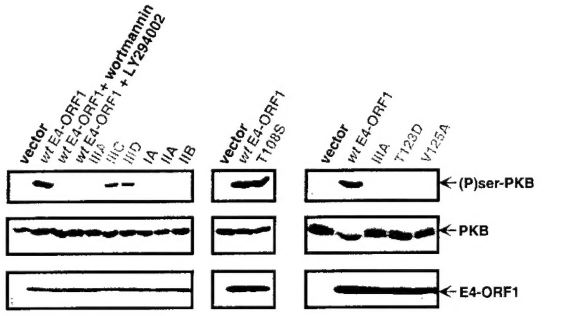

Fig. 5. Impaired PKB activation by Ad9 E4-ORF1 mutants in transient expression assays in CREF cells. CREF cells were lipofected with 2 μg of empty GW1 plasmid (vector) or a GW1 plasmid expressing wild-type or the indicated mutant E4-ORF1 protein. Cell proteins (100 μg) in sample buffer were separated by SDS-PAGE and then immunoblotted with α-phospho-Akt(Ser473) [(P)ser-PKB], α-Akt, or α-E4-ORF1 antibodies.

Our results with Region III Ad9 E4-ORF1 mutants presented in Figs. 4 and 5 above suggested that interactions of Ad9 E4-ORF1 with one or more of the four Ad9 E4-ORF1-associated PDZ proteins is required for activation of PKB. This finding prompted us to assess whether any of the Ad9 E4-ORF1-associated PDZ proteins may complex with components of the PI 3-K signaling-pathway. One such protein that we examined was the tumor suppressor protein PTEN, which is a lipid phosphatase that antagonizes PI 3-K in cells (see Fig. 1). Interestingly, like Ad9 E4-ORF1, PTEN has a PDZ domain-binding motif at its C-terminus. We found that PTEN co-immunoprecipitates with the Ad9 E4-ORF1-associated PDZ protein MAGI-1 from cell lysates (Fig. 6A). This interaction was mediated by four of the five MAGI-1 PDZ domains (Fig. 6B). Results with PTEN mutant V403A having a disrupted PDZ domain-binding motif further indicated that interaction of PTEN with three of the MAGI-1 PDZ domains (PDZ2, PDZ3, PDZ5) was dependent on the PTEN PDZ domain-binding motif whereas interaction of PTEN with MAGI-1 PDZ4 was not (Fig. 6B). The latter observation explained why the PTEN-V403A mutant retains approximately wild-type binding to MAGI-1 in co-immunoprecipitation assays (see Fig. 6A).

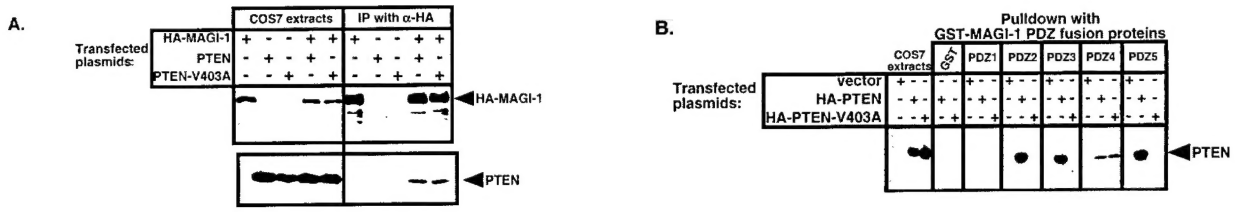

Fig. 6. PTEN binds to MAGI-1. (**A**) COS7 cells were transfected with an HA-MAGI-1 expression plasmid and a plasmid expressing either wild-type PTEN or mutant PTEN-V403A, which has a disrupted PDZ domain-binding motif. Cell proteins were immunoprecipitated with α-HA antibodies and then immunoblotted with the same antibodies or α-PTEN antibodies. (**B**) COS7 cells were transfected with a plasmid expressing either wild-type PTEN or mutant PTEN-V403A, and cell proteins were subjected to pulldown assays using GST fusion proteins containing each of the five MAGI-1 PDZ domains. These assays revealed that wild-type PTEN binds four of five MAGI-1 PDZ domains. Results with PTEN-V403A further show that the PDZ domain-binding motif of PTEN mediates binding to three such MAGI-1 PDZ domains.

To link the interaction between MAGI-1 and Ad9 E4-ORF1 to the ability of this viral oncoprotein to activate PKB in cells, we examined the consequences of MAGI-1 protein over-expression on Ad9 E4-ORF1-induced PKB activation. The results showed that over-expression of two different wild-type isoforms of MAGI-1, 1b and 1c, were able to block activation of PKB by Ad9 E4-ORF1 in CREF cells (Fig. 7). This effect was specific as MAGI-1 mutant ΔPDZ1&3, which fails to bind Ad9 E4-ORF1, was unable to diminish PKB activation by Ad9 E4-ORF1 in these assays.

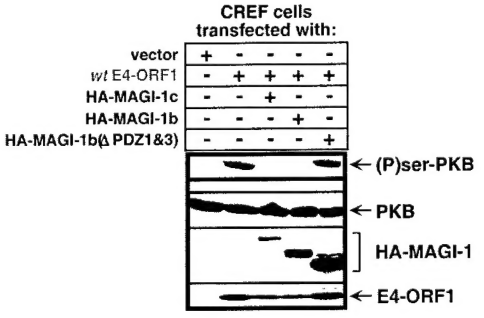

Fig. 7. Over-expression of MAGI-1 diminishes Ad9 E4-ORF1-induced PKB activation. CREF cells were lipofected with 0.2 μg of GW1-E4-ORF1 plasmid and 3 μg of either empty GW1 plasmid or a GW1 plasmid expressing wild-type HA-MAGI-1b isoform, wild-type HA-MAGI-1c isoform, or mutant HA-MAGI-1bΔPDZ1/3 (ΔPDZ1/3), which fails to bind to the E4-ORF1 protein. Cells lipofected with 3 μg of empty GW1 plasmid (vector) were included as a negative control. Cell proteins (100 μg) in sample buffer were immunoblotted with α-HA, α-phospho-Akt(Ser473), α-Akt, or α-E4-ORF1 antibodies.

Task 6: *Determine whether MAGI-1 and other Ad9 E4-ORF1-associated proteins enhance the function of PTEN in cells.*

Task 7: *Assess whether the interaction of Ad9 E4-ORF1 with MAGI-1 blocks the function of PTEN.*

In *Tasks 6-7*, we wanted to determine whether MAGI-1 and PTEN form functional complexes in cells. To test this idea, we co-transfected the Ad9 E4-ORF1 expression plasmid with either low or high amounts of MAGI-1 or PTEN expression plasmid alone or in combination. The results shown in Fig. 8 revealed that alone a low amount of MAGI-1 or PTEN caused a weak 1.5-fold or 1.4-fold reduction in Ad9 E4-ORF1-induced PKB activation, respectively, whereas the same low amount of each together synergized to produce a strong >6.3-fold reduction. Therefore, interaction with MAGI-1 enhances the ability of PTEN to inhibit PI 3-K signaling in cells, suggesting that MAGI-1 is an essential co-factor for the PTEN tumor suppressor protein. As we have shown that Ad9 E4-ORF1 aberrantly sequesters MAGI-1 in cells, we postulate that this viral protein would block the function of MAGI-1, as well as PTEN, under normal physiologic conditions. Such an activity for Ad9 E4-ORF1 would be expected to permit it to potently activate the PI 3-K signaling pathway.

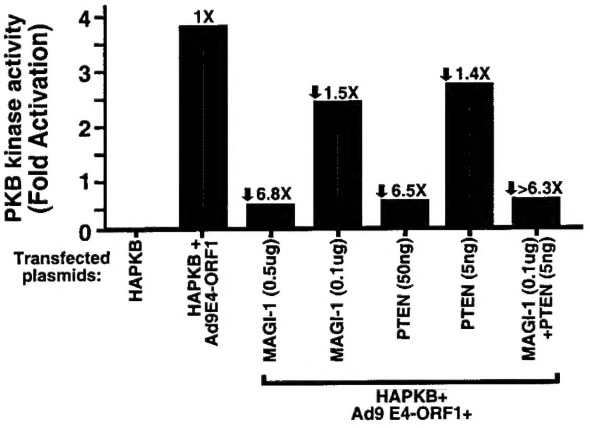

Fig. 8. MAGI-1 and PTEN synergize to antagonize Ad9 E4-ORF1-induced PKB activation. Human 293 cells were transfected with 50 ng of Ad9 E4-ORF1 plasmid, 0.5 μg of HA-PKB plasmid, and with the indicated amount of PTEN or MAGI-1 expression plasmid alone or in combination. At 48h post-transfection, equal amounts of HA-PKB were immunoprecipitated from cell lysates and subjected to PKB enzyme assays using histone 2B as a substrate. Histone 2B phosphorylation was quantified by phosphoimager analysis.

Task 8: *Determine whether Ad9 E4-ORF1 can activate PKB in PTEN-null cells.*

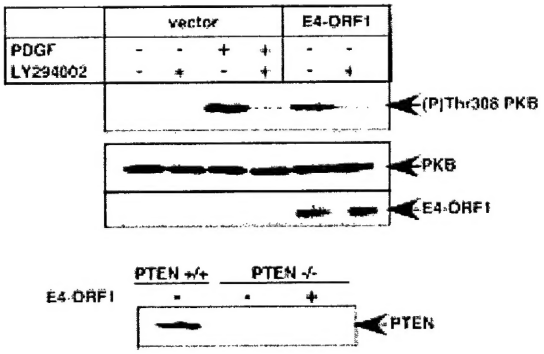

Fig. 9. Ad9 E4-ORF1 activates PKB in PTEN-null MEF. Cells were transfected with 50 ng of control plasmid (vector) or Ad9 E4-ORF1 expression plasmid and 0.5 μg of the HA-PKB (PKB) expression plasmid. At 48h post-transfection, an equivalent amount of each cell lysate was immunoblotted with either α-phospho-Akt(Ser473), α-Akt, α-E4-ORF1, α-PTEN antibodies.

For *Task 8*, we sought to ascertain whether Ad9 E4-ORF1-induced PKB activation is due entirely to an ability of this viral oncoprotein to inactivate PTEN in cells. This idea was examined by transfecting PTEN-null mouse embryo fibroblasts (MEF) with the Ad9 E4-ORF1 expression plasmid. The results shown in Fig. 9 demonstrated that, in the absence of PTEN, Ad9 E4-ORF1 retains the capacity to activate PKB. Coupled with results presented above in

Fig. 8, this finding argues that Ad9 E4-ORF1 activates PKB by both PTEN-dependent and –independent mechanisms.

Task 9: *Assess whether Ad9 E4-ORF1 activates PI 3-K in cells.*

Task 10: *Test whether Ad9 E4-ORF1 activates signaling proteins both upstream and downstream of PKB.*

Our results indicated that, although Ad9 E4-ORF1 likely interferes with PTEN function in cells, other mechanisms are also responsible for PKB activation by this viral oncoprotein. This idea prompted us to assess whether Ad9 E4-ORF1 affects components of this pathway both upstream and downstream of PKB (see Fig. 1). We found that, upstream of PKB, PI 3-K was activated (Fig. 10) and that, downstream of PKB, p27kip1 was downregulated (Fig. 11). Finding elevated PI 3-K enzyme levels in cells is consistent with our results showing that the PI 3-K inhibitors wortmannin and LY29004 block Ad9 E4-ORF1-induced PKB activation. In addition, the result showing that p27kip1 is downregulated in Ad9 E4-ORF1-expressing cells is significant in providing a plausible explanation for the transformed state of these cells.

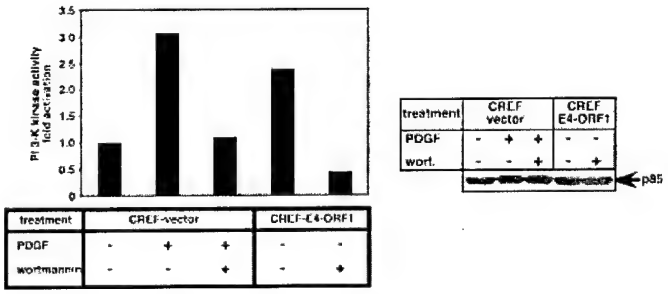

Fig. 10. Elevated levels of PI 3-K enzyme activity in Ad9 E4-ORF1-expressing cells. An equivalent amount of extract from the indicated CREF lines in 0.5% NP-40 buffer was subjected to a lipid kinase assay using PIP as the substrate. The 3-phosphorylated lipid product was separated by TLC and quantified by phosphorimager analysis (left panel). That an equivalent amount of PI 3-K protein was analyzed in each reaction was verified by immunoblot analysis with α-p85 antibodies (right panel).

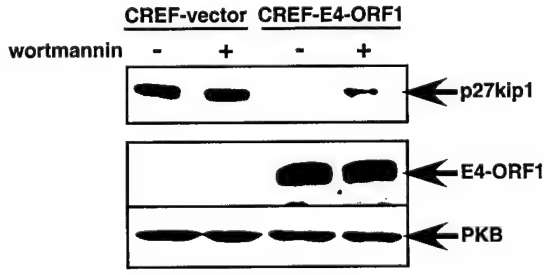

Fig. 11. Downregulation of p27kip1 in Ad9 E4-ORF1-expressing cells. An equivalent amount of extract from the indicated CREF line in RIPA buffer was subjected to immunoblot analysis with α-p27kip1, α-Ad9 E4-ORF1, or α-PKB antibodies.

Finally, it was also important to provide direct evidence that activation of PI 3-K signaling is essential for Ad9 E4-ORF1-mediated transformation. For this purpose, we transfected CREF cells with an Ad9 E4-ORF1 expression plasmid and then either mock treated (DMSO) or treated the cells with the PI 3-K inhibitor LY29004 (10 μM) or the S6 kinase inhibitor rapamycin (5 ng/mL). The latter drug was used because S6 kinase is downstream of PKB and is likewise activated in Ad9 E4-ORF1-expressing cells (data not shown). Significantly, both drugs dramatically inhibited Ad9 E4-ORF1-induced focus formation in CREF cells (Fig. 12), despite the fact that no effects on cell viability or proliferation were detected at these drug concentrations. Similar results have been obtained with an Ad9-induced mammary tumor line (data not shown). These findings are significant in demonstrating that transformation, and probably tumorigenesis, by Ad9 E4-ORF1 depend on its ability to stimulate PI 3-K signaling in cells.

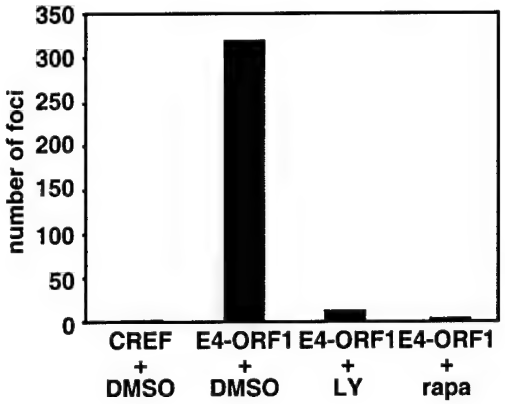

Fig. 12. LY29004 (LY) and rapamycin (rapa) block Ad9 E4-ORF1-mediated focud formation in CREF cells. Cells were transfected with 5 μg of an Ad9 E4-ORF1 expression plasmid. One week post-transfection, culture medium was either mock replaced (DMSO) or replaced with culture medium containing either LY29004 or rapamycin. Transformed foci were counted three weeks post transfection.

Key Research Accomplishments

- The Ad9 E4-ORF1 oncoprotein, which promotes solely mammary tumors in animals, selectively and potently activates phosphoinositide 3-kinase (PI 3-K) in cells.
- Ad9 E4-ORF1-mediated transformation of cultured cells and promotion of mammary tumors in animals is dependent on the ability of this viral oncoprotein to stimulate PI 3-K signaling.
- Activation of PI 3-K signaling by Ad9 E4-ORF1 is dependent on its interactions with its cellular PDZ-protein targets, most notably MAGI-1. Ad9 E4-ORF1 aberrantly sequesters its PDZ-protein targets in the cytoplasm of cells, suggesting that these cellular proteins are functionally inactivated.
- MAGI-1 forms a functional complex with the PTEN tumor suppressor protein, a lipid phosphatase that antagonizes PI 3-K in cells. As Ad9 E4-ORF1 likely inactivates MAGI-1 in cells, it would be expected that PTEN is similarly affected.
- Our findings suggest that Ad9 E4-ORF1 stimulates PI 3-K signaling in cells by novel PTEN-dependent and PTEN-independent mechanisms of action.

Reportable Outcomes

Manuscripts

1. Lee, S. S., Weiss, R. S., and Javier, R. T. (1997). Binding of Human Virus Oncoproteins to hDlg/SAP97, a Mammalian Homolog of the Drosophila Discs Large Tumor Suppressor Protein. Proc. Natl. Acad. Sci. USA 94:6670-6675.
2. D. Thomas, S. Shin, B. Jiang, H. Vogel, M. Ross, M. Kaplitt, T. Shenk, R. Javier. (1999). Early Region 1 Transforming Functions Are Dispensable for Mammary Tumorigenesis by Human Adenovirus Type 9. J. Virology 73:3071-3079.
3. D. Gardiol, C. Kuhne, B. Glaunsinger, S. Lee, R. Javier, L. Banks. (1999). Oncogenic Papillomavirus E6 Proteins Target the Discs Large Tumour Suppressor for Proteosome-Mediated Degradation. Oncogene 18:5487-5496.
4. Pim, D., Thomas, M., Javier, R., Gardiol, D. and Banks, L. (2000). HPV E6 Targeted Degradation of the Discs Large Protein: Evidence for the Involvement of a Novel Ubiquitin Ligase. Oncogene 19:719-725.
5. Barritt, D., Pearn, M., Zisch, A., Lee, S., Javier, R., Pasquale, E. and Stallcup, W. (2000). The Multi-PDZ Domain Protein MUPP1 Is a Cytoplasmic Ligand for the Membrane-Spanning Proteoglycan NG2. J. Cellular Biochem. 79:213-224.
6. Lee, S., B. Glaunsinger, F. Montavani, L. Banks, R. Javier. (2000). The Multi-PDZ Domain Protein MUPP1 Is a Cellular Target for Both Adenovirus E4-ORF1 and High-Risk Papillomavirus E6 Oncoproteins. J. Virology 74:9680-9693.
7. Glaunsinger, B., S. Lee, M. Thomas, L. Banks, and R. Javier. (2000). Interactions of the PDZ-Protein MAGI-1 with Adenovirus E4-ORF1 and Papillomavirus E6 Oncoproteins. Oncogene 19:5270-5280.
8. D. Thomas, J. Schaack, H. Vogel, and R. Javier. (2001). Several E4 Region Functions Influence Mammary Tumorigenesis by Human Adenovirus Type 9. J. Virology 75:557-68.
9. Thomas, M., B. Glaunsinger, D. Pim, R. Javier, and L. Banks. (2001). Human Papillomavirus E6 and MAGUK Protein Interactions: Determination of the Molecular Basis for Specific Protein Recognition and Degradation. Oncogene (in press).
10. Glaunsinger, B., R. Weiss, S. Lee, and R. Javier. (2001). The Unique Transforming and Tumorigenic Properties of the Adenovirus Type 9 E4-ORF1 Oncoprotein Are Linked to a Select Interaction with the Candidate Tumor Suppressor Protein ZO-2. (submitted).
11. K. Frese, Lee, S., D. Thomas, B. Glaunsinger, R. Weiss, and R. Javier. (2001). The Tumorigenic Potential of the Adenovirus E4-ORF1 Oncoprotein Depends on Its Ability to Activate the Phosphoinositide 3-Kinase Signaling Pathway. (manuscript in preparation).

Abstracts/Presentations

- S. Lee, R. Weiss and R. Javier. "The Human Adenovirus Type 9 E4 Region ORF1 Oncoprotein Binds to PDZ domain-Containing Cellular Proteins." Oral presentation, 1997 Small DNA Tumor Virus Meeting (Cambridge, England).

- S. Lee and R. Javier. "The Adenovirus Type 9 E4-ORF1 Oncoprotein Mislocalizes Cellular PDZ-Domain Proteins." Poster presentation, Pathways to Cancer Meeting. March 11-14, 1998 (Cold Spring Harbor Laboratory , NY).
- S. Lee and R. Javier. "The Adenovirus E4-ORF1 Oncoprotein Binds To and Mislocalizes the PDZ-Domain Protein 9BP-1 in Cells." Oral presentation, 1998 Small DNA Tumor Virus Meeting (Madison, Wisconsin).
- D. Gardiol, C. Kuhne, R. Javier, L. Banks. "Regulation of HPV-18 E6 Functions by Phosphorylation." Poster presentation, 1998 Small DNA Tumor Virus Meeting (Madison, Wisconsin).
- R. Javier. "Mammary Tumorigenesis by Human Adenovirus Type 9: A Role for Cellular PDZ Domain Proteins." Oral presentation for Symposium on Virus/Host Interactions in Pathogenesis at The American Society for Microbiology Meeting. May 30 - June 3, 1999.
- B. Glaunsinger, G. James, R. Javier. "MAGI-1 is a Common Cellular Target for Both Adenovirus E4-ORF1 and High-Risk Papillomavirus E6 Oncoproteins." Oral presentation, 1999 Small DNA Tumor Virus Meeting (Cambridge, England).
- D. Gardiol, C. Kuhne, D. Pim, B. Glaunsinger, S. Lee, R. Javier, L. Banks. "Oncogenic Human Papillomavirus E6 Proteins Target the Discs Large Tumour Suppressor for Proteasome-Mediated Degradation." Oral presentation, 1999 Small DNA Tumor Virus Meeting (Cambridge, England).
- R. Javier. "A Role for Cellular PDZ Proteins in Tumorigenesis by Viral Oncoproteins." Oral presentation for The Special Interest Subgroup Meeting MAGUKs and PDZs at The American Society for Cell Biology 39th Annual Meeting. December 11 - 15, 1999.
- R. Javier, S. Lee, B. Glaunsinger, R. Weiss, D. Thomas. "The Adenovirus E4-ORF1 Oncoprotein Activates the PI 3-K/PKB Signaling Pathway by a Mechanism Involving Cellular PDZ Proteins." Poster presentation for The Era of Hope Meeting in Atlanta, Georgia. June 8-11, 2000.
- D. Gardiol, B. Glaunsinger, R. Javier, F. Mantovani, P. Massimi, D. Pim, M. Thomas, L. Banks. "Regulation of HPV E6 Mediated Degradation of the Discs Large Tumour Suppressor Protein." Oral presentation, 2000 Small DNA Tumor Virus Meeting (Madison, Wisconsin).
- M. Thomas, B. Glaunsinger, R. Javier, L. Banks. "Comparison of HPV-18 and HPV-16 Interactions with the PDZ--Domain Containing Proteins DLG and MAGI-1." Poster presentation, 2000 Small DNA Tumor Virus Meeting (Madison, Wisconsin).
- S. Lee, B. Glaunsinger, R. Javier. "Phosphoinositide 3-Kinase-Dependent Activation of Protein Kinase B by the Adenovirus E4-ORF1 Oncoprotein." Oral presentation, 2000 Small DNA Tumor Virus Meeting (Madison, Wisconsin).

Conclusions

Our results show that in cells the Ad9 E4-ORF1 oncoprotein binds and aberrantly sequesters four different cellular PDZ proteins, MUPP1, MAGI-1, ZO-2, and DLG. Interestingly, ZO-2 is a candidate tumor suppressor protein implicated in the development of some human breast cancers. Although the precise functions of Ad9 E4-ORF1-associated PDZ proteins are not currently known, the domain structures of these polypeptides suggest that they function as adaptor proteins in cell signaling. In light of this observation, we tested whether Ad9 E4-ORF1 activates a known signaling pathway in cells. Our results indicate that the tumorigenic potential of Ad9 E4-ORF1 depends on its ability to activate phosphoinositide 3-kinase (PI 3-K) and its downstream effectors. Other results further showed that the capacity of wild-type Ad9 E4-ORF1 to stimulate this signaling pathway can be blocked either by disruption of its PDZ domain-binding motif or by overexpression of the Ad9 E4-ORF1-associated PDZ protein MAGI-1. These findings argue that activation of PI 3-K signaling by the Ad9 E4-ORF1 oncoprotein depends on its ability to complex with MAGI-1, and perhaps with other Ad9 E4-ORF1-associated cellular PDZ proteins. Significantly, we also showed that MAGI-1 forms a functional complex with the tumor suppressor protein PTEN, a lipid phosphatase that antagonizes PI 3-K signaling in cells.

"So What Section"

Our results suggest that MAGI-1 is an essential co-factor for the tumor suppressor protein PTEN and that activation of PI 3-K signaling by Ad9 E4-ORF1 is due in part to its ability to inactivate this PDZ protein in cells. Therefore, studies of the Ad9 E4-ORF1 oncoprotein are expected to reveal novel mechanisms whereby PI 3-K signaling can become disregulated in cells. These findings would be significant considering that uncontrolled stimulation of this signaling pathway is associated with the development of a wide range of human malignancies, including breast cancer.

References

None cited.

Appendices

Manuscripts

1. Lee, S. S., Weiss, R. S., and Javier, R. T. (1997). Binding of Human Virus Oncoproteins to hDlg/SAP97, a Mammalian Homolog of the Drosophila Discs Large Tumor Suppressor Protein. Proc. Natl. Acad. Sci. USA 94:6670-6675.
2. D. Thomas, S. Shin, B. Jiang, H. Vogel, M. Ross, M. Kaplitt, T. Shenk, R. Javier. (1999). Early Region 1 Transforming Functions Are Dispensable for Mammary Tumorigenesis by Human Adenovirus Type 9. J. Virology 73:3071-3079.
3. D. Gardiol, C. Kuhne, B. Glaunsinger, S. Lee, R. Javier, L. Banks. (1999). Oncogenic Papillomavirus E6 Proteins Target the Discs Large Tumour Suppressor for Proteosome-Mediated Degradation. Oncogene 18:5487-5496.
4. Lee, S., B. Glaunsinger, F. Montavani, L. Banks, R. Javier. (2000). The Multi-PDZ Domain Protein MUPP1 Is a Cellular Target for Both Adenovirus E4-ORF1 and High-Risk Papillomavirus E6 Oncoproteins. J. Virology 74:9680-9693.
5. Glaunsinger, B., S. Lee, M. Thomas, L. Banks, and R. Javier. (2000). Interactions of the PDZ-Protein MAGI-1 with Adenovirus E4-ORF1 and Papillomavirus E6 Oncoproteins. Oncogene 19:5270-5280.
6. D. Thomas, J. Schaack, H. Vogel, and R. Javier. (2001). Several E4 Region Functions Influence Mammary Tumorigenesis by Human Adenovirus Type 9. J. Virology 75:557-68.
7. Glaunsinger, B., R. Weiss, S. Lee, and R. Javier. (2001). The Unique Transforming and Tumorigenic Properties of the Adenovirus Type 9 E4-ORF1 Oncoprotein Are Linked to a Select Interaction with the Candidate Tumor Suppressor Protein ZO-2. (submitted).

Proc. Natl. Acad. Sci. USA
Vol. 94, pp. 6670–6675, June 1997
Biochemistry

Paper 1

Binding of human virus oncoproteins to hDlg/SAP97, a mammalian homolog of the *Drosophila* discs large tumor suppressor protein

SIU SYLVIA LEE, ROBERT S. WEISS, AND RONALD T. JAVIER*

Division of Molecular Virology, Baylor College of Medicine, One Baylor Plaza, Houston, TX 77030

Communicated by Thomas E. Shenk, Princeton University, Princeton, NJ, April 28, 1997 (received for review March 18, 1997)

ABSTRACT **The 9ORF1 gene encodes an adenovirus *E4* region oncoprotein that requires a C-terminal region for transforming activity. Screening a λgt11 cDNA expression library with a 9ORF1 protein probe yielded a novel cellular PDZ domain-containing protein, 9BP-1, which binds to wild-type, but not a transformation-defective, C-terminal, mutant 9ORF1 protein. The fact that PDZ domains complex with specific sequences at the free C-terminal end of some proteins led to the recognition that the 9ORF1 C-terminal region contained such a consensus-binding motif. This discovery prompted investigations into whether the 9ORF1 protein associates with additional cellular proteins having PDZ domains. It was found that the 9ORF1 protein interacts directly, *in vitro* and *in vivo*, with the PDZ domain-containing protein hDlg/SAP97 (DLG), which is a mammalian homolog of the *Drosophila* discs large tumor suppressor protein and which also binds the adenomatous polyposis coli tumor suppressor protein. Of interest, in forming complexes, the 9ORF1 protein preferentially associated with the second PDZ domain of DLG, similar to adenomatous polyposis coli protein. Human T cell leukemia virus type 1 Tax and most oncogenic human papillomavirus E6 oncoproteins also possessed PDZ domain-binding motifs at their C termini and, significantly, human T cell leukemia virus type 1 Tax and human papillomavirus 18 E6 proteins bound DLG *in vitro*. Considering the requirement of the 9ORF1 C-terminal region in transformation, these findings suggest that interactions with the cellular factor DLG may contribute to the tumorigenic potentials of several different human virus oncoproteins.**

Human adenoviruses are organized into six subgroups, A through F, and in people cause primarily respiratory, gastrointestinal, and eye infections (1). After infection of rodents, however, subgroup A and B and some subgroup D adenoviruses are tumorigenic. In animals, subgroup A and B adenoviruses produce undifferentiated sarcomas at the site of virus injection, and the viral *E1* region, consisting of the *E1A* and *E1B* genes, is both necessary and sufficient for this tumorigenicity. The transforming potentials of the nuclear E1A and E1B oncoproteins derive, at least in part, from an ability to complex with and inactivate the cellular tumor suppressor proteins pRB and p53, respectively (2).

Compared with the subgroup A and B adenoviruses, subgroup D adenovirus type 9 (Ad9) is unique in eliciting only estrogen-dependent mammary tumors in female rats (3) and requiring the viral *E4* region ORF1 gene (9ORF1) for oncogenicity (4, 5). The 9ORF1 gene codes for a 14-kDa cytoplasmic transforming protein (5, 6), and three separate regions of this viral polypeptide are important for transforming potential in cells (7), including a C-terminal region that mediates direct binding to several unidentified cellular proteins (p220, p180, p160, p155, p140/p130; R.S.W. and R.T.J., unpublished work). To reveal the molecular mechanisms of the novel 9ORF1 oncoprotein, we sought to identify these 9ORF1-associated cellular polypeptides.

We report here that the 9ORF1 protein possesses a C-terminal PDZ domain-binding motif that is necessary for binding to the PDZ domains of the cellular factor hDLg/SAP97 (DLG) (8, 9). This finding is significant because DLG is a mammalian homolog of the *Drosophila* discs large tumor suppressor protein (10) and, in mammalian cells, complexes with the product of the adenomatous polyposis coli (APC) tumor suppressor gene (11), which is mutated in most familial and sporadic colon cancers (12). Additionally, we show that the human T cell leukemia virus type 1 (HTLV-1) Tax and human papillomavirus (HPV) 18 E6 oncoproteins also encode consensus C-terminal PDZ domain-binding motifs and similarly bind to DLG. Therefore, DLG may represent an important cellular target for several different human virus oncoproteins.

EXPERIMENTAL PROCEDURES

Plasmids and Reagents. Portions of the SAP97 (rat DLG) ORF were PCR amplified with *pfu* DNA polymerase (Stratagene) from a pRK174-SAP97 plasmid (provided by C. C. Garner) (8) template using the following primer sets flanked by *Bam*HI and *Eco*RI sites: NT, (a) CTC GGA TCC ATG CCG GTC CGG AAG CAA and (b) CTC GAA TTC CTC ATA TTC ATA ATC TGC; 3PDZ, (c) CTC GGA TCC GCA GAT TAT GAA TAT GAG and (d) CTC GAA TTC GGT TCG GAG AGA CCC TGA; SH3/GuK, (e) CTC GAA TTC TTT CAG GGT CTC TCC GAA CC and (f) CTC GAA TTC TCA TAA TTT TTC TTT TGC TGG GAC CC; PDZ1–2, (c) and (g) CTC GAA TTC ACT TGT TGG TTT TGC CGC; PDZ2–3, (d) and (h) CTC GGA TCC CCT TCA GAA AAA ATC ATG; PDZ1, (c) and (i) CTC GAA TTC GAA GGC CTT CCG CCT TTT; PDZ2, (g) and (h); and PDZ3, (d) and (j) CTC GGA TCC ATG TAT ATA AAT GAT GGC. Full length and PCR-generated SAP97 fragments, as well as wild type and mutant E4 ORF1 genes, were cloned in-frame with the glutathione *S*-transferase (GST) gene of pGEX-2T or pGEX-2TK at the *Bam*HI and *Eco*RI sites. PCR products were verified to be correct by partial or complete sequence analysis. pGEX-2T plasmids containing HPV-11 and HPV-18 E6, HTLV-1 Tax, and HIV-1 Tat genes were gifts from P. Howley, S. Marriott, and A. Rice, respectively. GST fusion proteins were expressed in *Escherichia coli* and purified on glutathione–

The publication costs of this article were defrayed in part by page charge payment. This article must therefore be hereby marked "*advertisement*" in accordance with 18 U.S.C. §1734 solely to indicate this fact.

Abbreviations: 9ORF1, Ad9 E4 region ORF 1; GST, glutathione *S*-transferase; DLG, mammalian homolog of *Drosophila* discs large tumor suppressor protein; APC, adenomatous polyposis coli protein; HTLV-1, human T cell leukemia virus type 1; HPV, human papillomavirus.

Data deposition: The sequence reported in this paper has been deposited in the GenBank database (accession no. AF000168).

*To whom reprint requests should be addressed. e-mail: rjavier@bcm.tmc.edu.

Sepharose beads by standard methods (13). The λgt11 murine pancreatic cell cDNA library was provided by S. Tsai.

Cells and Cell Extracts. The rat embryo fibroblast cell line CREF, human osteosarcoma-derived cell line TE85, and G418-selected CREF cell pools containing an empty expression plasmid (vector) or expression plasmid encoding the wild-type or mutIII-A 9ORF1 gene were maintained as described (7, 14). For the preparation of cell lysates, cells were harvested, washed with PBS, and incubated in ≈5 vol of RIPA buffer [50 mM Tris·HCl, pH 8.0/150 mM NaCl/1% (vol/vol) Nonidet P-40/0.5% (wt/vol) sodium desoxycholate/0.1% (wt/vol) SDS] containing protease inhibitors (300 μg/ml phenylmethylsulfonyl fluoride and 6 μg/ml each of aprotinin and leupeptin) for 10 min on ice. Cell lysates were cleared of cell debris by centrifugation at 10,000 × *g* for 10 min. Protein concentrations were determined by the Bradford method.

Protein Blotting Assays. Protein blotting assays were performed with lambda phage plaques immobilized on nitrocellulose membranes or proteins separated by SDS/PAGE and transferred to poly(vinylidene fluoride) membranes (15). Membranes were blocked in TBST buffer [50 mM Tris·HCl, pH 7.5/200 mM NaCl/0.2% (vol/vol) Tween 20] containing 5% nonfat dried milk, incubated in blotting buffer (0.1% nonfat dry milk and 100 μg/ml unlabeled GST protein in TBST) containing [^{32}P]-labeled GST-9ORF1 protein probe (5×10^5 cpm/ml) for 12 h at 4°C, washed extensively with RIPA buffer, and developed by autoradiography. GST fusion protein probes were generated by incubating ≈3 μg of affinity-purified GST fusion protein bound to beads in reaction buffer [20 mM Tris·HCl, pH 7.5/100 mM NaCl/12 mM $MgCl_2$/20 μCi [^{32}P-γ-ATP] (6000 Ci/mmol)] containing 10 units of protein kinase A (Sigma) for 30 min on ice. Beads were washed extensively with RIPA buffer and eluted in elution buffer [20 mM Tris·HCl, pH 8.0/100 mM NaCl/1 mM EDTA/0.5% (vol/vol) Nonidet P-40/40 mM glutathione].

GST Pull-Down Reactions, Immunoprecipitations, and Immunoblots. GST pull-down reactions were performed by incubating cell lysates with ≈5 μg of affinity-purified GST fusion protein attached to glutathione–Sepharose beads. Immunoprecipitations were carried out by incubating cell lysates with 9ORF1 antiserum or affinity-purified DLG antibodies (supplied by M. Sheng) for 3 h and with 30 μl of protein A–Sepharose beads for 1 h on ice. After extensive RIPA buffer washes, cellular proteins bound to the respective beads were separated by 7.5% SDS/PAGE and transferred to a poly(vinylidene fluoride) membrane. Membranes were immunoblotted with either 9ORF1 rabbit polyclonal antiserum (5) or DLG antibodies (supplied by D. Branton and C. C. Garner) as described (6).

Database Searches. Protein database searches for polypeptides encoding C-terminal PDZ domain-binding motifs were performed using the command (S, T)X(V, I)> with the FindPatterns algorithm of the Genetics Computer Group (Madison, WI) software package.

RESULTS AND DISCUSSION

The 9ORF1 Protein Possesses a Consensus C-Terminal PDZ Domain-Binding Motif. To identify cellular factors interacting with the 9ORF1 C-terminal region, we screened a λgt11 cDNA expression library, derived from a murine pancreatic cell line that expresses 9ORF1-associated cellular proteins, with a radiolabeled GST-9ORF1 fusion protein probe. A single phage plaque was isolated that reacted with the wild-type but not with a mutIII-A 9ORF1 probe (data not shown). As a result of a C-terminal mutation, the mutIII-A 9ORF1 protein fails to transform cells (7) or bind any of the 9ORF1-associated cellular proteins (Table 1; unpublished results). The isolated phage contained a 2.7-kb partial cDNA coding for the C-terminal 526 amino acid residues of a novel

Table 1. Adenovirus E4 ORF1 transforming proteins possess consensus PDZ domain-binding motifs at their C termini*

PDZ domain-binding motif	Transforming activity†	Position −3	−2	−1	0
		X	(S/T)	X	(V/I)
9ORF1	+++++	A	T	L	V
mutIII-A	−	A	P		
mutIII-B	−	A	T	L	V
mutIII-C	+	D	T	L	V
mutIII-D	+	A	T	P	V
T123A	ND	A	A	L	V
T123D	ND	A	D	L	V
V125A	ND	A	T	L	A
12ORF1	+++++	A	S	L	I
3ORF1	+++++	A	T	M	I
5ORF1	+++++	A	S	N	V
APC	N/A	V	T	S	V

SACFL

*The four C-terminal amino acid residues of each wild-type protein are shown. Alterations of mutant 9ORF1 proteins are depicted as outlined amino acid residues.

†*In vitro* transforming activities of wild-type and mutant E4 ORF1 proteins (7, 15). +++++, strong transforming activity; +, weak transforming activity; −, no detectable transforming activity; ND, not done; N/A, not applicable.

cellular protein, designated 9BP-1 (9ORF1-Binding Protein 1) (Fig. 1). Although not found in the sequence databases, the recovered portion of 9BP-1 shared sequence similarity with many PDZ domain-containing proteins and, upon inspection of homologous regions, was found to consist of four PDZ domains separated by segments of unique protein sequence (Fig. 1).

PDZ domain-containing proteins normally localize to specialized sites of cell–cell contact, such as tight junctions in epithelial cells and synaptic densities in neurons, and are thought to function in signal transduction (16, 17). Like SRC homology region 2 (SH2), SH3, and phosphotyrosine-binding domains, PDZ domains are modular protein units that mediate protein–protein interactions, and certain PDZ domains bind directly to the consensus sequence S/T-X-V/I (X denotes any amino acid) at the free C-terminal end of some proteins (18–20). Significantly, 9ORF1 and other adenovirus E4 ORF1 transforming proteins (12ORF1, 3ORF1, and 5ORF1) (14) possessed this consensus, C-terminal, PDZ domain-binding motif (Table 1). Moreover, mutations within or adjacent to this motif decrease the ability of 9ORF1 to transform cells (mutIII-A, mutIII-B, mutIII-C, and mutIII-D; Table 1) (7) and bind some or all 9ORF1-associated cellular proteins. These observations led us to predict that, like 9BP-1, other cellular factors found to complex with the 9ORF1 protein through its C-terminal region would contain PDZ domains.

The 9ORF1 Protein Complexes with the PDZ Domain-Containing Cellular Protein DLG *in Vitro*. A search for known PDZ domain-containing proteins having an established or suspected role in neoplasia revealed one particularly attractive candidate protein, hDlg/SAP97 (DLG). DLG is the mammalian homolog for the *Drosophila* discs large tumor suppressor protein Dlg-A. Both DLG and Dlg-A are members of the membrane-associated guanylate kinase (MAGUK) family of proteins that contain, in addition to PDZ domains, an SH3 domain and a region with homology to guanylate kinases (16). In *Drosophila* imaginal disc epithelia, Dlg-A localizes to septate junctions, the equivalent of tight junctions in mammalian cells, and homozygous *Dlg-A* mutations lead to disruption of cell junctions, shape, and polarity, as well as neoplastic growth (21). For the mammalian homolog DLG, expression is found in many tissues *in vivo*, as well as cell lines derived from

```
aacttcatcagccttctgaagacggcaaaggcaactgtaaaactgatcgttcgagctgagaatccagcttgtccagctgttccttcttcagctgtaacagtcagtggagaaagg 114
 N  F  I  S  L  L  K  T  A  K  A  T  V  K  L  I  V  R  A  E  N  P  A  C  P  A  V  P  S  S  A  V  T  V  S  G  E  R
aaagacaactcccagactcctgcagtcccagctccagacctggaacccatcccaagtacaagcaggtcctccacaccagcagtctttgcttctgaccctgccccatc 228
 K  D  N  S  Q  T  P  A  V  P  A  P  D  L  E  P  I  P  S  T  S  R  S  S  T  P  A  V  F  A  S  D  P  A  T  C  P  I
atcccaggctgtgagacaacaattggagtttccaaaggccaaacaggcctgggactgagtattgttgggggctcagacacactgctgggtgctattattatccatgaagtttat 342
 I  P  G  C  E  T  T  I  G  V  S  K  G  Q  T  G  L  G  L  S  I  V  G  G  S  D  T  L  L  G  A  I  I  I  H  E  V  Y
gaagagggagcagcgtgtaaagatggaagactatgggctggagaccagattttagaggtaaatgggattgacttgcgaaaggctacacatgatgaagcaatcaatgtcctgagg 456
 E  E  G  A  A  C  K  D  G  R  L  W  A  G  D  Q  I  I  E  V  N  G  I  D  L  R  K  A  T  H  D  E  A  I  N  V  L  R
cagacgcctcaaagagtacgcgtgacgctctaccgagatgaggccccatacaaagaggaggatgtctgtgataccttcaccatcgagctgcagctgcagaagaggccaggcaaa 570
 Q  T  P  Q  R  V  R  V  T  L  Y  R  D  E  A  P  Y  K  E  E  D  V  C  D  T  F  T  I  E  L  Q  L  Q  K  R  P  G  K
ggccttgggttgagtattgttggcaaaagaaatgacactggagtatttgtatcagacattgtcaagggaggcattgcagacgccgatgggagactgatgcaaggggaccagatt 684
 G  L  G  L  S  I  V  G  K  R  N  D  T  G  V  F  V  S  D  I  V  K  G  G  I  A  D  A  D  G  R  L  M  Q  G  D  Q  I
ttaatggtgaatggagaagatgtccgtcatgccacccaggaggcagtcgctgccctgctaaagtgttccctaggtgcagtaaccctggaggttggaagagtcaaagctgcccca 798
 L  M  V  N  G  E  D  V  R  H  A  T  Q  E  A  V  A  A  L  L  K  C  S  L  G  A  V  T  L  E  V  G  R  V  K  A  A  P
ttccactcagaacggaggccttctcaaagcagccaggtgagtgagagcagcctgtcatctttcactcccccacttttctggaataaatacatcagagtcattggaaagtaactcg 912
 F  H  S  E  R  R  P  S  Q  S  S  Q  V  S  E  S  S  L  S  S  F  T  P  P  L  S  G  I  N  T  S  E  S  L  E  S  N  S
aagaaaaatgcattagcatctgaaattcagagactaagaacagtcgaaataaaaaaggggcctgctgactcgctgggactcagcattgctggaggagtgggcagcccgctcgga 1026
 K  K  N  A  L  A  S  E  I  Q  R  L  R  T  V  E  I  K  K  G  P  A  D  S  L  G  L  S  I  A  G  G  V  G  S  P  L  G
gatgtccctatatttattgcgatgatgcacccaaatggtgttgcagctcaaacacaaaaactcagagttggggataggattgtcaccatctgtggcacatccacggatgggatg 1140
 D  V  P  I  F  I  A  M  M  H  P  N  G  V  A  A  Q  T  Q  K  L  R  V  G  D  R  I  V  T  I  C  G  T  S  T  D  G  M
actcacacacaggcggttaacttgatgaaaaatgcctcaggctccattgaagtacaggtggttgctggaggagatgtgagtgtggtcacgggtcatcagcaagaacttgccaat 1254
 T  H  T  Q  A  V  N  L  M  K  N  A  S  G  S  I  E  V  Q  V  V  A  G  G  D  V  S  V  V  T  G  H  Q  Q  E  L  A  N
ccttgtcttgctttcactgggctgacatcaagcagtatatttccggatgatttaggccctccacagtctaagaccattacgctagaccgaggaccagatggcttaggcttcagc 1368
 P  C  L  A  P  T  G  L  T  S  S  S  I  F  P  D  D  L  G  P  P  Q  S  K  T  I  T  L  D  R  G  P  D  G  L  G  F  S
attgtaggcggctatggcagccctcatggagacttaccaatttatgtgaaaacagtgtttgcaaagggagcagcagcagaagatgggcgtctaaaaaggggcgatcagatcatt 1482
 I  V  G  G  Y  G  S  P  H  G  D  L  P  I  Y  V  K  T  V  F  A  K  G  A  A  A  E  D  G  R  L  K  R  G  D  Q  I  I
gctgtcaatgggcaaagtctagaaggagtgacccatgaagaagctgttgccatcctcaagaggacaaagggcaccgtcaccctcatggttctctcttgaagtgactgccagagc 1596
 A  V  N  G  Q  S  L  E  G  V  T  H  E  E  A  V  A  I  L  K  R  T  K  G  T  V  T  L  M  V  L  S  *
tgaagcagcccagccactggctcccctcctactgtaacagagaggacctgtttgtatgctgtgttggtcggagagggctacagtagggaggcgagaaacagagtgtttgttact 1710
cacagccaagcatcatttttccttttactctgcatttcatgatcatatactcaaaaagaagagatatttgcatagataaacctcagttttatctcgacaatatctaacaatttaa 1824
ggtcacgtggacaaaattattatatgttcatcttgttagtgaggaaacaaaatgatacaaagttaggcaattaggttaaagatggaatttagaaaaaaagaagacagttttgag 1938
ttttataggacttcttcaatccagcagtccaaaagaagaaaagaaagtgccttgcaatactttgaatagtctactgttttaaaattgtgacatattggtcctacttacctcta 2052
atgcatatttttctgctaaaattgtttagcagtccttgtaagctttaaaaagaaattcctgtttagtgcatatctcggtgtttgttttcagttttaacctgctatattttcatg 2166
ttgttataggtaaagtgctgatgctaccctgtgttggctagagttctaggaaacatccatgtagccatgggagacagagaaggagcccagagtgttctaatgctgatgtagcag 2280
actgatactacgtggaaaacatgttactgtaccatgctattgtttttccattagtattaatcttaatgacatagaaaaagacagcgtgttagtaattatttttggttgtatgcca 2394
ttagtaaattgacagaaaaattaaggggttaatgtaacttcatctcactgctgtatattaacatcttacaatacaatagtctaagactgaggaaacagatggggctgtttac 2508
tgagacaactggtgaggaattatgtgttcaatcccatttagagcgtgaaactcctacattagaatagataaagtcactttaaatactatctatatttgtaacagaagtcgtat 2622
acatatattttattatagcattcttgtgtaaatgcagaattaaagtgaataaataagtttctgtggtgcacaacaaaaaaa 2703
```

FIG. 1. Nucleotide and predicted amino acid sequences of the 2.7-kb partial murine 9BP-1 cDNA recovered from the 9BP-1 phage. The underlined and bold 82–84 amino acid residue segments designate four protein regions having sequence similarity to PDZ domains. Underlined nucleotides denote the putative 9BP-1 polyadenylylation signal.

fibroblasts and epithelial, B, and T cells, and, like Dlg-A, DLG localizes to regions of cell–cell contact in epithelial cells (8, 9). As another possible link to neoplasia, DLG complexes with the tumor suppressor protein APC in mammalian cells (11). Of interest, this interaction requires a PDZ domain of DLG and the APC C terminus, which encodes a consensus PDZ domain-binding motif (Table 1). Moreover, DLG migrates at 140-kDa in protein gels (8, 11), similar to the unidentified p140/p130 9ORF1-associated cellular proteins. These facts compelled us to investigate whether the 9ORF1 oncoprotein binds to this cellular factor.

Because, like 9BP-1, 9ORF1-associated cellular proteins immobilized on a membrane bind specifically to a wild-type GST-9ORF1 protein probe (R.S.W. and R.T.J., unpublished results), this approach was chosen initially to examine a possible interaction between the 9ORF1 and DLG polypeptides. Significantly, in such experiments, electrophoretically separated, membrane-immobilized, full length DLG fusion protein, but not GST alone (data not shown), reacted with the radiolabeled wild-type 9ORF1 probe (Fig. 2*A*). In contrast, full length DLG fusion protein did not react with a mutIII-A 9ORF1 probe (data not shown), indicating that the interaction between the wild-type 9ORF1 and DLG proteins was specific and mediated by the 9ORF1 C-terminal domain. To identify which region of DLG was binding to the wild-type 9ORF1 protein, we separated DLG into three protein fragments and analyzed each fragment fused to GST in similar assays. We found that the DLG fragment containing all three PDZ domains (GST-3PDZ) interacted with the 9ORF1 probe, but the unique N-terminal (GST-NT) and SH3 and guanylate kinase domain-containing C-terminal (GST-SH3/GuK) fragments did not (Fig. 2*A*). Further analyses to delineate which DLG PDZ domain interacted with the 9ORF1 protein revealed that the 9ORF1 probe bound most strongly to fragments containing the second DLG PDZ domain (GST-PDZ1–2, GST-PDZ2–3, GST-PDZ2) yet also reacted with the first (GST-PDZ1) and weakly with the third (GST-PDZ3) DLG PDZ domains individually (Fig. 3*A*). Of interest, APC also binds to the second PDZ domain of DLG (11). These results, summarized in Fig. 2*B*, indicated that the wild-type 9ORF1 protein binds directly to DLG and, as predicted, this interaction is mediated by the PDZ domains of this cellular protein.

We also demonstrated that the GST-9ORF1 protein interacts specifically with authentic cellular DLG. This was accomplished by incubating wild-type GST-9ORF1 protein with whole cell lysates and immunoblotting the recovered cellular proteins with a polyclonal antiserum against DLG. The wild-type GST-9ORF1 protein, as well as the related wild-type GST-12ORF1 and GST-5ORF1 proteins (14), bound to DLG in the cellular extracts whereas GST alone did not (Fig. 2*C*). The detection of several ≈140-kDa DLG species in these experiments was presumably due to the fact that it exists in four different alternatively spliced isoforms (9). These results were confirmed independently with an mAb to DLG (8) (data not shown). In the same experiments, we also included four transformation-defective C-terminal mutant 9ORF1 proteins (mutIII-A, mutIII-B, mutIII-C, mutIII-D; see Table 1) (7). With the exception of mutIII-C, all of these mutant 9ORF1 proteins failed to complex with DLG (Fig. 2*C*). The mutIII-A and mutIII-B proteins lack detectable transforming activity and binding to any 9ORF1-associated cellular proteins whereas the mutIII-C and mutIII-D proteins retain weak transforming activity and binding to some 9ORF1-associated cellular proteins (ref. 7 and R.S.W. and R.T.J., unpublished results). The mutIII-C protein uniquely preserves the capacity to complex with p140/p130 (DLG) but not other 9ORF1-associated cellular proteins, and, conversely, the mutIII-D

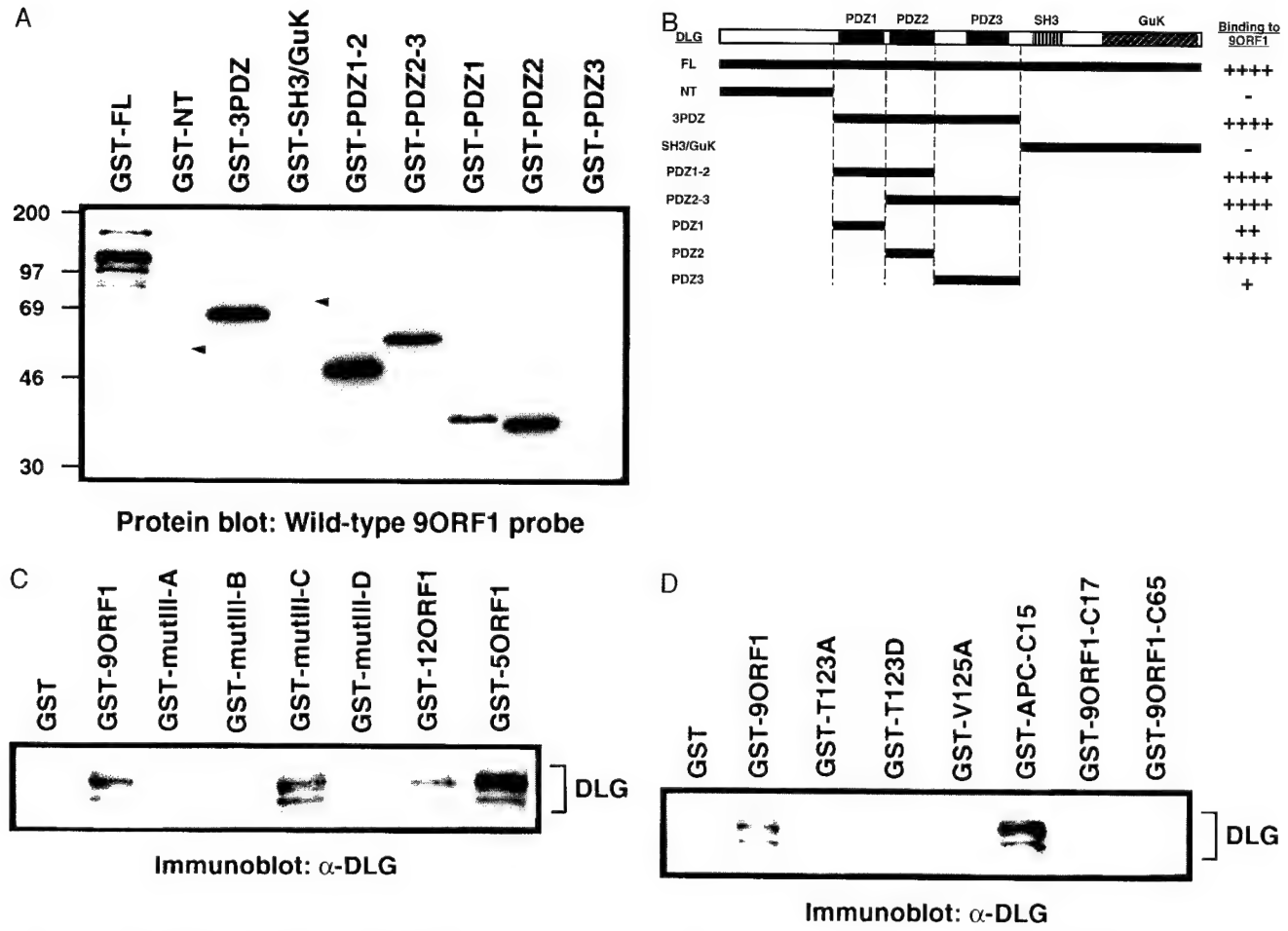

FIG. 2. Association of the 9ORF1 oncoprotein with the cellular factor DLG *in vitro*. (*A*) Binding of a wild-type GST-9ORF1 protein probe to bacterially expressed membrane-immobilized GST-DLG proteins (1 μg) in a protein blotting assay. Arrowheads show locations of GST-NT and GST-SH3/GuK proteins that did not bind to the GST-9ORF1 probe. The multiple bands seen with full length DLG fusion protein are probably proteolytic products of this large fusion protein. (*B*) An illustration of the DLG protein fragments used in *A* and summary of their corresponding 9ORF1 protein-binding activities. ++++, strong binding activity; ++, moderate binding activity; +, weak binding activity; −, no detectable binding activity. (*C*) Interaction of wild-type and transformation-defective C-terminal mutant 9ORF1 proteins with cellular DLG *in vitro*. GST pull-down reactions with the indicated GST fusion proteins were performed with 1 mg of protein from CREF cell lysates, and recovered cellular proteins were immunoblotted with rabbit polyclonal antiserum to DLG (9). Protein bands were visualized with an enhanced chemiluminescence detection system. (*D*) Interaction of C-terminal mutant 9ORF1 proteins and C-terminal 9ORF1 fragments with cellular DLG *in vitro*. GST pull-down reactions were performed as described in *C*. See Table 1 for description of mutant 9ORF1 proteins.

protein fails to interact with p140/p130 (DLG) but binds other 9ORF1-associated cellular proteins. Taken together, these results suggested that the 9ORF1 oncoprotein must complex with DLG, as well as one or more other 9ORF1-associated cellular proteins, to sustain full transforming potential.

Similar protein binding assays were carried out to further characterize the 9ORF1 C-terminal domain. For related PDZ domain-binding motifs, mutation of highly conserved amino acid residues at position −2 or position 0 from the C terminus results in loss of protein binding activity (20). Therefore, we introduced point mutations at equivalent amino acid residue positions of the 9ORF1 protein (T123A, T123D, V125A; see Table 1) to determine whether DLG-binding activity would likewise be eliminated. Concordant with results for other PDZ domain-binding motifs, such alterations significantly diminished binding of these mutant 9ORF1 polypeptides to DLG (Fig. 2*D*). In addition, because the 10–15 C-terminal amino acid residues of other PDZ domain-binding proteins retain protein binding activity (11, 19), we investigated also whether 9ORF1 C-terminal protein fragments would preserve reactivity toward DLG. Whereas the C-terminal 15 amino acid residues of APC (GST-APC-C15) possessed potent DLG-binding activity, the C-terminal 17 and 65 amino acid residues of the 9ORF1 protein (GST-9ORF1-C17 and GST-9ORF1-C65) failed to demonstrate detectable interactions with DLG (Fig. 2*D*). These C-terminal 9ORF1 fragments also either failed to bind or showed reduced binding to some of the other 9ORF1-associated cellular proteins (R.S.W. and R.T.J., unpublished results). Thus, while sharing many characteristics with related PDZ domain-binding motifs, the 9ORF1 C-terminal region exhibited the novel property of requiring an intact 9ORF1 polypeptide for retention of wild-type protein binding activity.

The 9ORF1 Protein Complexes with the PDZ Domain-Containing Cellular Protein DLG *in Vivo*. Although the results described thus far established that the 9ORF1 protein binds to DLG *in vitro*, it was essential to show that these polypeptides also form complexes *in vivo*. For this purpose, we subjected various cellular lysates to immunoprecipitation analyses with 9ORF1 antiserum and immunoblotted the recovered protein precipitates with anti-DLG polyclonal serum. In these experiments, the 9ORF1 antibodies coprecipitated DLG from wild-type 9ORF1-expressing cells but not from normal cells or from cells expressing mutIII-A 9ORF1 (Fig. 3A). A reciprocal analysis, in which cellular lysates were immunoprecipitated with an affinity-purified DLG polyclonal serum and recovered protein precipitates were immunoblotted with 9ORF1 antiserum, confirmed these findings because the DLG antibodies

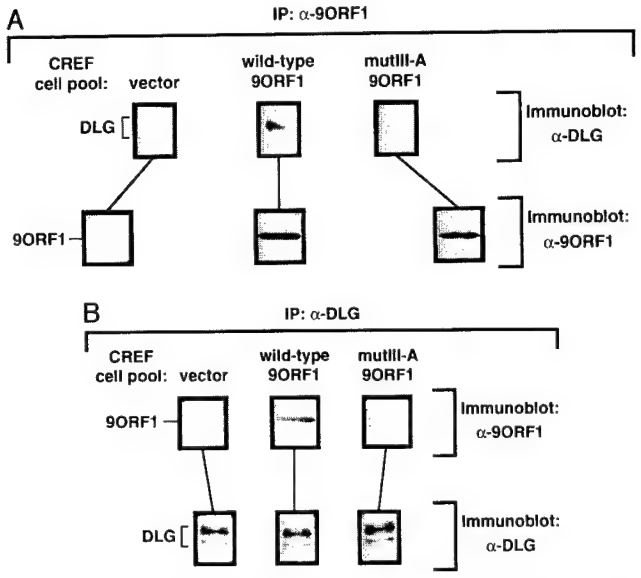

FIG. 3. Association of the 9ORF1 oncoprotein with DLG *in vivo*. (*A*) Coimmunoprecipitation of cellular DLG with the 9ORF1 protein. Two milligrams of protein from cell lysates prepared from the indicated CREF cell pool were subjected to immunoprecipitation with 2.5 μl of 9ORF1 rabbit polyclonal antiserum. Precipitated proteins were separated by SDS/PAGE, transferred to a poly(vinylidene fluoride) membrane, and immunoblotted with either DLG rabbit polyclonal antiserum (9) (upper three panels) or 9ORF1 antiserum (lower three panels). (*B*) Coimmunoprecipitation of the 9ORF1 protein with cellular DLG. These experiments were performed as described in *A* except that cellular lysates were immunoprecipitated with 0.4 μg of affinity-purified DLG rabbit polyclonal antibodies (34). Membranes were immunoblotted with either 9ORF1 antiserum (upper three panels) or DLG antiserum (lower three panels). IP, immunoprecipitation.

coprecipitated 9ORF1 protein from wild-type 9ORF1-expressing cells but not from normal cells or from cells expressing mutIII-A 9ORF1 (Fig. 3*B*). In addition, DLG also coimmunoprecipitated with 9ORF1 protein expressed in an Ad9-induced rat mammary tumor cell line (data not shown). These results indicated that the wild type, but not a C-terminal mutant 9ORF1 protein, forms complexes with DLG *in vivo*.

The HTLV-1 Tax and HPV-18 E6 Oncoproteins Possess Consensus C-Terminal PDZ Domain-Binding Motifs and Bind DLG *in Vitro*. Seemingly unrelated viral oncoproteins may share common strategies for cellular transformation, a concept illustrated by the fact that the simian virus 40 large T antigen, the papillomavirus E6 and E7 proteins, and the adenovirus E1A and E1B proteins similarly target the cellular tumor suppressor proteins pRB and p53 (22). Consequently, we considered the possibility that other viral oncoproteins, in addition to the 9ORF1 protein, might also bind DLG. This idea was initially explored by searching sequence databases for polypeptides encoding a consensus PDZ domain-binding motif at their free C-terminal ends. From this analysis, we discovered that the Tax oncoprotein from human T cell leukemia virus type 1 (HTLV-1) and many different E6 oncoproteins from HPVs of the genital tract also possessed a consensus C-terminal PDZ domain-binding motif (Table 2). The retrovirus HTLV-1 is the etiological agent of the aggressive and often fatal adult T cell leukemia (23) whereas certain HPVs are associated with the majority of cervical cancers (24). Of interest, with the exception of those encoded by HPV-16 and HPV-33, all E6 proteins from HPVs generating genital lesions with a risk for malignant progression (HPV types 16, 18, 30, 31, 33, 35, 39, 45, 51, 52, 56, 58) contained the putative PDZ domain-binding motif (25).

Table 2. HTLV-1 Tax and many HPV E6 oncoproteins have consensus PDZ domain-binding motifs at their C termini*

PDZ domain-binding motif	Position −3 X	−2 (S/T)	−1 X	0 (V/I)
HTLV-1 Tax	E	T	E	V
HIV-1 Tat	G	P	K	E
HPV E6 types				
11	D	L	L	P
18, 26, 31, 39, 45, 51	E	T	Q	V
30	E	T	A	V
34	A	T	V	V
35	E	T	E	V
52	V	T	Q	V
53	E	S	A	V
56	E	S	T	V
58	Q	T	Q	V

*The C-terminal four amino acid residues of each viral protein are shown. Note that HIV-1 Tat and, with the exception of those encoded by HPV-26, HPV-34, and HPV-53, E6 proteins from low risk HPVs (e.g., HPV-11 E6) do not encode the indicated consensus C-terminal PDZ domain-binding motif.

These observations prompted experiments to address whether HTLV-1 Tax and HPV E6 oncoproteins also would bind DLG. For this purpose, we examined Tax and one representative E6 protein, from HPV-18, which is designated as a high risk virus because of its strong association with cervical cancer. The HPV-18 E6 protein (18E6) also has the identical C-terminal sequence as five other E6 proteins, including those from two additional high risk viruses, HPV-31 and HPV-45 (Table 2). To assay binding to cellular DLG, we incubated GST-Tax and GST-18E6 proteins with protein extracts from a human cell line and immunoblotted the recovered proteins with anti-DLG polyclonal serum. Significantly, similar to GST-9ORF1, both GST-Tax and GST-18E6 specifically associated with cellular DLG (Fig. 4). GST alone as well as HIV-1, Tat (GST-Tat), and low risk HPV-11 E6 (GST-11E6) fusion proteins, which lacked the consensus C-terminal PDZ domain-binding motif (Table 2), failed to demonstrate detectable DLG-binding activity in these experiments (Fig. 4). Because the HTLV-1 Tax and HPV E6 proteins, aside from having nuclear components, also localize to the cytoplasm of cells similar to the 9ORF1 protein (26, 27), *in vivo* interactions with DLG seem possible. Moreover, DLG is expressed in both human T and cervical epithelial cell lines (9) (unpublished results), cell types infected by HTLV-1, and genital HPVs, respectively. Although transformation by the Tax or E6 oncoproteins is known to require binding to the

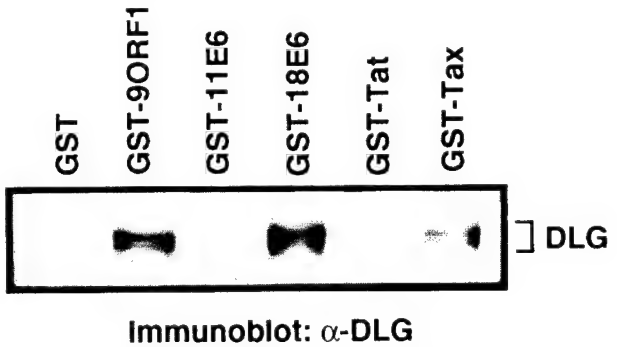

FIG. 4. Association of HTLV-1 Tax and HPV E6 oncoproteins with DLG *in vitro*. GST pull-down reactions with the indicated GST fusion protein were performed as described in the legend to Fig. 2 except that 500 μg of protein from human TE85 cell lysate was used per reaction.

cellular factors CREB, CBP, and NFKB2 (28–31) or p53, E6-AP, and E6BP (25, 26), respectively, the results suggest that these viral oncoproteins also complex with DLG. Thus, considering the findings with the 9ORF1 protein, DLG binding may also contribute to the transforming potential of these viral oncoproteins. In support of this idea, the Tax C-terminal 23 amino acid residues, which presumably mediate binding to DLG, have been implicated in Tax-mediated transformation (32).

PDZ domains serve to recruit and network plasma membrane and cytoskeletal proteins to regions of cell–cell contact (16, 17). Moreover, PDZ domain-containing polypeptides, like DLG, normally possess additional protein motifs, including SH3, guanylate kinase-like, pleckstrin, protein tyrosine phosphatase, or Ca+/calmodulin protein kinase II domains (33), suggesting that these cellular factors function as components of novel signal transduction pathways. This idea implies that the *Drosophila* tumor suppressor protein Dlg-A and perhaps its mammalian homolog DLG transmit growth-inhibitory signals from sites of cell–cell contact to downstream effectors. In cells, DLG binds to the free C-terminal end of the tumor suppressor protein APC (11). Considering that APC sustains C-terminal truncations in most sporadic and familial colon cancers (12), it is conceivable that DLG:APC complexes participate in blocking cell cycle progression. If so, one intriguing possibility is that, by binding to DLG, the 9ORF1, HTLV-1 Tax, and HPV E6 oncoproteins prevent the formation of DLG:APC complexes and, thereby, contribute to the promotion of unregulated cellular proliferation. Consistent with this proposal, we found that the 9ORF1 and APC proteins interact preferentially with the same PDZ domain of DLG. Determining the functional consequences of physical interactions between human virus oncoproteins and DLG should help clarify the role of this cellular factor in controlling normal cell growth and in oncogenesis.

We thank J. Butel and A. Rice for helpful discussions and J. Butel, L. Donehower, and D. Medina for critical reading of the manuscript. R.S.W. was the recipient of National Science Foundation and U.S. Army Breast Cancer Training Grant (DAMD17-94-J4204) predoctoral fellowships. This work was also supported by National Institutes of Health (CA58541) and American Cancer Society (RPG-97-068-01-VM) grants (R.T.J.).

1. Horwitz, M. S. (1996) in *Fields Virology*, eds. Fields, B. N., Knipe, D. M. & Howley, P. M. (Lippincott, Philadelphia), Vol. 2, pp. 2149–2171.
2. Javier, R., Raska, K., Jr., Macdonald, G. J. & Shenk, T. (1991) *J. Virol.* **65,** 3192–3202.
3. Shenk, T. (1996) in *Fields Virology*, eds. Fields, B. N., Knipe, D. M. & Howley, P. M. (Lippincott, Philadelphia), Vol. 2, pp. 2111–2148.
4. Javier, R., Raska, K., Jr. & Shenk, T. (1992) *Science* **257,** 1267–1271.
5. Javier, R. T. (1994) *J. Virol.* **68,** 3917–3924.
6. Weiss, R. S., McArthur, M. J. & Javier, R. T. (1996) *J. Virol.* **70,** 862–872.
7. Weiss, R. S., Gold, M. O., Vogel, H. & Javier, R. T. (1997) *J. Virol.* **71,** 4385–4394.
8. Muller, B. M., Kistner, U., Veh, R. W., Cases-Langhoff, C., Becker, B., Gundelfinger, E. D. & Garner, C. C. (1995) *J. Neurosci.* **15,** 2354–2366.
9. Lue, R. A., Marfatia, S. M., Branton, D. & Chishti, A. H. (1994) *Proc. Natl. Acad. Sci. USA* **91,** 9818–9822.
10. Woods, D. F. & Bryant, P. J. (1991) *Cell* **66,** 451–464.
11. Matsumine, A., Ogai, A., Senda, T., Okumura, N., Satoh, K., Baeg, G. H., Kawahara, T., Kobayashi, S., Okada, M., Toyoshima, K. & Akiyama, T. (1996) *Science* **272,** 1020–1023.
12. Polakis, P. (1995) *Curr. Opin. Genet. Dev.* **5,** 66–71.
13. Smith, D. B. & Corcoran, L. M. (1994) in *Current Protocols in Molecular Biology*, eds. Ausubel, F. M., Brent, R., Kingston, R. E., Moore, D. D., Seidman, J. G., Smith, J. A. & Struhl, K. (Wiley, New York), Vol. 2, pp. 16.7.1–16.7.7.
14. Weiss, R. S., Lee, S. S., Prasad, B. V. V. & Javier, R. T. (1997) *J. Virol.* **71,** 1857–1870.
15. Kaelin Jr., W. G., Krek, W., Sellers, W. R., DeCaprio, J. A., Ajchenbaum, F., Fuchs, C. S., Chittenden, T., Li, Y., Farnham, P. J., Blanar, M. A., Livingston, D. M. & Flemington, E. K. (1992) *Cell* **70,** 351–364.
16. Kim, S. K. (1995) *Curr. Opin. Cell Biol.* **7,** 641–649.
17. Sheng, M. (1996) *Neuron* **17,** 575–578.
18. Songyang, Z., Fanning, A. S., Fu, C., Xu, J., Marfatia, S. M., Chishti, A. H., Crompton, A., Chan, A. C., Anderson, J. M. & Cantley, L. C. (1997) *Science* **275,** 73–77.
19. Kornau, H. C., Schenker, L. T., Kennedy, M. B. & Seeburg, P. H. (1995) *Science* **269,** 1737–1740.
20. Kim, E., Niethammer, M., Rothschild, A. J., Y. N. & Sheng, M. (1995) *Nature (London)* **378,** 85–88.
21. Woods, D. F., Hough, C., Peel, D., Callaini, G. & Bryant, P. J. (1996) *J. Cell Biol.* **134,** 1469–1482.
22. Nevins, J. R. & Vogt, P. K. (1996) in *Fields Virology*, eds. Fields, B. N., Knipe, D. M. & Howley, P. M. (Lippincott, Philadelphia), Vol. 1, pp. 301–343.
23. Cann, A. J. & Chen, I. S. Y. (1996) in *Fields Virology*, eds. Fields, B. N., Knipe, D. M. & Howley, P. M. (Lippincott, Philadelphia), Vol. 2, pp. 1849–1880.
24. Howley, P. M. (1996) in *Fields Virology*, eds. Fields, B. N., Knipe, D. M. & Howley, P. M. (Lippincott, Philadelphia), Vol. 2, pp. 2045–2076.
25. Shah, K. V. & Howley, P. M. (1996) in *Fields Virology*, eds. Fields, B. N., Knipe, D. M. & Howley, P. M. (Lippincott, Philadelphia), Vol. 2, pp. 2077–2109.
26. Chen, J. J., Reid, C. E., Band, V. & Androphy, E. J. (1995) *Science* **269,** 529–531.
27. Desbois, C., Rousset, R., Bantignies, F. & Jalinot, P. (1996) *Science* **273,** 951–953.
28. Kwok, R. P., Laurance, M. E., Lundblad, J. R., Goldman, P. S., Shih, H., Connor, L. M., Marriott, S. J. & Goodman, R. H. (1996) *Nature (London)* **380,** 642–646.
29. Yamaoka, S., Inoue, H., Sakurai, M., Sugiyama, T., Hazama, M., Yamada, T. & Hatanaka, M. (1996) *EMBO J.* **15,** 873–887.
30. Wagner, S. & Green, M. R. (1993) *Science* **262,** 395–399.
31. Smith, M. R. & Greene, W. C. (1991) *J. Clin. Invest.* **88,** 1038–1042.
32. Semmes, O. J., Majone, F., Cantemir, C., Turchetto, L., Hjelle, B. & Jeang, K. T. (1996) *Virology* **217,** 373–379.
33. Ponting, C. P. & Phillips, C. (1995) *Trends Biochem. Sci.* **20,** 102–103.
34. Kim, E., Cho, K. O., Rothschild, A. & Sheng, M. (1996) *Neuron* **17,** 103–113.

JOURNAL OF VIROLOGY, Apr. 1999, p. 3071–3079 Vol. 73, No. 4
0022-538X/99/$04.00+0

Early Region 1 Transforming Functions Are Dispensable for Mammary Tumorigenesis by Human Adenovirus Type 9

DARBY L. THOMAS,[1,2] SOOK SHIN,[2]† BERNARD H. JIANG,[3]‡ HANNES VOGEL,[4] MARGERY A. ROSS,[3]§ MICHAEL KAPLITT,[3]‖ THOMAS E. SHENK,[3] AND RONALD T. JAVIER[2]*

Program in Cell and Molecular Biology,[1] Division of Molecular Virology,[2] and Department of Pathology,[4] Baylor College of Medicine, Houston, Texas 77030, and Department of Molecular Biology, Howard Hughes Medical Institute, Princeton University, Princeton, New Jersey 08544[3]

Received 3 December 1998/Accepted 4 January 1999

Some human adenoviruses are tumorigenic in rodents. Subgroup A and B human adenoviruses generally induce sarcomas in both male and female animals, and the gene products encoded within viral early region 1 (E1 region) are both necessary and sufficient for this tumorigenicity. In contrast, subgroup D human adenovirus type 9 (Ad9) induces estrogen-dependent mammary tumors in female rats and requires the E4 region-encoded ORF1 oncoprotein for its tumorigenicity. Considering the established importance of the viral E1 region for tumorigenesis by adenoviruses, we investigated whether this viral transcription unit is also necessary for Ad9 to generate mammary tumors. The nucleotide sequence of the Ad9 E1 region indicated that the gene organization and predicted E1A and E1B polypeptides of Ad9 are closely related to those of other human adenovirus E1 regions. In addition, an Ad9 E1 region plasmid demonstrated focus-forming activity in both low-passage-number and established rat embryo fibroblasts, whereas a large deletion within either the E1A or E1B gene of this plasmid diminished transforming activity. Surprisingly, we found that introducing the same transformation-inactivating E1A and E1B deletions into Ad9 results in mutant viruses that retain the ability to elicit mammary tumors in rats. These results are novel in showing that Ad9 represents a unique oncogenic adenovirus in which the E4 region, rather than the E1 region, encodes the major oncogenic determinant in the rat.

Human adenoviruses cause primarily respiratory, gastrointestinal, and eye infections in people and are divided into six subgroups (A to F) based upon several physical characteristics (25, 48). In rodents, however, the subgroup A and B adenoviruses are tumorigenic, eliciting undifferentiated sarcomas at the site of viral inoculation in both male and female animals (22, 54). Although subgroup D adenoviruses are nononcogenic in hamsters (54), subgroup D human adenovirus type 9 (Ad9) elicits mammary tumors in rats (3, 4, 29). Three months after subcutaneous injection with Ad9, female rats develop exclusively estrogen-dependent mammary tumors, while male rats fail to develop tumors of any kind. Tumors that form in the female rats are predominantly mammary fibroadenomas, the most common type of benign breast tumor found in young women (29, 44).

For the subgroup A and B adenoviruses, the E1A and E1B gene products encoded within the viral early region 1 (E1 region) are both necessary and sufficient for oncogenic transformation of primary rodent cell cultures (22, 49, 51). Individually, E1A is capable of immortalizing cells (26), whereas E1B displays no transforming potential (55). Together, however, these viral genes cooperate to produce transformed cells (22). The mechanism by which E1 region gene products transform cells can be attributed, in part, to their ability to inactivate the cellular tumor suppressor proteins pRB and p53 (48).

Unlike subgroup A and B adenoviruses, subgroup D Ad9 requires the E4 region ORF1 oncoprotein to generate tumors (30, 32). Nevertheless, the facts that (i) E1A mRNA is expressed in Ad9-induced mammary tumors (29) and (ii) the Ad9 E1 and E4 regions together cooperate to induce focus formation in CREF cells (30) suggest that the viral E1 region may also be required for Ad9-induced mammary tumorigenesis. To address this possibility, we constructed Ad9 mutant viruses containing transformation-defective E1A and E1B genes. Despite the critical role of the viral E1 region in oncogenesis by subgroup A and B adenoviruses, we present results here indicating that E1 region transforming functions are dispensable for Ad9 to induce mammary tumors in rats.

MATERIALS AND METHODS

Cell lines. Rat embryo fibroblasts (REFs) were cultured from 16-day Fisher rat embryos (Harlan Sprague-Dawley, Indianapolis, Ind.) by using standard methods (20). REF cultures, rat CREF (19) and 3Y1 cell lines (37), and human A549 and 293 cell lines (2, 23) were maintained in culture medium (Dulbecco's modified Eagle medium supplemented with 20 μg of gentamicin per ml and 6 or 10% fetal bovine serum) under a 5% CO_2 atmosphere at 37°C.

Nucleotide sequence analyses and plasmid construction. Plasmids pUC19-Ad9[0-7.5] and pSP72-Ad9[7.5-12.5] containing Ad9 DNA sequences from 0 to 7.5 and 7.5 to 12.5 map units (m.u.), respectively, were used to determine the nucleotide sequence of the Ad9 E1 region.

A DNA fragment (0 to 12.5 m.u.) containing the Ad9 E1 region was inserted into the *Kpn*I and *Bgl*II sites of plasmid pSP72 (Promega) to make pAd9E1. Deletions within the Ad9 E1A and E1B genes were first introduced into pUC19-Ad9[0-7.5] by removing the Ad9 *Sac*I-*Bsp*EI fragment (nucleotides [nt] 542 to 1049) and the Ad9 *Nae*I-*Cla*I fragment (nt 1609 to 2495), respectively. These two deletion mutations were subsequently transferred to pAd9E1 within the Ad9 *Bam*HI-*Eco*RI fragment (0 to 7.5 m.u.), resulting in pAd9E1(ΔE1A) and pAd9E1(ΔE1B), respectively. The presence of the correct deletion in each mutant plasmid was verified by restriction enzyme and limited sequence analyses.

* Corresponding author. Mailing address: Division of Molecular Virology, Baylor College of Medicine, One Baylor Plaza, Houston, TX 77030. Phone: (713) 798-3898. Fax: (713) 798-3586. E-mail: rjavier@bcm.tmc.edu.

† Present address: Department of Genetics, The Salk Institute, La Jolla, CA 92037.

‡ Present address: St. Joseph Mercy Hospital, Ann Arbor, MI 48106.

§ Present address: Department of Biochemistry, University of Connecticut Health Center, Farmington, CT 06032.

‖ Present address: Department of Neurosurgery, New York Hospital-Cornell University Medical College, New York, NY 10021.

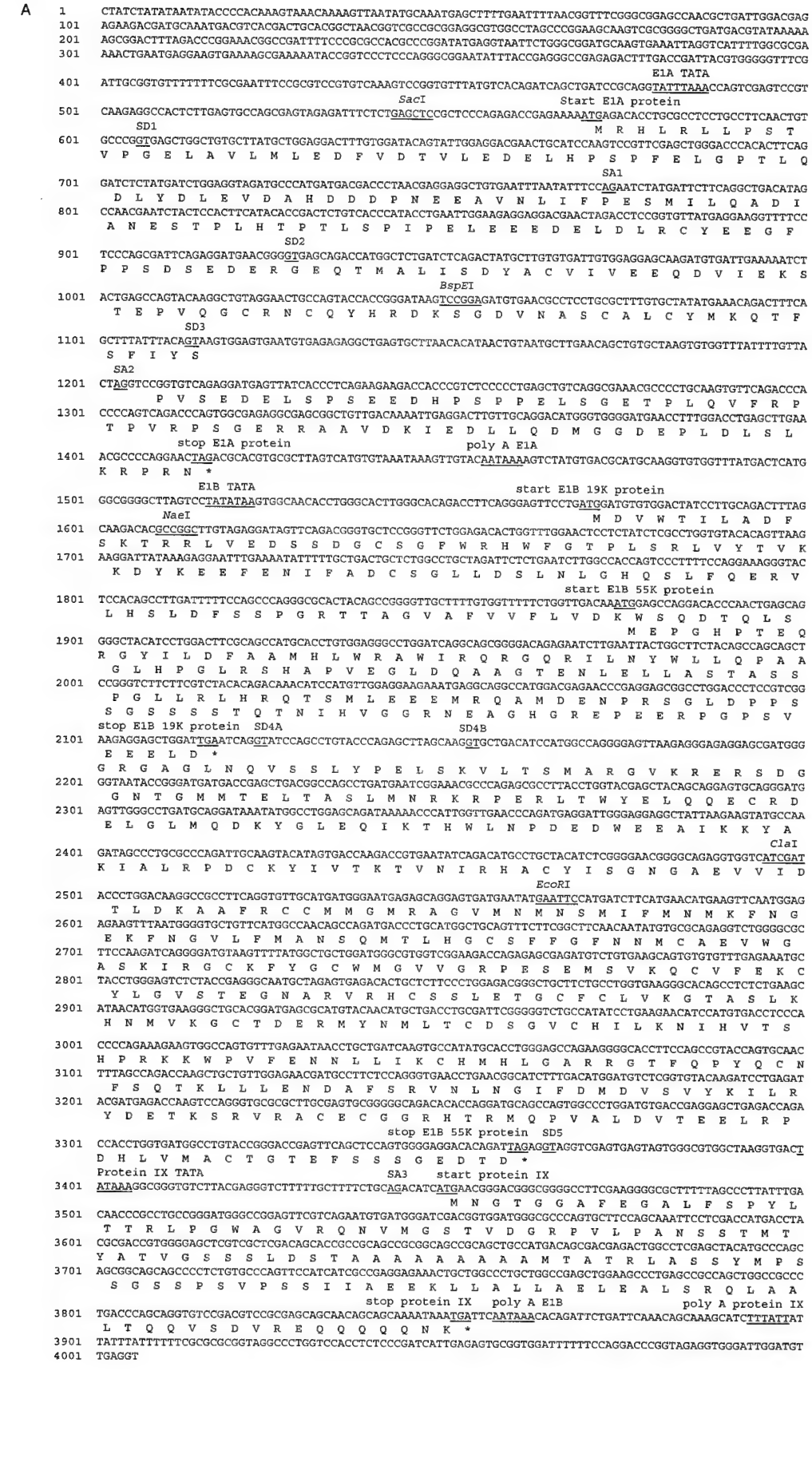
A
E1A TATA
SacI
Start E1A protein
SD1
SA1
SD2
BspEI
SD3
SA2
stop E1A protein
poly A E1A
E1B TATA
start E1B 19K protein
NaeI
start E1B 55K protein
stop E1B 19K protein
SD4A
SD4B
ClaI
EcoRI
stop E1B 55K protein
SD5
Protein IX TATA
SA3
start protein IX
stop protein IX
poly A E1B
poly A protein IX

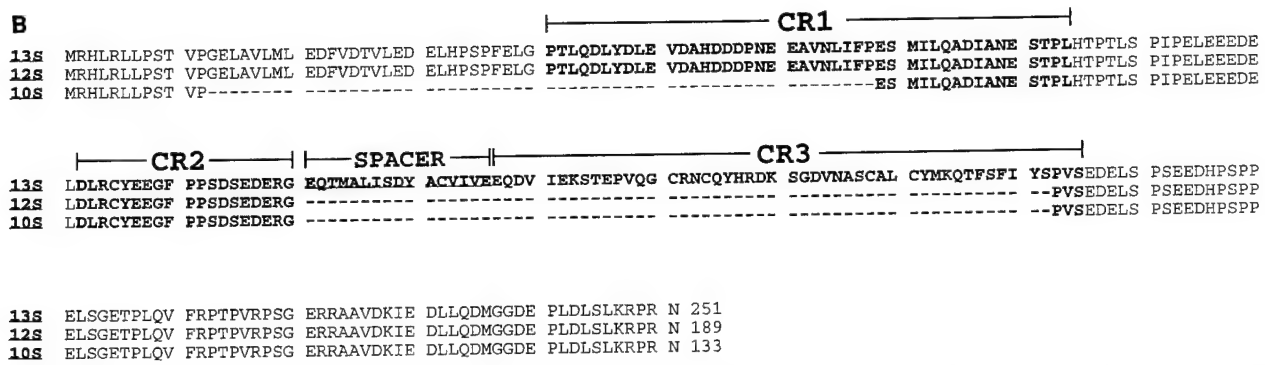

FIG. 1. (A) Nucleotide sequence of the Ad9 E1 region. The locations of E1A, E1B, and IX gene promoter TATA boxes, known and putative splice donor (SD) and splice acceptor (SA) sites, and poly(A) signal sequences are shown. Relevant restriction enzyme sites are indicated (underlined) on the nucleotide sequence. E1A and E1B mRNA splice variants result from the use of the following SD and SA sites: 10S E1A, SD1 and SA1 plus SD2 and SA2; 12S E1A, SD2 and SA2; 13S E1A, SD3 and SA2; 13S E1B, SD4A or SD4B and SA3; and 22S E1B, SD5 and SA3. The predicted amino acid sequences of the 13S E1A, 19K and 55K E1B, and pIX polypeptides are shown beneath their coding sequences. (B) Comparison of the Ad9 13S, 12S, and 10S E1A polypeptide sequences. CR1, CR2, spacer region, and CR3 are indicated (22, 33, 48, 53).

Construction of adenovirus mutants. Ad9 mutant viruses having the same E1A and E1B gene deletions described above for plasmids pAd9E1(ΔE1A) and pAd9E1(ΔE1B) were generated. Briefly, the full-length Ad9 genome (0 to 100 m.u.) consists of three *Eco*RI fragments: A (7.5 to 95 m.u.), B (0 to 7.5 m.u.), and C (95 to 100 m.u.). Deletions were first introduced into the Ad9 *Eco*RI B fragment of a plasmid, pAd9-EcoRI(B+C), which contains properly oriented terminal Ad9 *Eco*RI B and C fragments but lacks the intervening Ad9 *Eco*RI A fragment. Full-length mutant Ad9 genomes were subsequently assembled by inserting a virion-derived Ad9 *Eco*RI A fragment in the correct orientation at the unique *Eco*RI site of mutant pAd9-EcoRI(B+C) plasmids. The resulting infectious pAd9-EcoRI(A+B+C) plasmids were digested with *Spe*I to release intact linear viral genomes, which were transfected into 293 cells to complement expected E1 region deficiencies of the mutant viruses (2, 23). Recovered viruses were amplified and titrated in 293 cells (31, 48).

Isolation of RNA and Northern blot analyses. Total RNA was isolated from mock-infected or Ad9-infected A549 cells (multiplicity of infection of 10; 9 h postinfection). Cells were washed with ice-cold phosphate-buffered saline (4.3 mM Na_2HPO_4, 1.4 mM KH_2PO_4, 137 mM NaCl, 2.7 mM KCl) and lysed in guanidinium solution (4 M guanidinium isothiocyanate, 20 mM sodium acetate [pH 5.2], 0.1 mM dithiothreitol, and 0.5% [wt/vol] Sarkosyl) (12). The resulting lysate was drawn through a 20-gauge needle to shear cellular DNA, layered onto a 5.7 M CsCl cushion, and centrifuged at 150,000 × *g* for 18 h. The RNA pellet was dissolved in TES buffer (1 mM Tris-HCl [pH 7.5], 2.5 mM EDTA, 1% [wt/vol] sodium dodecyl sulfate [SDS]), precipitated with ethanol, and resuspended in water.

For Northern blot analyses, total RNA was separated on a formaldehyde agarose gel and transferred to a nitrocellulose membrane (13). The membrane was preincubated in hybridization buffer (0.5 M Na_2HPO_4 [pH 7.2], 1 mM EDTA, 7% [wt/vol] SDS) at 65°C for 4 h and then incubated in hybridization buffer containing a radiolabeled DNA probe (4.3×10^6 cpm/ml) at 65°C for 16 h. E1A and E1B probes, derived from Ad9 E1 region DNA fragments *Sac*I-*Sph*I (nt 542 to 1473) and *Nae*I-*Eco*RI (nt 1609 to 2563), respectively, were radiolabeled by the random priming method (17) and purified by gel filtration on NICK columns (Pharmacia). Probed membranes were washed in SSC wash buffer (45 mM NaCl, 4.5 mM sodium citrate, 0.1% [wt/vol] SDS) at 65°C.

Isolation of virion and cellular DNA. For isolation of adenovirus virion DNA, 293 cells were infected at a multiplicity of infection of 10 and, at 72 h postinfection, were harvested and lysed in lysis buffer (55 mM Tris-HCl [pH 9.0], 0.5 mM EDTA, 0.2% [wt/vol] sodium deoxycholate, 10% [vol/vol] ethanol, 0.5 mM spermine-HCl). Cell lysates were cleared by centrifugation, treated with proteinase K solution (0.75% [wt/vol] SDS, 12.5 mM EDTA, 2.5 mg of proteinase K per ml) at 37°C for 1 h, and extracted with phenol and chloroform. Virion DNA was precipitated with ethanol and resuspended in water.

For isolation of cellular DNA, 400 mg of frozen tumor tissue was ground in a liquid nitrogen-chilled mortar and pestle. The resulting frozen tumor powder was suspended in 4.8 ml of digestion buffer (10 mM Tris-HCl [pH 8.0], 100 mM NaCl, 25 mM EDTA, 0.5% [wt/vol] SDS, 0.1 mg of proteinase K per ml), incubated at 50°C for 16 h, and extracted with phenol (52). Cellular DNA was precipitated with ethanol and resuspended in TE buffer (10 mM Tris-HCl [pH 7.4], 1 mM EDTA).

PCR analyses. For PCR amplification of cDNAs (reverse transcription-PCR analysis), 2 μg of total RNA was reverse transcribed with Moloney murine leukemia virus reverse transcriptase, using random hexamers, as suggested by the manufacturer (Gibco-BRL). Ad9 E1A cDNAs were PCR amplified with *Taq* polymerase (Promega) by using E1A primers 1 (nt 551 to 570; 5′ CTC CTG CAG TCC CAG AGA CCG AGA AAA AT 3′) and 2 (nt 1430 to 1411; 5′ CTC AAG CTT AAG CGC ACG TGC GTC TAG TT 3′). *Pst*I and *Hin*dIII sites (underlined) engineered within the E1A oligonucleotides allowed PCR products to be inserted at the same sites of plasmid ds56rII6HI (1) for sequencing. Portions of the Ad9 E1A and E1B genes and the entire Ad9 E4 ORF1 gene were PCR amplified from tumor DNAs, using the following oligonucleotide pairs: E1A primers *a* (nt 487 to 513; 5′ CCA GTC GAG TCC GTC AAG AGG CCA CTC 3′) and *b* (nt 1487 to 1461; 5′ CCA CAC CTT GCA TGC GTC ACA TAG AC 3′); E1B primers *c* (nt 1584 to 1609; 5′ ATC CTT GCA GAC TTT AGC AAG ACA CG 3′) and *d* (nt 2651 to 2628; 5′ CAT GCA GGG TCA TCT GGC TGT TGG 3′); and Ad9 E4 ORF1 primers 1 (5′ ATG GCT GAA TCT CTG TAT GCT TTC 3′) and 2 (5′-CAT GGT TAG TAG AGA TGA GAG TCT GAA 3′). For E1A and E1B nested PCRs, DNA products derived from each of the first PCR amplifications described above were extracted with phenol, precipitated with ethanol, and resuspended in water. One-twentieth of each sample was subjected to a second round of PCR amplification using the following oligonucleotide pairs: E1A primers *e* (nt 726 to 746; 5′ CCC ATG ATG ACG ACC CTA ACG 3′) and *b*; and E1B primers *c* and *f* (nt 2116 to 2094; 5′ CAA TCC AGC TCC TCT TCC GAC GG 3′).

Immunoprecipitation and immunoblot analyses. Immunoprecipitations and immunoblot analyses were performed as described previously (32). Briefly, frozen tumor powder, generated as described above for the isolation of cellular DNA, was suspended in ice-cold radioimmunoprecipitation assay buffer (50 mM Tris-HCl [pH 8.0], 150 mM NaCl, 0.1% [wt/vol] SDS, 1% [vol/vol] Nonidet P-40, 0.5% [wt/vol] deoxycholate) containing protease inhibitors (2 μg of aprotinin, 2 μg of leupeptin, and 100 μg of phenylmethylsulfonyl fluoride per ml), sonicated briefly, and cleared by centrifugation (16,000 × *g*, 10 min). The protein concentration of tumor lysates was determined by the method of Bradford (9). Three milligrams of protein from tumor lysates was subjected to immunoprecipitation with 15 μl of Ad9 E4 ORF1 antiserum prebound to 30 μl of protein A-Sepharose beads (Pharmacia) (32). Beads were washed with ice-cold radioimmunoprecipitation assay buffer and boiled in 2× sample buffer (0.13 M Tris-HCl [pH 6.8], 4% [wt/vol] SDS, 20% [vol/vol] glycerol, 2% [vol/vol] β-mercaptoethanol, 0.003% [wt/vol] bromophenol blue). Proteins were separated by SDS-polyacrylamide gel electrophoresis (40) and electrophoretically transferred to a polyvinylidene difluoride membrane, which was blocked in TBST (50 mM Tris-HCl [pH 7.5], 200 mM NaCl, 0.1% [vol/vol] Tween 20) containing 5% (wt/vol) both nonfat dry milk and bovine serum albumin. In these assays, Ad9 E4 ORF1 antiserum (1:5,000 in TBST) (32) and horseradish peroxidase-conjugated goat anti-rabbit immunoglobulin G (1:5,000 in TBST; Southern Biotechnology Associates) were used as primary and secondary antibodies, respectively. After extensive washing with TBST, the membrane was developed by enhanced chemiluminescence (Pierce).

Focus assays. Plasmid DNA purified by CsCl density gradient centrifugation was transfected onto 50% confluent tertiary REF cultures or CREF cells on 100-mm-diameter dishes, using the calcium phosphate precipitation method with a glycerol shock (38). At 72 h posttransfection, REF and CREF cells were passaged 1:3 and maintained in culture medium containing 10 and 6% filtered fetal bovine serum, respectively. Four to six weeks posttransfection, cells were fixed in methanol and stained with Giemsa to quantify transformed foci (32).

Mammary tumorigenicity of viruses in rats. Female rats with 1- or 2-day-old litters were obtained from Harlan Sprague-Dawley; 12 to 24 h after arrival, newborn rats were injected subcutaneously with 0.4 ml of virus solution on their anterior flanks, using a 26-gauge needle. Beginning 2 months postinfection, animals were examined weekly by palpation for the presence of tumors, until the experiment was terminated at 8 months postinfection. At this time, animals were euthanized, and portions of tumors were removed and either fixed in 10% formalin for histological examination or frozen at −80°C for isolation of DNA or

TABLE 1. Amino acid sequence identities between subgroups A to D and F adenovirus E1A, E1B, and pIX proteins[a]

Virus	E1A 13S					E1B 19K					E1B 55K					pIX				
	Ad12	Ad7	Ad5	Ad9	Ad40	Ad12	Ad7	Ad5	Ad9	Ad40	Ad12	Ad7	Ad5	Ad9	Ad40	Ad12	Ad7	Ad5	Ad9	Ad40
Ad12	100					100					100					100				
Ad7	41.9	100				41.6	100				47.9	100				53.7	100			
Ad5	39.9	37.5	100			43.2	48.1	100			48.6	53.8	100			49.3	49.6	100		
Ad9	**39.3**	*43.1*	**38.1**	100		**43.2**	*52.4*	**47.6**	100		**45.3**	*56.2*	**52.2**	100		**50.0**	*58.2*	**46.5**	100	
Ad40	38.4	38.5	33.7	**40.1**	100	48.5	45.5	43.6	**41.8**	100	55.9	48.3	48.6	**44.5**	100	62.5	51.7	49.3	**49.6**	100

[a] Sequence identities were determined with the full-length sequence of each polypeptide by using the ALIGN program (50). Ad12, subgroup A; Ad7, subgroup B; Ad5, subgroup C; Ad9, subgroup D; Ad40, subgroup F. Boldface values indicate amino acid sequence comparisons between Ad9 E1 region polypeptides and other E1 region polypeptides; values in italics show that all Ad9 E1 region polypeptides are most closely related to those of subgroup B virus Ad7.

protein. Animals were cared for and handled according to institutional guidelines.

Protein sequence alignments. Sequences of Ad12, Ad7, Ad5, and Ad40 E1 region polypeptides were obtained from GenBank. Alignments were made by using the Pairwise Sequence Alignment program (ALIGN) of the BCM Search Launcher (50).

Nucleotide sequence accession number. The nucleotide and polypeptide sequences reported in this paper were submitted to GenBank (accession no. AF099665).

RESULTS

Gene organization and predicted polypeptides of the Ad9 E1 region. To initiate our characterization of the subgroup D Ad9 E1 region, we determined the sequence of the left 4006 nt of the Ad9 genome. From this analysis, we found that the gene organization of the Ad9 E1 region closely resembles that of other human adenovirus E1 regions (Fig. 1A) (48). In addition, the predicted Ad9 13S E1A, 19K and 55K E1B, and pIX proteins displayed significant sequence similarity with the corresponding proteins from other human adenoviruses, although they were most closely related to the E1 region polypeptides of subgroup B adenoviruses (Table 1).

Northern blot analyses of total cellular RNA isolated from Ad9-infected A549 cells were also performed to detect Ad9 E1A and E1B mRNAs. In these assays, a diffuse E1A mRNA band migrating at approximately 1 kb and distinct 1.2- and 2.2-kb E1B mRNA bands were observed (Fig. 2). The size of the E1A mRNA band was consistent with that predicted for the 12S and 13S transcripts (see below), and the two E1B mRNAs corresponded well with the sizes predicted for 13S and 22S transcripts (47).

Because E1A but not E1B mRNA is detected in Ad9-induced rat mammary tumors (29), we determined the structures of Ad9 E1A transcripts by using reverse transcription-PCR techniques on total RNA from Ad9-infected A549 cells. Sequencing of PCR products obtained from these analyses revealed three Ad9 E1A splice-variant transcripts resembling 13S, 12S, and 10S mRNAs from other human adenoviruses (Fig. 1A) (47). Ad9 E1A mRNA having a size consistent with that expected for the 10S mRNA was not detected by Northern blot analyses (Fig. 2), presumably due to its low abundance at early times after infection. The 13S, 12S, and 10S Ad9 E1A cDNAs are predicted to encode 251-, 189-, and 133-amino-acid-residue polypeptides, respectively (Fig. 1B). Between conserved regions 2 (CR2) and 3 (CR3), the 13S E1A protein of subgroup A virus Ad12 possesses an alanine-rich spacer region which is, in part, responsible for the highly oncogenic phenotype of this virus (33, 53). In contrast, the Ad9 13S E1A protein was found to contain a non-alanine-rich spacer region similar to the one present in 13S E1A proteins of weakly oncogenic subgroup B adenoviruses (Fig. 1B).

A large deletion within the E1A or E1B gene abolishes focus-forming activity by the Ad9 E1 region. To investigate the transforming potential of the Ad9 E1 region, we constructed an Ad9 E1 region (0 to 12.5 m.u.) plasmid, pAd9E1, and examined its ability to induce transformed foci on low-passage-number REF cultures. Unlike other adenovirus E1 regions, the Ad9 E1 region is unable to transform primary REF or baby rat kidney cell cultures (28). Consistent with these previous findings, pAd9E1 alone failed to generate transformed foci on REFs (Table 2). Nevertheless, whereas an activated *ras* plasmid alone also lacked detectable focus-forming activity on REFs, pAd9E1 and the activated *ras* plasmid together cooperated to produce transformed foci on these cells (Table 2). To determine whether Ad9 E1A and E1B gene functions were required for this cooperation, we introduced a large deletion into each of these genes within pAd9E1. A segment of the E1A gene coding for the initiation codon, conserved region 1 (CR1), CR2, and half of CR3 (48) was removed in plasmid pAd9E1(ΔE1A), and E1B gene coding sequences downstream of E1B-19K amino acid residue 14, as well as the first 208 amino acid residues of the 495-residue E1B-55K protein, were removed in plasmid pAd9E1(ΔE1B) (Fig. 3). Each deletion would be anticipated to inactivate the transforming potential of the relevant gene (21, 22, 57). When cotransfected with the activated *ras* plasmid, pAd9E1(ΔE1A) failed to generate any foci on REFs, whereas pAd9E1(ΔE1B) retained significant focus-forming activity, albeit at a reduced efficiency compared to wild-type pAd9E1 (Table 2). These results are concordant with previous results showing that activated *ras* cooperates with the Ad5 E1A but not the E1B gene (18). Therefore, our findings provided evidence that the transforming potential of the E1A gene is inactivated in pAd9E1(ΔE1A); however, it was un-

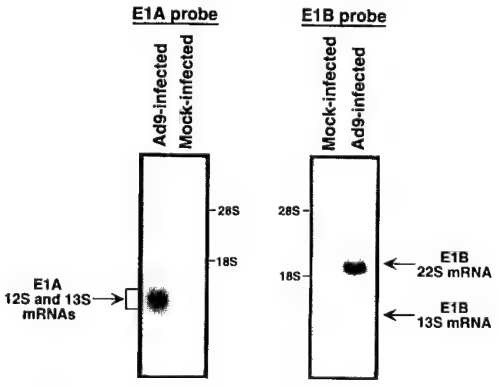

FIG. 2. Northern blot analyses of Ad9 E1A and E1B mRNAs. Total RNA (23 μg), isolated from Ad9-infected (9 h postinfection) or mock-infected A549 cells, was separated on a formaldehyde agarose gel, transferred to a nitrocellulose membrane, and hybridized to either an E1A or E1B ^{32}P-labeled DNA probe. RNA bands were visualized by autoradiography. Locations of 28S and 18S rRNAs are indicated. The indicated Ad9 mRNA species are predicted from their sizes.

TABLE 2. Focus formation by wild-type and mutant Ad9 E1 region plasmids on low-passage-number REF cultures and the CREF cell line[a]

Plasmid(s)	No. of transformed foci/ 2 100-mm-diam dishes					
	REF cultures[b]				CREF cell line[c]	
	−*ras*		+*ras*		Expt 1	Expt 2
	Expt 1	Expt 2	Expt 1	Expt 2		
pSP72	0	0	0	0	0	1
pAd9E1	0	0	24	53	71	116
pAd9E1(ΔE1A)	0	0	0	0	2	3
pAd9E1(ΔE1B)	0	0	12	14	0	0
pAd9E1(ΔE1A) + pAd9E1(ΔE1B)	ND[d]	ND	ND	ND	36	45

[a] 50% confluent tertiary REF or CREF cells on 100-mm-diameter dishes were transfected with the indicated plasmid(s). At 72 h posttransfection, cells were passaged 1:3 and then maintained in culture medium. REF and CREF cells were fixed in methanol and stained with Giemsa at 4 and 6 weeks posttransfection, respectively, to quantify the number of transformed foci.

[b] 15 μg of the indicated Ad9 E1 region plasmid plus 5 μg of empty pSP72 (−*ras*) or 5 μg of pSP72-*ras* (+*ras*) plasmid (18) were transfected into REF cells.

[c] 10 μg of the indicated Ad9 E1 region plasmid plus 10 μg of empty pSP72 plasmid were transfected into CREF cells. For the pAd9E1(ΔE1A)-plus-pAd9E1(ΔE1B) cotransfection, 10 μg of each plasmid was used.

[d] ND, not determined.

clear from these REF assays whether the deletion in pAd9E1 (ΔE1B) similarly affects the transforming potential of the E1B gene.

In an attempt to reveal more striking transforming deficiencies for pAd9E1(ΔE1B), we next performed focus assays in the established REF cell line CREF (19). Contrary to results obtained in REFs, transfection of pAd9E1 alone into CREF cells led to the formation of numerous transformed foci (Table 2). The fact that a plasmid containing Ad9 sequences from 0 to 17.5 m.u. exhibits weaker transforming activity in CREF cells (30) may indicate that Ad9 sequences from 12.5 to 17.5 m.u. interfere with focus formation in these cells. More important, when transfected individually into CREF cells, both pAd9E1 (ΔE1A) and pAd9E1(ΔE1B) displayed significantly impaired focus-forming activity compared to wild-type pAd9E1 (Table 2). Cotransfection of pAd9E1(ΔE1A) and pAd9E1(ΔE1B) into CREF cells, however, resulted in a moderate number of transformed foci, revealing cooperation between the functional E1A and E1B genes retained collectively in the two plasmids. Taken together, the results obtained for low-passage-number REFs and the cell line CREF showed that the deletions within pAd9E1(ΔE1A) and pAd9E1(ΔE1B) greatly diminish the transforming activity of the Ad9 E1A and E1B genes, respectively.

Isolation of Ad9 E1A or E1B deletion mutant viruses. The importance of the Ad9 E1 region in mammary oncogenesis was assessed by introducing the same E1A and E1B deletion mutations of pAd9E1(ΔE1A) and pAd9E1(ΔE1B) into infectious Ad9 plasmids for recovery of mutant viruses. To complement their E1 region deficiencies, we transfected each of the mutant viral DNAs into human 293 cells, which stably express Ad5 E1 region proteins (2, 23). In 293 cells, the E1A mutant virus Ad9ΔE1A replicated to titers comparable to those of wild-type Ad9, whereas the E1B mutant virus Ad9ΔE1B replicated to titers approximately 10-fold lower. Because wild-type Ad9 fails to complement the replication defects of the Ad5 E1B-55K mutant *dl*252 (28), the reduced replication of Ad9ΔE1B conversely may be due to it being poorly complemented by Ad5 E1B proteins expressed in 293 cells. Restriction enzyme analyses of virion DNA verified that Ad9ΔE1A and Ad9ΔE1B contained the expected deletions and further showed that these viruses had not acquired Ad5 E1 region sequences from the 293 cells (Fig. 4).

Ad9 E1A and E1B mutant viruses retain the ability to elicit mammary tumors in rats. We next tested the ability of mutant viruses Ad9ΔE1A and Ad9ΔE1B to generate mammary tumors in Wistar-Furth rats. In accordance with our previous results (29, 30), wild-type Ad9 elicited mammary tumors in all of the female rats but none of the male rats, whereas subgroup D Ad26 failed to elicit tumors in any animals (Table 3). Significantly, we found that both Ad9ΔE1A and Ad9ΔE1B retained the ability to generate mammary tumors in female rats, despite the fact that Ad9ΔE1B-infected animals received a ninefold-lower dose of virus than did animals infected with either wild-type Ad9 or Ad9ΔE1A (Table 3). The tumorigenic phenotype of Ad9ΔE1B may not be surprising, considering that, unlike E1A mRNA, E1B mRNA is not detected in Ad9-induced mammary tumors (29). Furthermore, although mammary tumors elicited by all of the viruses were histologically identical (Table 4), the tumors produced by Ad9ΔE1A were generally smaller than those induced by either wild-type Ad9 or Ad9ΔE1B, both of which generated tumors of similar size (data not shown).

Mutant Ad9 virus-induced tumors do not contain wild-type Ad9 E1 region sequences. Because retention of tumorigenicity by both Ad9ΔE1A and Ad9ΔE1B was unanticipated, it was important to demonstrate that the mammary tumors caused by these viruses do not contain wild-type Ad9 DNA. For this

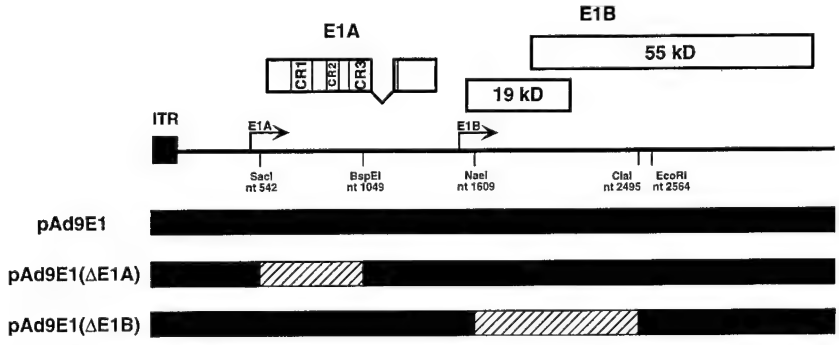

FIG. 3. Illustration of E1A and E1B deletion mutations introduced into the Ad9 E1 region of plasmid pAd9E1. Wild-type Ad9 sequences are represented by a black line; deleted sequences are represented by a hatched line. The restriction enzyme sites used to generate the deletions are shown. The locations of E1A CR1, CR2, and CR3 (22, 48) are also indicated. ITR, inverted terminal repeat.

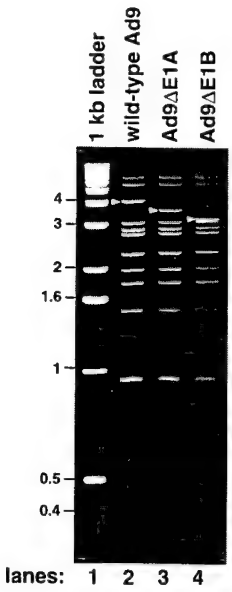

FIG. 4. *Sma*I digestion pattern of wild-type and E1A and E1B mutant Ad9 virion DNAs. The wild-type Ad9 E1 region-containing *Sma*I DNA band migrating at approximately 4 kb, as well as the corresponding faster-migrating DNA bands of the Ad9 E1A mutant virus Ad9ΔE1A and of the Ad9 E1B mutant virus Ad9ΔE1B, are indicated with arrows. A 1-kb ladder (Gibco-BRL) was used as a DNA size marker (lane 1).

analysis, we subjected tumor DNAs to a two-step nested PCR procedure (Fig. 5). In the first step, DNAs were PCR amplified with E1A primers (*a* plus *b*) or E1B primers (*c* plus *d*) flanking the deleted regions (Fig. 5A). From these reactions, wild-type Ad9-induced tumors yielded the expected 1,001-bp E1A product and 1,068-bp E1B product, but Ad9ΔE1A-induced tumors and Ad9ΔE1B-induced tumors yielded only the expected smaller 550-bp E1A product and 180-bp E1B product, respectively (Fig. 5B). To rule out the possibility of low-level contamination by wild-type Ad9 genomes in these mutant virus-induced tumors, we next used a nested set of E1A primers (*e* plus *b*) or E1B primers (*c* plus *f*) to subject the DNA products of the first PCRs described above to a second PCR (Fig. 5A). Using these nested primers in control PCRs, we were able to amplify the expected 762-bp E1A and 533-bp E1B products directly from the DNA of a wild-type Ad9-induced tumor (Fig. 5C). In contrast, we failed to amplify any such wild-type Ad9 DNA products from the first E1A and E1B PCRs of mutant virus-induced tumor DNAs (Fig. 5C). These results indicated that wild-type Ad9 E1 region sequences are absent from the mutant virus-induced mammary tumors and, consequently, that Ad9ΔE1A and Ad9ΔE1B are able to produce mammary tumors in rats.

TABLE 3. Tumorigenicities of wild-type and mutant Ad9 viruses in Wistar-Furth rats[a]

Virus	No. of rats that developed tumors/no. infected with virus	
	Females	Males
Ad9	3/3	0/2
Ad9ΔE1A	8/8	0/2
Ad9ΔE1B[b]	3/3	0/3
Ad26[c]	0/3	0/3

[a] Two- to three-day-old Wistar-Furth rats were injected subcutaneously with 7×10^7 PFU of virus. Animals were monitored by palpation for tumor development over an 8-month period.

[b] Due to replication deficiencies of virus Ad9ΔE1B in 293 cells, the dose used to infect rats with this virus (8×10^6 PFU) was approximately ninefold lower than that used for the other viruses.

[c] Ad26, a nononcogenic subgroup D human adenovirus closely related to Ad9 (31), served as a negative control in this experiment.

TABLE 4. Histologies of wild-type and mutant Ad9-induced tumors[a]

Virus	Tumor sample	Histology
Wild-type Ad9	1	Fibroadenoma
	2	Fibroadenoma
	3	Fibroadenoma
Ad9ΔE1A	1	Fibroadenoma, one area of increased cellularity
	2	Focally cellular fibroadenoma
	3	Fibroadenoma
	4	Cellular fibroadenoma, focally increased mitoses, and focal phyllodes-like tumor[b]
	5	Fibroadenoma
	6	Fibroadenoma
	7	Fibroadenoma
	8	Fibroadenoma
Ad9ΔE1B	1	Fibroadenoma
	2	Fibroadenoma
	3	Fibroadenoma

[a] For histological examination, tumor samples were fixed in 10% formalin, and sections were stained with hematoxylin and eosin.

[b] A section of this tumor contained an area resembling a phyllodes-like tumor, a type of mammary tumor occasionally observed in rats infected by wild-type Ad9 (29).

Mammary tumors contain and express the Ad9 E4 ORF1 gene. As E4 ORF1 is an essential viral determinant for tumorigenesis by Ad9 (32), we next sought to confirm that Ad9 mutant virus-induced mammary tumors retain this gene and express the protein. By PCR amplification or immunoblot analysis, we detected the Ad9 E4 ORF1 gene (Fig. 6A) or its protein expression (Fig. 6B), respectively, in all mammary tumors, including those elicited by viruses Ad9ΔE1A and Ad9ΔE1B. As smaller tumors had arisen in Ad9ΔE1A virus-infected animals, it was noteworthy that the levels of Ad9 E4 ORF1 protein in Ad9ΔE1A-induced tumors were lower than those in both wild-type Ad9-induced and Ad9ΔE1B-induced tumors (Fig. 6B).

DISCUSSION

In this study, we determined the nucleotide sequence of the subgroup D Ad9 E1 region and showed that its gene organization and predicted protein products are highly related to those of E1 regions from other human adenoviruses. Additionally, to investigate the role of the Ad9 E1 region in Ad9-induced mammary oncogenesis, we engineered the same E1A and E1B deletion mutations into both Ad9 E1 region plasmids and Ad9 viruses. We found that while E1A and E1B mutant Ad9 E1 region plasmids displayed significantly impaired focus-forming activity in vitro, the corresponding E1A and E1B mutant Ad9 viruses retained the ability to generate mammary tumors in rats. These results indicate that although the Ad9 E1 region alone or in cooperation with activated *ras* exhibits transforming activity in vitro, this activity is not required for mammary tumorigenesis by Ad9 in vivo. Similar examples in which transformation in vitro fails to predict tumorigenicity in vivo are also known for other viral and cellular transforming proteins (6, 8, 35, 45, 48, 56).

In addition to showing that Ad9 E1 region transforming functions are dispensable for mammary tumorigenesis by Ad9,

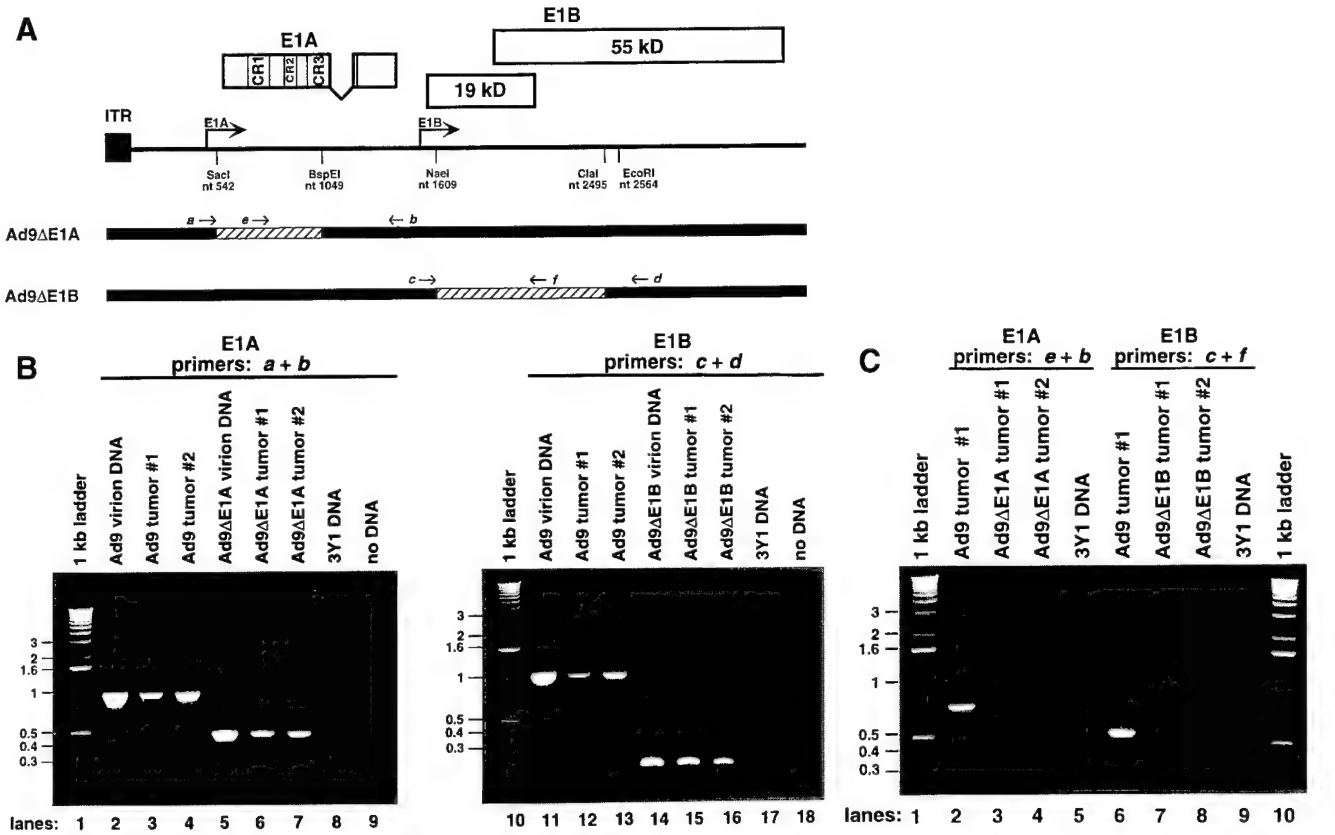

FIG. 5. Tumors induced by viruses Ad9ΔE1A and Ad9ΔE1B do not contain wild-type Ad9 E1 region sequences. (A) Locations of Ad9 E1 region primers used in PCRs. ITR, inverted terminal repeat. (B) PCR 1 utilized either E1A primers *a* and *b* or E1B primers *c* and *d*. Genomic DNA from rat 3Y1 cells or water (no DNA) represented negative controls in these reactions; 1.5 μg of genomic DNA or 10 ng of virion DNA was used as a template. (C) Nested PCR 2 utilized E1A primers *e* and *b* or E1B primers *c* and *f*. In these reactions, DNA from a wild-type Ad9-induced tumor and 3Y1 genomic DNA represented positive and negative controls, respectively; 1/20 of the DNA products from PCR (B) was used as a template for PCR 2. PCR conditions: 30 cycles of denaturation at 94°C for 1 min, annealing at 65°C (E1A reaction 1), 58°C (E1A reaction 2), or 60°C (E1B reactions 1 and 2) for 1 min, and extension at 72°C for 1 min, followed by a final 72°C extension for 15 min. DNA products were separated by agarose gel electrophoresis and visualized with ethidium bromide.

our results further argue that the Ad9 E4 region-encoded ORF1 transforming gene represents the major oncogenic determinant of this virus. In this respect, Ad9 represents the first example of an oncogenic adenovirus for which the E1 region is not the major oncogenic determinant. The fact that the oncogenic avian adenovirus CELO lacks genes related to the human adenovirus E1A and E1B oncogenes (11) further suggests that additional examples non-E1 region oncogenic determinants for adenoviruses will be found.

Although the mechanism by which Ad9 reaches the mammary glands of rats after subcutaneous inoculation has not been established, we hypothesize that the inoculated Ad9 virions are able to directly infect mammary cells to cause tumors in the animals. This idea is based on the fact that rodent cells are generally nonpermissive for replication of human adenoviruses (48), a property that would limit spread of the virus by successive rounds of viral replication in tissues of rats. Moreover, in this study, we found that Ad9 E1A and E1B mutant viruses (Ad9ΔE1A and Ad9ΔE1B, respectively) retained the capacity to generate mammary tumors in these animals. Because E1A and E1B genes encode critical functions needed for efficient replication of adenoviruses (48), these new results with E1A and E1B mutant viruses provide additional support for the idea that viral replication in rats is not required for Ad9 to produce mammary tumors.

Although tumors elicited by wild-type and E1 region mutant Ad9 viruses in this study were found to be histologically identical, the tumors induced by the E1A mutant Ad9 virus were generally smaller than those generated by both the wild-type and E1B mutant Ad9 viruses. This finding suggests that E1A transforming functions may, in fact, enhance the growth of Ad9-induced mammary tumors. Nevertheless, it must also be considered that, separate from its transforming functions, E1A also serves an important role in the viral life cycle by transcriptionally activating other viral gene regions, including the E4 region (7, 34, 42). In the E1A mutant virus Ad9ΔE1A, we introduced a large deletion extending from the E1A initiation codon through half of CR3, a mutation which in addition to abolishing the transforming potential of E1A would also be expected to block transcriptional activation mediated by this gene. With regard to such a lack of E1A transcriptional activity in virus Ad9ΔE1A, it may be relevant that mammary tumors generated by this virus expressed reduced levels of the E4 ORF1 protein (Fig. 6B). This finding may indicate that E1A plays an accessory role in Ad9 mammary tumorigenesis by transcriptionally activating the viral E4 region and, thereby, elevating expression of the Ad9 E4 ORF1 oncogenic determinant. Similar indirect roles in viral oncogenesis have been ascribed to the bovine papillomavirus type 1 E2 and the Epstein-Barr herpesvirus EBNA2 transactivators, which participate in tumor formation by increasing expression of

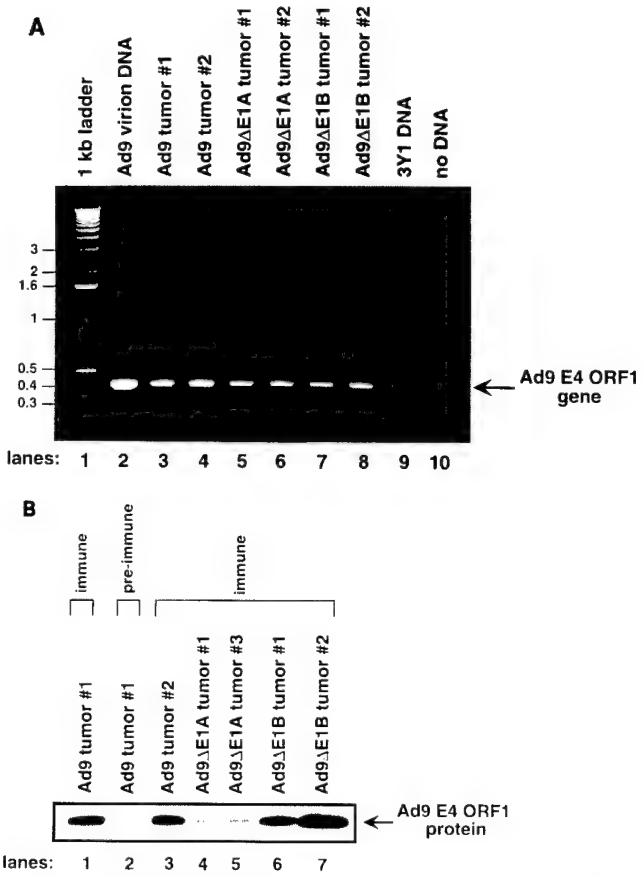

FIG. 6. (A) PCR amplification of the Ad9 E4 ORF1 gene from tumor DNAs. PCRs were performed with Ad9 E4 ORF1 primers as described for Fig. 5 except that a 55°C annealing temperature was used. Genomic DNA from rat 3Y1 cells represented a negative control in these reactions. (B) Detection of Ad9 E4 ORF1 protein in tumors. Tumor lysates containing 3 mg of protein were subjected to immunoprecipitation followed by immunoblot analysis using Ad9 E4 ORF1 polyclonal antiserum. Preimmune serum served as a negative control for immunoprecipitations (lane 2).

the transforming genes of their respective viruses (14, 16, 24, 36, 43).

In addition to promoting tumorigenesis, the oncoproteins of DNA tumor viruses may also contribute to determining which particular tissues are targeted for neoplasia. Comparisons of two related families of viruses, the papillomaviruses (PVs) and fibropapillomaviruses (FPVs), can be used to illustrate this idea. Although members of both families of viruses encode three different, structurally conserved transforming proteins, E5, E6, and E7 (5, 10, 15, 27, 39, 46), PVs and FPVs target distinct tissues in vivo, with PVs causing papillomas in epithelial keratinocytes and FPVs causing fibropapillomas in dermal fibroblasts (27). It has been established that E6 and E7 represent the major transforming proteins of PVs, whereas the E5 gene product is the major transforming protein of FPVs (27). Such observations have led to the hypothesis that the use of functionally different oncogenic determinants contributes to the unique tumorigenic tissue tropisms of PVs and FPVs (27). Likewise, Ad9 causes estrogen-dependent mammary tumors, whereas other oncogenic adenoviruses induce sarcomas in rodents. Therefore, one intriguing possibility is that novel molecular mechanisms which underly the transforming activity of Ad9 E4 ORF1 (41) permit Ad9 to selectively target mammary cells for tumorigenesis.

ACKNOWLEDGMENTS

We thank Stephen Hoang for technical assistance and Sylvia Lee for generously supplying REF cultures. We also thank Sylvia Lee, Britt Glaunsinger, Ezequiel Fuentes, and Nader Ghebranious for helpful suggestions.

D.L.T. was supported by National Research Service Award CA09197 from the National Cancer Institute and by the Federal Work-Study program of the U.S. Department of Education. This work was funded by grants from the NIH (NCI R01 CA/AI58541), ACS (RP6-97-068-01-VM), and Department of the Army (DAMD17-97-1-7082) to R.T.J. and by an NIH grant (POI CA41086) to T.E.S. T.E.S. is an American Cancer Society Professor and an Investigator of the Howard Hughes Medical Institute.

REFERENCES

1. **Abate, C., D. Luk, R. Gentz, F. Rauscher, and T. Curran.** 1990. Expression and purification of the leucine zipper and DNA-binding domains of fos and jun: both fos and jun contact DNA directly. Proc. Natl. Acad. Sci. USA **87:** 1032–1036.
2. **Aiello, L., R. Guilfoyle, K. Huebner, and R. Weinmann.** 1979. Adenovirus 5 DNA sequences present and RNA sequences transcribed in transformed human embryo kidney cells. Virology **94:**460–469.
3. **Ankerst, J., and N. Jonsson.** 1989. Adenovirus type 9-induced tumorigenesis in the rat mammary gland related to sex hormonal state. J. Natl. Cancer Inst. **81:**294–298.
4. **Ankerst, J., N. Jonsson, L. Kjellen, E. Norrby, and H. O. Sjogren.** 1974. Induction of mammary fibroadenomas in rats by adenovirus type 9. Int. J. Cancer. **13:**286–290.
5. **Baker, C. C.** 1987. Sequence analysis of papillomavirus genomes, p. 321–385. *In* N. Salzman and P. M. Howley (ed.), The Papovaviridae, vol. 2. Plenum Publishing Corp., New York, N.Y.
6. **Barbosa, M. S., and R. Schlegel.** 1989. The E6 and E7 genes of HPV-18 are sufficient for inducing two-stage in vitro transformation of human keratinocytes. Oncogene **4:**1529–1532.
7. **Berk, A. J., F. Lee, T. Harrison, J. Williams, and P. A. Sharp.** 1979. Pre-early adenovirus 5 gene product regulates synthesis of early viral messenger RNAs. Cell **17:**935–944.
8. **Bos, J. L., A. G. Jochemsen, R. Bernards, P. I. Schrier, H. van Ormondt, and A. J. van der Eb.** 1983. Deletion mutants of region E1a of AD12 E1 plasmids: effect on oncogenic transformation. Virology **129:**393–400.
9. **Bradford, M. M.** 1976. A rapid and sensitive method for the quantitation of microgram quantities of protein utilizing the principle of protein dye binding. Anal. Biochem. **72:**248–254.
10. **Bubb, V., D. J. McCance, and R. Schlegel.** 1988. DNA sequence of the HPV-16 E5 ORF and the structural conservation of its encoded protein. Virology **163:**243–246.
11. **Chiocca, S., R. Kurzbauer, G. Schaffner, A. Baker, V. Mautner, and M. Cotten.** 1996. The complete DNA sequence and genomic organization of the avian adenovirus CELO. J. Virol. **70:**2939–2949.
12. **Chomczynski, P., and N. Sacchi.** 1987. Single-step method of RNA isolation by acid guanidinium thiocyanate-phenol-chloroform extraction. Anal. Biochem. **162:**156–159.
13. **Chomczynski, R.** 1992. One-hour downward alkaline capillary transfer for blotting of DNA and RNA. Anal. Biochem. **201:**134–139.
14. **Cohen, J. I., F. Wang, and E. Kieff.** 1991. Epstein-Barr virus nuclear protein 2 mutations define essential domains for transformation and transactivation. J. Virol. **65:**2545–2554.
15. **Danos, O., L. W. Engel, E. Y. Chen, M. Yaniv, and P. M. Howley.** 1983. Comparative analysis of the human type 1a and bovine type 1 papillomavirus genomes. J. Virol. **46:**557–566.
16. **DiMaio, D., J. Metherall, and K. Neary.** 1986. Nonsense mutation in open reading frame E2 of bovine papillomavirus DNA. J. Virol. **57:**475–480.
17. **Feinberg, A. P., and B. Vogelstein.** 1983. A technique for radiolabeling DNA restriction endonuclease fragments to high specific activity. Anal. Biochem. **132:**6–13.
18. **Finlay, C. A., P. W. Hinds, and A. J. Levine.** 1989. The p53 proto-oncogene can act as a suppressor of transformation. Cell **57:**1083–1093.
19. **Fisher, P. B., L. E. Babiss, I. B. Weinstein, and H. S. Ginsberg.** 1982. Analysis of type 5 adenovirus transformation with a cloned rat embryo cell line (CREF). Proc. Natl. Acad. Sci. USA **79:**3527–3531.
20. **Freshney, R. I.** 1987. Culture of animal cells: a manual of basic technique, 2nd ed., p. 107–126. Alan R. Liss, Inc., New York, N.Y.
21. **Fukui, Y., I. Saito, K. Shiroki, and H. Shimojo.** 1984. Isolation of transformation-defective, replication-nondefective early region 1B mutants of adenovirus type 12. J. Virol. **49:**154–161.
22. **Graham, F.** 1984. Transformation by and oncogenicity of human adenoviruses, p. 339–398. *In* H. Ginsberg (ed.), The adenoviruses. Plenum Press, New York, N.Y.
23. **Graham, F. L., J. Smiley, W. C. Russell, and R. Nairn.** 1977. Characteristics

of a human cell line transformed by DNA from human adenovirus type 5. J. Gen. Virol. **36:**59–72.
24. **Groff, D. E., and W. D. Lancaster.** 1986. Genetic analysis of the 3′ early region transformation and replication functions of bovine papillomavirus type 1. Virology **150:**221–230.
25. **Horwitz, M. S.** 1996. Adenoviruses, p. 2149–2171. *In* B. N. Fields, D. M. Knipe, and P. M. Howley (ed.), Fields virology, vol. 2. Lippincott, Philadelphia, Pa.
26. **Houweling, A., P. van den Elsen, and A. van der Eb.** 1980. Partial transformation of primary rat cells by the leftmost 4.5% fragment of adenovirus 5 DNA. Virology **105:**537–550.
27. **Howley, P. M.** 1996. Papillomavirinae: the viruses and their replication, p. 2045–2076. *In* B. N. Fields, D. M. Knipe, and P. M. Howley (ed.), Fields virology, vol. 2. Lippincott, Philadelphia, Pa.
28. **Jannun, R., and G. Chinnadurai.** 1987. Functional relatedness between the E1a and E1b regions of group C and group D human adenoviruses. Virus Res. **7:**33–48.
29. **Javier, R., K. Raska, Jr., G. J. Macdonald, and T. Shenk.** 1991. Human adenovirus type 9-induced rat mammary tumors. J. Virol. **65:**3192–3202.
30. **Javier, R., K. Raska, Jr., and T. Shenk.** 1992. Requirement for the adenovirus type 9 E4 region in production of mammary tumors. Science **257:**1267–1271.
31. **Javier, R., and T. Shenk.** 1996. Mammary tumors induced by human adenovirus type 9: a role for the viral early region 4 gene. Breast Cancer Res. Treat. **39:**57–67.
32. **Javier, R. T.** 1994. Adenovirus type 9 E4 open reading frame 1 encodes a transforming protein required for the production of mammary tumors in rats. J. Virol. **68:**3917–3924.
33. **Jelinek, T., D. S. Pereira, and F. L. Graham.** 1994. Tumorigenicity of adenovirus-transformed rodent cells is influenced by at least two regions of adenovirus type 12 early region 1A. J. Virol. **68:**888–896.
34. **Jones, N., and T. Shenk.** 1979. An adenovirus type 5 early gene function regulates expression of other early viral genes. Proc. Natl. Acad. Sci. USA **76:** 3665–3669.
35. **Kaur, P., and J. K. McDougall.** 1988. Characterization of primary human keratinocytes transformed by human papillomavirus type 18. J. Virol. **62:** 1917–1924.
36. **Kieff, E.** 1996. Epstein-Barr Virus and its replication, p. 2343–2396. *In* B. N. Fields, D. M. Knipe, and P. M. Howley (ed.), Fields virology, vol. 2. Lippincott, Philadelphia, Pa.
37. **Kimura, G., A. Itagaki, and J. Summers.** 1975. Rat cell line 3Y1 and its virogenic polyoma and SV40 transformed derivatives. Int. J. Cancer **15:**694–706.
38. **Kingston, R. E., C. A. Chen, and H. Okayama.** 1990. Calcium phosphate transfection, p. 9.1.1–9.1.9. *In* F. M. Ausubel, R. Brent, R. E. Kingston, D. D. Moore, J. G. Seidman, J. A. Smith, and K. Struhl (ed.), Current protocols in molecular biology. Greene Publishing Associates and Wiley-Interscience, New York, N.Y.
39. **Kulke, R., and D. DiMaio.** 1991. Biological activities of the E5 protein of the deer papillomavirus in mouse C127 cells: morphologic transformation, induction of cellular DNA synthesis, and activation of the platelet-derived growth factor receptor. J. Virol. **65:**4943–4949.
40. **Laemmli, U. K.** 1970. Cleavage of structural proteins during the assembly of the head of bacteriophage T4. Nature **227:**680–685.
41. **Lee, S. S., R. S. Weiss, and R. T. Javier.** 1997. Binding of human virus oncoproteins to hDlg/SAP97, a mammalian homolog of the *Drosophila* discs large tumor suppressor protein. Proc. Natl. Acad. Sci. USA **94:**6670–6675.
42. **Nevins, J.** 1981. Mechanism of activation of early viral transcription by the adenovirus E1A gene product. Cell **26:**213–220.
43. **Rabson, M. S., C. Yee, Y.-C. Yang, and P. M. Howley.** 1986. Bovine papillomavirus type 1 3′ early region transformation and plasmid maintenance functions. J. Virol. **60:**626–634.
44. **Robbins, S. L., M. Angell, and V. Kumar.** 1981. Basic pathology, p. 564–595. The W. B. Saunders Co., Philadelphia, Pa.
45. **Schlegel, R., W. C. Phelps, Y.-L. Zhang, and M. Barbosa.** 1988. Quantitative keratinocyte assay detects two biological activities of human papillomavirus DNA and identifies viral types associated with cervical carcinoma. EMBO J. **7:**3181–3187.
46. **Schwarz, E., M. Durst, C. Demankowski, O. Lattermann, R. Zech, E. Wolfsperger, S. Suhai, and H. zur Hausen.** 1983. DNA sequence and genome organization of genital human papillomavirus type 6b. EMBO J. **2:**2341–2348.
47. **Sharp, P. A.** 1984. Adenovirus transcription, p. 173–204. *In* H. Ginsberg (ed.), The adenoviruses. Plenum Press, New York, N.Y.
48. **Shenk, T.** 1996. Adenoviridae: the viruses and their replication, p. 2111–2148. *In* B. N. Fields, D. M. Knipe, and P. M. Howley (ed.), Fields virology, vol. 2. Lippincott, Philadelphia, Pa.
49. **Shenk, T., and J. Flint.** 1991. Transcriptional and transforming activities of the adenovirus E1A proteins. Adv. Cancer Res. **57:**47–85.
50. **Smith, R. F., B. A. Wiese, M. K. Wojzynski, D. B. Davison, and K. C. Worley.** 1996. BCM Search Launcher—an integrated interface to molecular biology database search and analysis services available on the World Wide Web. Genome Res. **6:**454–462.
51. **Stillman, B.** 1986. Functions of the adenovirus E1B tumor antigens. Cancer Surv. **5:**389–404.
52. **Strauss, W. M.** 1994. Preparation of genomic DNA from mammalian tissue, p. 2.2.1–2.2.3. *In* F. M. Ausubel, R. Brent, R. E. Kingston, D. D. Moore, J. G. Seidman, J. A. Smith, and K. Struhl (ed.), Current protocols in molecular biology, vol. 1. Greene Publishing Associates and Wiley-Interscience, New York, N.Y.
53. **Telling, G. C., and J. Williams.** 1994. Constructing chimeric type 12/type 5 adenovirus E1A genes and using them to identify an oncogenic determinant of adenovirus type 12. J. Virol. **68:**877–887.
54. **Trentin, J., Y. Yabe, and G. Taylor.** 1962. The quest for human cancer viruses: a new approach to an old problem reveals cancer induction in hamster by human adenovirus. Science **137:**835–841.
55. **van den Elsen, P., A. Houweling, and A. van der Eb.** 1983. Expression of region E1b of human adenoviruses in the absence of region E1a is not sufficient for complete transformation. Virology **128:**377–390.
56. **van Leeuwen, F. N., R. A. van der Kammen, G. G. M. Habets, and J. G. Collard.** 1995. Oncogenic activity of Tiam 1 and Rac1 in NIH3T3 cells. Oncogene **11:**2215–2221.
57. **Yew, P. R., C. C. Kao, and A. J. Berk.** 1990. Dissection of functional domains in the adenovirus 2 early 1B 55K polypeptide by suppressor-linker insertional mutagenesis. Virology **179:**795–805.

Paper 3

Oncogene (1999) 18, 5487–5496

http://www.stockton-press.co.uk/onc

Oncogenic human papillomavirus E6 proteins target the discs large tumour suppressor for proteasome-mediated degradation

Daniela Gardiol[1], Christian Kühne[1], Britt Glaunsinger[2], Siu Sylvia Lee[2], Ron Javier[2] and Lawrence Banks*,[1]

[1]*International Centre for Genetic Engineering and Biotechnology, Padriciano 99, I-34012 Trieste, Italy;* [2]*Division of Molecular Virology, Baylor College of Medicine, One Baylor Plaza, Houston, Texas, TX 77030, USA*

Previous studies have shown that the oncogenic HPV E6 proteins form a complex with the human homologue of the *Drosophila* tumour suppressor protein, discs large (Dlg). This is mediated by the carboxy terminus of the E6 proteins and involves recognition of at least one PDZ domain of Dlg. This region of E6 is not conserved amongst E6 proteins from the low risk papillomavirus types and, hence, binding of HPV E6 proteins to Dlg correlates with the oncogenic potential of these viruses. We have performed studies to investigate the consequences of the interaction between E6 and Dlg. Mutational analysis of both the HPV18 E6 and Dlg proteins has further defined the regions of E6 and Dlg necessary for complex formation. Strikingly, co-expression of wild type HPV18 E6 with Dlg *in vitro* or *in vivo* results in a dramatic decrease in the amount of Dlg protein, whereas mutants of E6 which fail to complex with Dlg have minimal effect on Dlg protein levels. The oncogenic HPV16 E6 also decreased the Dlg levels, but this was not observed with the low risk HPV11 E6 protein. Moreover, a region within the first 544 amino acids of Dlg containing the three PDZ domains confers susceptibility to E6 mediated degradation. Finally, treatment of cells with a proteasome inhibitor overrides the capacity of E6 to degrade Dlg. These results demonstrate that Dlg is targeted by high risk HPV E6 proteins for proteasome mediated degradation.

Keywords: HPV E6; DLG; proteasome; transformation

Introduction

Certain Human Papillomaviruses (HPVs), such as HPV16 and HPV18, are closely associated with the development of a number of human cancers (zur Hausen and Schneider, 1987; zur Hausen, 1991). The major transforming activity of these viruses is encoded by the E6 and E7 genes (Vousden, 1994). These proteins contribute to the oncogenic process by inactivating key cellular proteins involved in the control of cell proliferation. E7 was demonstrated to bind and inactivate the retinoblastoma tumour suppressor protein (pRB) (Dyson *et al.*, 1989; Münger *et al.*, 1989), as well as the related p107 and p130 proteins (Davies *et al.*, 1993). The principal activity of the tumour-associated E6 proteins is the ability to bind to the p53 tumour suppressor protein and stimulate its rapid degradation via the ubiquitin proteolytic pathway (Scheffner *et al.*, 1990). There is however, a growing list of evidence indicating that, in addition to inactivating p53, E6 has other activities which may contribute to its oncogenic potential. It has been shown that HPV16 E6 interacts with the focal adhesion protein paxillin, resulting in a disruption of the actin cytoskeleton (Tong and Howley, 1997). The E6 oncoproteins also bind to the calcium binding protein ERC55 (E6BP) (Chen *et al.*, 1995), and it has been recently reported that HPV16 E6 stimulates the ubiquitin-mediated degradation of c-*myc* and Bak (Gross-Mesilaty *et al.*, 1998; Thomas and Banks, 1998).

Sequence analysis of the E6 proteins derived from high risk mucosotropic HPVs reveals a high degree of homology in their C-terminal domains. This highly conserved region of E6 is not involved in the ability of E6 to bind and promote the degradation of p53 (Crook *et al.*, 1991; Pim *et al.*, 1994), suggesting that other activities important for cell transformation may be regulated by this region. Recent studies have shown that this conserved C-terminal motif of oncogenic E6 proteins mediates an interaction with the PDZ domain-containing protein hDlg, the human homologue of the *Drosophila* tumour suppressor, discs large protein (DlgA) (Woods and Bryant, 1991; Lee *et al.*, 1997; Kiyono *et al.*, 1997). In fact, this E6 motif (XTXV/L) is remarkably similar to the C-terminal peptide domain XS/TXV which has been shown previously to interact with the hydrophobic groove of the PDZ sites (Doyle *et al.*, 1996; Songyang *et al.*, 1997). PDZ domains (PSD-95/disc large/ZO-1) are 80–90 amino acid motifs present in several proteins of distinct origin and function as specific protein-recognition modules (Ponting and Phillips, 1995; Saras and Heldin, 1996; Kim, 1997). They can target cytoplasmic proteins to form complexes at the inner surface of the plasma membrane, and are important for clustering membrane proteins, as well as for linking signalling molecules in multiprotein complexes at specialized membrane sites (Kim *et al.*, 1995; Marfatia *et al.*, 1996; Kim, 1997). hDlg-1 (homologous to the rat SAP97 and hereafter termed DLG) belongs to the family of proteins termed MAGUKs (membrane-associated guanylate kinase homologues) (Lue *et al.*, 1994; Muller *et al.*, 1995). These proteins share amino-terminal PDZ domains, an SH3 domain and a carboxy-terminal guanylate kinase (GuK) homology domain. MAGUKs are multifunctional proteins localized at the membrane-cytoskeleton interface at cell-cell junctions, where they have

*Correspondence: L Banks
Received 17 November 1998; revised 15 April 1999; accepted 20 April 1999

structural as well as signalling roles (Anderson, 1996). hDlg is expressed in a variety of cell types including epithelia, where it is localized at regions of cell-cell contact (Lue *et al*., 1994). Interestingly, mutations in *Drosophila dlg* causes epithelial cells to lose polarity and undergo neoplastic proliferation (Woods *et al*., 1996).

Taking into account the activity of E6 with respect to p53, we initiated a series of studies to investigate the effects of E6 upon the steady-state levels of DLG. We show both *in vitro* and *in vivo* that co-expression of HPV18 E6 with DLG results in a dramatic reduction in the levels of DLG expression. Mutational analysis of both E6 and DLG shows that this effect correlates with the ability of E6 and DLG to form a protein complex. A similar activity is exerted by HPV16 E6 but not by the low risk HPV11 E6 and, in addition, the reduction in DLG levels by E6 can be reversed by proteasome inhibition. These results demonstrate that oncogenic HPV E6 proteins target DLG for proteasome mediated degradation both *in vitro* and *in vivo*.

Results

The Thr156 residue of the HPV18 E6 protein is important for binding to DLG in vitro

Recent reports have shown the binding of oncogenic E6 proteins to DLG, a PDZ domain-containing protein (Lee *et al*., 1997; Kiyono *et al*., 1997). These studies highlighted the importance of the highly conserved C-terminus of the E6 proteins for this interaction, and the similarity of this region to previously defined PDZ domain-binding motifs (Doyle *et al*., 1996; Songyang *et al*., 1997). To further analyse the E6-DLG interaction, we first investigated the importance of E6 Thr156 for binding DLG, since this residue represents a potential PKA phosphorylation site and is also part of the PDZ domain-binding motif (Figure 1). We constructed two different HPV18 E6 mutants: Thr156Glu and Thr156Val and tested them for the ability to bind DLG *in vitro*. Wild type and mutant E6 proteins were expressed by *in vitro* translation and subjected to GST pulldown analyses by incubation with GST-DLG fusion protein (Lee *et al*., 1997). The results shown in Figure 2 demonstrate that both mutants are greatly reduced in their ability to bind DLG compared with wild type HPV18 E6. As an additional control, another mutant, Arg153Lys, bearing a point mutation in the C-terminus of E6 upstream of the PDZ domain-binding motif, was also included. As can be seen, the Arg153Lys mutant binds DLG as efficiently as the wild type protein. These results demonstrate that the Thr residue at position 156 within the consensus C terminal binding motif of E6 is necessary for interaction with DLG. This is in agreement with the crystal structure of the PSD-95 PDZ domain-peptide complex, which showed that the hydroxyl oxygen of the T/S residue in the PDZ binding motif of the peptide is directly involved in the interaction with the PDZ domain (Doyle *et al*., 1996).

HPV18 E6 binds to all three PDZ domains of DLG in vitro

Previous studies have shown that HPV16 E6 binds principally to the second PDZ domain of DLG (Kiyono *et al*., 1997). Since HPV18 E6 has been reported to bind DLG more strongly than HPV16 E6 (Kiyono *et al*., 1997; R Weiss and R Javier, personal observations), we were interested in identifying which DLG PDZ domains were necessary for complex formation with HPV18 E6. A series of GST-DLG deletion constructs (Figure 3A) (Lee *et al*., 1997) were used to assess HPV18 E6 binding. Similar amounts of each DLG fusion protein were immobilized on PVDF membrane and then incubated with purified radiola-

```
HPV18    AGHYRGQCHS CCNRARQERL QRRRETQV
HPV45    AGQYRGQCNT CCDQARQERL RRRRETQV
HPV16    RGRWTGRCMS CC.....RSS RTRRETQL
HPV31    GGRWTGRCIA CW......R. RPRTETQV
HPV33    SGRWAGRCAA CW......R. SRRRETAL
HPV51    AGRWTGQCAN CW.....QRT RQRNETQV

HPV11                          CLHCWTTCMEDLLP

PDZ consensus                  XTXV
                                S
```

Figure 1 Alignment of the C-terminal ends of E6 proteins derived from HPV types associated with genital infections. HPV18, 16, 45, 31, 33 and 51 are high risk HPVs associated with cervical cancer. HPV11 is a low risk type associated with benign genital lesions. The alignment was performed relative to the last cysteine of the second zinc-finger of the E6 sequence. The conserved PDZ consensus binding site is shown

belled HPV18 E6 protein probe. The binding of the HPV18 E6 protein to the DLG fusion proteins was determined by autoradiography. The results shown in Figure 3B demonstrate that HPV18 E6 binds equally well to each of the three PDZ domains of DLG. This binding is specific since the HPV18 E6 probe did not react with the DLG constructs NT and SH3/GuK, which lack PDZ domains. This is in contrast to the results previously obtained with HPV16 E6 which was found to bind largely to DLG PDZ2 (Kiyono *et al.*, 1997). These divergent results are likely to explain the apparent stronger affinity of HPV18 E6 for DLG compared with HPV16 E6.

Degradation of DLG protein by HPV18 E6 in vitro

A major activity of the tumour-associated E6 proteins is the ability to target a number of cellular proteins for ubiquitin mediated degradation (Scheffner *et al.*, 1990; Gross-Mesilaty *et al.*, 1998; Thomas and Banks, 1998; Kühne and Banks, 1998). Therefore, we were interested in determining whether HPV18 E6 had a similar activity with respect to DLG. To examine this, we first performed an *in vitro* degradation assay. DLG and HPV18 E6 were translated *in vitro* with rabbit reticulocyte lysate, and subsequently, were mixed together and incubated at 30°C for 60 min. The proteins were then run on SDS–PAGE, and DLG protein was detected by autoradiography (Figure 4A). The results show a reduced level of DLG protein following incubation with wild type E6. In contrast, no change in the levels of DLG is seen when it was incubated either with the E6 Thr156Glu mutant, which cannot bind DLG, or with control water primed reticulocyte lysate. For comparison, the same assay was performed with p53 and, as can be seen in Figure 4B, both the wild type and the mutant Thr156Glu E6 proteins similarly reduced the level of p53. Equivalent results were also obtained when the experiment was performed by simultaneously co-translating the E6 and DLG proteins and then monitoring DLG levels by SDS–PAGE and autoradiography (Figure 4C). In this experiment, DLG was also co-translated in the presence of HPV16 E7 as an additional negative control. These data demonstrate that the wild type HPV18 E6 protein specifically stimulates the degradation of DLG in reticulocyte lysates *in vitro* and that this activity is dependent on the ability of E6 to interact with DLG.

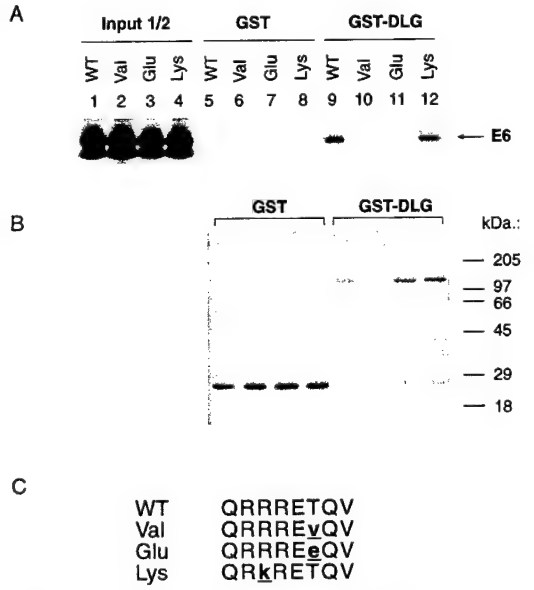

Figure 2 Binding of HPV18 E6 to GST-DLG *in vitro*. (**A**) Radiolabelled *in vitro* translated E6 proteins were incubated with GST-DLG or GST alone as a control. The bound E6 proteins were assessed by autoradiography. Wild type (WT) and the mutant E6 proteins tested are indicated, and amount of input protein is shown on the left of the gel. (**B**) Coomassie Blue stained gel showing equal levels of fusion protein loading. (**C**) Sequence of the C terminal domain of the wild type and mutant E6 proteins used in the assay. The amino acid substitutions are shown with respect to the wild type HPV18 E6 sequence and are underlined

DLG is targeted by HPV18 E6 for degradation in vivo

Having shown that HPV18 E6 could induce the degradation of DLG *in vitro*, we were next interested in analysing whether this would take place *in vivo*. To test this possibility, we performed a series of *in vivo* degradation assays. Human 293 cells were co-transfected with influenza haemaglutinin (HA) epitope-tagged DLG (Kim and Sheng, 1996) plus either wild type or the Thr156Glu mutant of HPV18 E6. After 24 h, the cells were harvested and the levels of DLG were ascertained by Western blot analysis using an anti-HA monoclonal antibody. The results shown in Figure 5A (upper panel) indicate that the levels of DLG were greatly reduced in the presence of wild type HPV18 E6 but were unaffected in the presence of the E6 Thr156Glu mutant. Therefore, HPV18 E6 targets DLG for degradation *in vivo*, and this correlates with the ability of E6 to bind DLG *in vitro*. To investigate whether E6 proteins derived from other genital HPV types could promote the degradation of DLG, we examined the HPV16 E6 and HPV11 E6 proteins in the same assay. As can be seen in Figure 5A (upper panel), HPV16 E6 also promotes degradation of DLG, albeit to a lesser extent than HPV18 E6, whereas no reduction in the levels of DLG was observed in the presence of HPV11 E6. HPV16 E6 has previously been shown to bind DLG both *in vivo* and *in vitro*; in contrast, HPV11 E6 lacks the consensus PDZ domain-binding motif and cannot bind DLG (Lee *et al.*, 1997; Kiyono *et al.*, 1997). Thus, high risk HPV E6 proteins share the ability to target DLG for degradation *in vivo*, but low risk E6 proteins which fail to bind DLG do not.

To exclude the possibility that the reduced levels of DLG expression obtained *in vivo* in the presence of E6 were due to sequestration within insoluble complexes rather than degradation, we analysed the levels of the DLG protein in the insoluble fractions of cells in both the presence and absence of HPV E6. The results obtained are shown in Figure 5A (lower panel) and demonstrate that in the insoluble fractions, the levels of DLG are reduced in the presence of HPV18 E6 and to a somewhat lesser extent with HPV16 E6. In contrast there is no decrease in the levels of DLG in the presence of either the Thr156Glu mutant or HPV11 E6. This result confirms that E6 reduces the total

amount of DLG within the cell, and that the reduced levels of DLG observed are not due to the generation of protein complexes which fail to be extracted under the conditions of these assays.

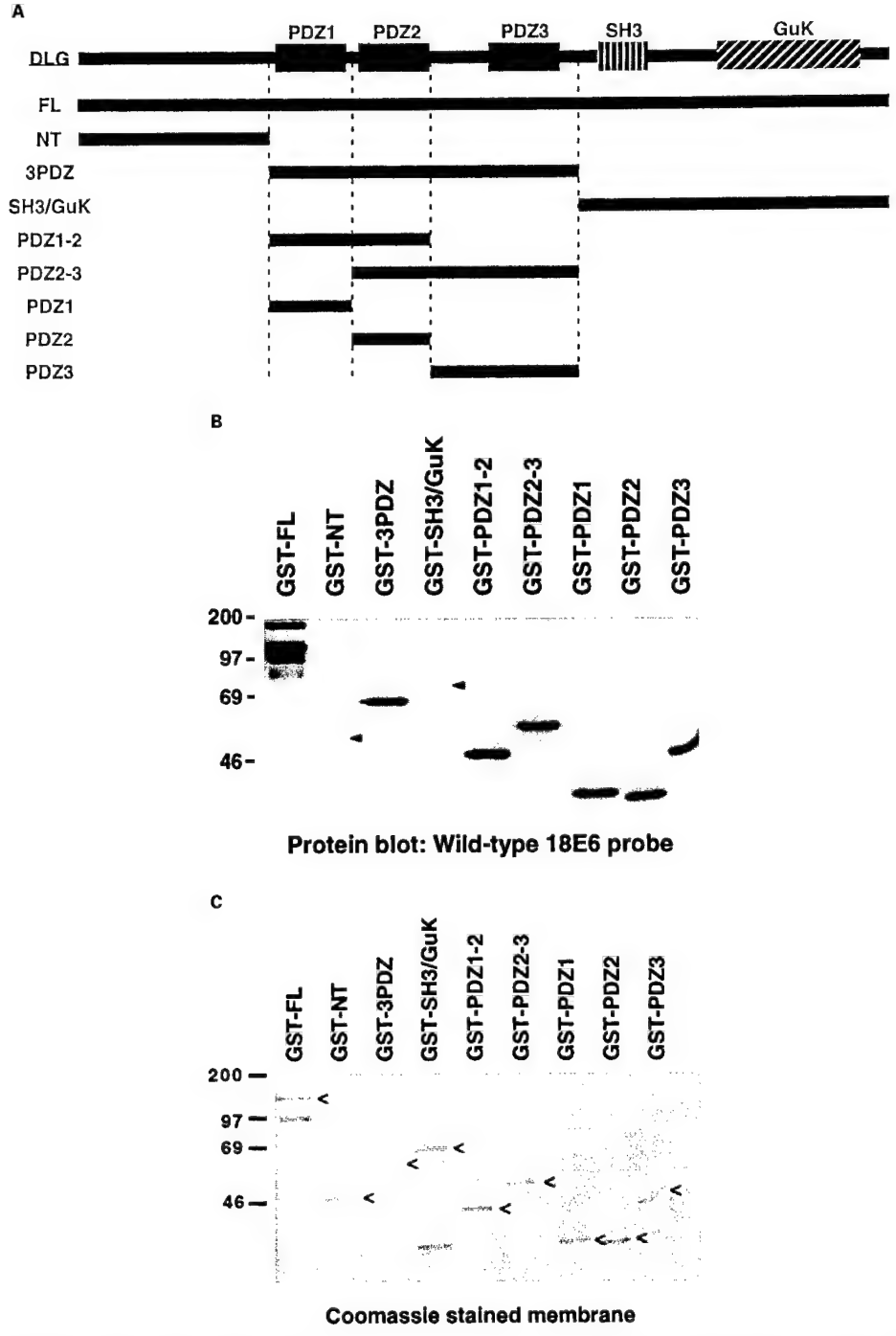

Figure 3 HPV18 E6 binds to all three individual PDZ domains of DLG *in vitro*. (**A**) Schematic representation of the full-length (FL) and truncated DLG proteins used in the binding assays. (**B**) GST-DLG fusion proteins were transferred to a PVDF membrane, which was then incubated with purified radiolabelled HPV18 E6 protein (5×10^5 c.p.m./ml), and washed extensively. Bound E6 was detected by autoradiography. Arrows indicate the positions of truncated GST-DLG fusion proteins which did not bind the E6 protein probe. (**C**) Coomassie stain of the PVDF membrane after performing the binding assay showing equal levels of fusion protein loading

In order to exclude the possibility that differences in the ability of the E6 proteins to target DLG for degradation were due to differences in levels of E6 expression, a parallel p53 *in vivo* degradation assay was also performed. Saos-2 cells were transfected with a p53 expression plasmid together with either HPV18, HPV16, HPV11 E6 or the Thr156Glu HPV18 E6 mutant. The cells were harvested after 24 h and the results obtained are shown in Figure 5B. As can be seen, both HPV18 E6 and HPV16 E6 induce complete degradation of the p53 protein. This indicates that the differences in the ability of these two E6 proteins to degrade DLG most likely reflects intrinsic differences in their respective abilities to target DLG for degradation rather than differences in their levels of expression. Likewise the Thr156Glu mutant displays almost wild type levels of p53 degradation. This confirms in a functional assay that this mutant E6 protein is expressed and, in addition, that this region of E6 is not involved in the p53 interaction. Finally, a weak reduction in p53 levels was obtained following transfection with HPV11 E6. This is in agreement with our previous observations (Storey *et al*., 1998) and also demonstrates functional expression of this protein.

To determine which regions of DLG render it susceptible to E6 mediated degradation, we performed *in vivo* degradation assays using two truncated derivatives of DLG: DLG-NT3PDZ (amino acids 1–544) contains the N-terminus and the three PDZ domains of the protein, and DLG-SH3GuK (amino acids 539-end) contains the GuK

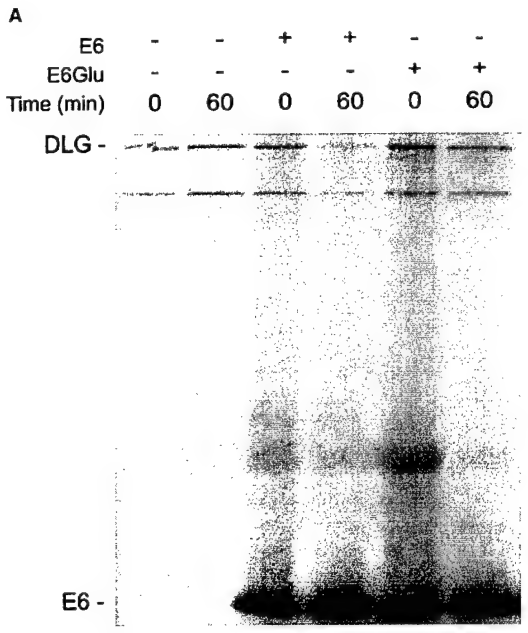

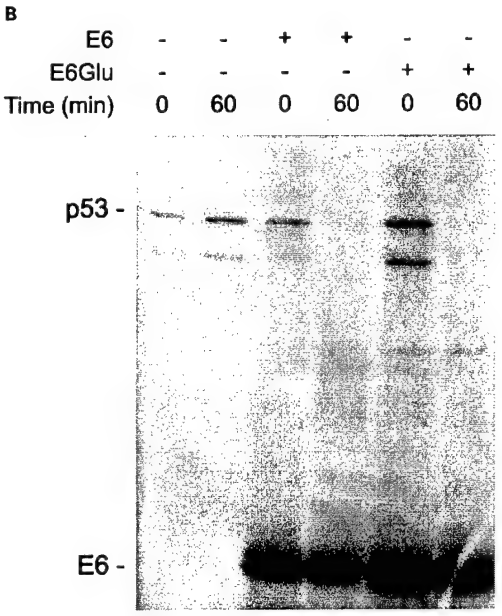

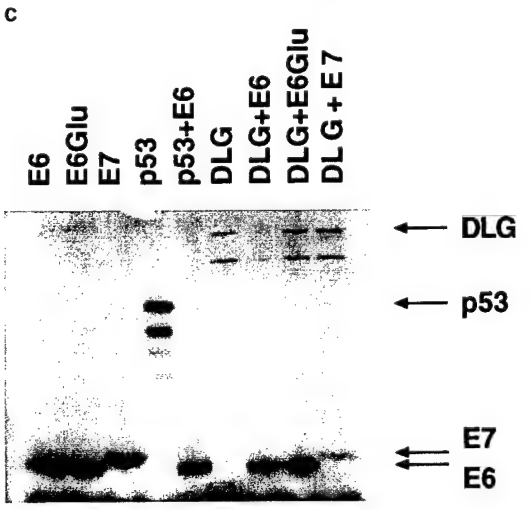

Figure 4 E6-mediated degradation of DLG *in vitro*. **(A)** *In vitro* translated DLG was incubated in the presence of *in vitro* translated wild type E6, Thr156Glu E6 mutant (E6Glu) or water-primed lysate for 0 or 60 min as indicated. The amount of DLG remaining after the incubations was assessed by SDS–PAGE and autoradiography. The position of E6 and DLG is indicated. **(B)** The same assay was carried out with p53 protein as a positive control. The amount of p53 remaining after the incubations was assessed by SDS–PAGE and autoradiography. The position of E6 and p53 is indicated. **(C)** DLG protein was cotranslated *in vitro* with E6, the Thr156Glu (E6Glu) mutant or E7 for 90 min at 30°C as indicated. The samples were then analysed by SDS–PAGE and autoradiography. p53 served as a positive control and the left hand three lanes show E6, E6Glu and E7 translated alone. Arrows indicate the positions of DLG, p53, E7 and E6

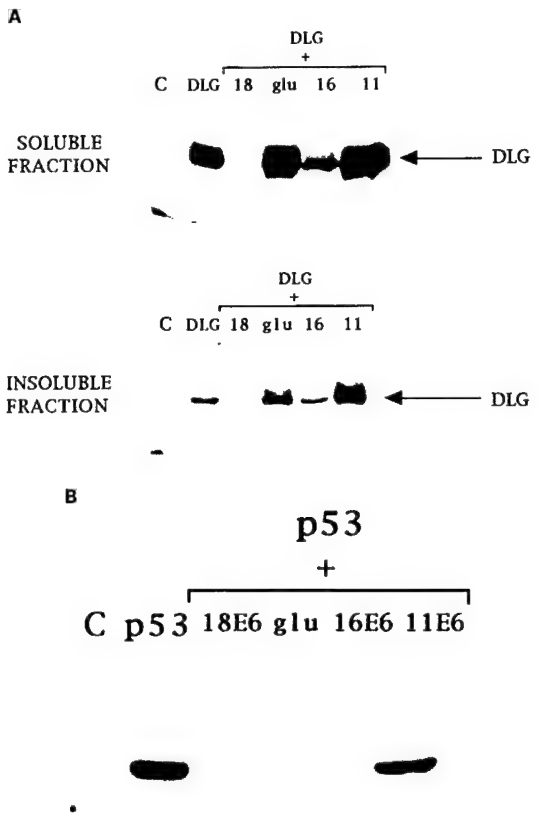

Figure 5 E6 mediated degradation of DLG *in vivo*. (**A**) 293 cells were transfected with 4 μg of HA-tagged DLG expression plasmid, in the absence (DLG) or presence of 4 μg of HPV18 E6 (18), the Thr156Glu (glu) mutant, HPV16 E6 (16) and HPV11 E6 (11). After 24 h, the proteins were extracted (soluble and insoluble fractions as indicated) and equal amounts were separated by SDS–PAGE. The levels of DLG were ascertained by Western blot analysis with anti-HA monoclonal antibody (Boehringer-Mannheim). (**B**) A parallel transfection was performed in Saos-2 cells with 4 μg of p53 expression plasmid in the absence or presence of 4 μg HPV18 E6 (18), the Thr156Glu (glu) mutant, HPV16E6 (16) and HPV11 E6 (11). After 24 h, the proteins were extracted and equal amounts were separated by SDS–PAGE. The levels of p53 were ascertained by Western blot analysis with a pool of anti-p53 monoclonal antibodies

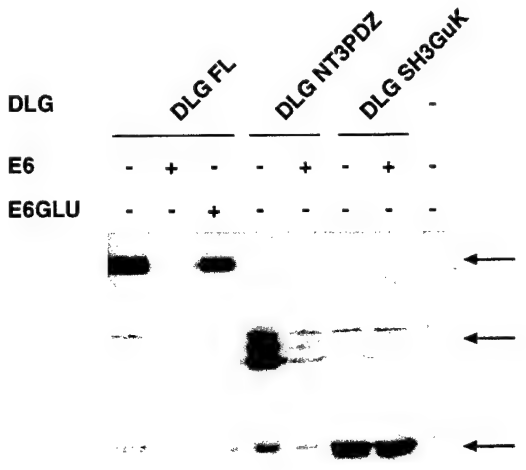

Figure 6 *In vivo* degradation comparing full-length DLG with truncated mutants. The *in vivo* degradation assay was performed as in Figure 5. All transfections contained 4 μg of the HA-tagged DLG expression plasmid and 4 μg of the indicated E6 expression plasmids. The HA-tagged proteins used are also indicated (FL indicating full length), and arrows show the position of the wild type and mutant DLG proteins. The truncated DLG mutants are described in Figure 3

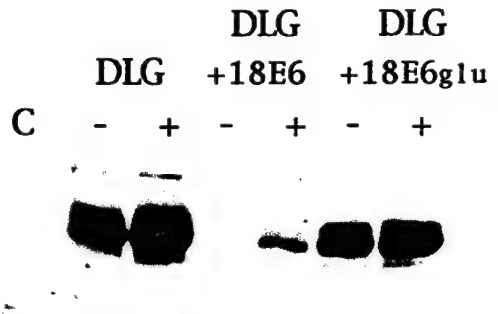

Figure 7 HPV18 E6 enhances DLG degradation via the proteasome. An *in vivo* degradation assay was performed as described for Figure 5. Cells were transfected with DLG alone (DLG) or together with either HPV18E6 (18E6) or the Thr156Glu mutant (18E6glu) and proteasome inhibitor was added to the cells 2 h before harvesting as indicated (+). Residual DLG was ascertained by Western blotting with the anti-HA antibody

and SH3 motifs but lacks the PDZ domains. Both mutants were HA-tagged and the degradation assay was performed as described above. The results shown in Figure 6 demonstrate that the levels of the DLG-NT3PDZ were reduced by wild type E6 to a level similar to that of the full length DLG (DLG FL) protein. In contrast, the levels of the DLG-SH3GuK protein, which lacks the three PDZ domains, were completely unaffected by the presence of the HPV18 E6 protein. These results demonstrate that the binding of E6 to DLG is required for the degradation of DLG *in vivo* and, in addition, that the sequences necessary and sufficient for efficient degradation of DLG by HPV18 E6 lie within the first 544 amino acid residues of the protein, encompassing the three PDZ domains.

HPV18 E6 stimulates the degradation of DLG via the proteasome pathway

To characterize the mechanism by which HPV18 E6 promotes degradation of DLG, we examined the involvement of the proteasome proteolytic pathway. An *in vivo* degradation assay was performed as described above, but the transfected cells were treated with the proteasome inhibitor (N-CBZ-LEU-LEU-LEU-AL) for 2 h before protein extraction. The levels of DLG were ascertained by Western blotting and the results obtained are shown in Figure 7. The presence of HPV18 E6 again results in a dramatic decrease in the levels of the DLG protein. Interestingly, addition of

proteasome inhibitor results in a partial restoration of DLG protein levels in the presence of HPV18 E6, indicating proteasome involvement in the E6 mediated degradation of DLG. It is interesting to note that DLG levels in the absence of E6 are also increased in the presence of the proteasome inhibitor suggesting that DLG may normally be regulated via the proteasome.

To investigate whether DLG protein levels are regulated by ubiquitination, we performed a series of *in vivo* ubiquitination assays. Cells were transfected with plasmids expressing full length DLG, and the two truncated derivatives NT3PDZ and SH3GuK. After 24 h cells were extracted under denaturing conditions and DLG proteins were detected by Western blot analysis. The results obtained are shown in Figure 8A and, as can be seen, ladders increasing as multiples of 8 kd, characteristic of ubiquitination, were detected with the full length DLG and with the NT3PDZ derivative. In contrast, the SH3GuK derivative, which was not susceptible to E6 mediated degradation did not exhibit laddering. To further confirm these observations and to show that the full length DLG protein was indeed ubiquitinated *in vivo*, cells were transfected with a 'six Histidine' tagged DLG expression plasmid together with a plasmid expressing HA tagged ubiquitin. After 24 h cells were extracted under denaturing conditions and extracts were affinity purified on Ni^{++} agarose columns as described previously (Kühne and Banks, 1998). Bound ubiqui-

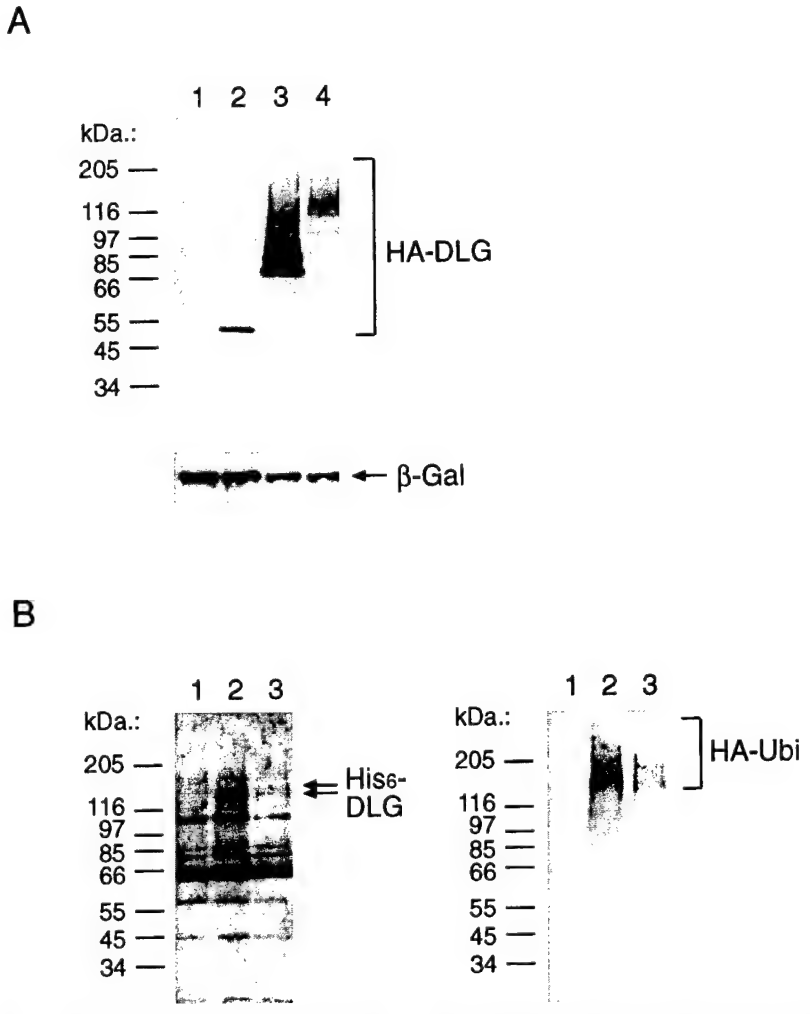

Figure 8 DLG is ubiquitinated *in vivo*. (**A**) 293 cells were transfected with HA-tagged full length DLG (lane 4) the DLGNT3PDZ derivative (lane 3) and the DLGSH3GuK derivative (lane 2) or control expression plasmid (lane 1). After 24 h cells were harvested in the presence of 2 M Guanidinium Hydrochloride and proteins analysed by Western blot with anti HA-specific monoclonal antibodies (upper panel). A plasmid expressing β-galactosidase (pCDNA3-LacZ) served as an internal transfection control and the parallel Western blot was developed with anti β-galactosidase antibodies (lower panel). (**B**) A plasmid expressing 'six Histidine' tagged DLG (pCDNAHis-DLG) was expressed in the presence of a plasmid expressing HA tagged ubiquitin (pHA-Ubi) in 293 cells. The DLG protein was affinity purified on Ni^{++} agarose under denaturing conditions. Western blots were performed with anti GST-DLG antibody (left hand panel) or anti HA antibody (right hand panel). The lanes represent cells transfected with pHA-Ubi (1), pCDNAHis-DLG and pHA-Ubi (2) and pCDNAHis-DLG, pHA-Ubi and pCDNA-18E6 (3). The positions of the His-DLG and HA-ubi ladders are indicated

tin was then assessed by Western blot analysis with the anti HA monoclonal antibody and the results obtained are shown in Figure 8B. As can be seen, in cells expressing either DLG alone, or in the presence of HPV18 E6, specific retention of high molecular weight ubiquitin ladders were obtained. These results confirm that DLG is ubiquitinated both in the absence and presence of HPV18 E6 and demonstrates that DLG levels are regulated in the cell by ubiquitination.

Discussion

The high risk HPV E6 proteins share several stretches of homology in different regions of the protein that define specific functional domains. The C-terminus is very highly conserved, and it has been shown to be involved in the binding to cellular proteins bearing PDZ domains. The conserved C-terminal motif of E6 also contains an RXXT consensus sequence for the cyclic AMP-dependent protein kinase A (PKA). We have shown that the Thr156 of HPV18 E6 is critical for the *in vitro* binding to DLG, with both neutral and acidic charge mutations abolishing binding. Interestingly, in the case of the binding of the K^+ channel protein Kir2.3 to the PDZ domain-containing protein PSD-95, it has been reported that the Ser residue at the C-terminus of Kir2.3 is vital for the interaction (Cohen *et al*., 1996). Moreover, this Ser residue on Kir2.3 is also a substrate for PKA, and phosphorylation was found to negatively regulate the association with the PSD-95 protein. Taken together, these data suggest that potential PKA phosphorylation of E6 may also negatively regulate E6 binding to DLG.

HPV E6 proteins can stimulate the ubiquitin-mediated degradation of a number of the cellular proteins to which they bind. A number of these cellular targets are tumour suppressors, and it has been proposed that the degradation of such cellular control proteins is responsible for the oncogenic activity of E6 (Scheffner *et al*., 1990; Gross-Mesilaty *et al*., 1998; Thomas and Banks, 1998; Kühne and Banks, 1998). We show, both *in vitro* and *in vivo*, that the recently reported E6 target protein, DLG, is also susceptible to enhanced degradation in the presence of HPV18 E6. The Thr156Glu E6 mutant, which fails to bind to DLG, had no effect on the stability of DLG in either assay, indicating that E6's binding to DLG is important for the stimulation of degradation.

We then extended the study to E6 proteins derived from other genital HPV types. The degradation assays showed that while HPV16 E6 could reduce DLG levels, the HPV11 E6 protein had minimal effect. The C-terminal motif of HPV16 E6, ETQL, is not identical to the consensus XTXV PDZ binding domains, although a previous report has shown that HPV16 E6 is capable of binding DLG *in vitro* and *in vivo* (Kiyono *et al*., 1997). In contrast, the C-terminus of HPV11 E6 lacks any homology with the consensus PDZ binding site, and does not bind to DLG *in vitro* (Lee *et al*., 1997). It has also been shown that a mutant of HPV16 E6 which was defective in DLG binding was also defective in rat cell transformation assays (Kiyono *et al*., 1997). Taken together, these results suggest that this activity of E6 may contribute to the process of transformation and carcinogenesis mediated by the high risk HPVs.

Previous studies have shown that among the three PDZ domains of DLG, the second PDZ domain is essential for HPV16 E6 binding (Kiyono *et al*., 1997). In contrast, we have shown that HPV18 E6 binds efficiently to each of the three isolated PDZ domains *in vitro*, although the assays used are not identical and this may account for some of the differences. However, the data suggest that the HPV16 and HPV18 E6 proteins bind DLG slightly differently, and this may be a reflection of differences in the consensus PDZ binding domains of the two proteins. The *in vivo* degradation assays would also tend to support this conclusion since HPV16 E6 is consistently weaker than HPV18 E6 in its ability to degrade DLG. It will now be interesting to determine whether this is reflected in differences in the pathology of HPV16 and HPV18, since there are a number of reports which indicate a poorer prognosis for individuals with cervical tumours harbouring HPV18 DNA rather than HPV16 DNA (Burnett *et al*., 1992; Franco, 1992; Zhang *et al*., 1995).

The *in vivo* degradation assays performed with the deletion derivatives of DLG showed that the amino terminus and the three PDZ domains are sufficient for degradation by E6. In contrast, deletion of this region renders DLG resistant to E6 mediated degradation, and demonstrates that the region of DLG which confers susceptibility to E6 mediated degradation lies within the first 544 residues of the protein.

We next investigated whether the reduction in DLG protein levels in the presence of E6 was proteasome mediated. The results demonstrated that the treatment of cells with a specific proteasome inhibitor partially stabilized DLG protein in the presence of E6. Complete protection of DLG over the time frame of the assay was never attained. Whether this is a reflection of a very high DLG turnover, low levels of DLG translation or a combination of the two, remains to be determined. We also noted that DLG levels increased following proteasome inhibition in the absence of E6 protein, indicating that DLG may be normally regulated via the proteasome. This was investigated further with a series of assays designed to determine whether DLG was indeed ubiquitinated. In the absence of E6, full length DLG and the NT3PDZ derivative were found to form high molecular weight complexes indicative of ubiquitinylation. Strikingly, the SH3GuK derivative of DLG which was not susceptible to E6 mediated degradation did not form these high molecular weight complexes. Using His tagged DLG with HA tagged ubiquitin (Treier *et al*., 1994) it was further possible to demonstrate that DLG is modified by ubiquitin both in the absence and presence of HPV18 E6 protein *in vivo*. These results enable us to conclude that DLG is indeed normally regulated through ubiquitination which implies turnover via the proteasome.

The biological significance of the degradation of DLG by E6 in natural infections can be addressed by considering the functions of DLG. DLG is expressed in epithelial cells, the natural host cells of HPV (Lue *et al*., 1994). Epithelia form sheets of polarized cells, with the apical and basolateral sides separated by tight junctions (Kim, 1997), and DLG is requried for the organization of these junctional complexes. Tight

junctions form a continuous intercellular contact and their absence is associated with defective cell-cell adhesion, a loss of cell polarity and unregulated proliferation (Anderson, 1996; Woods *et al.*, 1996). Maintenance of cell polarity is crucial for normal differentiation, and the localization of polarity signalling receptors to the basolateral membrane is apparently mediated by PDZ proteins (Woods and Bryant, 1993). Reducing the levels of DLG may contribute to a disorganization of these tightly controlled signal transduction pathways. This could lead to a loss of control of cell proliferation or to an alteration in the proper pattern of keratinocyte differentiation. Significantly, the well-characterized Dlg-A of *Drosophila* was shown to form part of a developmental pathway essential for blocking cell proliferation, invasion and migration in a defined pattern. In addition, it was found that invasive cells bearing certain Dlg-A mutations resemble malignant cells in several ways, including migratory ability (Goode and Perrimon, 1997). The fact that high risk HPV E6 proteins are able to modulate DLG abundance may also contribute to the invasiveness of cancerous cells infected by these viruses.

In summary, degradation of DLG would be expected to induce alterations in DLG dependent signal transduction pathways, leading to changes in cytoskeletal organization and cellular migration. These alterations could contribute to the transformed, undifferentiated phenotype of cells expressing high risk HPV E6 proteins.

Materials and methods

Plasmids

The E6, E7 and p53 proteins were cloned under the control of the CMV promoter into the pCDNA-3 expression plasmid. The E6 mutants were constructed using PCR directed mutagenesis. HA-tagged SAP97 expression plasmid was kindly provided by Kyung-Ok Cho and the His tagged derivative was obtained by subcloning SAP97 in frame into a 'six His' containing pCDNA-3 expression plasmid. Deleted derivatives of SAP97 were expressed from the CMV promoter in the GW1 plasmid (Kim and Sheng, 1996). pGEX-2T-SAP97 was described previously (Lee *et al.*, 1997) as was the HA-tagged ubiquitin expression plasmid (Treier *et al.*, 1994).

Cells and tissue culture

Human 293 and Saos-2 cells were grown in DMEM with 10% foetal calf serum. All the transient transfections were carried out using the calcium phosphate precipitation procedure as described previously (Matlashewski *et al.*, 1987).

GST fusion protein expression and binding assays

GST-SAP97 fusion protein purification and GST pulldown assays were performed as described previously (Thomas *et al.*, 1995). Protein blotting assays using truncated derivatives of GST-DLG fusion proteins with radiolabelled HPV18 E6 were done as described previously (Lee *et al.*, 1997).

In vitro *and* in vivo *degradation assays*

The *in vitro* degradation assays were performed as described previously (Pim *et al.*, 1994). For the *in vivo* assays cells were harvested in extraction buffer (250 mM NaCl, 0.1% NP40, 50 mM HEPES pH 7.0, 1% aprotinin) 24 h after transfection. Equal amounts of proteins were separated by SDS–PAGE and transferred to nitrocellulose. The levels of remaining HA-tagged DLG or p53 were determined by immunoblot analysis using either the anti-HA monoclonal antibody (Boehringer-Mannheim) or a pool of anti p53 monoclonal antibodies, pAb1801, 1802 and 1803 (Banks *et al.*, 1986). Blots were developed using the Amersham ECL technique according to the manufacturer's instructions. Cells were treated with the proteasome inhibitor (N-CBZ-LEU-LEU-LEU-AL, 40 μM), as indicated in the text, 2 h prior to protein extraction.

In vivo *ubiquitination assays*

Cells were transfected with His tagged DLG together with a plasmid expressing HA-tagged ubiquitin. After 24 h extracts were prepared as described previously (Kühne and Banks, 1998) and affinity purified on Ni^{++} agarose columns. Bound ubiquitin was detected by Western blot analysis with anti HA monoclonal antibodies.

Acknowledgements

The authors are grateful to Charles Lacey for valuable discussions and to Miranda Thomas and David Pim for comments on the manuscript. This work was supported in part by a research grant from the Associazione Italiana per la Ricerca sul Cancro to L Banks and Research grants from National Cancer Institute (ROI CA58541), American Cancer Society (RPG-97-668-01-VM) and the US Army (DAMD17-97-1-7082) to R Javier.

References

Anderson JM. (1996). *Curr. Biol.*, **6**, 382–384.

Banks L, Matlashewski G and Crawford L. (1986). *Eur. J. Biochem.*, **159**, 529–534.

Burnett AF, Barnes WA, Johnson JC, Grendys E, Willett GD, Barter JF and Doniger J. (1992). *Gynecol. Oncol.*, **47**, 343–347.

Chen J, Reid C, Band V and Androphy E. (1995). *Science*, **269**, 529–531.

Cohen N, Benman J, Snyder S and Bredt D. (1996). *Neuron*, **17**, 759–767.

Crook T, Tidy JA and Vousden K. (1991). *Cell*, **67**, 547–556.

Davies R, Hicks R, Crook T, Morris J and Vousden K. (1993). *J. Virol.*, **67**, 2521–2528.

Doyle D, Lee A, Lewis J, Kim E, Sheng M and MacKinnon R. (1996). *Cell*, **85**, 1067–1076.

Dyson N, Howley P, Münger K and Harlow E. (1989). *Science*, **243**, 934–937.

Franco EL. (1992). *Cancer Epid. Biom. Prev.*, **1**, 499–504.

Goode S and Perrimon N. (1997). *Genes Dev.*, **11**, 2532–2544.

Gross-Mesilaty S, Reinstein E, Bercovich B, Tobias K, Schwartz A, Kahana C and Ciechanover A. (1998). *Proc. Natl. Acad. Sci. USA*, **95**, 8058–8063.

Kim S. (1997). *Curr. Opin. Cell Biol.*, **9**, 853–859.

Kim E, Niethammer M, Rothschild A, Nung Jan Y and Sheng M. (1995). *Nature*, **378**, 85–88.

Kim E and Sheng M. (1996). *Neuropharm.*, **35**, 993–1000.

Kiyono T, Hiraiwa A, Fujita M, Hayashi Y, Akiyama T and Ishibashi M. (1997). *Proc. Natl. Acad. Sci. USA*, **94**, 11612–11616.

Kühne C and Banks L. (1998). *J. Biol. Chem.*, **273,** 34302–34309.

Lee SS, Weiss R and Javier R. (1997). *Proc. Natl. Acad. Sci. USA*, **94,** 6670–6675.

Lue R, Marfatia S, Branton D and Chishti A. (1994). *Proc. Natl. Acad. Sci. USA*, **91,** 9818–9822.

Marfatia S, Morais Cabral J, Lin L, Hough C, Bryant P, Stolz L and Chishti A. (1996). *J. Cell Biol.*, **135,** 753–766.

Matlashewski G, Schneider J, Banks L, Jones N, Murray A and Crawford L. (1987). *EMBO J.*, **6,** 1741–1746.

Muller B, Kistner U, Veh R, Cases-Langhoff C, Becker B, Gundelfinger E and Garner C. (1995). *J. Neurosci.* **15,** 2354–2366.

Münger K, Werness B, Dyson N, Phelps W, Harlow E and Howley P. (1989). *EMBO J.*, **8,** 4099–4105.

Pim D, Storey A, Thomas M, Massimi P and Banks L. (1994). *Oncogene*, **9,** 1869–1876.

Ponting C and Phillips C. (1995). *Trends Biochem. Sci.*, **20,** 102–103.

Saras J and Heldin C. (1996). *Trends Biochem. Sci.*, **21,** 455–458.

Scheffner M, Werness BA, Huibregtse JM, Levine AJ and Howley PM. (1990). *Cell*, **63,** 1129–1136.

Songyang Z, Fanning A, Fu C, Xu J, Marfatia S, Chishti A, Crompton A, Chan A, Anderson J and Cantley L. (1997). *Science*, **275,** 73–77.

Storey A, Thomas M, Kalita A, Harwood C, Gardiol D, Mantovani F, Breuer J, Leigh I, Matlashewski G and Banks L. (1998). *Nature*, **393,** 229–234.

Thomas M, Massimi P, Jenkins J and Banks L. (1995). *Oncogene*, **10,** 261–268.

Thomas M and Banks L. (1998). *Oncogene*, **17,** 2943–2954.

Tong X and Howley P. (1997). *Proc. Natl. Acad. Sci. USA*, **94,** 4412–4417.

Treier M, Staszewski LM and Bohmann D. (1994). *Cell*, **78,** 787–798.

Vousden K. (1994). *Adv. Cancer Res.*, **64,** 1–24.

Woods D and Bryant P. (1991). *Cell*, **66,** 451–464.

Woods D and Bryant P. (1993). *Mech. Dev.*, **44,** 85–89.

Woods D, Hough C, Peel D, Callaini G and Bryant P. (1996). *J. Cell Biol.*, **134,** 1469–1482.

Zhang J, Rose BR, Thompson CH, Jarrett C, Russell P, Houghton RS and Cossart YE. (1995). *Gynecol. Oncol.*, **57,** 170–177.

zur Hausen H and Schneider A. (1987). In: Salzman N and Howley PM. (eds.). *The Papovaviridae*. vol. 2. Plenum Press: New York pp. 245–263.

zur Hausen H. (1991). *Virology*, **184,** 9–13.

JOURNAL OF VIROLOGY, Oct. 2000, p. 9680–9693 Vol. 74, No. 20
0022-538X/00/$04.00+0

Multi-PDZ Domain Protein MUPP1 Is a Cellular Target for both Adenovirus E4-ORF1 and High-Risk Papillomavirus Type 18 E6 Oncoproteins

SIU SYLVIA LEE,[1] BRITT GLAUNSINGER,[1] FIAMMA MANTOVANI,[2] LAWRENCE BANKS,[2] AND RONALD T. JAVIER[1]*

Department of Molecular Virology and Microbiology, Baylor College of Medicine, Houston, Texas 77030,[1] and International Center for Genetic Engineering and Biotechnology, I-34012 Trieste, Italy[2]

Received 10 April 2000/Accepted 13 July 2000

A general theme that has emerged from studies of DNA tumor viruses is that otherwise unrelated oncoproteins encoded by these viruses often target the same important cellular factors. Major oncogenic determinants for human adenovirus type 9 (Ad9) and high-risk human papillomaviruses (HPV) are the E4-ORF1 and E6 oncoproteins, respectively, and although otherwise unrelated, both of these viral proteins possess a functional PDZ domain-binding motif that is essential for their transforming activity and for binding to the PDZ domain-containing and putative tumor suppressor protein DLG. We report here that the PDZ domain-binding motifs of Ad9 E4-ORF1 and high-risk HPV-18 E6 also mediate binding to the widely expressed cellular factor MUPP1, a large multi-PDZ domain protein predicted to function as an adapter in signal transduction. With regard to the consequences of these interactions in cells, we showed that Ad9 E4-ORF1 aberrantly sequesters MUPP1 within the cytoplasm of cells whereas HPV-18 E6 targets this cellular protein for degradation. These effects were specific because mutant viral proteins unable to bind MUPP1 lack these activities. From these results, we propose that the multi-PDZ domain protein MUPP1 is involved in negatively regulating cellular proliferation and that the transforming activities of two different viral oncoproteins depend, in part, on their ability to inactivate this cellular factor.

Human adenovirus type 9 (Ad9) is a unique oncogenic virus that generates estrogen-dependent mammary tumors in rats (22). Whereas the viral E1A and E1B oncoproteins are responsible for tumorigenesis by most human adenoviruses (44), the primary oncogenic determinant for Ad9 is its E4-ORF1 (9ORF1) transforming protein (21, 23, 52, 59). Mutational analyses of the 125-amino-acid (aa) 9ORF1 protein implicate three separate regions (regions I, II, and III) as being critical for transformation (56). Although the activities associated with regions I and II have not been determined, region III at the extreme carboxyl terminus of 9ORF1 mediates interactions with multiple cellular polypeptides (p220, p180, p160, p155, and p140/p130) (57). This carboxyl-terminal 9ORF1 domain was recently discovered to define a functional PDZ domain-binding motif (28) and, consistent with this finding, 9ORF1-associated protein p140/130 was identified as the cellular PDZ protein DLG (28), a mammalian homolog of the *Drosophila* discs large tumor suppressor protein dlg-A (29, 33).

In humans, infections with human T-cell leukemia virus type 1 and high-risk human papillomaviruses (HPV) are associated with the development of adult T-cell leukemia and cervical carcinoma, respectively (5, 43). Finding a functional PDZ domain-binding motif at the carboxyl terminus of 9ORF1 subsequently led us to discover that human T-cell leukemia virus type 1 Tax and high-risk but not low-risk HPV E6 oncoproteins possess similar binding motifs at their carboxyl termini and, in addition, bind DLG (28). Although it is well established that transformation by high-risk HPV E6 proteins depends in part on an ability to target the tumor suppressor protein p53 for degradation (42), other E6 functions are also known to be important (27, 38, 47). In this regard, high-risk HPV-16 E6 mutant proteins having a disrupted PDZ domain-binding motif lose the capacity to oncogenically transform rat 3Y1 fibroblasts (26). Moreover, we recently showed that high-risk HPV E6 proteins target the PDZ protein DLG for degradation in cells (11). Therefore, a common ability of several different human virus oncoproteins to complex with cellular PDZ domain proteins probably contributes to their transforming potentials.

PDZ domains are approximately 80-aa modular units that mediate protein-protein interactions (6, 7). PDZ domain-containing proteins represent a diverse family of polypeptides that contain single or multiple PDZ domains, other types of protein-protein interaction modules including SH3, WW, PTB or pleckstrin homology domains, and protein kinase or phosphatase domains (35, 40). Consistent with such domain structures, many PDZ proteins play a role in signal transduction. In this capacity, these cellular factors serve to localize receptors and cytosolic signaling proteins to specialized membrane sites in cells and, in addition, to act as scaffolding proteins to organize these cellular targets into large supramolecular complexes (6, 8, 37). The PDZ domains of these cellular factors typically recognize specific peptide sequence motifs located at the extreme carboxyl termini of their target proteins (48), although PDZ domains can also mediate other types of protein interactions (3, 30, 63). To date, three different types of carboxyl-terminal PDZ domain-binding motifs have been identified (31, 48, 50), and at their extreme carboxyl-termini, the Ad 9ORF1, HTLV-1 Tax, and high-risk HPV E6 oncoproteins possess a type I binding motif with the consensus sequence -(S/T)-X-(V/I/L)-COOH (where X is any residue) (28).

Although our findings (28, 56, 57) and those of others (26) suggest that DLG is an important cellular target for transformation by both human Ad E4-ORF1 and high-risk HPV E6

* Corresponding author. Mailing address: Department of Molecular Virology and Microbiology, Baylor College of Medicine, One Baylor Plaza, Houston, TX 77030. Phone: (713) 798-3898. Fax: (713) 798-3586. E-mail: rjavier@bcm.tmc.edu.

oncoproteins, our previous results with the 9ORF1 protein also argue for the existence of additional important cellular PDZ protein targets. Specifically, disruption of the 9ORF1 PDZ domain-binding motif abolishes the interaction of 9ORF1 with DLG, as well as with several other unidentified cellular proteins (p220, p180, p160, and p155) (57). Consistent with this observation, we now report that the 9ORF1-associated protein p220 is the multi-PDZ domain protein MUPP1 (55) and that 9ORF1 abnormally sequesters this cellular factor within the cytoplasm of cells. We further show that the high-risk HPV-18 E6 (18E6) oncoprotein likewise complexes with MUPP1 but instead targets this cellular factor for degradation in cells. These findings suggest that the transforming potentials of the human Ad E4-ORF1 and 18E6 proteins depend on their ability to block the function of MUPP1, a large multi-PDZ domain protein predicted to function as a scaffolding factor in cell signaling.

MATERIALS AND METHODS

Cells. NIH 3T3 (20), CREF (9), COS7 (13), TE85 (32), and 293 (14) cell lines, as well as the Ad9-induced rat mammary tumor cell line 20-8, were maintained in culture medium (Dulbecco's modified Eagle's medium supplemented with 10% fetal bovine serum) under a 5% CO_2 atmosphere in a humidified incubator at 37°C. CREF cell pools (group 16) stably expressing wild-type or mutant 9ORF1 protein (56) and a CREF cell pool stably expressing an influenza virus hemagglutinin (HA) epitope-tagged 9ORF1 protein (58) were maintained in culture medium supplemented with G418 (Gibco BRL).

Plasmids. The partial murine 9BP-1 cDNA (28) encoding the carboxyl-terminal 526 aa of 9BP-1 was inserted between the *Bam*HI and *Hin*dIII sites of plasmid pQE9 (Qiagen) to make plasmid pQE9-9BP1-CT526. The full-length rat MUPP1 cDNA from pBSK-MUPP1 (55) was introduced between either the *Sac*II and *Eco*RV sites of plasmid pSL301 (Invitrogen) or the *Hin*dIII and *Eco*RI sites of cytomegalovirus expression plasmid GW1 (British Biotechnology) to create plasmid pSL301-MUPP1 or GW1-MUPP1, respectively. Plasmid GW1-HAMUPP1 was derived from GW1-MUPP1 by introducing an HA epitope tag at the amino terminus of MUPP1 by PCR methods. Plasmids GW1-HAMUPP1ΔPDZ7, GW1-HAMUPP1ΔPDZ10, and GW1-HAMUPP1ΔPDZ7/10 were derived from GW1-HAMUPP1 by deletion of MUPP1 sequences coding for either PDZ7 (aa 1166 to 1232) or PDZ10 (aa 1616 to 1656) or both of these PDZ domains, respectively, by PCR methods.

Plasmids GW1-9ORF1wt, GW1-9ORF1IIIA, GW1-9ORF1IIIC, GW1-9ORF1IIID, and GW1-18E6 contain the respective wild-type or mutant 9ORF1 (56) or wild-type 18E6 gene inserted between the *Hin*dIII and *Eco*RI sites of plasmid GW1. The wild-type 18E6 cDNA was also introduced between the *Hin*dIII and *Eco*RI sites of plasmid pSP64 (Promega) to make plasmid pSP64-18E6. Substitution of 18E6 valine residue 158 with alanine (18E6-V158A) or of threonine and valine residues 156 and 158 with aspartic acid and alanine (18E6-T156D/V158A), as well as introduction of an HA epitope tag at the amino termini of 18E6, HPV-11 E6 (11E6), rat DLG (33), and human ZO-1 (61) proteins, was accomplished by PCR methods. Altered E6 and DLG cDNAs were introduced between the *Hin*dIII and *Eco*RI sites of plasmid GW1 to make plasmids GW1-HA18E6, GW1-HA18E6-V158A, GW1-HA18E6-T156D/V158A, GW1-HA11E6, and GW1-HADLG, whereas the HAZO-1 cDNA was inserted between the *Kpn*I and *Bgl*II sites of plasmid GW1 to make plasmid GW1-HAZO-1. Plasmids pcDNA3-DLG and pSP64-p53 were described previously (11, 36).

For the construction of glutathione *S*-transferase (GST) fusion protein expression plasmids, cDNA sequences coding for 9BP1-US9/10 (aa 179 to 251), MUPP1-NT (aa 1 to 123), MUPP1-PDZ1–3 (aa 118 to 504), MUPP1-PDZ4-5 (aa 489 to 785), MUPP1-US5/6 (aa 780 to 990), MUPP1-PDZ6 (aa 985 to 1110), MUPP1-PDZ7 (aa 1105 to 1312), MUPP1-PDZ8–9 (aa 1307 to 1611), MUPP1-PDZ10 (aa 1606 to 1706), MUPP1-PDZ11 (aa 1701 to 1830), MUPP1-PDZ12–13 (aa 1825 to 2054), 18E6-V158A, and 18E6-T156D/V158A were PCR amplified and introduced in frame with the GST gene of plasmid pGEX-2T or pGEX-4T-1 (Pharmacia). pGEX-2T plasmids containing wild-type or mutant E4-ORF1 genes have been described previously (57). pGEX-2T plasmids containing wild-type 18E6 and 11E6 cDNAs were kindly provided by P. Howley.

PCR amplifications were performed with *pfu* polymerase (Stratagene), and plasmids were verified by restriction enzyme and limited sequence analyses.

Lambda phage cDNA library screening. A DNA fragment from the 9BP-1 cDNA (nucleotides 134 to 544) (28) was radiolabeled by the random-priming method (51) and used to screen a mouse pancreatic cell λgt11 cDNA library, kindly provided by S. Tsai, by standard methods (49).

Antisera and antibodies. The His_6-tagged 9BP1-CT526, GST-9BP1-US9/10, and GST-MUPP1-US5/6 fusion proteins were expressed in bacteria and purified with either Ni-nitrilotriacetic acid agarose (Qiagen) or glutathione beads (Pharmacia) (46), as recommended by the manufacturers. Rabbits were immunized with purified 9BP1-CT526 or MUPP1-US5/6 fusion proteins to generate polyclonal antisera by standard methods (17). The purified GST-9BP1-US9/10 fusion protein was covalently linked to Affi-Gel 10 beads (Bio-Rad) and used to affinity purify 9BP-1 antibodies by standard methods (17). Commercially available HA (12CA5) monoclonal antibodies (BABCO), horseradish peroxidase-conjugated goat anti-rabbit immunoglobulin G (IgG) or goat anti-mouse IgG antibodies (Southern Biotechnology Associates), fluorescein isothiocyanate-conjugated goat anti-rabbit IgG (Gibco BRL), and Texas red-conjugated goat anti-mouse IgG antibodies (Molecular Probes, Eugene, Oreg.) were utilized. p53, DLG, and 9ORF1 antisera were described previously (1, 11, 23).

Transfections and cell extracts. COS7 cells were transfected with Lipofectin or Lipofectamine (Gibco BRL) as recommended by the manufacturer and harvested 48 h posttransfection. For preparation of cell extracts, cells were washed with ice-cold phosphate-buffered saline (4.3 mM Na_2HPO_4, 1.4 mM KH_2PO_4, 137 mM NaCl, 2.7 mM KCl) and either lysed in sample buffer (0.065 M Tris-HCl [pH 6.8], 2% [wt/vol] sodium dodecyl sulfate (SDS), 10% [vol/vol] β-mercaptoethanol, 0.005% bromophenol blue) and boiled immediately or lysed for 10 min on ice in RIPA buffer (50 mM Tris-HCl [pH 8.0], 150 mM NaCl, 1% [vol/vol] Nonidet P-40, 0.5% [wt/vol] sodium deoxycholate, 0.1% [wt/vol] SDS) containing protease inhibitors (300 μg of phenylmethylsulfonyl fluoride per ml, 6 μg each of aprotinin and leupeptin per ml) and phosphatase inhibitors (50 mM NaF, 0.1 mM Na_3VO_4) and cleared by centrifugation (14,000 × *g* for 20 min at 4°C). Protein concentrations of cell extracts were determined by the Bradford method (45). For crude cell fractionation assays, the pellet recovered after centrifugation of RIPA buffer-lysed cells was solubilized in sample buffer using an equivalent volume to that originally used to lyse the cells in RIPA buffer.

GST pulldown, immunoprecipitation, and immunoblot assays. For both GST pulldown and immunoprecipitation assays, glutathione- or protein A-Sepharose beads (Pharmacia) bound to GST fusion proteins or antibodies, respectively, were incubated with cell extracts in RIPA buffer (3 h at 4°C), washed extensively with RIPA buffer, and boiled in sample buffer. Recovered proteins were separated by SDS-polyacrylamide gel electrophoresis (PAGE). For each GST pulldown reaction, 5 μg of each GST fusion protein was used and verified in each experiment by staining relevant portions of the protein gel with Coomassie brilliant blue dye. Each immunoprecipitation reaction was carried out with 1 or 12 μg of p53 or HA antibodies, respectively, 1 μl of DLG antiserum, or 5 μl of either 9ORF1, 9BP-1, or MUPP1 antiserum or the corresponding matched preimmune serum.

For immunoblot assays, proteins separated by SDS-PAGE were electrotransferred to a polyvinylidene difluoride membrane, which was incubated for 1 h with blocking buffer, consisting of TBST (50 mM Tris-HCl [pH 7.5], 200 mM NaCl, 0.2% [vol/vol] Tween 20) containing 5% nonfat dry milk, for 2 h with the appropriate primary antiserum or antibody (1:5,000 dilution of either 9ORF1, 9BP-1, or MUPP1 antiserum or 1.2 μg of HA antibodies per ml), and then for 1 h with horseradish peroxidase-conjugated goat anti-rabbit IgG or goat anti-mouse IgG secondary antibodies (1:5,000). Antibodies were diluted in TBST containing 0.5% nonfat dry milk, and incubations were performed at room temperature. After extensive washes in TBST buffer, the membranes were developed by enhanced chemiluminescence methods (Pierce).

Protein-blotting assays. Protein-blotting assays and preparation of ^{32}P-radiolabeled 9ORF1 fusion protein probes were performed as described previously (57). Briefly, MUPP1 fusion proteins were separated by SDS-PAGE and electrotransferred to a polyvinylidene difluoride membrane. The membranes were incubated with blocking buffer and then for 12 h at 4°C with the ^{32}P-labeled GST-9ORF1 protein probe (5×10^5 cpm/ml) in TBST, washed extensively with RIPA buffer, and developed by autoradiography.

In vitro translation and degradation assays. pcDNA3-DLG, pSP64-p53, pSL301-MUPP1, or pSP64-18E6 was transcribed and translated in vitro using the TNT-coupled rabbit reticulocyte system (Promega) and 10 μCi of [^{35}S]cysteine (1,000 Ci/mmol) (Amersham), as specified by Promega. In vitro degradation assays were performed as described previously (11). Briefly, the specified in vitro translation reaction mixtures were mixed and incubated at 30°C for the indicated times and proteins were immunoprecipitated, separated by SDS-PAGE, and detected by autoradiography.

Pulse-chase labeling of cell proteins. Transfected COS7 cells were preincubated for 30 min in culture medium lacking methionine and cysteine, metabolically labeled for 10 min with 0.4 mCi of EXPRE^{35}S^{35}S [^{35}S]protein-labeling mix (New England Nuclear) in 1.5 ml of culture medium lacking methionine and cysteine, and chased with culture medium containing excess unlabeled methionine (15 mg/liter) (2). At various times postchase, cells were harvested and lysed in RIPA buffer and cell proteins were immunoprecipitated with HA antibodies, separated by SDS-PAGE, and developed by autoradiography. The amount of radioactivity present within each protein band of interest was quantified using a Storm Molecular Dynamics PhosphorImager.

IF microscopy. Indirect-immunofluorescence (IF) microscopy assays were performed by standard methods (17). Cells were grown on glass coverslips, fixed in methanol for 20 min at −20°C, blocked with IF buffer (TBS [50 mM Tris-HCl, pH 7.5, 200 mM NaCl] containing 10% goat serum), and reacted first with either preimmune serum or MUPP1 antiserum (1:500) and then with fluorescein isothiocyanate-conjugated goat anti-rabbit IgG secondary antibodies (1:250) (Gibco BRL). For double-labeling IF experiments, cells on coverslips were incubated

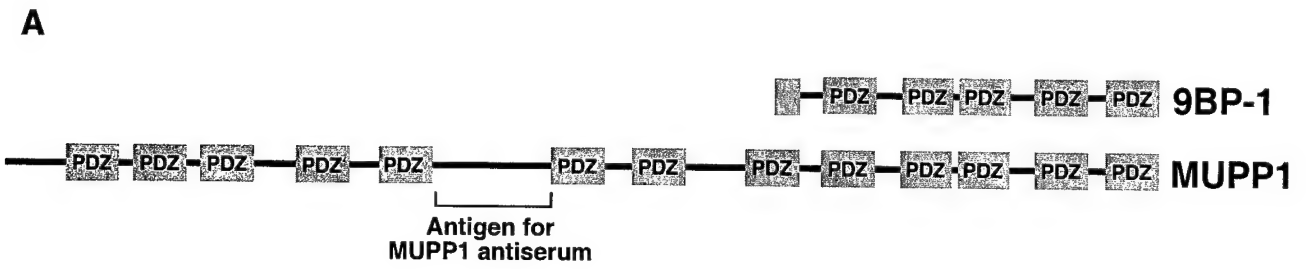

B

```
9BP-1     1 IDPTGAAGRDGRLQIADELLEINGQILYGRSHQNASSIIKCAPSKVKIIFIRNADAVNQTAVCPGIAADSPSSTSDSPQN 80
            :::::::::::::::::::::::::::::::::::::::::::::::::::::::::::: ::::::::::::::::::::
MUPP1  1368 IDPTGAAGRDGRLQIADELLEINGQILYGRSHQNASSIIKCAPSKVKIIFIRNADAVNQMAVCPGIAADSPSSTSDSPQN 1447

9BP-1    81 KEVEPCSTTSASAADLSSLTDVYQLELPKDQGGLGIAICEEVTINGVMIESLTEHGGAAKDGRLKPGDHILAVDDEVVAG 160
            :::::::::::::::::::::::::::::::::::::::: :::::::::::::::::::::::::::::::::::::::
MUPP1  1448 KEVEPCSTTSASAADLSSLTDVYQLELPKDQGGLGIAICEEDTINGVMIESLTEHGGAAKDGRLKPGDHILAVDDEVVAG 1527

9BP-1   161 CPVEKFISLLKTAKATVKLIVRAENPACPAVPSSAVTVSGERKDNSQTPAVPAPDLEPIPSTSRSSTPAVFASDPATCPI 240
            :::::::::::::::::::: :::::::::::::::::::::::::::::::::::: ::::::::::::::::::::
MUPP1  1528 CPVEKFISLLKTAKATVKLTVRAENPACPAVPSSAVTVSGERKDNSQTPAVPAPDLEPIPSPSRSSTPAVFASDPATCPI 1607

9BP-1   241 IPGCETTIEISKGQTGLGLSIVGGSDTLLGAIIIHEVYEEGAACKDGRLWAGDQILEVNGIDLRKATHDEAINVLRQTPQ 320
            ::::::::::::::::::::::::::::::::::::::::::::::::::::::::::::::::::::::::::::::::
MUPP1  1608 IPGCETTIEISKGQTGLGLSIVGGSDTLLGAIIIHEVYEEGAACKDGRLWAGDQILEVNGIDLRKATHDEAINVLRQTPQ 1687

9BP-1   321 RVRLTLYRDEAPYKEEDVCDTFTIELQKRPGKGLGLSIVGKRNDTGVFVSDIVKGGIADADGRLMQGDQILMVNGEDVRH 400
            ::::::::::::::::::::::::::::::::::::::::::::::::::::::::::::::::::::::::::::::::
MUPP1  1688 RVRLTLYRDEAPYKEEDVCDTFTIELQKRPGKGLGLSIVGKRNDTGVFVSDIVKGGIADADGRLMQGDQILMVNGEDVRH 1767

9BP-1   401 ATQEAVAALLKCSLGAVTLEVGRVKAAPFHSERRPSQSSQVSESSLSSFTPPLSGINTSESLESNSKKNALASEIQRLRT 480
            :::::::::::::::::::::::::::::::::::::::::::::::::::::::::::::::::::::::: :::
MUPP1  1768 ATQEAVAALLKCSLGAVTLEVGRVKAAPFHSERRPSQSSQVSESSLSSFTPPLSGINTSESLESNSKKNALASEIQGLRT 1847

9BP-1   481 VEIKKGPADSLGLSIAGGVGSPLGDVPIFIAMMHPNGVAAQTQKLRVGDRIVTICGTSTDGMTHTQAVNLMKNASGSIEV 560
            ::::::::::::::::::::::::::::::::::::::::::::::::::::::::::::::::::::::::::::::::
MUPP1  1848 VEIKKGPADSLGLSIAGGVGSPLGDVPIFIAMMHPNGVAAQTQKLRVGDRIVTICGTSTDGMTHTQAVNLMKNASGSIEV 1927

9BP-1   561 QVVAGGDVSVVTGHQQELANPCLAFTGLTSSSIFPDDLGPPQSKTITLDRGPDGLGFSIVGGYGSPHGDLPIYVKTVFAK 640
            :::::::::::::::::::::::::::::::::::::::: :::::::::::::::::.:::::::::::::::::::::
MUPP1  1928 QVVAGGDVSVVTGHQQELANPCLAFTGLTSSSIFPDDLGPSQSKTITLDRGPDGLSFNIVGGYGSPHGDLPIYVKTVFAK 2007

9BP-1   641 GAAAEDGRLKRGDQIIAVNGQSLEGVTHEEAVAILKRTKGTVTLMVLS 688
            :::::::::::::::::::::::::::::::::::::::::::::::::
MUPP1  2008 GAAAEDGRLKRGDQIIAVNGQSLEGVTHEEAVAILKRTKGTVTLMVLS 2055
```

FIG. 1. The partial mouse protein 9BP-1 represents the carboxyl terminus of the mouse multi-PDZ protein MUPP1. (A) PDZ domain organizations of the partial mouse protein 9BP-1 (688 aa) and the mouse multi-PDZ domain protein MUPP1 (2,055 aa). Note that the domain organization of 9BP-1 is identical to that of the carboxyl-terminal region of MUPP1. The unique protein region used to generate MUPP1 antisera is indicated. (B) The partial mouse protein 9BP-1 exhibits 99% amino acid sequence identity to the carboxyl-terminal region of the mouse MUPP1 protein (aa 1368 to 2055). Highlighted sequences denote PDZ homology domains. Sequence alignment was performed using the Align Global Sequence Alignment algorithm from the Baylor College of Medicine Search Launcher Web site.

with both MUPP1 antiserum (1:500) and HA monoclonal antibodies (66 μg/ml) and then with both fluorescein isothiocyanate-conjugated goat anti-rabbit IgG (1:250) (Gibco BRL) and Texas red-conjugated goat anti-mouse IgG secondary antibodies (1:300) (Molecular Probes). All antibodies were diluted in IF buffer, and incubations were performed at 37°C. Coverslips with attached cells were rinsed briefly in a 0.5 mg of 4′,6-diamidino-2-phenylindole (DAPI) solution per ml to stain nuclei and affixed to slides with mounting medium (VectorShield). Images were collected with a Zeiss Axiophot fluorescence microscope and digitally processed using Adobe PhotoShop software.

Sequence alignment. Pairwise sequence alignments were performed using the Align algorithm of the BCM Search Launcher web browser (http://dot.imgen.bcm.tmc.edu:9331/seq-search/alignment.html). Mouse, rat, and human MUPP1 sequences (accession numbers AJ131869, AJ001320, and AJ001319, respectively) were obtained from GenBank.

RESULTS

9BP-1 and 9ORF1-associated protein p220 have similar characteristics. By screening λgt11 cDNA expression libraries with a 9ORF1 protein probe, we previously isolated a partial cDNA coding for the carboxyl-terminal 526 aa of the novel mouse multi-PDZ domain protein 9BP-1 (28). Subsequent rescreening of the same λgt11 library with a 9BP-1 DNA probe led to the isolation of a cDNA coding for a larger partial carboxyl-terminal 688-aa 9BP-1 polypeptide that contains five PDZ homology domains (Fig. 1A).

To assess initially whether 9BP-1 may represent one of the

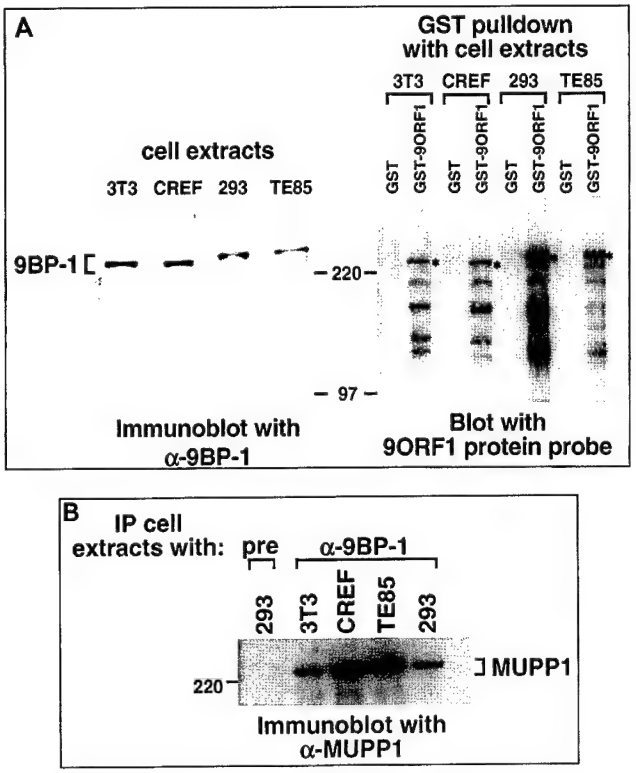

FIG. 2. 9ORF1-associated protein p220 displays similar properties to both 9BP-1 and MUPP1. (A) 9BP-1 and 9ORF1-associated protein p220 comigrate and exhibit identical species-specific gel mobilities. Proteins from RIPA buffer-lysed mouse NIH 3T3, rat CREF, human 293, and human TE85 cell lines were either immunoblotted with 9BP-1 antiserum (left) or first subjected to a GST pulldown assay with the indicated fusion protein and then blotted with a radiolabeled 9ORF1 protein probe (right). For the experiment shown in the left or right panel, 100 or 2.5 mg of cell proteins was used, respectively, and the protein gels were run in parallel. Asterisks indicate 9ORF1-associated protein p220. (B) MUPP1 antiserum cross-reacts with 9BP-1 protein derived from several different species. Cell proteins (2.5 mg) in RIPA buffer from the indicated cell lines were first immunoprecipitated (IP) with either 9BP-1 antiserum (α-9BP-1) or the matched preimmune serum (pre) and then immunoblotted with MUPP1 antiserum. Also note that the 9BP-1 protein detected in panel A (left) and the MUPP1 protein detected here exhibited identical species-specific gel mobilities.

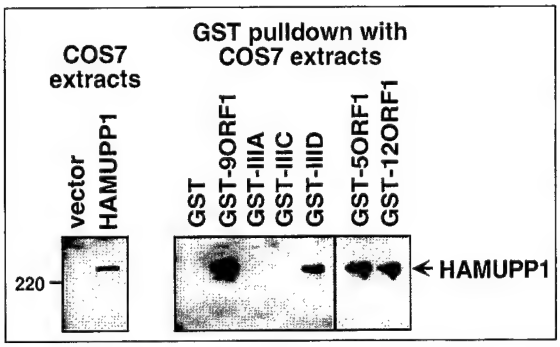

FIG. 3. 9ORF1 binds MUPP1 in vitro. GST-9ORF1 binds HA epitope-tagged rat MUPP1 protein (HAMUPP1) expressed in COS7 cells. Cells were lipofected with 4 μg of either empty GW1 plasmid (vector) or GW1-HAMUPP1 plasmid, and cell proteins in RIPA buffer were either immunoblotted with HA antibodies (left) or first subjected to a GST pulldown assay with the indicated wild-type or mutant E4-ORF1 fusion protein (Table 1) and then immunoblotted with HA antibodies (right). COS7 cell proteins at 100 μg or 1 mg were used in the experiment shown in the left and right panels, respectively.

unidentified 9ORF1-associated cellular proteins (p220, p180, p160, or p155), we raised polyclonal antisera to the carboxyl-terminal 526 aa of this partial polypeptide (28). By immunoblot analysis, two independent 9BP-1 antisera specifically recognized an approximately 250-kDa protein which, in cell lines derived from various species, exhibited slightly different gel mobilities (Fig. 2A and data not shown). The latter observation presumably reflects species-specific differences for this polypeptide. More important, 9BP-1 was found to be complexed with 9ORF1 in lysates of 9ORF1-expressing cells (see below; data not shown). Additionally, comparison of the gel mobility of 9BP-1 with that of each 9ORF1-associated protein showed that 9BP-1 and 9ORF1-associated protein p220 comigrate and exhibit identical species-specific gel mobilities (Fig. 2A), suggesting that these proteins are the same.

9BP-1 is the multi-PDZ domain protein MUPP1. From BLAST searches of protein sequence databases, we subsequently found that the partial mouse 9BP-1 polypeptide exhibits 99% amino acid sequence identity to the carboxyl-terminal region of the 2,055-aa mouse multi-PDZ domain protein MUPP1 (Fig. 1), as well as 94 or 82% amino acid sequence identity to the carboxyl-terminal region of rat MUPP1 (2,054 aa) or human MUPP1 (2,042 aa), respectively (data not shown). MUPP1 is a widely expressed polypeptide, containing 13 PDZ domains and no other recognizable protein motifs, and was isolated by virtue of its ability to bind the cytoplasmic domain of the 5-HT_{2C} serotonin receptor in yeast two-hybrid screens (55).

To confirm that 9BP-1 and MUPP1 are indeed the same polypeptide, we generated polyclonal antisera to a unique 210-aa rat MUPP1 region that lies between PDZ5 and PDZ6 and that lacks sequence similarity to other known proteins (Fig. 1A). As with the 9BP-1 antisera, these MUPP1 antisera specifically recognized an approximately 250-kDa cellular protein in cell lysates (data not shown) and, in addition, cross-reacted with 9BP-1 protein immunoprecipitated from human, rat, and mouse cell lines (Fig. 2B).

9ORF1 binds MUPP1. We utilized GST pulldown assays to show that the wild-type 9ORF1 protein can bind to MUPP1. In these assays, we found that the GST-9ORF1 fusion protein bound both to HA epitope-tagged rat MUPP1 (HAMUPP1)

TABLE 1. Carboxyl-terminal amino acid sequences of human Ad E4-ORF1 and HPV E6 proteins[a]

Protein[b]	Carboxyl-terminal amino acid sequence with respect to the consensus type I PDZ domain-binding motif[c]:			
	X	(S/T)	X	(V/I/L)-COOH
wt 9ORF1	A	T	L	V
IIIA 9ORF1	A	**P**		
IIIC 9ORF1	**D**	T	L	V
IIID 9ORF1	A	T	**P**	V
wt 5ORF1	A	S	N	V
wt 12ORF1	A	S	L	**I**
wt 18E6	E	T	Q	V
18E6-V158A	E	T	Q	**A**
18E6-T156D/V158A	E	**D**	Q	**A**
wt 11E6	D	L	L	P

[a] The sequence of the last 4 aa at the carboxyl terminus of E4-ORF1 proteins from Ad9 (9ORF1), Ad5 (5ORF1), and Ad12 (12ORF1) and the HPV-18 E6 (18E6) protein define a consensus type I PDZ domain-binding motif, whereas the HPV-11 E6 (11E6) protein lacks such a motif. Also shown are 9ORF1 and 18E6 mutant proteins having altered or disrupted PDZ domain-binding motifs.

[b] wt, wild type.

[c] Substitution mutations are depicted as bold amino acid residues.

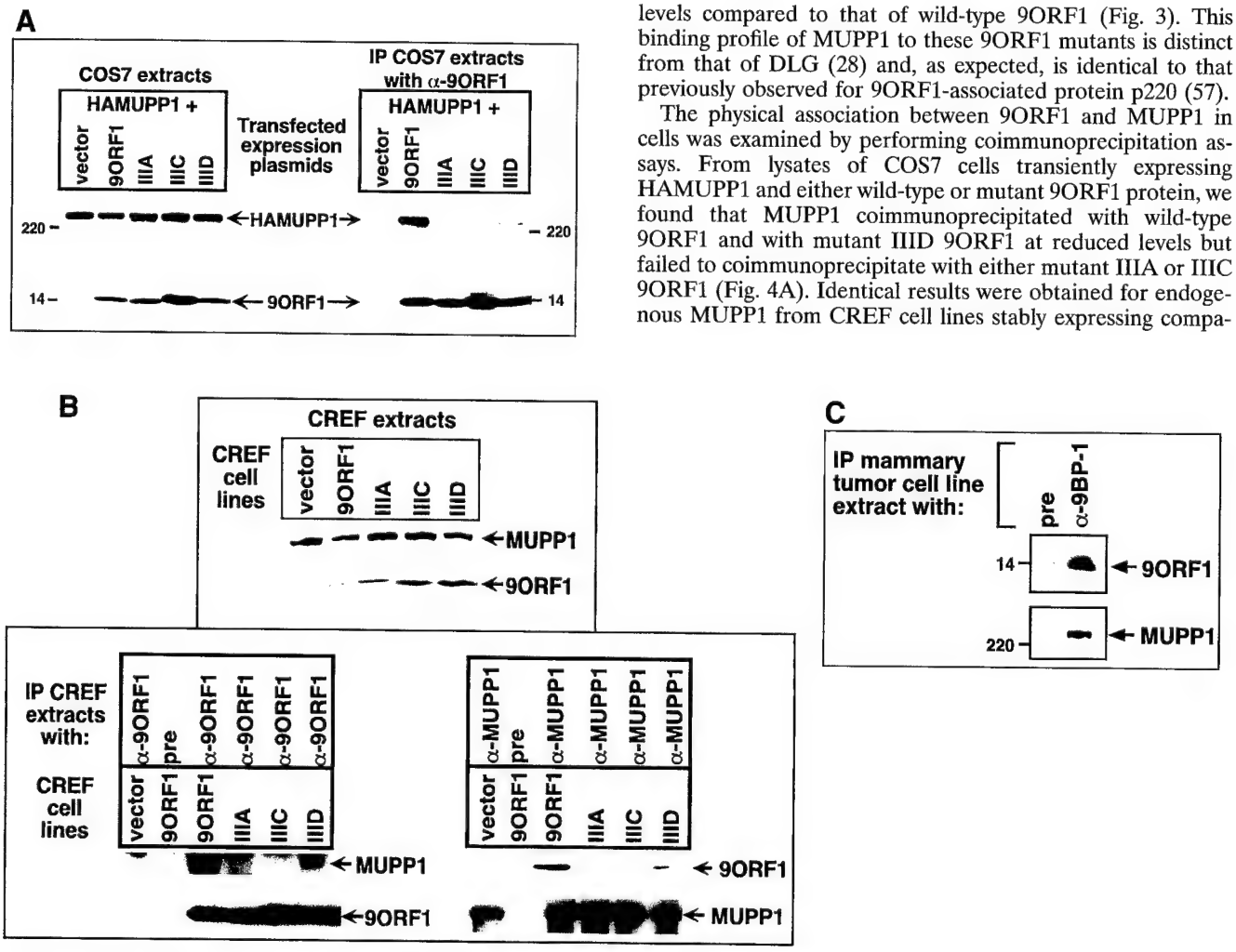

FIG. 4. 9ORF1 complexes with MUPP1 in cells. (A) 9ORF1 complexes with HA epitope-tagged rat MUPP1 protein (HAMUPP1) expressed in COS7 cells. Cells were lipofected with 6 μg of GW1-HAMUPP1 plasmid and 2 μg of either empty GW1 plasmid (vector) or a GW1 plasmid expressing wild-type or the indicated mutant 9ORF1 protein. Cell proteins in RIPA buffer were either immunoblotted with HA antibodies or 9ORF1 antiserum (left) or first immunoprecipitated (IP) with 9ORF1 antiserum (α-9ORF1) and then immunoblotted with HA antibodies or 9ORF1 antiserum (right). Cell proteins at 100 or 800 μg were used in the experiment shown in the left and right panels, respectively. (B) 9ORF1 complexes with endogenous MUPP1 of CREF cells. Cell proteins in RIPA buffer were either immunoblotted with MUPP1 or 9ORF1 antiserum (top) or first immunoprecipitated (IP) with 9ORF1 antiserum or the matched preimmune serum (pre) (bottom left) or, alternatively, with either MUPP1 antiserum (α-MUPP1) or the matched preimmune serum (pre) (bottom right) and then immunoblotted with either MUPP1 or 9ORF1 antiserum. CREF cell proteins at 100 μg, 3 mg, and 3 mg were used in the experiments in the top, bottom left, and bottom right panels, respectively. (C) 9ORF1 complexes with MUPP1 in the Ad9-induced rat mammary tumor cell line 20-8. This tumor cell line contains a single integrated copy of the entire Ad9 genome (unpublished results). Cell proteins (3 mg) in RIPA buffer were first immunoprecipitated (IP) with either 9BP-1 antiserum (α-9BP-1) or the matched preimmune serum and then immunoblotted with either 9ORF1 or 9BP-1 antiserum.

levels compared to that of wild-type 9ORF1 (Fig. 3). This binding profile of MUPP1 to these 9ORF1 mutants is distinct from that of DLG (28) and, as expected, is identical to that previously observed for 9ORF1-associated protein p220 (57).

The physical association between 9ORF1 and MUPP1 in cells was examined by performing coimmunoprecipitation assays. From lysates of COS7 cells transiently expressing HAMUPP1 and either wild-type or mutant 9ORF1 protein, we found that MUPP1 coimmunoprecipitated with wild-type 9ORF1 and with mutant IIID 9ORF1 at reduced levels but failed to coimmunoprecipitate with either mutant IIIA or IIIC 9ORF1 (Fig. 4A). Identical results were obtained for endogenous MUPP1 from CREF cell lines stably expressing comparable levels of wild-type or mutant 9ORF1 protein (Fig. 4B). These findings with COS7 and CREF cells were fully concordant with the GST pulldown assay results (Fig. 3). It was also noteworthy that MUPP1 similarly coimmunoprecipitated with wild-type 9ORF1 from lysates of an Ad9-induced rat mammary tumor cell line (Fig. 4C). Taken together, the results of GST pulldown and coimmunoprecipitation assays demonstrated that 9ORF1 utilizes its PDZ domain-binding motif to mediate a specific interaction with the multi-PDZ domain protein MUPP1 in cells.

transiently expressed in COS7 cells (Fig. 3) and to endogenous MUPP1 from CREF rat embryo fibroblasts (data not shown), as did GST fusion proteins of the related wild-type Ad5 and Ad12 E4-ORF1 transforming proteins (GST-5ORF1 and GST-12ORF1, respectively) (58). To assess whether these binding results with 9ORF1 were specific, we also examined in these same assays three different transformation-defective 9ORF1 mutant proteins having disrupted (mutant IIIA) or altered (mutants IIIC and IIID) carboxyl-terminal PDZ domain-binding motifs (Table 1) (28, 56). With respect to the residues mutated in 9ORF1 mutants IIIC and IIID, such sequences surrounding the conserved residues of type I PDZ domain-binding motifs are known to influence the binding to some PDZ domains (48). In GST pulldown assays with the three 9ORF1 mutant proteins, we found that only mutant IIID was able to bind to MUPP1, albeit at substantially reduced

9ORF1 binds selectively to MUPP1 PDZ7 and PDZ10. To reveal which of the 13 MUPP1 PDZ domains interacted with 9ORF1, we constructed a panel of fusion proteins containing 10 different, nonoverlapping MUPP1 protein fragments (Fig. 5A), which collectively represented the entire full-length MUPP1 polypeptide. A similar quantity of each MUPP1 fusion

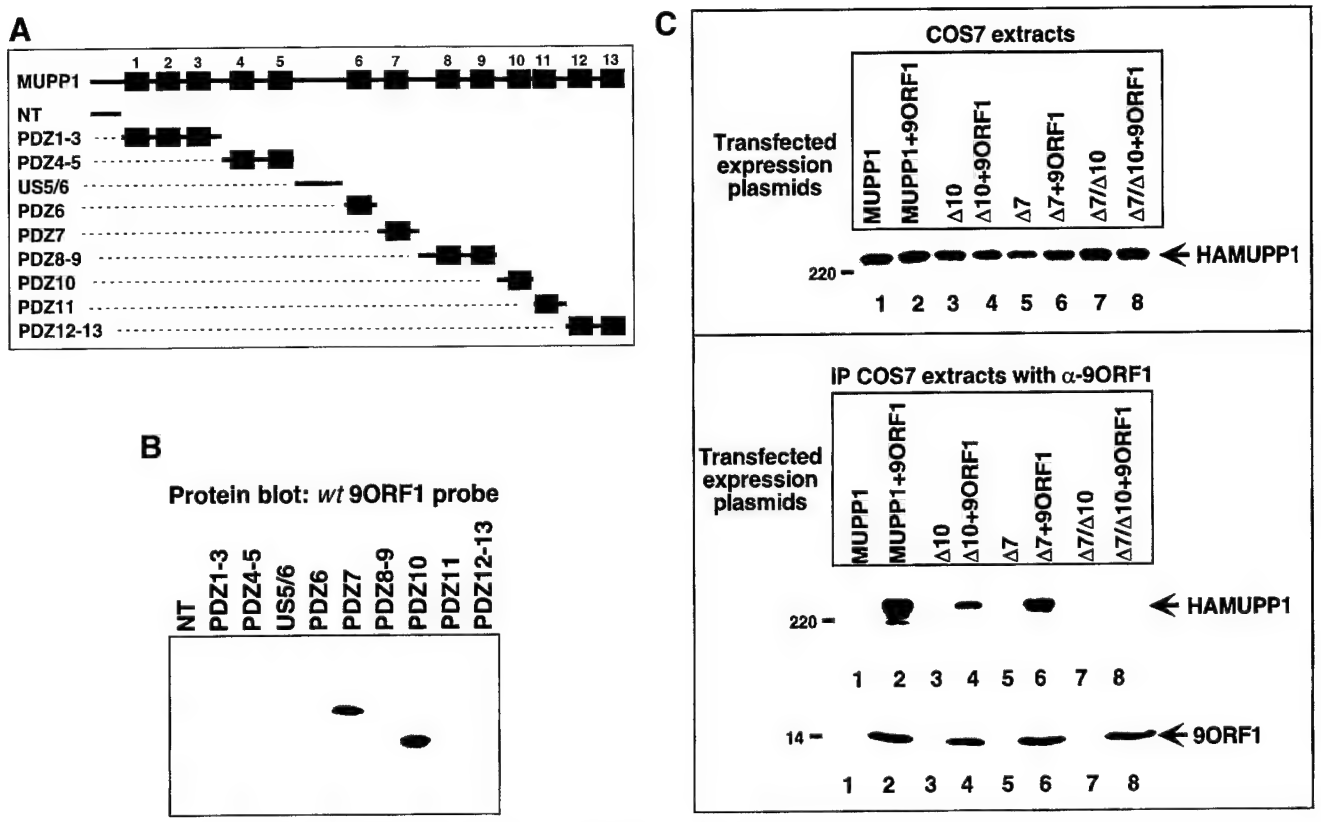

FIG. 5. MUPP1 PDZ7 and PDZ10 mediate binding to 9ORF1. (A) Illustration of the full-length MUPP1 polypeptide and 10 different MUPP1 GST fusion protein constructs used in protein blotting assays. (B) 9ORF1 binds MUPP1 PDZ7 and PDZ10 in vitro. Approximately 1 μg of each indicated MUPP1 GST fusion protein was immobilized on a membrane and protein blotted with a radiolabeled 9ORF1 protein probe. As a control, the membrane was stained with Coomassie brilliant blue dye to verify that an equivalent amount of each fusion protein was used in the experiment (data not shown). (C) A MUPP1 deletion mutant lacking both PDZ7 and PDZ10 fails to complex with 9ORF1 in COS7 cells. Cells were lipofected with 6 μg of a GW1 plasmid expressing wild-type or the indicated deletion mutant MUPP1 protein together with 2 μg of either empty GW1 plasmid (vector) or the GW1-9ORF1wt plasmid. Cell proteins in RIPA buffer were either immunoblotted with HA antibodies (top) or first immunoprecipitated (IP) with 9ORF1 antiserum (α-9ORF1) and then immunoblotted with HA antibodies or 9ORF1 antiserum (bottom). Cell proteins at 50 and 750 μg were used in the experiments in the top and bottom panels, respectively.

protein was immobilized on a membrane (data not shown) and blotted with a radiolabeled 9ORF1 protein probe. In these experiments, 9ORF1 bound to MUPP1 PDZ7 and PDZ10 but not to any other region of this cellular protein (Fig. 5B). A functional 9ORF1 PDZ domain-binding motif was required for these interactions, since a mutant GST-IIIA 9ORF1 protein probe failed to react with any of the MUPP1 fusion proteins in similar assays (data not shown).

To relate the in vitro binding results to the formation of 9ORF1-MUPP1 protein complexes in cells, we constructed MUPP1 deletion mutants lacking PDZ7 (HAMUPP1ΔPDZ7), PDZ10 (HAMUPP1ΔPDZ10), or both domains (HAMUPP1-ΔPDZ7/10) and tested these MUPP1 mutants for their ability to coimmunoprecipitate with 9ORF1 from COS7 cell lysates. The results showed that HAMUPP1ΔPDZ7 coimmunoprecipitated with 9ORF1 at wild-type levels and that HAMUPP1-ΔPDZ10 coimmunoprecipitated with 9ORF1 at slightly reduced levels but that HAMUPP1ΔPDZ7/10 failed to coimmunoprecipitate with 9ORF1 in these assays (Fig. 5C). These findings corroborated our in vitro binding results in showing that, among the 13 MUPP1 PDZ domains, only PDZ7 and PDZ10 are capable of mediating the binding of MUPP1 to 9ORF1 in vivo.

9ORF1 aberrantly sequesters MUPP1 within punctate bodies in the cytoplasm of cells. Using IF microscopy assays, we sought to ascertain the subcellular distribution of MUPP1 in normal CREF cells, as well as in CREF cell lines stably expressing wild-type or mutant 9ORF1 protein. In normal CREF cells, MUPP1 displayed mostly diffuse and somewhat perinuclear staining in the cytoplasm, although some MUPP1 protein was also detected at discrete points of cell-cell contact (Fig. 6A). The latter finding is consistent with the observation that PDZ proteins frequently localize to membranes at specialized regions of cell-cell contact in epithelial cells (8). Because 9ORF1 exists primarily within punctate bodies in the cytoplasm of cells (59), we reasoned that the subcellular localization of MUPP1 may be perturbed in 9ORF1-expressing CREF cells. Significantly, in contrast to results obtained with normal CREF cells, MUPP1 was found to be sequestered within punctate bodies in the cytoplasm of more than 95% of CREF cells expressing wild-type 9ORF1 (Fig. 6A), similar to the staining pattern observed for 9ORF1 (59). Using a CREF cell line stably expressing an HA epitope-tagged 9ORF1 protein, we were able to demonstrate that 9ORF1 and MUPP1 colocalize within these cytoplasmic bodies (Fig. 6B).

Additional IF assay results indicated that the cytoplasmic sequestration of MUPP1 by 9ORF1 depended on an ability of 9ORF1 to complex with this cellular PDZ protein. Specifically, CREF cell lines expressing 9ORF1 mutants IIIA and IIIC, which fail to bind MUPP1, showed a MUPP1 staining pattern similar to that seen in normal CREF cells. Moreover, the CREF cell line expressing 9ORF1 mutant IIID, which exhibits

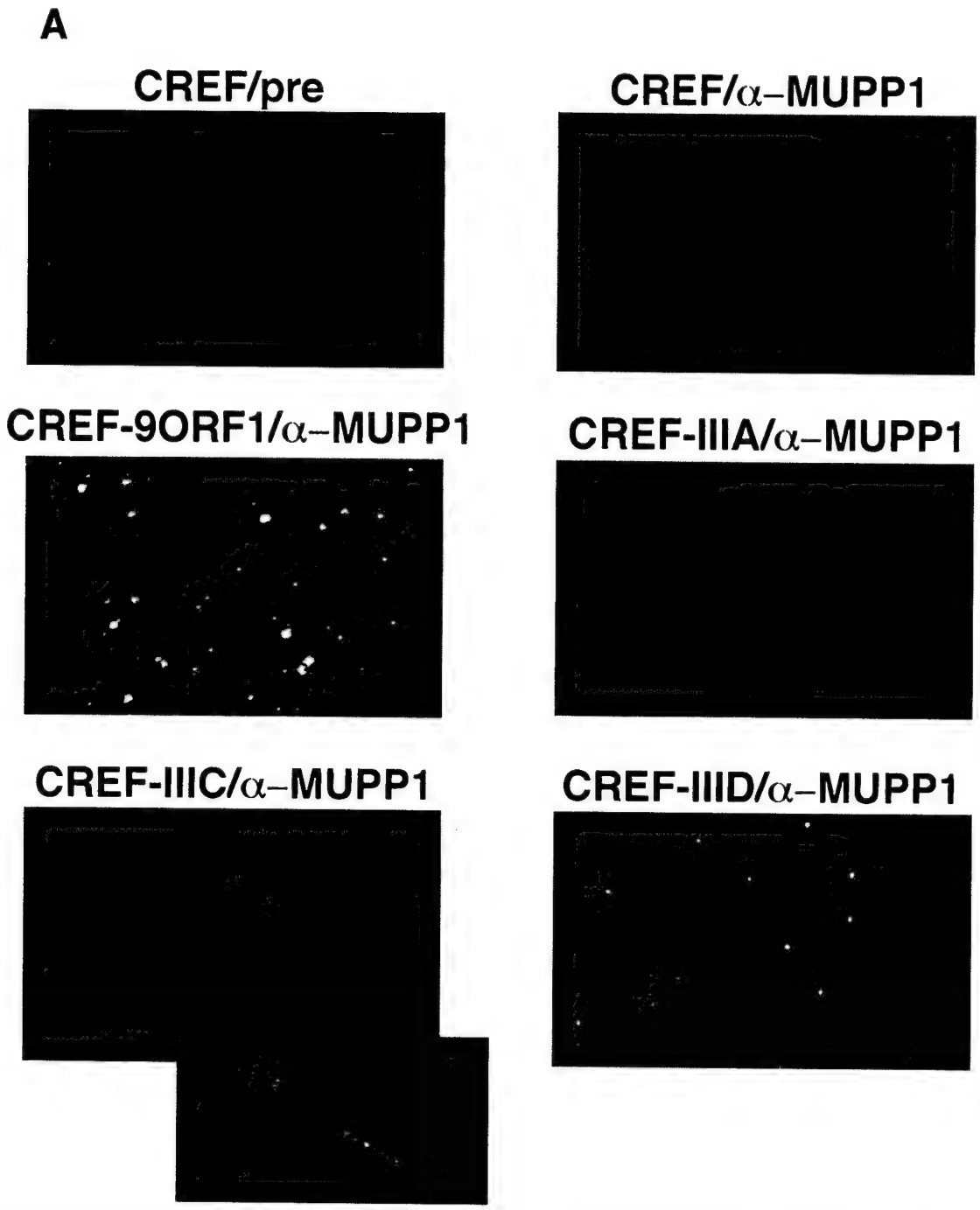

FIG. 6. 9ORF1 aberrantly sequesters MUPP1 within punctate bodies in the cytoplasm of cells. (A) Determination of the subcellular localization of MUPP1 in normal CREF cells (CREF) or CREF cell lines stably expressing wild-type (CREF-9ORF1) or the indicated mutant 9ORF1 protein (CREF-IIIA, CREF-IIIC, and CREF-IIID). IF microscopy assays were performed with either MUPP1 antiserum (α-MUPP1) or the matched preimmune serum (pre). Although all of the CREF cell lines expressed similar amounts of MUPP1 protein (see Fig. 7A), the MUPP1 staining for CREF-9ORF1 cells appeared brighter than that for the other CREF lines. This effect probably resulted from the large amounts of MUPP1 protein concentrated within the cytoplasmic punctate bodies. Discontinuous cell-cell contact staining for MUPP1 was most evident in normal CREF cells, and CREF-IIIA and CREF-IIIC lines, all of which exhibited similar MUPP1 staining patterns. As an example of this cell-cell contact staining, two adjacent CREF-IIIC cells within the delimited rectangular region are shown offset at higher magnification. (B) 9ORF1 and MUPP1 colocalize within punctate bodies in the cytoplasm of CREF cells. Double-labeling IF microscopy assays using both MUPP1 antiserum and HA antibodies (α-HA) were performed with CREF cells stably expressing HA epitope-tagged 9ORF1 protein (CREF-HA9ORF1). Each of the three panels shows the identical field containing the same three cells. The top left and top right panels show the MUPP1 and 9ORF1 staining patterns, respectively, whereas the bottom panel shows the merged images.

weak binding to MUPP1, showed some cytoplasmic punctate staining for MUPP1, although substantially less than that observed in the CREF cell line expressing wild-type 9ORF1 (Fig. 6A). It is worth mentioning that, similar to the wild-type 9ORF1 protein, these three 9ORF1 mutant proteins also display punctate staining in the cytoplasm of CREF cells (56).

To corroborate the IF assay results, we performed crude cell fractionation experiments with the same CREF cell lines. Fol-

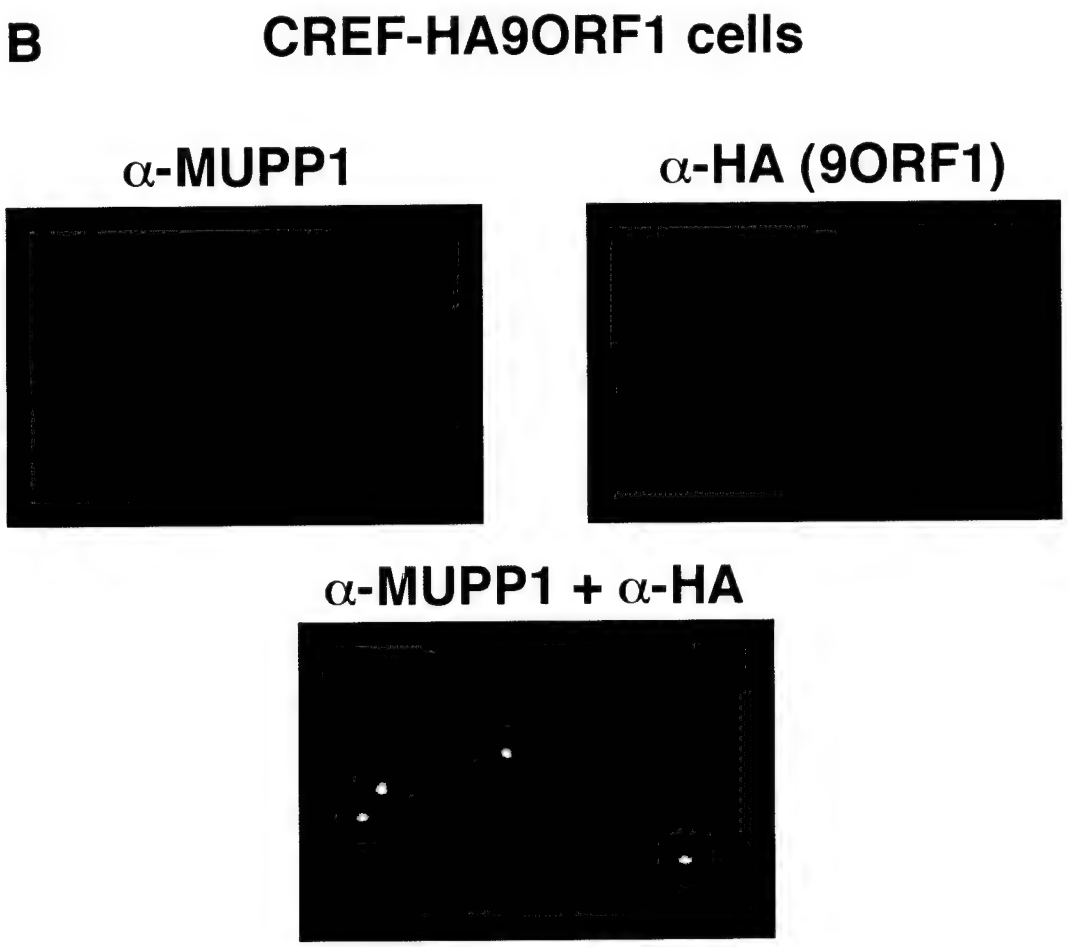

FIG. 6—*Continued.*

lowing direct lysis in 2% SDS, each cell line was found to express comparable levels of both MUPP1 and 9ORF1 proteins (Fig. 7A). CREF cell lysates were also prepared in RIPA buffer and separated by centrifugation into a RIPA buffer-soluble supernatant fraction and a RIPA buffer-insoluble pellet fraction. Immunoblot analyses of these two fractions with MUPP1 antiserum revealed that wild-type-9ORF1-expressing CREF cells contain substantially less RIPA buffer-soluble MUPP1 protein and concomitantly more RIPA buffer-insoluble MUPP1 protein than do normal CREF cells (Fig. 7B). The fact that the portion of MUPP1 protein retained in the RIPA buffer-soluble fraction of the wild-type-9ORF1-expressing cells could be depleted by quantitative immunoprecipitation of 9ORF1 (Fig. 7C) indicated that the vast majority of MUPP1 protein in these cells is complexed with 9ORF1.

The redistribution of MUPP1 into the RIPA buffer-insoluble fraction of wild-type-9ORF1-expressing CREF cells was also related to the ability of 9ORF1 to bind this cellular protein, because mutant IIIA and IIIC 9ORF1 largely failed to aberrantly redistribute MUPP1 in CREF cells whereas mutant IIID 9ORF1 retained a reduced capacity to induce this effect (Fig. 7B). These differences are not likely to be due to the smaller amounts of RIPA buffer-insoluble mutant IIIA and IIIC 9ORF1 proteins present in these CREF cells (Fig. 7B), since transiently transfected 293 cells contained equivalent amounts of RIPA buffer-insoluble wild-type and mutant 9ORF1 proteins but still yielded a pattern of MUPP1 redistribution similar to that of the CREF cell lines (Fig. 7D). That 9ORF1 redistributed MUPP1 into the RIPA buffer-insoluble fraction of 293 cells more effectively than it did in CREF cells may be due to the higher protein levels attained for 9ORF1 and MUPP1 in transient transfections of the 293 cells. Together, the results of IF and crude cell fractionation assays argued that 9ORF1 aberrantly sequesters MUPP1 within RIPA buffer-insoluble complexes in the cytoplasm of cells.

The high-risk 18E6 oncoprotein binds MUPP1 and targets this cellular protein for degradation in cells. Because, like 9ORF1, high-risk HPV E6 oncoproteins possess a functional PDZ domain-binding motif and complex with DLG (27, 29), we next explored the possibility that such HPV E6 proteins likewise bind to MUPP1. In GST pulldown assays, the wild-type high-risk 18E6 protein associated both with HAMUPP1 protein expressed in COS7 cells (Fig. 8) and with endogenous MUPP1 from CREF cells (data not shown). This binding was specific and dependent on a functional PDZ domain-binding motif because in these assays the 18E6-V158A and 18E6-T156D/V158A mutant proteins, which have disrupted PDZ-domain binding motifs (Table 1), failed to complex with MUPP1 (Fig. 8 and data not shown), as did the wild-type low-risk HPV-11 E6 (11E6) protein, which lacks a PDZ domain-binding motif (Table 1). It is notable that HPV-16 E6 mutants having functionally disrupted PDZ domain-binding motifs, like those of 18E6-V158A and 18E6-T156D/V158A,

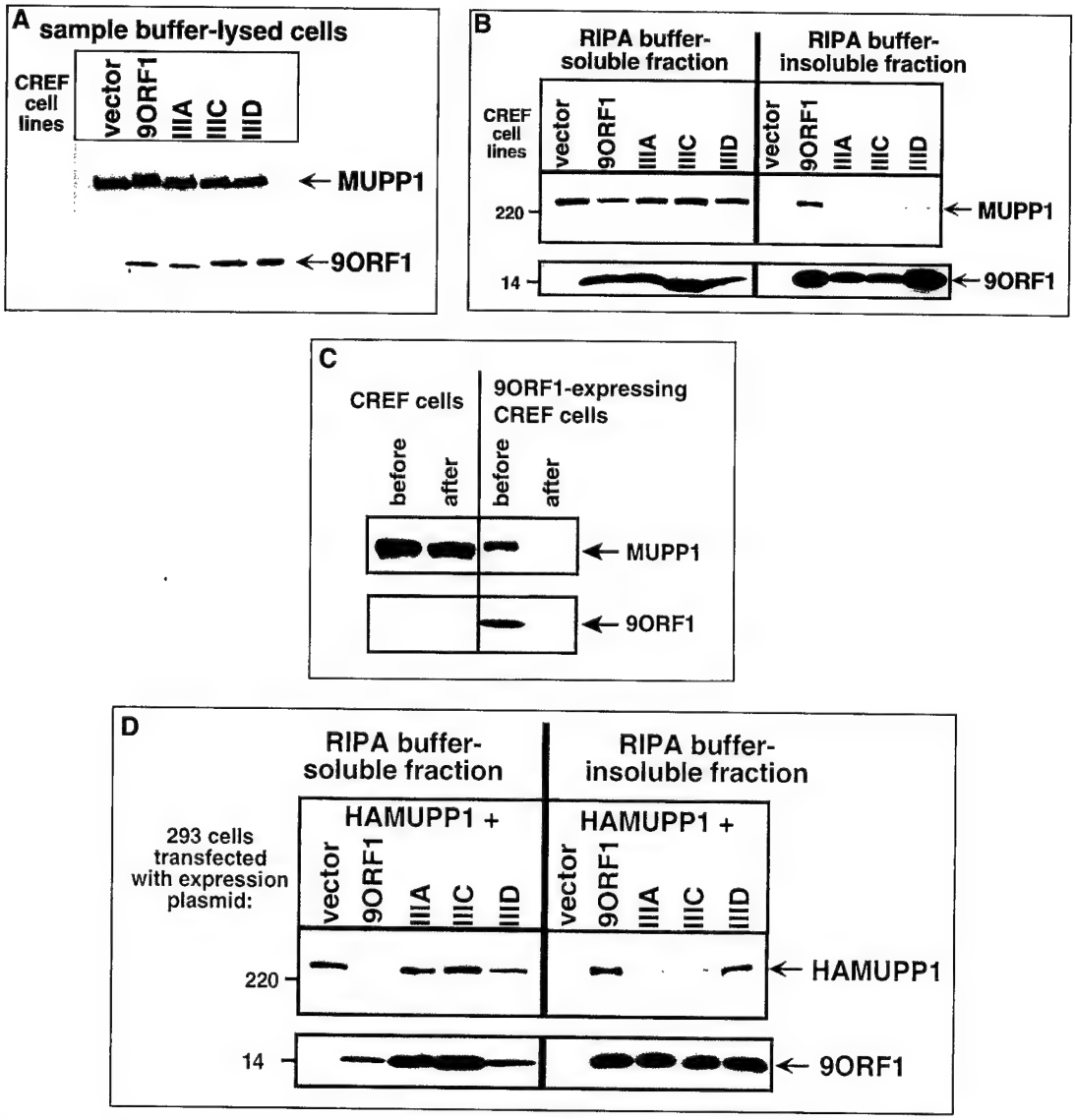

FIG. 7. 9ORF1 aberrantly redistributes MUPP1 into the RIPA buffer-insoluble fraction of cells. (A) Similar amounts of MUPP1 and 9ORF1 proteins within CREF cell lines stably expressing wild-type and mutant 9ORF1 proteins. Cell proteins (100 μg) extracted with sample buffer were immunoblotted with MUPP1 antiserum or 9ORF1 antiserum. (B) Wild-type 9ORF1 specifically redistributes MUPP1 into the RIPA buffer-insoluble fraction of CREF cells. Cells from the indicated CREF lines were lysed in RIPA buffer and centrifuged to yield a RIPA buffer-soluble supernatant fraction and a RIPA buffer-insoluble pellet fraction (see Materials and Methods). Cell proteins from an equivalent volume of either the soluble or insoluble fraction were immunoblotted with MUPP1 or 9ORF1 antiserum. (C) Most MUPP1 protein is complexed with 9ORF1 in 9ORF1-expressing CREF cells. Cell proteins (3 mg) in the RIPA buffer-soluble fraction of normal CREF cells or wild-type 9ORF1-expressing CREF cells were subjected to five serial immunoprecipitations with 9ORF1 antiserum. Relative amounts of MUPP1 and 9ORF1 protein remaining in this fraction (100 μg of protein) "before" and "after" performing the serial immunoprecipitations were determined by immunoblot analysis. (D) Wild-type 9ORF1 also specifically redistributes HA epitope-tagged rat MUPP1 (HAMUPP1) into the RIPA buffer-insoluble fraction of 293 cells. Cells were lipofected with 1 μg of GW1-HAMUPP1 plasmid and 3 μg of either empty GW1 plasmid (vector) or a GW1 plasmid expressing wild-type or the indicated mutant 9ORF1 protein. Cell fractionation assays were performed as described for panel B, except that cell proteins were immunoblotted with HA antibodies or 9ORF1 antiserum.

are no longer able to oncogenically transform rodent fibroblasts (26).

The fact that high-risk HPV E6 oncoproteins promote the degradation of several cellular factors (10, 15, 53), including the tumor suppressor protein p53 (42) and DLG (11), prompted us to test whether 18E6 has similar effects on MUPP1. Incubation of in vitro-translated high-risk HPV E6 proteins with p53 leads to degradation of this cellular factor (42), and so we first examined MUPP1 in similar assays. Although 18E6-induced degradation of both p53 and DLG was more efficient, a modest reduction in MUPP1 protein levels was reproducibly observed following a 3-h incubation with 18E6 (Fig. 9). This effect was also consistently greater than that observed in control water-primed in vitro translation reactions.

Whether 18E6 may target MUPP1 for degradation in cells was examined by expressing HAMUPP1 alone or together with 18E6 in COS7 cells. We found that in these assays, compared to cells expressing MUPP1 alone, cells coexpressing MUPP1 and 18E6 showed substantially lower steady-state levels of MUPP1 protein (Fig. 10A). It is important to mention that this effect is distinct from that seen in the RIPA buffer-soluble fraction of 9ORF1-expressing cells (Fig. 7B and D), since MUPP1 was not sequestered within the RIPA buffer-insoluble fraction of 18E6-expressing cells (data not shown). To produce

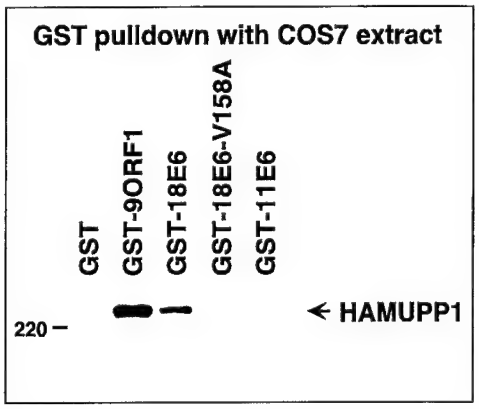

FIG. 8. 18E6 binds MUPP1 in vitro. GST-18E6 binds HA epitope-tagged rat MUPP1 (HAMUPP1) exogenously expressed in COS7 cells. Cells were lipofected with 8 μg of GW1-HAMUPP1 plasmid, and cell proteins (250 μg) in RIPA buffer were first subjected to a GST pulldown assay with the indicated fusion protein and then immunoblotted with HA antibodies.

this effect, 18E6 required a functional PDZ domain-binding motif because mutants 18E6-V158A and 18E6-T156D/V158A, as well as wild-type 11E6, failed to reduce MUPP1 protein levels in COS7 cells. Additionally, only specific cellular PDZ proteins were affected by 18E6, since 18E6 neither bound the DLG-related PDZ-protein ZO-1 (Fig. 10B) (61) nor reduced its protein levels in these cells (Fig. 10C).

To verify that the 18E6-mediated reduction in MUPP1 steady-state protein levels was due to decreased stability of this cellular protein in cells, we performed pulse-chase experiments with COS7 cells either expressing HAMUPP1 alone or coexpressing HAMUPP1 and 18E6. The results showed that MUPP1 protein levels modestly declined after a 6-h chase period in the absence of 18E6 whereas they were more extensively reduced after only a 3-h chase period in the presence of 18E6 (Fig. 11). By quantifying the amounts of radioactivity present in MUPP1 protein bands at each time point, we estimated that the half-life of the MUPP1 protein was shortened from 5.7 h in control COS7 cells to 1.3 h in 18E6-expressing COS7 cells. This greater than fourfold decrease in the half-life of the MUPP1 protein argues that 18E6 targets this cellular factor for degradation in cells.

DISCUSSION

The results presented in this paper demonstrate that the widely expressed multi-PDZ protein MUPP1 is a direct cellular target for the Ad9 E4-ORF1 oncoprotein (9ORF1), as well as for the related E4-ORF1 transforming proteins derived from Ad5 and Ad12 (5ORF1 and 12ORF1, respectively) (Fig. 3). We also showed that interactions between 9ORF1 and MUPP1 are mediated by the carboxyl-terminal PDZ domain-binding motif of 9ORF1 and the PDZ7 and PDZ10 domains of MUPP1 (Fig. 3 to 5). Since 5ORF1 and 12ORF1 also possess carboxyl-terminal PDZ domain-binding motifs, these viral proteins probably complex with MUPP1 in a similar fashion. More important, the fact that transformation-defective 9ORF1 mutants with altered PDZ domain-binding motifs either fail or have reduced capacities to complex with MUPP1 in cells argues that binding of 9ORF1 to MUPP1 is critical for 9ORF1-

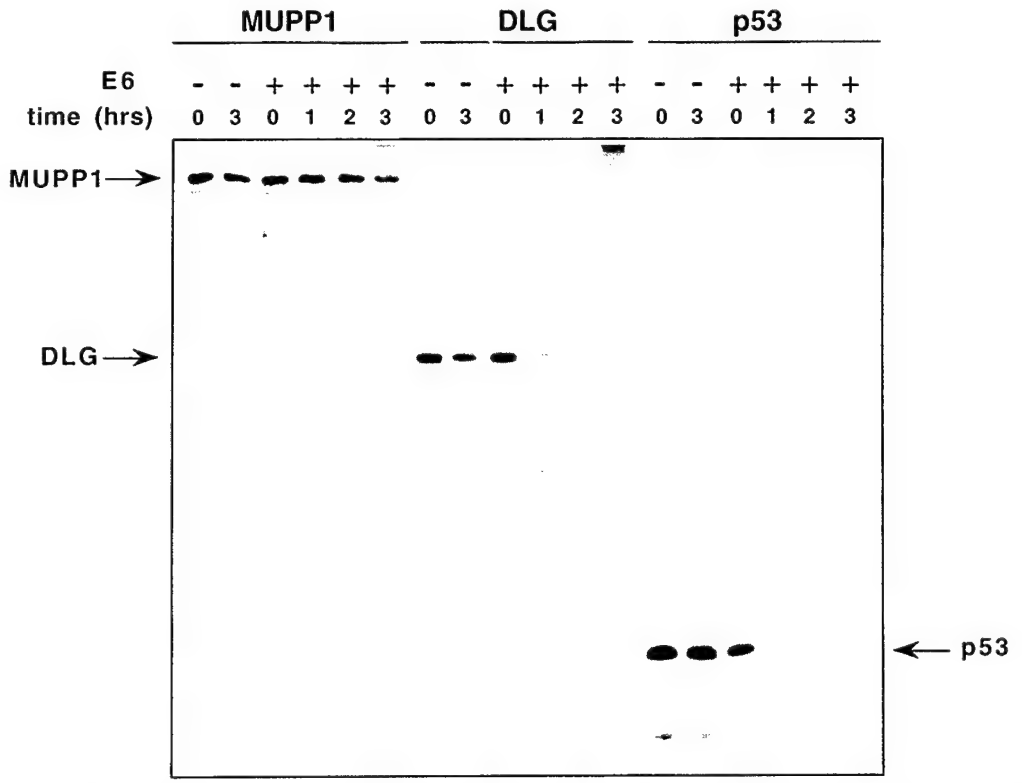

FIG. 9. 18E6 promotes the degradation of the MUPP1 protein in vitro. In vitro-translated MUPP1, DLG, or p53 protein was incubated for the indicated times with a 5- to 10-fold molar excess of in vitro-translated 18E6 protein (+) or with an equivalent volume of a water-primed in vitro translation reaction mixture (−). Proteins from each reaction were subjected to immunoprecipitation with MUPP1, DLG, or p53 antibodies, respectively, and detected by autoradiography.

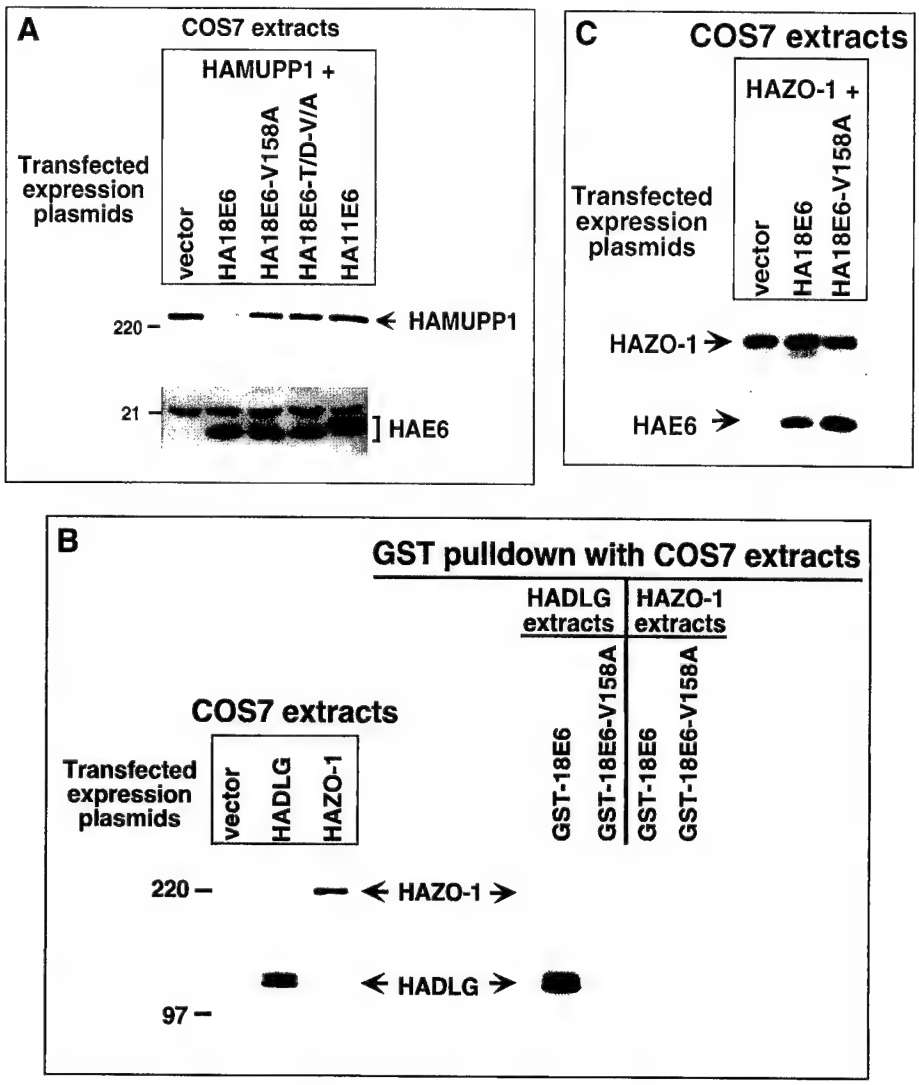

FIG. 10. 18E6 reduces the steady-state levels of MUPP1 protein in cells. (A) 18E6 reduces the steady-state levels of HA epitope-tagged rat MUPP1 (HAMUPP1) protein expressed in COS7 cells. Cells were lipofected with 1 μg of GW1-HAMUPP1 plasmid and 4 μg of either empty GW1 plasmid (vector) or a GW1 plasmid expressing HA epitope-tagged wild-type or the indicated mutant 18E6 protein or expressing HA epitope-tagged wild-type 11E6 protein. Cell proteins (30 μg) in RIPA buffer were immunoblotted with HA antibodies. (B) 18E6 does not bind HA epitope-tagged PDZ-protein ZO-1 (HAZO-1). Cells were lipofected with 3 μg of either empty GW1 plasmid (vector), GW1-HADLG plasmid, or GW1-HAZO-1 plasmid, and cell proteins in RIPA buffer were either immunoblotted with HA antibodies (left) or first subjected to a GST pulldown assay with the indicated fusion protein and then immunoblotted with HA antibodies (right). COS7 cell proteins at 10 and 75 μg were used in the experiments in the left and right panels, respectively. HADLG was included as a positive control in these binding assays (28). (C) 18E6 does not reduce HAZO-1 protein levels in COS7 cells. COS7 cells were lipofected with 0.01 μg of GW1-HAZO-1 plasmid and 4 μg of either empty GW1 plasmid (vector) or a GW1 plasmid expressing HA epitope-tagged wild-type or the indicated mutant 18E6 protein. Cell proteins (30 μg) in RIPA buffer were immunoblotted with HA antibodies.

induced transformation (Fig. 3 and 4). Our finding that 9ORF1 associates with MUPP1 in an Ad9-induced mammary tumor cell line (Fig. 4C) further suggests that this interaction also contributes to Ad9-induced mammary tumorigenesis in rats. With the findings presented in this paper, 9ORF1 has now been shown to complex with two different cellular PDZ proteins, MUPP1 and DLG (28). Since the weakly transforming 9ORF1 mutants IIIC and IIID bind only one of these two PDZ proteins whereas the completely transformation-defective 9ORF1 mutant IIIA fails to bind either PDZ protein, we believe that interaction of 9ORF1 with both MUPP1 and DLG is important for full 9ORF1 transforming activity.

It is also worth noting that we have failed to detect any binding of 9ORF1 to several other cellular PDZ proteins (B. Glaunsinger and R. Javier, unpublished results), suggesting that 9ORF1 interacts with only a select group of these cellular factors. We hypothesize that such selective binding of 9ORF1 is achieved through sequences surrounding its PDZ domain-binding motif. In this model, specific amino acid residues adjacent to the 9ORF1 PDZ domain-binding motif would play differential roles in mediating the binding to each 9ORF1-associated PDZ protein. Consistent with this idea, 9ORF1 mutant IIIC retains wild-type binding to DLG (28) but fails to bind MUPP1 and, conversely, 9ORF1 mutant IIID fails to bind DLG (28) but retains an ability to bind MUPP1 (Table 1 and Fig. 3 and 4).

The domain structure of MUPP1 suggests that this cellular factor functions as an adapter protein in signal transduction (55). Moreover, having the largest number of PDZ domains (i.e., 13) yet reported in a polypeptide, MUPP1 has the capac-

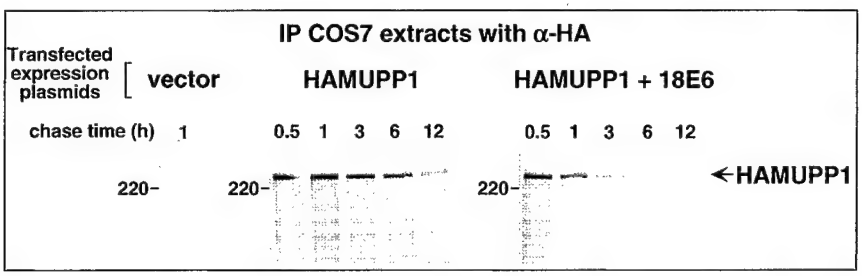

FIG. 11. 18E6 decreases the half-life of the MUPP1 protein in cells. A total of 5.5×10^5 COS7 cells were lipofected with 5 μg of empty GW1 plasmid (vector) or 1 μg of GW1-HAMUPP1 plasmid and 4 μg of either empty GW1 plasmid (HAMUPP1) or the GW1-18E6 plasmid (HAMUPP1 + 18E6). At 24 h posttransfection, cells were pulse-labeled and then chased for the indicated times (see Materials and Methods). Cell proteins (200 μg) were immunoprecipitated with HA antibodies (α-HA), and HAMUPP1 protein was detected by autoradiography and quantified with a PhosphorImager.

ity to assemble a large array of cellular targets into a multitude of different signaling complexes. As further support for a presumed role in cell signaling, MUPP1 was isolated in yeast two-hybrid screens for its ability to interact with the cytoplasmic carboxyl-terminal domain of the 5-HT_{2C} serotonin receptor (55), which, in the central nervous system, is implicated in a variety sensory, motor, and behavioral processes (18). The putative interaction between the 5-HT_{2C} receptor and MUPP1 in cells is suspected to involve a type I PDZ domain-binding motif at the extreme carboxyl terminus of the 5-HT_{2C} receptor and at least one MUPP1 PDZ domain (55). The fact that overexpression of the 5-HT_{2C} receptor has been shown to confer a transformed state on 3T3 fibroblasts (60) also suggests a possible link between MUPP1 and signaling pathways involved in regulating cellular proliferation.

We found that most of the MUPP1 protein in CREF fibroblasts is present within the cytoplasm, although some MUPP1 protein is also detected at discrete regions of cell-cell contact (Fig. 6). Consistent with the notion that MUPP1 functions in signal transduction, PDZ proteins that play known roles in cell signaling also localize to membranes at regions of cell-cell contact in epithelial cells (8) and, in some cases, within the cytoplasm (62, 64). With respect to how MUPP1 may function in cells, studies with the *Drosophila* MUPP1-related multi-PDZ protein InaD are likely to provide the most useful paradigm. The polypeptide InaD, consisting of five PDZ domains, functions to regulate the rhodopsin light-activated signaling pathway in retinal neurons. Each of the InaD PDZ domains mediates binding to a different signaling protein, including the calcium channel TRP, phospholipase C-β, and protein kinase C. InaD serves to organize these cellular targets into large signaling complexes and localize them to specialized cell membranes, and, in so doing, it allows rapid and efficient activation and deactivation of the light response (54). Although the PDZ protein-regulated signaling pathways perturbed by 9ORF1 in cells have yet to be identified, we previously showed that two prominent transformed properties of 9ORF1-expressing CREF cells in culture are anchorage-independent growth and an ability to grow to high saturation densities (59). Since proliferation of normal cells is inhibited by either detachment from a substrate matrix or formation of extensive cell-cell contacts (12, 16), one intriguing possibility is that 9ORF1 interferes with the ability of MUPP1 to regulate cell growth-controlling signaling cascades that emanate from these important plasma membrane contact points.

Of the 13 MUPP1 PDZ domains, 9ORF1 specifically targets only 2, namely, PDZ7 and PDZ10 (Fig. 5). This selective interaction may serve to block MUPP1 from associating with cellular targets of these particular domains or, alternatively, to bring 9ORF1 into close proximity with other MUPP1 cellular targets in order to modify their activities. A recently discovered activity for some PDZ proteins is the ability to direct their cellular targets to the proper location within cells (4, 24, 39, 54). One notable example comes from studies of vulval development in *Caenorhabditis elegans*. In this system, LET-23, an epidermal growth factor receptor-like protein, must be localized to the basolateral membrane of the vulval epithelial cells for this receptor to associate with its growth factor ligand (25). Three different PDZ domain-containing proteins, LIN-7, LIN-2, and LIN-10, which complex with LET-23, are responsible for directing this receptor to its proper site in cells (24). Therefore, considering that 9ORF1 aberrantly sequesters MUPP1 in the cytoplasm of cells (Fig. 6 and 7), it is reasonable to assume that 9ORF1 completely abolishes the function of MUPP1 by preventing this PDZ protein and its cellular targets from reaching their proper destinations in the cell.

We also showed that the high-risk 18E6 oncoprotein utilizes a PDZ domain-binding motif to complex with and promote degradation of the MUPP1 protein in cells (Fig. 8 to 11). Whether 18E6 targets MUPP1 for ubiquitin-mediated, proteasome-dependent proteolysis, as it does for p53 (41), was not determined. The modest 18E6-induced MUPP1 degradation observed after mixing in vitro-translated proteins (Fig. 9) may indicate that 18E6 utilizes a different mechanism to degrade MUPP1 from the one it uses to degrade p53 and DLG. Nevertheless, the degradation of MUPP1 that we observed in 18E6-expressing COS7 cells implies that MUPP1 function is abrogated in cells infected by HPV-18. Because the carboxyl-terminal PDZ domain-binding motif sequence of high-risk HPV-31, HPV-39, HPV-45, and HPV-51 E6 proteins is identical to that of 18E6 (28), MUPP1 is also likely to be targeted for degradation by these and probably other high-risk HPV E6 oncoproteins. Our additional finding that the low-risk 11E6 protein neither binds MUPP1 nor targets this cellular protein for degradation in cells (Fig. 8 and 10) provides additional support for the idea that binding of high-risk E6 proteins to MUPP1 may contribute to HPV-induced carcinogenesis.

Our results argue that an ability to bind cellular PDZ proteins contributes to the transforming activities of both the Ad E4-ORF1 and high-risk HPV E6 oncoproteins. With respect to possible roles in the life cycles of Ad and HPV, these interactions are expected to help create an optimal environment for viral replication within infected host cells by overcoming normal defense mechanisms that block abnormal progression into S phase. Such an activity is common to the oncoproteins of DNA tumor viruses and is invariably mediated by their interactions with host cell factors intimately involved in regulating cellular proliferation and differentiation (34). In this regard,

the fact that two unrelated viral oncoproteins, Ad E4-ORF1 and high-risk HPV E6, have both evolved to target the MUPP1 protein in cells strengthens the hypothesis that interactions with this cellular factor are pertinent to transformation. It is well known that the Ad5 E1B oncoprotein sequesters the tumor suppressor protein p53 in cells (44) whereas the unrelated high-risk HPV E6 oncoproteins promote the degradation of this cellular factor (19). In these examples, functional inactivation of p53 is the ultimate outcome of these interactions, but the mechanisms by which these viral oncoproteins accomplish this effect are distinct. Our findings suggest that the Ad E4-ORF1 and HPV E6 oncoproteins likewise inactivate MUPP1 by different mechanisms. This interesting parallel with the tumor suppressor protein p53, together with the fact that the PDZ protein DLG is a putative tumor suppressor protein, hints that MUPP1 may function to negatively regulate cellular proliferation and thus may represent a novel tumor suppressor protein. Consequently, revealing the cellular functions for this multi-PDZ domain adapter protein may provide new insights into mechanisms that contribute to the development of human malignancies.

ACKNOWLEDGMENTS

We are grateful to Christoph Ullmer and Alan Fanning for generously providing the pBSK-MUPP1 and pSK-ZO-1 plasmids, respectively. We thank Richard Sutton for helpful discussions and critical reading of the manuscript. We also thank Hank Adams and Frank Herbert (Microscopy Core, Department of Cell Biology, Baylor College of Medicine) for assistance.

S.S.L. was the recipient of a U.S. Army Breast Cancer Training Grant (DAMD17-94-J4204), and B.G. was the recipient of a Molecular Virology Training Grant (T32 AI07471). This work was supported by National Institutes of Health (ROI CA58541), American Cancer Society (RPG-97-668-01-VM), and U.S. Army (DAMD17-97-1-7082) grants to R.T.J. and an Associazione Italiana per la Ricerca sul Cancro grant to L.B.

REFERENCES

1. **Banks, L., G. Matlashewski, and L. Crawford.** 1986. Isolation of human-p53-specific monoclonal antibodies and their use in the studies of human p53 expression. Eur. J. Biochem. **159:**529–534.
2. **Bonifacino, J. S.** 1991. Biosynthetic labeling of proteins, p. 10.18.1–10.18.9. *In* F. M. Ausubel, R. Brent, R. E. Kingston, D. D. Moore, J. G. Seidman, J. A. Smith, and K. Struhl (ed.), Current protocols in molecular biology, vol. 2. Greene Publishing Associates and Wiley-Interscience, New York, N.Y.
3. **Brenman, J. E., D. S. Chao, S. H. Gee, A. W. McGee, S. E. Craven, D. R. Santillano, Z. Wu, F. Huang, H. Xia, M. F. Peters, S. C. Froehner, and D. S. Bredt.** 1996. Interaction of nitric oxide synthase with the postsynaptic density protein PSD-95 and alpha1-syntrophin mediated by PDZ domains. Cell **84:**757–767.
4. **Butz, S., M. Okamoto, and T. C. Sudhof.** 1998. A tripartite protein complex with the potential to couple synaptic vesicle exocytosis to cell adhesion in brain. Cell **94:**773–782.
5. **Cann, A. J., and I. S. Y. Chen.** 1996. Human T-cell leukemia virus types I and II, p. 1849–1880. *In* B. N. Fields, D. M. Knipe, and P. M. Howley (ed.), Fields virology, 3rd ed., vol. 2. Lippincott-Raven, Philadelphia, Pa.
6. **Craven, S. E., and D. S. Bredt.** 1998. PDZ proteins organize synaptic signaling pathways. Cell **93:**495–498.
7. **Fanning, A. S., and J. M. Anderson.** 1998. PDZ domains and the formation of protein networks at the plasma membrane. Curr. Top. Microbiol. Immunol. **228:**209–233.
8. **Fanning, A. S., and J. M. Anderson.** 1999. PDZ domains: fundamental building blocks in the organization of protein complexes at the plasma membrane. J. Clin. Investig. **103:**767–772.
9. **Fisher, P. B., L. E. Babiss, I. B. Weinstein, and H. S. Ginsberg.** 1982. Analysis of type 5 adenovirus transformation with a cloned rat embryo cell line (CREF). Proc. Natl. Acad. Sci. USA **79:**3527–3531.
10. **Gao, Q., S. Srinivasan, S. N. Boyer, D. E. Wazer, and V. Band.** 1999. The E6 oncoproteins of high-risk papillomaviruses bind to a novel putative GAP protein, E6TP1, and target it for degradation. Mol. Cell. Biol. **19:**733–744.
11. **Gardiol, D., C. Kuhne, B. Glaunsinger, S. S. Lee, R. Javier, and L. Banks.** 1999. Oncogenic human papillomavirus E6 proteins target the discs large tumour suppressor for proteasome-mediated degradation. Oncogene **18:** 5487–5496.
12. **Giancotti, F. G., and E. Ruoslahti.** 1999. Integrin signaling. Science **285:** 1028–1032.
13. **Gluzman, Y.** 1981. SV40-transformed simian cells support the replication of early SV40 mutants. Cell **23:**175–182.
14. **Graham, F. L., J. Smiley, W. C. Russell, and R. Nairn.** 1977. Characteristics of a human cell line transformed by DNA from human adenovirus type 5. J. Gen. Virol. **36:**59–74.
15. **Gross-Mesilaty, S., E. Reinstein, B. Bercovich, K. E. Tobias, A. L. Schwartz, C. Kahana, and A. Ciechanover.** 1998. Basal and human papillomavirus E6 oncoprotein-induced degradation of Myc proteins by the ubiquitin pathway. Proc. Natl. Acad. Sci. USA **95:**8058–8063.
16. **Gumbiner, B. M.** 1996. Cell adhesion: the molecular basis of tissue architecture and morphogenesis. Cell **84:**345–357.
17. **Harlow, E., and D. Lane.** 1988. Antibodies. A laboratory manual, p. 55–137, 283–318, and 359–420. Cold Spring Harbor Laboratory, Cold Spring Harbor, N.Y.
18. **Heisler, L. K., H. M. Chu, and L. H. Tecott.** 1998. Epilepsy and obesity in serotonin 5-HT2C receptor mutant mice. Ann. N. Y. Acad. Sci. **861:**74–78.
19. **Howley, P. M.** 1996. Papillomavirinae: the viruses and their replication, p. 2045–2076. *In* B. N. Fields, D. M. Knipe, and P. M. Howley (ed.), Fields virology, 3rd ed., vol. 2. Lippincott-Raven, Philadelphia, Pa.
20. **Jainchill, J. L., S. A. Aaronson, and G. J. Todaro.** 1969. Murine sarcoma and leukemia viruses: assay using clonal lines of contact-inhibited mouse cells. J. Virol. **4:**549–553.
21. **Javier, R., K. Raska, Jr., and T. Shenk.** 1992. Requirement for the adenovirus type 9 E4 region in production of mammary tumors. Science **257:**1267–1271.
22. **Javier, R., and T. Shenk.** 1996. Mammary tumors induced by human adenovirus type 9: a role for the viral early region 4 gene. Breast Cancer Res. Treat. **39:**57–67.
23. **Javier, R. T.** 1994. Adenovirus type 9 E4 open reading frame 1 encodes a transforming protein required for the production of mammary tumors in rats. J. Virol. **68:**3917–3924.
24. **Kaech, S. M., C. W. Whitfield, and S. K. Kim.** 1998. The LIN-2/LIN-7/LIN-10 complex mediates basolateral membrane localization of the *C. elegans* EGF receptor LET-23 in vulval epithelial cells. Cell **94:**761–771.
25. **Kim, S. K.** 1997. Polarized signaling: basolateral receptor localization in epithelial cells by PDZ-containing proteins. Curr. Opin. Cell Biol. **9:**853–859.
26. **Kiyono, T., A. Hiraiwa, M. Fujita, Y. Hayashi, T. Akiyama, and M. Ishibashi.** 1997. Binding of high-risk human papillomavirus E6 oncoproteins to the human homologue of the *Drosophila* discs large tumor suppressor protein. Proc. Natl. Acad. Sci. USA **94:**11612–11616.
27. **Kubbutat, M. H., and K. H. Vousden.** 1998. New HPV E6 binding proteins: dangerous liaisons? Trends Microbiol. **6:**173–175.
28. **Lee, S. S., R. S. Weiss, and R. T. Javier.** 1997. Binding of human virus oncoproteins to hDlg/SAP97, a mammalian homolog of the *Drosophila* discs large tumor suppressor protein. Proc. Natl. Acad. Sci. USA **94:**6670–6675.
29. **Lue, R. A., S. M. Marfatia, D. Branton, and A. H. Chishti.** 1994. Cloning and characterization of hdlg: the human homologue of the *Drosophila* discs large tumor suppressor binds to protein 4.1. Proc. Natl. Acad. Sci. USA **91:**9818–9822.
30. **Maekawa, K., N. Imagawa, A. Naito, S. Harada, O. Yoshie, and S. Takagi.** 1999. Association of protein-tyrosine phosphatase PTP-BAS with the transcription-factor-inhibitory protein IkappaBalpha through interaction between the PDZ1 domain and ankyrin repeats. Biochem. J. **337:**179–184.
31. **Maximov, A., T. C. Sudhof, and I. Bezprozvanny.** 1999. Association of neuronal calcium channels with modular adaptor proteins. J. Biol. Chem. **274:** 24453–24456.
32. **McAllister, R. M., M. B. Gardner, A. E. Greene, C. Bradt, W. W. Nichols, and B. H. Landing.** 1971. Cultivation in vitro of cells derived from a human osteosarcoma. Cancer **27:**397–402.
33. **Muller, B. M., U. Kistner, R. W. Veh, C. Cases-Langhoff, B. Becker, E. D. Gundelfinger, and C. C. Garner.** 1995. Molecular characterization and spatial distribution of SAP97, a novel presynaptic protein homologous to SAP90 and the *Drosophila* discs-large tumor suppressor protein. J. Neurosci. **15:** 2354–2366.
34. **Nevins, J. R., and P. K. Vogt.** 1996. Cell transformation by viruses, p. 301–343. *In* B. N. Fields, D. M. Knipe, and P. M. Howley (ed.), Fields virology, 3rd ed., vol. 1. Lippincott-Raven, Philadelphia, Pa.
35. **Pawson, T., and J. D. Scott.** 1997. Signaling through scaffold, anchoring, and adaptor proteins. Science **278:**2075–2080.
36. **Pim, D., A. Storey, M. Thomas, P. Massimi, and L. Banks.** 1994. Mutational analysis of HPV-18 E6 identifies domains required for p53 degradation in vitro, abolition of p53 transactivation in vivo and immortalisation of primary BMK cells. Oncogene **9:**1869–1876.
37. **Ranganathan, R., and E. M. Ross.** 1997. PDZ domain proteins: scaffolds for signaling complexes. Curr. Biol. **7:**R770–R773.
38. **Rapp, L., and J. J. Chen.** 1998. The papillomavirus E6 proteins. Biochim. Biophys. Acta **1378:**F1–F19.
39. **Rongo, C., C. W. Whitfield, A. Rodal, S. K. Kim, and J. M. Kaplan.** 1998. LIN-10 is a shared component of the polarized protein localization pathways in neurons and epithelia. Cell **94:**751–759.

40. **Saras, J., and C. H. Heldin.** 1996. PDZ domains bind carboxy-terminal sequences of target proteins. Trends Biochem. Sci. **21:**455–458.
41. **Scheffner, M., J. M. Huibregtse, R. D. Vierstra, and P. M. Howley.** 1993. The HPV-16 E6 and E6-AP complex functions as a ubiquitin-protein ligase in the ubiquitination of p53. Cell **75:**495–505.
42. **Scheffner, M., B. A. Werness, J. M. Huibregtse, A. J. Levine, and P. M. Howley.** 1990. The E6 oncoprotein encoded by human papillomavirus types 16 and 18 promotes the degradation of p53. Cell **63:**1129–1136.
43. **Shah, K. V., and P. M. Howley.** 1996. Papillomaviruses, p. 2077–2109. *In* B. N. Fields, D. M. Knipe, and P. M. Howley (ed.), Fields virology, 3rd ed., vol. 2. Lippincott-Raven, Philadelphia, Pa.
44. **Shenk, T.** 1996. Adenoviridae: the viruses and their replication, p. 2111–2148. *In* B. N. Fields, D. M. Knipe, and P. M. Howley (ed.), Fields virology, 3rd ed., vol. 2. Lippincott-Raven, Philadelphia, Pa.
45. **Simonian, M. H., and J. A. Smith.** 1996. Quantitation of proteins, p. 10.1.1–10.1.10. *In* F. M. Ausubel, R. Brent, R. E. Kingston, D. D. Moore, J. G. Seidman, J. A. Smith, and K. Struhl (ed.), Current protocols in molecular biology, vol. 2. Greene Publishing Associates and Wiley-Interscience, New York, N.Y.
46. **Smith, D. B., and L. M. Corcoran.** 1994. Expression and purification of glutathione-*S*-transferase fusion proteins, p. 16.7.1–16.7.7. *In* F. M. Ausubel, R. Brent, R. E. Kingston, D. D. Moore, J. G. Seidman, J. A. Smith, and K. Struhl (ed.), Current protocols in molecular biology, vol. 2. Greene Publishing Associates and Wiley-Interscience, New York, N.Y.
47. **Song, S., H. C. Pitot, and P. F. Lambert.** 1999. The human papillomavirus type 16 E6 gene alone is sufficient to induce carcinomas in transgenic animals. J. Virol. **73:**5887–5893.
48. **Songyang, Z., A. S. Fanning, C. Fu, J. Xu, S. M. Marfatia, A. H. Chishti, A. Crompton, A. C. Chan, J. M. Anderson, and L. C. Cantley.** 1997. Recognition of unique carboxyl-terminal motifs by distinct PDZ domains. Science **275:**73–77.
49. **Strauss, W. M.** 1993. Hybridization with radioactive probes, p. 6.3.1–6.3.6. *In* F. M. Ausubel, R. Brent, R. E. Kingston, D. D. Moore, J. G. Seidman, J. A. Smith, and K. Struhl (ed.), Current protocols in molecular biology, vol. 1. Greene Publishing Associates and Wiley-Interscience, New York, N.Y.
50. **Stricker, N. L., K. S. Christopherson, B. A. Yi, P. J. Schatz, R. W. Raab, G. Dawes, D. E. Bassett, Jr., D. S. Bredt, and M. Li.** 1997. PDZ domain of neuronal nitric oxide synthase recognizes novel C-terminal peptide sequences. Nat. Biotechnol. **15:**336–342.
51. **Tabor, S., K. Struhl, S. J. Scharf, and D. H. Gelfand.** 1990. DNA-dependent DNA polymerases, p. 3.5.1–3.5.15. *In* F. M. Ausubel, R. Brent, R. E. Kingston, D. D. Moore, J. G. Seidman, J. A. Smith, and K. Struhl (ed.), Current protocols in molecular biology, vol. 1. Greene Publishing Associates and Wiley-Interscience, New York, N.Y.
52. **Thomas, D. L., S. Shin, B. H. Jiang, H. Vogel, M. A. Ross, M. Kaplitt, T. E. Shenk, and R. T. Javier.** 1999. Early region 1 transforming functions are dispensable for mammary tumorigenesis by human adenovirus type 9. J. Virol. **73:**3071–3079.
53. **Thomas, M., and L. Banks.** 1998. Inhibition of Bak-induced apoptosis by HPV-18 E6. Oncogene **17:**2943–2954.
54. **Tsunoda, S., J. Sierralta, Y. Sun, R. Bodner, E. Suzuki, A. Becker, M. Socolich, and C. S. Zuker.** 1997. A multivalent PDZ-domain protein assembles signalling complexes in a G-protein-coupled cascade. Nature **388:**243–249.
55. **Ullmer, C., K. Schmuck, A. Figge, and H. Lubbert.** 1998. Cloning and characterization of MUPP1, a novel PDZ domain protein. FEBS Lett. **424:** 63–68.
56. **Weiss, R. S., M. O. Gold, H. Vogel, and R. T. Javier.** 1997. Mutant adenovirus type 9 E4 ORF1 genes define three protein regions required for transformation of CREF cells. J. Virol. **71:**4385–4394.
57. **Weiss, R. S., and R. T. Javier.** 1997. A carboxy-terminal region required by the adenovirus type 9 E4 ORF1 oncoprotein for transformation mediates direct binding to cellular polypeptides. J. Virol. **71:**7873–7880.
58. **Weiss, R. S., S. S. Lee, B. V. Prasad, and R. T. Javier.** 1997. Human adenovirus early region 4 open reading frame 1 genes encode growth-transforming proteins that may be distantly related to dUTP pyrophosphatase enzymes. J. Virol. **71:**1857–1870.
59. **Weiss, R. S., M. J. McArthur, and R. T. Javier.** 1996. Human adenovirus type 9 E4 open reading frame 1 encodes a cytoplasmic transforming protein capable of increasing the oncogenicity of CREF cells. J. Virol. **70:**862–872.
60. **Westphal, R. S., and E. Sanders-Bush.** 1996. Differences in agonist-independent and -dependent 5-hydroxytryptamine 2C receptor-mediated cell division. Mol. Pharmacol. **49:**474–480.
61. **Willott, E., M. S. Balda, A. S. Fanning, B. Jameson, C. Van Itallie, and J. M. Anderson.** 1993. The tight junction protein ZO-1 is homologous to the *Drosophila* discs-large tumor suppressor protein of septate junctions. Proc. Natl. Acad. Sci. USA **90:**7834–7838.
62. **Wu, H., S. M. Reuver, S. Kuhlendahl, W. J. Chung, and C. C. Garner.** 1998. Subcellular targeting and cytoskeletal attachment of SAP97 to the epithelial lateral membrane. J. Cell Sci. **111:**2365–2376.
63. **Xia, H., S. T. Winokur, W. L. Kuo, M. R. Altherr, and D. S. Bredt.** 1997. Actinin-associated LIM protein: identification of a domain interaction between PDZ and spectrin-like repeat motifs. J. Cell Biol. **139:**507–515.
64. **Yang, N., O. Higuchi, and K. Mizuno.** 1998. Cytoplasmic localization of LIM-kinase 1 is directed by a short sequence within the PDZ domain. Exp. Cell Res. **241:**242–252.

Oncogene (2000) 19, 5270–5280

www.nature.com/onc

Paper 5

Interactions of the PDZ-protein MAGI-1 with adenovirus E4-ORF1 and high-risk papillomavirus E6 oncoproteins

Britt A Glaunsinger[1], Siu Sylvia Lee[1], Miranda Thomas[2], Lawrence Banks[2] and Ronald Javier*[,1]

[1]*Department of Molecular Virology and Microbiology, Baylor College of Medicine, Houston, Texas, TX 77030, USA;*
[2]*International Center for Genetic Engineering and Biotechnology, Padriciano 99, I-34012 Trieste, Italy*

The oncoproteins of small DNA tumor viruses promote tumorigenesis by complexing with cellular factors intimately involved in the control of cell proliferation. The major oncogenic determinants for human adenovirus type 9 (Ad9) and high-risk human papillomaviruses (HPV) are the E4-ORF1 and E6 proteins, respectively. These seemingly unrelated viral oncoproteins are similar in that their transforming activities in cells depend, in part, on a carboxyl-terminal PDZ domain-binding motif which mediates interactions with the cellular PDZ-protein DLG. Here we demonstrated that both Ad9 E4-ORF1 and high-risk HPV E6 proteins also bind to the DLG-related PDZ-protein MAGI-1. These interactions resulted in MAGI-1 being aberrantly sequestered in the cytoplasm by the Ad9 E4-ORF1 protein or being targeted for degradation by high-risk HPV E6 proteins. Transformation-defective mutant viral proteins, however, were deficient for these activities. Our findings indicate that MAGI-1 is a member of a select group of cellular PDZ proteins targeted by both adenovirus E4-ORF1 and high-risk HPV E6 proteins and, in addition, suggest that the tumorigenic potentials of these viral oncoproteins depend, in part, on an ability to inhibit the function of MAGI-1 in cells. *Oncogene* (2000) **19,** 5270–5280.

Keywords: adenovirus E4-ORF1; MAGI-1; papillomavirus E6; PDZ

Introduction

Human adenoviruses are associated primarily with respiratory, gastrointestinal, and eye infections in people but, in rodents, some of these viruses have the capacity to induce tumors (Shenk, 1996). Based on the types of tumors elicited and the oncoproteins that determine their tumorigenicity, two different classes of oncogenic human adenoviruses can be distinguished. Human adenoviruses from subgroups A and B induce primarily undifferentiated sarcomas at the site of injection, and the tumorigenic potential of these viruses depends solely on their nuclear E1A and E1B transforming proteins (Shenk, 1996). In contrast, subgroup D human adenovirus type 9 (Ad9) generates exclusively estrogen-dependent mammary tumors (Javier *et al.*, 1991), and the tumorigenic potential of this virus relies on its cytoplasmic Ad9 E4-ORF1 (9ORF1) transforming protein (Javier, 1994; Thomas *et al.*, 1999).

*Correspondence: R Javier
Received 19 April 2000; revised 11 August 2000; accepted 4 September 2000

Human papillomaviruses (HPV) are the etiological agents of warts in people. With regard to HPVs that infect the genital tract, high-risk HPVs (types 16, 18, 31, and 45) are strongly associated with cervical cancer whereas low-risk HPVs (types 6 and 11) are weakly or not associated with this disease (Howley, 1996). In addition, the major oncogenic determinants of high-risk HPVs are their E7 and E6 gene products. Interestingly, the tumorigenic potentials of high-risk HPV E7 and E6 and adenovirus E1A and E1B, as well as SV40 large T-antigen, similarly depend in part on their capacity to complex with and inactivate the tumor suppressor proteins pRb and p53 (Nevins and Vogt, 1996). Such findings have revealed that seemingly unrelated oncoproteins from DNA tumor viruses often target common cellular factors having critical roles in the control of cellular proliferation. We and others recently showed that the seemingly unrelated adenovirus E4-ORF1 and high-risk HPV E6 proteins, as well as the human T-cell leukemia virus type I (HTLV-1) Tax protein, likewise target a common cellular factor (Lee *et al.*, 1997). It was found that these viral oncoproteins similarly bind to the cellular PDZ domain-containing protein DLG (Kiyono *et al.*, 1997; Lee *et al.*, 1997), which is a mammalian homolog of the *Drosophila* tumor suppressor protein dlg (Lue *et al.*, 1994; Muller *et al.*, 1995).

PDZ domains are 80–90 amino-acid protein-protein interaction modules most often found within cellular factors that function in signal transduction (Fanning and Anderson, 1999). These domains typically bind specific sequence motifs located at the extreme carboxyl-terminus of target proteins, although they also participate in other types of protein interactions. Three different types of carboxyl-terminal PDZ domain-binding motifs are recognized and, at their extreme carboxyl-termini, adenovirus E4-ORF1, high-risk HPV E6, and HTLV-1 Tax proteins possess a type I motif having the consensus sequence -(T/S)-X-(V/I)-COOH (X, any amino-acid [aa] residue) (Lee *et al.*, 1997). These PDZ domain-binding motifs mediate interactions with one or more PDZ domains of DLG and, for the 9ORF1 and high-risk HPV-16 E6 proteins, disruption of this motif abolishes their transforming activity (Kiyono *et al.*, 1997; Lee *et al.*, 1997). These findings suggest that transformation by these viral oncoproteins depends in part on their ability to block the function of DLG.

Drosophila dlg has been designated as a tumor suppressor protein because, for larvae carrying homozygous *dlg* mutations, imaginal disc epithelial cells exhibit loss of polarity and neoplastic outgrowth and, in addition, certain neuronal cells of the brain undergo hyperplastic growth (Woods and Bryant, 1991). The

fact that DLG rescues the phenotypic defects of *Drosophila* unable to express functional dlg indicates that these two proteins are functionally homologous (Thomas *et al.*, 1997). These two closely-related proteins are members of the membrane-associated guanylate kinase (MAGUK) family of proteins, which typically have a domain structure consisting of one or more amino-terminal PDZ domains, an internal SH3 domain, and a carboxyl-terminal guanylate kinase-homology domain (Craven and Bredt, 1998). In general, this family of polypeptides functions to properly localize membrane and cytosolic proteins to the plasma membrane at specialized regions of cell-cell contact, as well as to organize these targets into large signaling complexes (Fanning and Anderson, 1999). These results, together with our recent finding that high-risk HPV E6 proteins target DLG for degradation in cells (Gardiol *et al.*, 1999), suggest a model whereby the proposed cell signaling regulatory activities of DLG function to suppress inappropriate proliferation of cells.

Our previous findings with the 9ORF1 oncoprotein suggest that its oncogenic potential depends not only on interactions with DLG (Lee *et al.*, 1997), but also with other unidentified cellular PDZ proteins (p220, p180, p160, p155) (Weiss *et al.*, 1997a). In this paper, we screened a panel of large cellular PDZ proteins for an ability to bind the 9ORF1 protein in order to identify additional cellular factors that contribute to 9ORF1-induced transformation. We found that 9ORF1, as well as high-risk HPV E6 oncoproteins, selectively complex with the widely-expressed cellular PDZ-protein MAGI-1, a MAGUK protein related to DLG. Additional results showed that MAGI-1 is aberrantly sequestered in the cytoplasm of cells by the 9ORF1 protein and is targeted for degradation in cells by high-risk HPV E6 proteins, suggesting that the transforming potentials of two unrelated viral oncoproteins depend in part on an ability to inactivate this cellular PDZ protein.

Results

9ORF1 complexes with the PDZ-protein MAGI-1 in cells

The transforming activity of the 9ORF1 oncoprotein depends on its carboxyl-terminal PDZ domain-binding motif (Table 1) (Lee *et al.*, 1997), which mediates direct interactions with multiple large cellular polypeptides (p220, p180, p160, p155, and p140/p130) (Weiss *et al.*, 1997a). Whereas 9ORF1-associated protein p140/p130 was previously identified as the PDZ-protein DLG (Lee *et al.*, 1997), the identities of the remaining 9ORF1-associated proteins have not been determined. Reasoning that, like DLG, these unidentified 9ORF1-associated polypeptides contain PDZ domains and also considering their predicted sizes (155–220 kD), we examined a group of cellular PDZ-proteins that included FAP-1 (273 kD) (Sato *et al.*, 1995), ZO-1 (220 kD) (Willott *et al.*, 1993), AF-6 (182 kD) (Prasad *et al.*, 1993), hINADL (167 kD) (Philipp and Flockerzi, 1997), MAGI-1 (152 kD) (Dobrosotskaya *et al.*, 1997), and ZO-3 (130 kD) (Haskins *et al.*, 1998) for binding to 9ORF1. Using a variety of assays, we demonstrated that 9ORF1 bound to the widely-expressed PDZ-protein MAGI-1 (see below), but not to the other PDZ-proteins indicated above (data not shown).

Although its function is not known, MAGI-1 is a MAGUK protein related to DLG (Dobrosotskaya *et al.*, 1997). MAGI-1 is structurally inverted relative to DLG, however, as MAGI-1 has a guanylate kinase-homology domain at its amino-terminus and five PDZ domains at its carboxyl-terminus (Figure 1). In addition, MAGI-1 possesses two WW domains rather than the SH3 domain of DLG. Three MAGI-1 isoforms (a, b and c), identical except for sequences carboxyl-terminal to PDZ5, have been identified (Figure 1). The presence of a consensus bipartite nuclear localization signal within the unique carboxyl-terminal sequences of MAGI-1c hints that this particular isoform may under certain conditions have functions in the nucleus.

To show binding of MAGI-1 to the 9ORF1 protein, we subjected extracts of COS-7 cells expressing HA epitope-tagged mouse MAGI-1b (HAMAGI-1b) or MAGI-1c (HAMAGI-1c) to GST-pulldown assays with a wild-type 9ORF1 fusion protein. We found that wild-type 9ORF1 complexed similarly with both MAGI-1b (data not shown) and MAGI-1c (Figure 2a; upper panel). Like 9ORF1, the related E4-ORF1 transforming proteins of adenovirus types 5 (5ORF1)

Table 1 Carboxyl-terminal amino-acid sequences of wild-type and mutant adenovirus E4-ORF1 and human papillomavirus (HPV) E6 proteins*

Proteins	*Carboxyl-terminal amino-acid sequence*			
	Consensus type I PDZ domain-binding motif			
	X	*(S/T)*	*X*	*(V/I/L)-COOH*
Adenovirus E4-ORF1				
wt 9ORF1	A	T	L	V
mutant IIIA	A	**P**		
mutant IIIC	**D**	T	L	V
mutant IIID	A	T	**P**	V
wt 5ORF1	A	S	N	V
wt 12ORF1	A	S	L	I
HPV E6				
wt 18E6	E	T	Q	V
mutant 18E6-V158A	E	T	Q	**A**
wt 16E6	E	T	Q	L
mutant 16E6-T149D/L151A	E	**D**	Q	**A**
wt 11E6	D	L	L	P

*The carboxyl-terminal sequences of Ad9 E4 ORF1 (9ORF1), HPV-18 E6 (18E6), and HPV-16 E6 (16E6) define a type I PDZ domain-binding motif, which is not present at the carboxyl-terminus of HPV-11 E6 (11E6). Substitution mutations are indicated by bold amino-acid residues

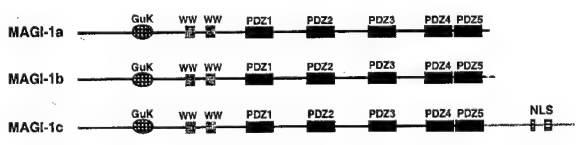

Figure 1 Three isoforms of MAGI-1. MAGI-1 has an inverted MAGUK domain structure with a guanylate kinase-homology domain (GuK) at its amino-terminus and PDZ domains at its carboxyl-terminus. MAGI-1a, -1b, and -1c isoforms are identical except that their sequences diverge carboxyl-terminal to PDZ5. WW, WW domain; NLS, putative bipartite nuclear localization signal

and 12 (12ORF1) also possess carboxyl-terminal PDZ domain-binding motifs (Table 1) and likewise bound to both MAGI-1b (data not shown) and MAGI-1c in these assays (Figure 2a; lower panel). With the use of MAGI-1-specific antibodies (Dobrosotskaya *et al.*, 1997), we also showed that 9ORF1 is similarly able to associate with endogenous MAGI-1 protein derived from extracts of CREF rat embryo fibroblasts (Figure 2b). Which MAGI-1 isoform(s) is expressed in CREF cells was not determined, but the size of the detected polypeptide is most consistent with that of MAGI-1c. Also notable was that MAGI-1 and 9ORF1-associated protein p180 co-migrated in protein gels, suggesting that these proteins are the same (Figure 3).

The specificity of the binding results described above in Figure 2 was demonstrated by inclusion of 9ORF1 mutant proteins in the same experiments. The PDZ domain-binding motif of severely transformation-defective 9ORF1 mutant IIIA is disrupted by deletion (Table 1), which renders this mutant unable to complex with any 9ORF1-associated proteins (Weiss *et al.*, 1997a; Weiss and Javier, 1997). In contrast, the PDZ domain-binding motifs of the weak-transforming 9ORF1 mutants IIIC and IIID have less disruptive missense mutations (Table 1), which permit these mutants to bind a subset of 9ORF1-associated proteins, albeit at substantially reduced levels in most cases (Weiss *et al.*, 1997a; Weiss and Javier, 1997). In GST-pulldown assays, we found that MAGI-1 failed to

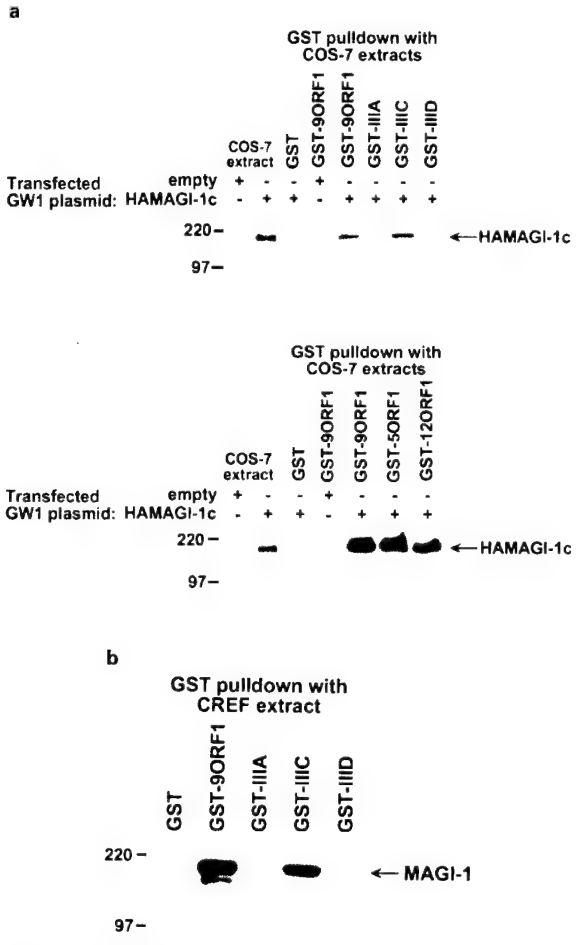

Figure 2 Binding of 9ORF1 to MAGI-1 *in vitro*. (**a**) 9ORF1 protein binding to mouse MAGI-1c detected in GST-pulldown assays. Extracts of RIPA buffer-lysed COS-7 cells transfected with 5 μg of empty GW1 or 5 μg of GWI-HAMAGI-1c plasmid were used in GST-pulldown reactions with the indicated GST fusion protein, and recovered proteins were immunoblotted with HA antibodies. Upper panel, MAGI-1 binding to wild-type and mutant 9ORF1 proteins (see Table 1). Lower panel, MAGI-1 binding to the wild-type E4-ORF1 proteins of Ad9, Ad5 (5ORF1), and Ad12 (12ORF1). COS-7 extracts representing one-half the amount used in GST pulldown reactions were also directly immunoblotted with HA antibodies as a control. (**b**) 9ORF1 binding to endogenous rat MAGI-1 of CREF cells using GST-pulldown assays. CREF cell extracts in RIPA buffer were subjected to GST-pulldown assays and then immunoblotted with MAGI-1 antibodies

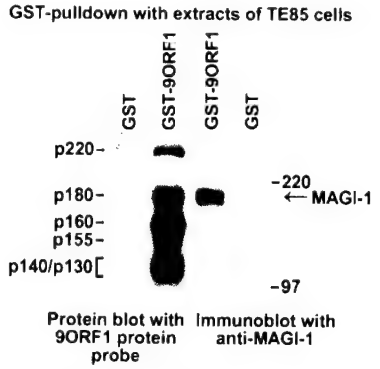

Figure 3 Co-migration of MAGI-1 and 9ORF1-associated protein p180 in a protein gel. GST-pulldown reactions using GST or GST-9ORF1 protein were performed with extracts of human TE85 cells in RIPA buffer. Recovered proteins from duplicate GST-pulldown reactions were separated in parallel by SDS–PAGE and transferred to a membrane, and membranes were either blotted with a radiolabeled 9ORF1 protein probe (left) or with MAGI-1 antibodies (right)

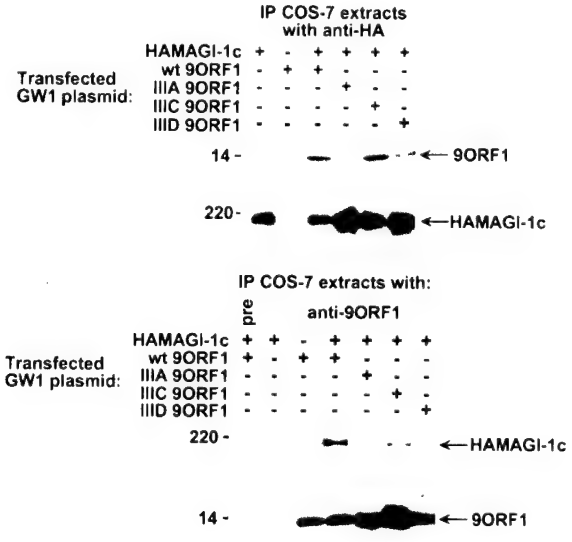

Figure 4 Binding of 9ORF1 to MAGI-1 *in vivo*. Co-immunoprecipitation assays were performed with extracts of COS-7 cells transfected with 4 μg of GW1-HAMAGI-1 plasmid and either 4 μg empty GW1 or 4 μg of GW1 plasmid expressing wild-type or the indicated mutant 9ORF1 protein. COS-7 extracts in RIPA buffer were subjected to immunoprecipitation with either HA antibodies (upper panel) or 9ORF1 antibodies (lower panel), and recovered proteins were separately immunoblotted with the same two antibodies. In the lower panel, immunoprecipitation of the COS-7 extract with pre-immune serum (pre) was included as a negative control

complex with mutant IIIA, yet complexed with mutant IIIC at approximately wild-type levels or with mutant IIID at substantially reduced levels (Figures 2a, b). The fact that this binding profile of MAGI-1 to wild-type and mutant 9ORF1 proteins was identical to that previously observed for 9ORF1-associated protein p180 (Weiss and Javier, 1997) provided further support for the idea that these proteins are the same. More important, these findings indicated that 9ORF1 binding to MAGI-1 is specific and depends on a functional 9ORF1 PDZ domain-binding motif.

We next performed reciprocal co-immunoprecipitation assays with extracts of COS-7 cells co-expressing HAMAGI-1c and either wild-type or mutant 9ORF1 protein. We found that MAGI-1 co-precipitated with wild-type 9ORF1 but failed to co-precipitate with mutant IIIA (Figure 4). MAGI-1 also co-precipitated with mutants IIIC and IIID, but at levels slightly below or substantially below, respectively, that of the wild-type 9ORF1 protein (Figure 4). These results were concordant with those of the GST-pulldown assays (see Figure 2) and also indicated that 9ORF1 and MAGI-1 form specific complexes in cells.

9ORF1 interacts primarily with MAGI-1 PDZ1 and PDZ3

The fact that disrupting the PDZ domain-binding motif of 9ORF1 impairs its binding to MAGI-1 implies that this viral protein binds one or more MAGI-1 PDZ domains. To verify this prediction, we performed protein blotting assays by incubating membrane-immobilized fusion proteins of individual MAGI-1 PDZ domains with a radiolabeled 9ORF1 protein probe. In these assays, the wild-type 9ORF1 protein probe bound strongly with PDZ1 and PDZ3, weakly with PDZ2, but failed to bind either PDZ4 or PDZ5 (Figure 5a). Additionally, none of these MAGI-1 PDZ domains reacted with a mutant IIIA protein probe (data not shown), indicating that the detected binding was specific and dependent on a functional 9ORF1 PDZ domain-binding motif.

As 9ORF1 mutants IIIC and IIID displayed nearly wild-type or reduced binding, respectively, to MAGI-1 (see Figures 2 and 4), these mutant proteins were also used as probes in protein blotting assays. In these experiments, mutants IIIC and IIID displayed recipro-

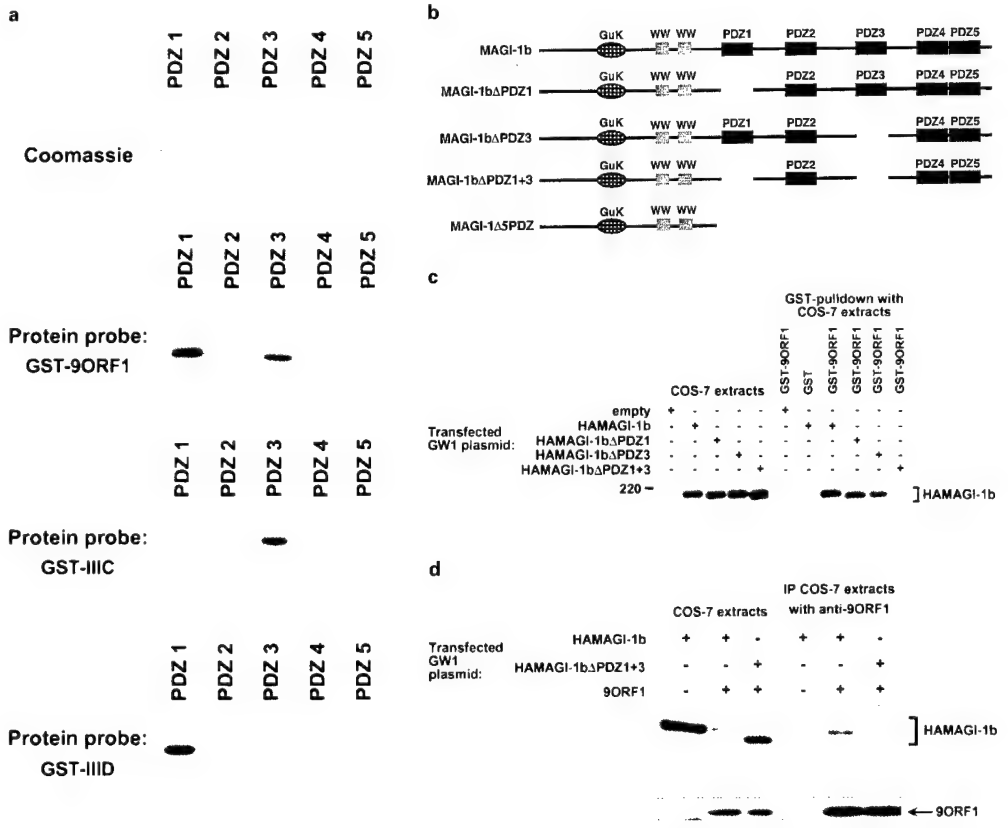

Figure 5 Binding of 9ORF1 to MAGI-1 PDZ1 and PDZ3. (**a**) Strong binding of 9ORF1 to two of five MAGI-1 PDZ domains. GST proteins fused to individual MAGI-1 PDZ domains were separated by SDS–PAGE, immobilized on duplicate membranes, and either stained with coomassie or protein blotted with the indicated wild-type or mutant 9ORF1 fusion protein probe. (**b**) Illustration of MAGI-1 deletion mutants. (**c**) A MAGI-1 mutant missing PDZ1 and PDZ3 fails to interact with 9ORF1 in GST pulldown assays. Extracts of RIPA buffer-lysed COS-7 cells transfected with 5 μg of GW1 plasmid expressing either HA-tagged wild-type or the indicated mutant MAGI-1 protein were subjected to GST-pulldown reactions with either GST or GST-9ORF1 fusion protein, and recovered proteins were immunoblotted with HA antibodies. COS-7 extracts representing one-tenth the amount used in GST pulldown reactions were also directly immunoblotted with HA antibodies as a control. (**d**) A MAGI-1 mutant missing PDZ1 and PDZ3 fails to interact with 9ORF1 in co-immunoprecipitation assays. Co-immunoprecipitation assays were performed with extracts of COS-7 cells transfected with 4 μg of wild-type or mutant GW1-HAMAGI-1 plasmid and either 4 μg empty GW1 or 4 μg of GW1-9ORF1 plasmid. COS-7 extracts in RIPA buffer were subjected to immunoprecipitation with 9ORF1 antibodies, and recovered proteins were separately immunoblotted with either HA antibodies (upper panels) or 9ORF1 antibodies (lower panels)

cal defects in binding to MAGI-1 PDZ1 and PDZ3. Specifically, mutant IIIC reacted with PDZ3 but not with PDZ1 and mutant IIID reacted with PDZ1 but not with PDZ3 (Figure 5a). Also, mutant IIID bound to MAGI-1 PDZ2, but mutant IIIC did not interact detectably with this domain. These results revealed that, although they are able to bind MAGI-1, mutants IIIC and IIID both have impaired domain interactions with this PDZ protein.

To confirm that MAGI-1 PDZ1 and PDZ3 primarily determine binding of 9ORF1 to the full-length MAGI-1 polypeptide, we constructed a MAGI-1 double-deletion mutant missing both PDZ1 and PDZ3 (HAMAGI-1ΔPDZ1+3) (Figure 5b). In agreement with the results of protein blotting assays (see Figure 5a), 9ORF1 failed to bind HAMAGI-1ΔPDZ1+3 both in GST-pulldown assays (Figure 5c) and in co-immunoprecipitation assays (Figure 5d). Although 9ORF1 can bind to MAGI-1 PDZ2 (see Figure 5a), this weak interaction was presumably too low to detect in these experiments. These findings showed that MAGI-1 PDZ1 and PDZ3, and no other region of MAGI-1, largely mediate binding to 9ORF1.

Contrary to results obtained with the HAMAGI-1ΔPDZ1+3 double-deletion mutant, MAGI-1 single-deletion mutants missing either only PDZ1 (HAMAGI-1ΔPDZ1) or only PDZ3 (HAMAGI-1ΔPDZ3) (Figure 5b) associated with 9ORF1 at approximately wild-type levels (Figure 5c), demonstrating that either PDZ1 alone or PDZ3 alone is sufficient to confer upon

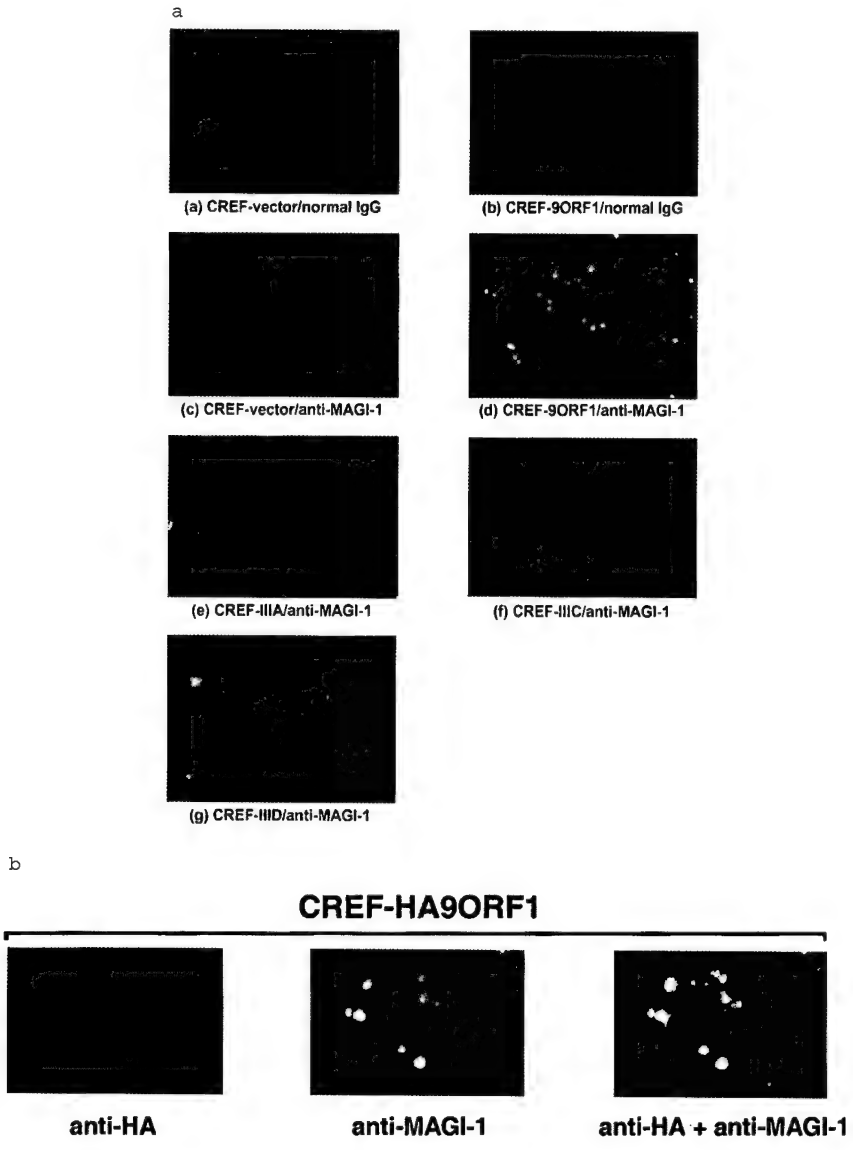

Figure 6 Aberrant sequestration of MAGI-1 in the cytoplasm of 9ORF1-expressing CREF cells. (**a**) Localization of MAGI-1 in normal CREF cells or CREF cells expressing wild-type or mutant 9ORF1 proteins. Indirect immunofluorescence assays were performed with normal CREF cells (panels a and c) or CREF cells stably expressing wild-type 9ORF1 (panels b and d), mutant IIIA (panel e), mutant IIIC (panel f), or mutant IIID (panel g). Cells were reacted with either normal rabbit IgG (panels a–b) or MAGI-1 antibodies (panels c–g) and visualized by fluorescence microscopy. (**b**) Co-localization of 9ORF1 and MAGI-1 proteins in CREF cells. Double-label indirect immunofluorescence assays were performed by reacting CREF cells stably expressing HA epitope-tagged 9ORF1 (CREF-HA9ORF1) with both HA and MAGI-1 antibodies. Each of the three panels represents the same field containing a single representative cell stained for 9ORF1 (left panel), MAGI-1 (center panel), or the merged images (right panel)

MAGI-1 wild-type binding to 9ORF1. This finding also suggested that the strong binding of mutant IIIC to MAGI-1 (see Figures 2 and 4) is due to this mutant retaining approximately wild-type affinity for PDZ3 and that the weak binding of mutant IIID to MAGI-1 (see Figures 2 and 4) is due to this mutant having reduced affinity for PDZ1. The reason that the predicted reduced affinity of mutant IIID for PDZ1 was not revealed in protein blotting assays (see Figure 5a) is not clear, but it may be due to differences in the specific activity of each protein probe.

9ORF1 aberrantly sequesters MAGI-1 in the cytoplasm of cells

Indirect immunofluorescence (IF) microscopy assays were used to ascertain the subcellular distribution of MAGI-1 in cells. We found that, in normal CREF fibroblasts, MAGI-1 was primarily distributed diffusely within the cytoplasm (Figure 6a). Other PDZ proteins also localize in the cytoplasm (Wu *et al*., 1998; Yang *et al*., 1998), although these types of polypeptides more often associate with the plasma membrane at sites of cell-cell contact in epithelial cells (Fanning and Anderson, 1999). Because 9ORF1 is present within punctate bodies in the cytoplasm of CREF cells (Weiss *et al*., 1996), we hypothesized that the staining pattern of MAGI-1 in 9ORF1-expressing CREF cells would be dramatically altered from that of normal CREF cells, resembling that of 9ORF1. As expected, MAGI-1 was redistributed within punctate bodies in the cytoplasm of CREF cells expressing wild-type 9ORF1 (CREF-9ORF1) (Figure 6a). This aberrant localization of MAGI-1 was due to association of 9ORF1 with MAGI-1, as these proteins co-localized in these cells (Figure 6b).

We also examined the subcellular distribution of MAGI-1 in CREF cell lines stably expressing mutant 9ORF1 proteins (see Table 1) which, similar to wild-type 9ORF1, exhibit punctate cytoplasmic staining in CREF cells (Weiss *et al*., 1997a). Despite the fact that each of the different CREF cell lines expressed 9ORF1 protein at comparable levels (Figure 7, upper panel),

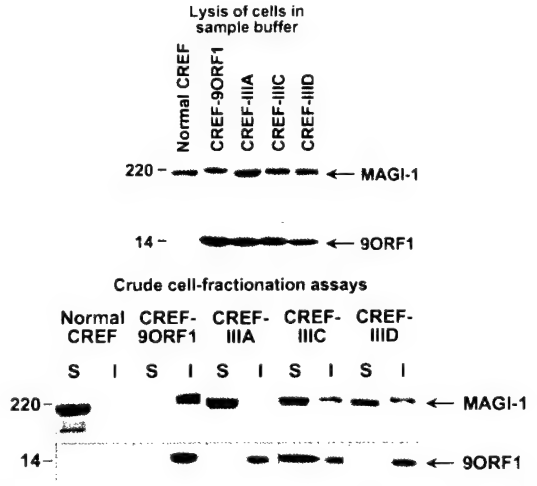

Figure 7 Aberrant sequestration of MAGI-1 within RIPA buffer-insoluble complexes in 9ORF1-expressing CREF cells. Normal CREF cells or CREF cells stably expressing wild-type or mutant 9ORF1 protein were lysed either in sample buffer (upper panel) or in RIPA buffer and subsequently centrifuged to yield RIPA buffer-soluble supernatant (S) and RIPA buffer-insoluble pellet (I) fractions (lower panel). Extracts of sample buffer-lysed cells or equal volumes of the S and I fractions from RIPA buffer-lysed cells were separately immunoblotted with MAGI-1 antibodies or 9ORF1 antiserum

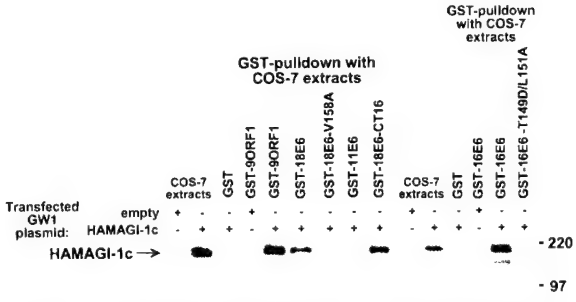

Figure 8 Binding of high-risk HPV E6 oncoproteins to MAGI-1 *in vitro*. Extracts of COS-7 cells transfected with 5 μg of empty GW1 or 5 μg of GWI-HAMAGI-1c plasmid were subjected to GST-pulldown reactions with the indicated GST fusion protein, and recovered proteins were immunoblotted with HA antibodies. GST pulldown assays with the indicated GST fusion protein were performed with COS-7 extracts in RIPA buffer or NETN buffer. COS-7 extracts representing one-tenth the amount used in GST pulldown reactions were also directly immunoblotted with HA antibodies as a control

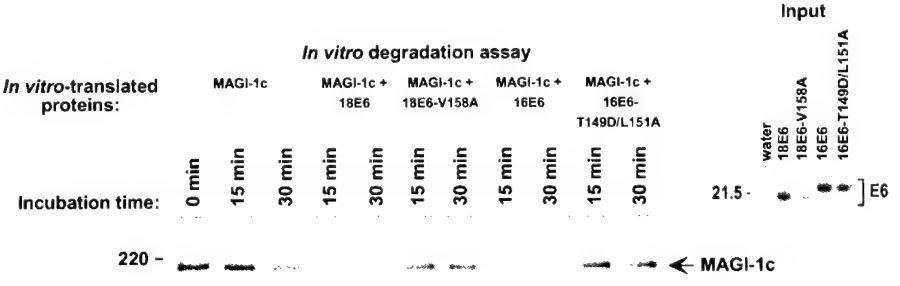

Figure 9 HPV-18 E6-induced degradation of MAGI-1 *in vitro*. *In vitro*-translated FLAG epitope-tagged MAGI-1c (MAGI-1c) was mixed with *in vitro*-translated wild-type 18E6, mutant 18E6-V158A, wild-type 16E6, mutant 16E6-T149D/L151A, or control water-primed lysates and incubated at 30°C for the indicated times. At each time point, reactions were immunoprecipitated with FLAG antibodies, and recovered proteins were separated by SDS–PAGE and visualized by autoradiography (left panel). The amount of *in vitro*-translated E6 protein used in each assay is shown (right panel)

the staining pattern of MAGI-1 in the CREF cell line expressing mutant IIIA (CREF-IIIA; Figure 6a), which fails to bind MAGI-1 (see Figure 2), was similar to that of normal CREF cells, whereas substantially less aberrant punctate staining for MAGI-1 was detected in the cytoplasm of the CREF cell line expressing mutant IIID (CREF-IIID; Figure 6a), which binds weakly to MAGI-1 (see Figure 2). Interestingly, the CREF cell line expressing mutant IIIC (CREF-IIIC), which binds MAGI-1 at nearly wild-type levels (see Figure 2), showed a MAGI-1 staining pattern similar to that of normal CREF cells (Figure 6a). Therefore, in addition to having defective PDZ-domain interactions with MAGI-1 (see Figure 5a), mutants IIIC and IIID also either failed or showed a substantially reduced capacity, respectively, to sequester MAGI-1 within punctate bodies in the cytoplasm of CREF cells.

To confirm the aberrant sequestration of MAGI-1 by 9ORF1 detected in IF assays, we performed crude cell-fractionation assays with the same CREF cell lines. In these experiments, cells lysed in RIPA buffer were separated by centrifugation into RIPA buffer-soluble supernatant and RIPA buffer-insoluble pellet fractions, each of which was immunoblotted for the presence of MAGI-1 protein. In normal CREF cells, the majority of MAGI-1 protein was detected in the RIPA buffer-soluble fraction but, in CREF-9ORF1 cells, MAGI-1 was exclusively present within the RIPA buffer-insoluble fraction (Figure 7, lower panel). It was this inability to recover soluble MAGI-1 protein from extracts of CREF-9ORF1 cells that prevented us from showing co-immunoprecipitation of 9ORF1 and MAGI-1 with this particular cell line. This observation also explained the substantially lower levels of MAGI-1 protein recovered in lysates of COS-7 cells co-expressing MAGI-1 and 9ORF1 compared to those recovered in COS-7 cells expressing MAGI-1 alone (see Figure 5d). Additionally, the results of crude cell-fractionation assays with CREF cells expressing mutant 9ORF1 proteins were in accordance with the IF findings because MAGI-1 protein was recovered primarily in the RIPA buffer-soluble fraction of the CREF-IIIA, CREF-IIIC, and CREF-IIID cell lines (Figure 7, lower panel).

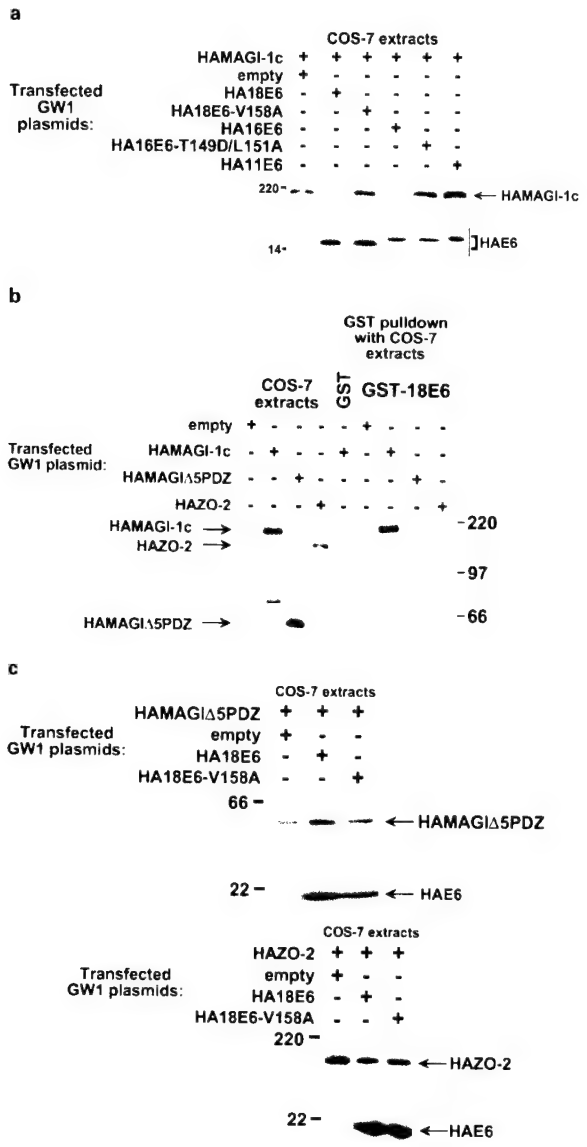

Figure 10 Selective reduction in MAGI-1 protein levels *in vivo* by high-risk HPV E6 proteins. (**a**) Decrease in the steady-state protein levels of MAGI-1 induced by high-risk HPV E6 oncoproteins. Extracts of RIPA buffer-lysed COS-7 cells transfected with 0.5 μg of GW1-HAMAGI-1c plasmid alone or in combination with 4 μg of a GW1 plasmid expressing the indicated wild-type or mutant HPV E6 protein were immunoblotted with HA antibodies. (**b**) Failure of 18E6 to bind a MAGI-1 deletion mutant missing all five PDZ domains (MAGI-1Δ5PDZ) or the wild-type ZO-2 protein. Extracts of RIPA buffer-lysed COS-7 cells transfected with 5 μg of the indicated GW1 expression plasmid were subjected to GST-pulldown reactions with either GST or GST-18E6 protein. Recovered proteins were immunoblotted with HA antibodies. COS-7 extracts representing one-tenth the amount used in GST pulldown reactions were also directly immunoblotted with HA antibodies as a control. (**c**) Inability of 18E6 to reduce the steady-state protein levels of MAGI-1Δ5PDZ or ZO-2 in cells. Extracts of RIPA buffer-lysed COS-7 cells transfected with 0.1 μg of GWI-HAMAGIΔ5PDZ plasmid (upper panel) or with 0.01 μg of GW1-HAZO-2 plasmid (lower panel), alone or in combination with 4 μg of GW1 plasmid expressing wild-type or mutant HA18E6, were immunoblotted with HA antibodies

High-risk human papillomavirus E6 oncoproteins also complex with MAGI-1

We (Lee *et al*., 1997) and others (Kiyono *et al*., 1997) previously showed that, like 9ORF1, high-risk but not

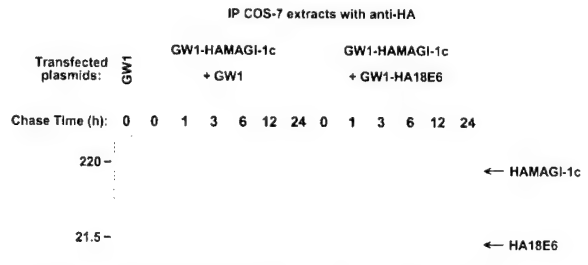

Figure 11 Decrease in MAGI-1 protein half-life induced by the high-risk HPV-18 E6 protein. COS-7 cells transfected with 0.5 μg of GW1-HAMAGI-1c plasmid in combination with 4 μg of empty GW1 or GW1-HA18E6 plasmid were pulse-labeled for 15 min with [^{35}S] EXPRESS protein label and subsequently chased with unlabeled culture medium for the indicated times. At each time point, cell extracts were immunoprecipitated with HA antibodies. Recovered MAGI-1 protein was visualized by autoradiography and quantified by phosphorimager analysis

low-risk HPV E6 oncoproteins contain functional PDZ domain-binding motifs at their carboxyl-termini (Table 1) and bind DLG. To determine whether high-risk HPV E6 oncoproteins also bind MAGI-1, we performed GST-pulldown assays with lysates of COS-7 cells expressing the HAMAGI-1c protein. The results indicated that wild-type high-risk 16E6 and 18E6, but not low-risk HPV-11 E6 (11E6), bind MAGI-1 in these assays (Figure 8). Moreover, the mutants 16E6-T149D/L151A and 18E6-V158A, which have disrupted PDZ domain-binding motifs (Table 1), failed to bind MAGI-1, indicating that the interactions between wild-type high-risk E6 oncoproteins and MAGI-1 were specific and required a functional PDZ domain-binding motif. We further demonstrated that a 16 aa-residue carboxyl-terminal 18E6 peptide (18E6-CT16) containing the PDZ domain-binding motif was sufficient to mediate binding to MAGI-1 (Figure 8).

High-risk HPV E6 oncoproteins target MAGI-1 for degradation

High-risk HPV E6 oncoproteins promote degradation of the p53 tumor suppressor protein in cells by ubiquitin-dependent proteolysis (Scheffner *et al*., 1990). As we recently showed that DLG is also targeted for degradation by high-risk HPV E6 proteins (Gardiol *et al*., 1999), it was of interest to determine whether MAGI-1 is similarly affected by these viral proteins. This possibility was initially examined by mixing and incubating *in vitro*-translated FLAG epitope-tagged MAGI-1 with wild-type or mutant 18E6 and 16E6 proteins. We found that, following incubation with either wild-type 18E6 or 16E6, MAGI-1 protein levels were substantially more reduced than following incubation with mutant 18E6-V158A or 16E6-T149D/L151A, or with a water-primed *in vitro*-translation reaction (Figure 9).

To determine whether high-risk HPV E6 proteins also specifically target MAGI-1 for degradation in cells, we compared the steady-state protein levels of MAGI-1 in COS-7 cells either expressing MAGI-1 alone or co-expressing MAGI-1 and wild-type or mutant E6 proteins. Consistent with our *in vitro* results, MAGI-1 protein levels were substantially reduced in cells expressing either wild-type 18E6 or 16E6 (Figure 10a). The results of additional experiments indicated that the reduction of MAGI-1 protein levels in cells expressing these wild-type E6 proteins was specific and due to proteolysis. First, no decrease in MAGI-1 protein levels was detected in cells expressing either the 18E6-V158A or 16E6-T149D/L151A mutant protein, or the low-risk 11E6 protein (Figure 10a). Second, consistent with our inability to detect binding of 18E6 to a truncated MAGI-1 protein lacking all five PDZ domains (MAGI-1Δ5PDZ) (see Figure 5b) or to the wild-type MAGUK-family PDZ-protein ZO-2 (Jesaitis and Goodenough, 1994) (Figure 10b), 18E6 failed to reduce the protein levels of either polypeptide in cells (Figure 10c). Finally, the results of pulse-chase experiments in COS-7 cells expressing MAGI-1 alone or co-expressing MAGI-1 and 18E6 demonstrated that the half-life of the MAGI-1 protein is drastically decreased from approximately 24 h in normal cells to approximately 1 h in 18E6-expressing cells (Figure 11). From these results, we conclude that high-risk HPV E6 oncoproteins specifically target the PDZ-protein MAGI-1 for degradation in cells.

Discussion

Interactions of the 9ORF1 oncoprotein with the MAGUK-protein DLG and with several other unidentified cellular factors (p220, p180, p160, p155) correlate with the ability of this viral protein to transform cells (Weiss and Javier, 1997). Thus, identification and characterization of the unidentified cellular proteins is expected to aid in fully revealing the mechanisms of 9ORF1-induced transformation. In this study, we showed that, in addition to DLG, 9ORF1 also binds to the related MAGUK-protein MAGI-1 and that this cellular PDZ protein likely represents the previously unidentified 9ORF1-associated protein p180. Particularly noteworthy is that all transformation-defective 9ORF1 mutants having an altered PDZ domain-binding motif displayed impaired interactions with MAGI-1. For example, the severely transformation-defective mutant IIIA and the weak-transforming mutant IIID failed or showed a substantially reduced capacity, respectively, to bind MAGI-1. In addition, although the weak-transforming mutant IIIC bound to MAGI-1 at nearly wild-type levels in cells, this mutant protein was impaired both for interacting with certain MAGI-1 PDZ domains and for aberrantly sequestering MAGI-1 within RIPA buffer-insoluble complexes in the cytoplasm of cells. With respect to the latter observation, we noted that, in contrast to wild-type 9ORF1, substantial amounts of mutant IIIC protein exist in the RIPA buffer-soluble fraction of cells, suggesting that this mutant may be inherently unable to sequester PDZ proteins in the cytoplasm of cells. Taken together, results with transformation-defective 9ORF1 mutants argue that the abilities of 9ORF1 to bind and aberrantly sequester MAGI-1 in cells contribute to 9ORF1-mediated cellular transformation. The fact that transformation-defective 9ORF1 mutants also fail to bind other 9ORF1-associated PDZ-proteins (Lee *et al*., 1997), however, suggests that interactions of 9ORF1 with additional PDZ proteins are likewise important.

It is also noteworthy that, among six different PDZ proteins examined, only MAGI-1 was found to interact with 9ORF1. This finding indicates that 9ORF1 targets only select PDZ proteins in cells. This idea is further evidenced by the select interaction of 9ORF1 with two of the five PDZ domains of MAGI-1 and two of the three PDZ domains of DLG (Lee *et al*., 1997). These observations, coupled with the fact that 9ORF1 mutants IIIC and IIID bind only one MAGI-1 PDZ domain, argue that precise sequence requirements both within the PDZ domain-binding motif of 9ORF1 and within each PDZ domain of the 9ORF1-associated targets determine these highly specific protein-protein interactions.

The fact that MAGI-1 is a MAGUK-family protein suggests that this PDZ protein functions to assemble numerous cellular targets into large signaling complexes in cells. In contrast to many PDZ proteins, however, MAGI-1 was found to localize predominantly in the cytoplasm of CREF fibroblasts. Although we cannot discount the possibility that a minor fraction of

MAGI-1 is present at the membrane of CREF cells, this finding may indicate that MAGI-1 functions primarily in the cytoplasm. Alternatively, it is feasible that MAGI-1 does function at the membrane, but its translocation to this site occurs only following specific cellular stimuli. Besides possible cytoplasmic and membrane activities, the MAGI-1c isoform, which contains a consensus bipartite nuclear localization signal (Dobrosotskaya *et al.*, 1997), may additionally function in the nucleus, perhaps to regulate the transcription of certain cellular genes. Again, we did not detect MAGI-1 in the nucleus of cells, but nuclear localization may occur only under specific conditions, as has been reported for the related MAGUK-family protein ZO-1 (Gottardi *et al.*, 1996). Regardless of where in the cell MAGI-1 functions, however, this cellular factor would likely be inactivated in 9ORF1-expressing cells, as we found that 9ORF1 aberrantly sequesters MAGI-1 in the cytoplasm of cells. Also considering that 9ORF1 binds strongly to MAGI-1 PDZ1 and PDZ3, 9ORF1 would be expected to block MAGI-1 from complexing with the normal cellular targets of these PDZ domains. Therefore, aberrant sequestration and disruption of protein complexes, as well as perturbation of associated protein activities, may all be envisioned as possible mechanisms by which 9ORF1 could inhibit the normal functions of MAGI-1 in cells.

Like 9ORF1, all known high-risk HPV E6 oncoproteins also possess a carboxyl-terminal PDZ domain-binding motif (Lee *et al.*, 1997). Significantly, disruption of the PDZ domain-binding motif of 16E6 renders this viral protein transformation-defective in rat 3Y1 fibroblasts (Kiyono *et al.*, 1997). As infections with high-risk HPV-16 and HPV-18 are associated with approximately 75% of cervical carcinomas (Bosch *et al.*, 1995), our finding that both the 16E6 and 18E6 oncoproteins, but not the low-risk 11E6 protein, utilize their carboxyl-terminal PDZ domain-binding motif to bind the PDZ-protein MAGI-1 is also likely to be important. This idea is further underscored by the facts that 16E6 and 18E6 mutant proteins having disrupted PDZ domain-binding motifs fail to bind MAGI-1 and that the wild-type viral proteins do not complex with the related MAGUK proteins ZO-1 (unpublished results) and ZO-2. Such specific and selective interactions suggest that the ability of high-risk HPV E6 oncoproteins to associate with MAGI-1 in cells may contribute to the development of HPV-associated cancers in people.

A common mechanism by which the oncoproteins of DNA tumor viruses promote tumorigenesis is the inactivation of cellular tumor suppressor proteins. For example, both the adenovirus E1B and high-risk HPV E6 oncoproteins functionally inactivate the tumor suppressor protein p53, yet by distinct mechanisms. In this regard, E1B sequesters p53 in an inactive state (Shenk, 1996), whereas high-risk HPV E6 targets p53 for ubiquitin-mediated proteolysis (Howley, 1996). Likewise, we found that the 9ORF1 oncoprotein sequesters MAGI-1 in the cytoplasm of cells whereas the high-risk HPV E6 proteins target MAGI-1 for degradation in cells. These findings argue that adenovirus E4-ORF1 and high-risk HPV E6 oncoproteins similarly inactivate MAGI-1 by distinct mechanisms. As MAGI-1 is related to DLG and both proteins are selectively targeted by two otherwise unrelated viral oncoproteins, it seems plausible that these PDZ proteins have related functions in cells. Therefore, we hypothesize that MAGI-1 similarly functions to suppress inappropriate cellular proliferation and, consequently, represents a new candidate tumor suppressor protein.

Materials and methods

Cells and cell extracts

CREF (Fisher *et al.*, 1982), TE85 (McAllister *et al.*, 1971), and COS-7 (Gluzman, 1981) cell lines were maintained in culture medium (Dulbecco's Modified Eagle Medium supplemented with gentamicin (20 μg/ml) and 6 or 10% fetal bovine serum (FBS)). CREF cell pools (group 16) stably expressing wild-type or mutant 9ORF1 protein (Weiss *et al.*, 1997a), as well as a CREF cell pool stably expressing an influenza hemagglutinin (HA) epitope-tagged 9ORF1 protein (Weiss *et al.*, 1997b), were maintained in culture medium supplemented with G418.

Cell extracts were prepared in either RIPA buffer (50 mM Tris-HCl pH 8.0, 150 mM NaCl, 1% (vol/vol) Nonidet P-40, 0.5% (wt/vol) sodium deoxycholate, 0.1% (wt/vol) sodium dodecyl sulfate (SDS)) or NETN buffer (20 mM Tris, pH 8.0, 100 mM NaCl, 1 mM EDTA, 0.5% Nonidet P-40 (vol/vol)) as described previously (Lee *et al.*, 1997). Alternatively, cells were lysed directly in sample buffer (0.15 M Tris-HCl pH 6.8, 2% (wt/vol) SDS, 10% (vol/vol) glycerol, 1% (vol/vol) β-mercaptoethanol, 0.0015% (wt/vol) bromophenol blue). For crude cell-fractionation assays, the pellet obtained after centrifugation of RIPA buffer-lysed cells was solublized in sample buffer using the same volume originally used to lyse the cells in RIPA buffer. Protein concentrations of cell extracts were determined by the Bradford assay (Bradford, 1976).

Plasmids

pCDNA3 (Invitrogen) plasmids coding for amino-terminal FLAG epitope-tagged mouse MAGI-1 isoform b (MAGI-1b), MAGI-1 isoform c (MAGI-1c), and MAGI-1b missing either PDZ1 (aa 453–549; MAGI-1bΔPDZ1), PDZ2 (aa 625–702; MAGI-1bΔPDZ2), or PDZ3 (aa 796–875; MAGI-1bΔPDZ3), as well as pGEX-KG (Pharmacia) plasmids coding for MAGI-1 PDZ1 (aa 431–545), PDZ2 (aa 601–702), PDZ4 (aa 925–1034), or PDZ5 (aa 1013–1116) were generously provided by Guy James. cDNA sequences coding for MAGI-1 PDZ3 (aa 763–880) were amplified by PCR and introduced in-frame with the glutathione *S*-transferase (GST) gene of pGEX-2T to make pGEX-MAGI-1PDZ3. pGEX-2T and pGEX-2TK plasmids coding for wild-type Ad5 and Ad12 E4-ORF1 proteins (5ORF1 and 12ORF1, respectively), as well as for wild-type or mutant 9ORF1 proteins were described previously (Weiss and Javier, 1997). The cDNAs of HPV-18 E6 (18E6) mutant 18E6-V158A, wild-type HPV-16 E6 (16E6), and mutant 16E6-T149D/L151A were introduced into the *Hin*dIII and *Eco*RI sites of pSP64 (Promega) to generate pSP64-18E6-V158A, pSP64-16E6, and pSP64-16E6-T149D/L151A, respectively. An HA-epitope tag was introduced at the amino-terminus of MAGI-1b, MAGI-1c, MAGI-1Δ5PDZ (aa 1–424), 16E6, mutant 16E6-T149D/L151A, and canine ZO-2 by PCR methods. cDNAs coding for the HA-epitope-tagged MAGI-1 and 16E6 proteins were introduced between the *Hin*dIII and *Eco*RI sites of CMV expression plasmid GW1 (British Biotechnology) to generate GW1-HAMAGI-1b, GW1-HAMAGI-1c, GW1-HAMAGI-1Δ5PDZ, GW1-HA16E6, and GW1-HA16E6-T149D/L151A. The HA-epitope-tagged ZO-2 cDNA was introduced

into the *Sma*I site of GW1 to generate GW1-HAZO-2. The deletions of pCDNA3-FLAGMAGI-1bΔPDZ1 and pCDNA3-FLAGMAGI-1bΔPDZ3 were subcloned individually or in combination into GW1-HAMAGI-1b to generate GW1-HAMAGI-1bΔPDZ1, GW1-HAMAGI-1bΔPDZ3, and GW1-HAMAGI-1bΔPDZ1+3. PCR reactions were performed with *Pfu* polymerase (Stratagene), and plasmids were verified by restriction enzyme and limited sequence analyses. Plasmids GW1-HA18E6, GW1-HA18E6-V158A, GW1-HA11E6, GWI-9ORF1wt, GW1-9ORF1IIIA, GW1-9ORF1IIIC, GW1-9ORF1IIID, and pSP64-18E6 were described elsewhere (Gardiol *et al.*, 1999).

Antisera and antibodies

Rabbit polyclonal antiserum raised to the unique amino-terminal region of MAGI-1 (aa 2–140) was generously provided by Guy James (Dobrosotskaya *et al.*, 1997). 9ORF1 antiserum was described previously (Javier, 1994). Commercially-available FLAG antibodies (Santa Cruz Biotechnology), 12CA5 HA monoclonal antibodies (BABCO; Boehringer Mannheim), normal rabbit IgG, peroxidase-conjugated goat anti-rabbit or goat anti-mouse IgG (Southern Biotechnology Associates), FITC-conjugated goat anti-rabbit or goat anti-mouse IgG (Gibco BRL), or Texas red-conjugated goat anti-mouse IgG (Molecular Probe) were used.

GST-pulldown, immunoprecipitation, and immunoblot assays

GST-pulldown and immunoprecipitation assays were performed with cell extracts in RIPA buffer as described previously (Lee *et al.*, 1997). Immunoblot assays were carried out as described previously (Weiss *et al.*, 1996) using either 9ORF1 (1:5000), HA (0.2 μg/ml), or MAGI-1 (1 μg/ml) primary antibodies and either horseradish peroxidase-conjugated goat anti-rabbit IgG or goat anti-mouse IgG (1:5000) secondary antibodies. Immunoblotted assays were developed by enhanced chemiluminescence (Pierce).

Protein blotting assays

Individual MAGI-1 PDZ domains were expressed as GST-fusion proteins in bacteria, purified on glutathione sepharose beads (Pharmacia) (Smith and Corcoran, 1994), separated by SDS-polyacrylamide gel electrophoresis (PAGE), and transferred to a nitrocellulose membrane. Methods for preparing radiolabeled GST fusion probes and for performing protein blotting assays with such probes have been described (Lee *et al.*, 1997).

Immunofluorescence microscopy assays

For indirect immunofluorescence (IF) microscopy assays (Harlow and Lane, 1988), cells were grown on coverslips, fixed in methanol for 20 min at −20°C, blocked in IF buffer (TBS (50 mM Tris-HCl pH 7.5, 200 mM NaCl) containing 10% goat serum (Sigma)) for 1 h at RT and, then, incubated with either MAGI-1 antibodies (5 μg/ml), HA antibodies (0.24 mg/ml) or normal rabbit IgG (5 μg/ml) for 3 h at 37°C. Cells were subsequently washed with TBS, blocked as described above, incubated with either FITC-conjugated goat anti-rabbit or goat anti-mouse IgG antibodies (1:250) or Texas red-conjugated goat anti-mouse IgG antibodies (1:250) for 1 h at 37°C, and washed with TBS. All antibodies were diluted in IF buffer. Cells were visualized by fluorescence microscopy using a Zeiss Axiophot microscope, and images were processed using Adobe PhotoShop software.

In vitro-*degradation assays*

pCDNA3-FLAGMAGI-1c, pSP64-18E6, pSP64-18E6-V158A, pSP64-16E6, and pSP64-16E6-T149D/L151A plasmids were transcribed and translated *in vitro* using the TnT coupled rabbit reticulocyte lysate system (Promega) and 50 μCi [^{35}S]-cysteine (1200 Ci mmol) (Amersham), according to the manufacturer's instructions. The amount of radioactivity introduced into *in vitro*-translated proteins per microliter of reaction was determined by resolving an aliquot of each reaction by SDS–PAGE and quantifying CPM within relevant protein bands using a Storm Molecular Dynamics phosphorimager. For *in vitro*-degradation assays, a reaction volume equivalent to 50 c.p.m. of *in vitro*-translated FLAGMAGI-1c protein was mixed with a reaction volume equivalent to 250 c.p.m. of *in vitro*-translated 18E6, 18E6-V158A, 16E6, or 16E6-T149D/L151A protein. All assay volumes were equalized with a water-primed *in vitro*-translation reaction and, at selected time points, an aliquot from each assay mixture was removed and subjected to immunoprecipitation analysis. Recovered proteins were resolved by SDS–PAGE and visualized by audioradiography.

Pulse-chase labeling of proteins in cells

At 48 h post-transfection, COS-7 cells were incubated with methionine- and cysteine-free DMEM containing 5% dialyzed FBS (5% FBS-DMEM-MC) for 30 min and, then, pulse labeled for 15 min in the same medium containing 0.2 mCi ml [^{35}S] EXPRESS protein label (Dupont). Following several washes with 5% FBS-DMEM-MC, pulse radiolabeled cells were chased by incubation with culture medium containing fivefold excess methionine (15 mg/l) for various times, harvested, and lysed in RIPA buffer. Cell extracts were subjected to immunoprecipitation with HA antibodies, and recovered proteins were resolved by SDS–PAGE and visualized by autoradiography. Amounts of protein immunoprecipitated were quantified using a phosphorimager.

Acknowledgments
We are indebted to Guy James (University of Texas Health Sciences Center, San Antonio) for generously providing MAGI-1 reagents. We also thank Bruce Stevenson for providing the canine ZO-2 expression plasmid. BA Glaunsinger and SS Lee were recipients of a Molecular Virology Training Grant (T32 AI07471) and the US Army Breast Cancer Training Grant (DAMD17-94-J4204), respectively. This work was supported by grants from the National Institutes of Health (RO1 CA58541), the American Cancer Society (RPG-97-668-01-VM), and the US Army (DAMD17-97-1-7082) to RT Javier and an Associazione Italiana per la Ricerca sul Cancro grant to L Banks.

References

Bosch FX, Manos MM, Munoz N, Sherman M, Jansen AM, Peto J, Schiffman MH, Moreno V, Kurman R and Shah KV. (1995). *J. Natl. Cancer Inst.*, **87,** 796–802.
Bradford MM. (1976). *Anal. Biochem.*, **72,** 248–254.
Craven SE and Bredt DS. (1998). *Cell,* **93,** 495–498.
Dobrosotskaya I, Guy RK and James GL. (1997). *J. Biol. Chem.*, **272,** 31589–31597.
Fanning AS and Anderson JM. (1999). *J. Clin. Invest.*, **103,** 767–772.

Fisher PB, Babiss LE, Weinstein IB and Ginsberg HS. (1982). *Proc. Natl. Acad. Sci. USA,* **79,** 3527–3531.
Gardiol D, Kuhne C, Glaunsinger B, Lee S, Javier R and Banks L. (1999). *Oncogene,* **18,** 5487–5496.
Gluzman Y. (1981). *Cell,* **23,** 175–182.
Gottardi CJ, Arpin M, Fanning AS and Louvard D. (1996). *Proc. Natl. Acad. Sci. USA,* **93,** 10779–10784.
Harlow E and Lane D. (1988). *Antibodies: a laboratory manual.* Harlow E and Lane D. (eds). Cold Spring Harbor Laboratory: Cold Spring Harbor, N.Y., pp 359–420.
Haskins J, Gu L, Wittchen ES, Hibbard J and Stevenson BR. (1998). *J. Cell. Biol.,* **141,** 199–208.
Howley PM. (1996). *Fields Virology, Vol. 2.* Fields BN, Knipe DM and Howley PM. (eds). Lippincott-Raven: Philadelphia, pp 2045–2076.
Javier R, Raska Jr K, Macdonald GJ and Shenk T. (1991). *J. Virol.,* **65,** 3192–3202.
Javier RT. (1994). *J. Virol.,* **68,** 3917–3924.
Jesaitis LA and Goodenough DA. (1994). *J. Cell. Biol.,* **124,** 949–961.
Kiyono T, Hiraiwa A, Fujita M, Hayashi Y, Akiyama T and Ishibashi M. (1997). *Proc. Natl. Acad. Sci. USA,* **94,** 11612–11616.
Lee SS, Weiss RS and Javier RT. (1997). *Proc. Natl. Acad. Sci. USA,* **94,** 6670–6675.
Lue RA, Marfatia SM, Branton D and Chishti AH. (1994). *Proc. Natl. Acad. Sci. USA,* **91,** 9818–9822.
McAllister RM, Filbert JE, Nicolson MO, Rongey RW, Gardner MB, Gilden RV and Huebner RJ. (1971). *Nat. New Biol.,* **230,** 279–282.
Muller BM, Kistner U, Veh RW, Cases-Langhoff C, Becker B, Gundelfinger ED and Garner CC. (1995). *J. Neurosci.,* **15,** 2354–2366.
Nevins JR and Vogt PK. (1996). *Fields Virology, Vol. 1.* Fields BN, Knipe DM and Howley PM. (eds). Lippincott-Raven Publishers: Philadelphia, pp 301–343.
Philipp S and Flockerzi V. (1997). *FEBS Lett.,* **413,** 243–248.
Prasad R, Gu Y, Alder H, Nakamura T, Canaani O, Saito H, Huebner K, Gale RP, Nowell PC, Kuriyama K, Miyazaki Y, Croce CM and Cacaani E. (1993). *Cancer Res.,* **53,** 5624–5628.
Sato T, Irie S, Kitada S and Reed JC. (1995). *Science,* **268,** 411–415.
Scheffner M, Werness BA, Huibregtse JM, Levine AJ and Howley PM. (1990). *Cell,* **63,** 1129–1136.
Shenk T. (1996). *Fields Virology, Vol. 2.* Fields BN, Knipe DM and Howley PM. (eds). Lippincott-Raven Publishers: Philadelphia, pp 2111–2148.
Smith DB and Corcoran LM. (1994). *Current Protocols in Molecular Biology, Vol. 2.* Ausubel, FM, Brent R, Kingston RE, Moore DD, Seidman JG, Smith JA and Struhl K. (eds). John Wiley and Sons, Inc.: New York, pp 16.7.1–16.7.7.
Thomas DL, Shin S, Jiang BH, Vogel H, Ross MA, Kaplitt M, Shenk TE and Javier RT. (1999). *J. Virol.,* **73,** 3071–3079.
Thomas U, Phannavong B, Muller B, Garner CC and Gundelfinger ED. (1997). *Mech. Dev.,* **62,** 161–174.
Weiss RS, Gold MO, Vogel H and Javier RT. (1997a). *J. Virol.,* **71,** 4385–4394.
Weiss RS and Javier RT. (1997). *J. Virol.,* **71,** 7873–7880.
Weiss RS, Lee SS, Prasad BVV and Javier RT. (1997b). *J. Virol.,* **71,** 1857–1870.
Weiss RS, McArthur MJ and Javier RT. (1996). *J. Virol.,* **70,** 862–872.
Willott E, Balda MS, Fanning AS, Jameson B, Van Itallie C and Anderson JM. (1993). *Proc. Natl. Acad. Sci. USA,* **90,** 7834–7838.
Woods DF and Bryant PJ. (1991). *Cell,* **66,** 451–464.
Wu H, Reuver SM, Kuhlendahl S, Chung WJ and Garner CC. (1998). *J. Cell. Sci.,* **111,** 2365–2376.
Yang N, Higuchi O and Mizuno K. (1998). *Exp. Cell Res.,* **241,** 242–252.

JOURNAL OF VIROLOGY, Jan. 2001, p. 557–568 Vol. 75, No. 2
0022-538X/01/$04.00+0 DOI: 10.1128/JVI.75.2.557–568.2001

Several E4 Region Functions Influence Mammary Tumorigenesis by Human Adenovirus Type 9

DARBY L. THOMAS,[1,2]† JEROME SCHAACK,[3] HANNES VOGEL,[4] AND RONALD JAVIER[1]*

Department of Molecular Virology and Microbiology,[1] Program in Cell and Molecular Biology,[2] and Department of Pathology,[4] Baylor College of Medicine, Houston, Texas 77030, and Department of Microbiology, Program in Molecular Biology, and University of Colorado Cancer Center, University of Colorado Health Sciences Center, Denver, Colorado 80262[3]

Received 18 August 2000/Accepted 10 October 2000

Among oncogenic adenoviruses, human adenovirus type 9 (Ad9) is unique in eliciting exclusively estrogen-dependent mammary tumors in rats and in not requiring viral E1 region transforming genes for tumorigenicity. Instead, studies with hybrid viruses generated between Ad9 and the closely related nontumorigenic virus Ad26 have roughly localized an Ad9 oncogenic determinant(s) to a segment of the viral E4 region containing open reading frame 1 (E4-ORF1), E4-ORF2, and part of E4-ORF3. Although subsequent findings have shown that E4-ORF1 codes for an oncoprotein essential for tumorigenesis by Ad9, it is not known whether other E4 region functions may similarly play a role in this process. We report here that new results with Ad9/Ad26 hybrid viruses demonstrated that the minimal essential Ad9 E4-region DNA sequences include portions of both E4-ORF1 and E4-ORF2. Investigations with Ad9 mutant viruses additionally showed that the E4-ORF1 protein and certain E4-ORF2 DNA sequences are necessary for Ad9-induced tumorigenesis, whereas the E4-ORF2 and E4-ORF3 proteins are not. In fact, the E4-ORF3 protein was found to antagonize this process. Also pertinent was that certain crucial nucleotide differences between Ad9 and Ad26 within E4-ORF1 and E4-ORF2 were found to be silent with respect to the amino acid sequences of the corresponding proteins. Furthermore, supporting a prominent role for the E4-ORF1 oncoprotein in Ad9-induced tumorigenesis, an E1 region-deficient Ad5 vector that expresses the Ad9 but not the Ad26 E4-ORF1 protein was tumorigenic in rats and, like Ad9, promoted solely mammary tumors. These findings argue that the E4-ORF1 oncoprotein is the major oncogenic determinant of Ad9 and that an undefined regulatory element(s) within the E4 region represents a previously unidentified second function likewise necessary for tumorigenesis by this virus.

Human adenoviruses, which are classified into six subgroups (A through F), cause a variety of human illnesses associated with infections of the respiratory and gastrointestinal tracts, as well as the eye (15). Although these viruses are not linked to human cancers, a subset of them, including all subgroup A and B viruses and two members of the subgroup D viruses, have the capacity to promote tumors in rodents. Following subcutaneous inoculation of animals, the subgroup A and B viruses induce undifferentiated sarcomas at the site of injection (13), whereas the subgroup D viruses Ad9 (adenovirus serotype 9) and Ad10 cause exclusively estrogen-dependent mammary tumors (1, 2, 17). Furthermore, it has been established that tumorigenesis by subgroup A and B viruses relies solely on their E1 region-encoded E1A and E1B oncoproteins (37). On the contrary, we have shown that tumorigenesis by subgroup D virus Ad9 lacks such a requirement for E1 region-encoded gene products and rather depends on the viral E4 region-encoded open reading frame 1 (E4-ORF1) oncoprotein (20, 41). Thus, two classes of oncogenic human adenoviruses can be distinguished based on the types of tumors they elicit in animals and the viral oncoproteins responsible for their tumorigenic potential.

* Corresponding author. Mailing address: Department of Molecular Virology and Microbiology, Baylor College of Medicine, One Baylor Plaza, Houston, TX 77030. Phone: (713) 798-3898. Fax: (713) 798-3586. E-mail: rjavier@bcm.tmc.edu.

† Present address: Department of Microbiology, University of Pennsylvania School of Medicine, Philadelphia, PA 19104.

One rationale for studying DNA tumor viruses such as adenovirus stems from the fact that such investigations have contributed greatly to our understanding of mechanisms responsible for the development of cancer (9). For example, the tumorigenic potentials of the nuclear adenovirus E1A and E1B oncoproteins, as well as the nuclear simian virus 40 (SV40) large T antigen, have been shown to depend in part on their abilities to complex with products of the pRb and p53 tumor suppressor genes (16, 31), two of the most commonly mutated genes in human cancers. These findings, together with succeeding studies of such interactions, have proven instrumental in defining functions for these two remarkably important tumor suppressor proteins.

While the mechanisms underlying the tumor-promoting capacity of the cytoplasmic Ad9 E4-ORF1 polypeptide have not been determined, our results suggest that transformation by this viral oncoprotein depends in part on its ability to complex with a select group of cellular PDZ domain-containing proteins, including DLG, MUPP1, and MAGI-1 (11, 23, 24, 44). These types of cellular factors generally act as scaffolding proteins in cell signaling (6, 8, 32), yet precise functions for the Ad9 E4-ORF1-associated PDZ proteins are not known. Nevertheless, DLG is a functional homologue of the *Drosophila* discs large (dlg) tumor suppressor protein (25, 28, 42) and, significantly, is likewise a cellular target for both the Tax oncoprotein of human T-cell leukemia virus type 1 and the E6 oncoproteins of high-risk but not low-risk human papillomaviruses (10, 21, 24, 40). These observations hint that important

new mechanisms of oncogenesis may be uncovered through studies of the Ad9 tumor model system.

A prior study of hybrid viruses generated between Ad9 and the closely related nontumorigenic subgroup D virus Ad26 has shown that an essential determinant(s) for Ad9-induced tumorigenesis is encoded somewhere within the Ad9 E4 region DNA sequences encompassing E4-ORF1, E4-ORF2, and part of E4-ORF3 (18). The experiments reported here were undertaken to establish whether the genetic differences responsible for the disparate tumorigenic phenotypes of Ad9 and Ad26 map to one or more of these three E4 region functions. In light of the fact that the Ad9 E4-ORF1 oncoprotein, but not the E4-ORF2 or E4-ORF3 protein, has been found to represent a crucial determinant for Ad9-induced tumorigenesis (20), however, we anticipated that all pertinent genetic differences between Ad9 and Ad26 would be confined to E4-ORF1 DNA sequences. We report that new results with Ad9/Ad26 hybrid viruses unexpectedly demonstrated that such genetic differences actually localize within both the E4-ORF1 and E4-ORF2 coding regions. Additional findings presented in this study indicated that although the E4-ORF1 protein is the principal oncogenic determinant of Ad9, the essential E4-ORF1 and E4-ORF2 DNA sequences also likely define a previously unrecognized E4 region regulatory element(s) similarly necessary for tumorigenesis by Ad9.

MATERIALS AND METHODS

Cells. Human 293 (ATCC CRL-1573) and A549 (ATCC CCL-185) cell lines were maintained in culture medium (Dulbecco's modified Eagle medium supplemented with gentamicin [20 μg/ml] and 10% fetal bovine serum) under a humidified 5% CO_2 atmosphere at 37°C.

Construction of Ad5 recombinant vectors. E1 region-deficient, replication-defective Ad5 recombinant vectors that express either Ad9 or Ad26 E4-ORF1 from a cytomegalovirus (CMV) promoter-driven cassette ($dl327/_{9E4ORF1}$ or $dl327/_{26E4ORF1}$, respectively) were constructed as described previously (35). Briefly, Ad9 or Ad26 E4-ORF1 coding sequences (nucleotides [nt] 471 to 855) were first introduced into the *Bam*HI and *Eco*RI sites of the CMV expression cassette situated between the two correctly oriented Ad5 DNA fragments 0 to 1.3 and 9.3 to 17 map units (mu) within plasmid pACCMVpLpA (12). Ad5 recombinant vectors were generated by cotransfection of recombinant pACCMVpLpA plasmids and *Bst*BI-digested $dl327_{Bst}$β-gal virion DNA into 293 cells. Resultant viral plaques failing to stain blue in the presence of X-Gal (5-bromo-4-chloro-3-indolyl-β-D-galactopyranoside) were isolated, and the cloned viruses were amplified and titrated on 293 cells. Virion DNAs were prepared from these viruses as described previously (41) and subjected to restriction enzyme analyses to verify proper genomic structures.

Construction of Ad9/Ad26 hybrid and Ad9 mutant viruses. Two different two-step procedures were used to construct Ad9/Ad26 hybrid viruses. First, with the use of common restriction enzyme sites or by PCR methods, Ad9/Ad26 hybrid E4 regions were assembled either within plasmid $p26_{XbaIA}$ (18), containing the Ad26 DNA fragment *Xba*I-A (65 to 100 mu), or within plasmid $p26_{EcoRI(B+C)}$, containing correctly oriented Ad26 DNA fragments *Eco*RI-C (0 to 7.5 mu) and *Eco*RI-B (89.5 to 100 mu). Second, for isolation of hybrid viruses by overlap recombination (5), Ad9/Ad26 hybrid $p26_{XbaIA}$ plasmids were cotransfected into A549 cells with plasmid $p26_{EcoRI(A+C)}$ containing the Ad26 DNA fragment 0 to 89.5 mu (18). Alternatively, for isolation of hybrid viruses from whole virus genome plasmids (41), the Ad26 virion-derived DNA fragment *Eco*RI-A (7.5 to 89.5 mu) was introduced in the correct orientation into the unique *Eco*RI site of Ad9/Ad26 hybrid $p26_{EcoRI(B+C)}$ plasmids, and resultant infectious, whole virus genome $p26_{EcoRI(A+B+C)}$ plasmids were transfected into 293 cells.

For construction of Ad9 mutant viruses, E4 region-containing DNA fragments were mutated either by disruption of appropriate restriction enzyme sites or by PCR methods. With the use of convenient restriction enzyme sites, mutant E4 regions were subsequently introduced into plasmid $p9_{EcoRI(B+C)}$ (41), containing correctly oriented Ad9 DNA fragments *Eco*RI-B (0 to 7.5 mu) and *Eco*RI-C (95 to 100 mu). The virion-derived Ad9 DNA fragment *Eco*RI-A (7.5 to 95 mu) was subsequently introduced in the correct orientation into the unique *Eco*RI site of $p9_{EcoRI(B+C)}$ mutant plasmids. For isolation of mutant viruses, resultant infectious, whole virus genome $p9_{EcoRI(A+B+C)}$ plasmids were transfected into 293 cells.

Ad9/Ad26 hybrid and Ad9 mutant viruses were amplified and titrated in either 293 or A549 cells (19). A combination of limited sequence and restriction enzyme analyses was used to verify the genomic structures of all viruses.

Tumor assays. One- or two-day-old male and female Wistar/Furth rats (Harlan Sprague-Dawley, Indianapolis, Ind.) were inoculated subcutaneously on both flanks with the indicated dose of virus and then monitored for tumors over an 8-month period as previously described (19). Portions of tumors were either fixed in 10% neutral-buffered formalin for histological examination or frozen at −80°C for DNA and protein analyses. Caring and handling of animals were in accordance with institutional guidelines.

Antisera, cell extracts, and immunoblot assays. Ad9 E4-ORF2 coding sequences, PCR amplified with primers 5′AGC TGG ATC CAT GCT TCA GCG ACG CG3′ and 5′CGC GAA TTC TCA TAA TAG AAA CAG ATC C3′, were introduced between the *Bam*HI and *Eco*RI sites of plasmid pGEX-2T (Pharmacia) in frame with the glutathione *S*-transferase (GST) gene. GST–Ad9 E4-ORF2 fusion protein was expressed in bacteria, purified, and used as an antigen to generate rabbit polyclonal antisera (39).

At 24 h postinfection, virus-infected A549 or 293 cells (10 PFU/cell) were washed in ice-cold phosphate-buffered saline and lysed in sample buffer (0.065 M Tris-HCl [pH 6.8], 2% [wt/vol] sodium dodecyl sulfate, 10% [vol/vol] glycerol, 1% [vol/vol] β-mercaptoethanol, 0.0015% [wt/vol] bromophenol blue). Resultant cell extracts were boiled and centrifuged (16,000 × *g*, 10 min). Protein concentrations of these cleared cell extracts were determined by the Bradford assay (4). For immunoblot analyses, proteins from cell extracts were separated by sodium dodecyl sulfate-polyacrylamide gel electrophoresis and electrotransferred to polyvinylidene difluoride membranes, which were sequentially incubated with blocking buffer (5% nonfat dry milk in TBST [50 mM Tris-HCl {pH 7.4}, 200 mM NaCl, 2% Tween 20]), with Ad9 E4-ORF1 antiserum (20) or Ad9 E4-ORF2 antiserum (1:5,000 in TBST), and then with horseradish peroxidase-conjugated goat anti-rabbit immunoglobulin G secondary antibodies (Southern Biotechnology Associates). Membranes were developed by enhanced chemiluminescence (Pierce).

PCR assays. Virion, cellular, and tumor DNAs were isolated by standard methods (41). PCR amplifications were performed with *Taq* polymerase (Stratagene) as recommended by the manufacturer. Ad9 E4-ORF1 expression cassette and Ad5 E1 region DNA sequences were PCR amplified with primer pairs Ad9 E4-ORF1 [nt 471-494] (5′ATG GCT GAA TCT CTG TAT GCT TTC3′)/SV40 cassette (5′GCG GAA TTC TTC AGG GGG AGG TGT GGG AG3′) and Ad5 [nt 2504-2525] (5′GCA GCC AGG GGA TGA TTT TGA G3′)/Ad5 [nt 3053-3075] (5′CCT CGC AGT TGC CAC ATA CCA TG3′), respectively.

RESULTS

Tumorigenesis by Ad9 depends on DNA sequences located within both E4-ORF1 and E4-ORF2. Our previous results with Ad9/Ad26 hybrid viruses indicate that an approximately 1.2-kb segment of the Ad9 E4 region encodes a determinant(s) for tumorigenesis by Ad9 (Fig. 1A) (18). With the extreme right end of the adenovirus genome defined as nt 1, this segment extends from the *Nru*I site at nt 299 to the *Mlu*I site at nt 1481 (Fig. 1B). These sequences either partially or completely code for four separate functions, including the E4 promoter/5′ untranslated region, E4-ORF1, E4-ORF2, and E4-ORF3. Additionally, alignment of these Ad9 sequences with the corresponding Ad26 sequences reveals a total of 74 nucleotide differences distributed within all four functional elements contained in the defined segment (Fig. 1B). Although this particular finding fails to aid more precise localization of the Ad9 E4 region oncogenic determinant(s), we have previously shown that Ad9 E4-ORF1 codes for a transforming protein (20, 46) and that expression of this polypeptide is required for Ad9-induced tumorigenesis (20). From these observations, we postulated that specific nucleotide differences within the E4-

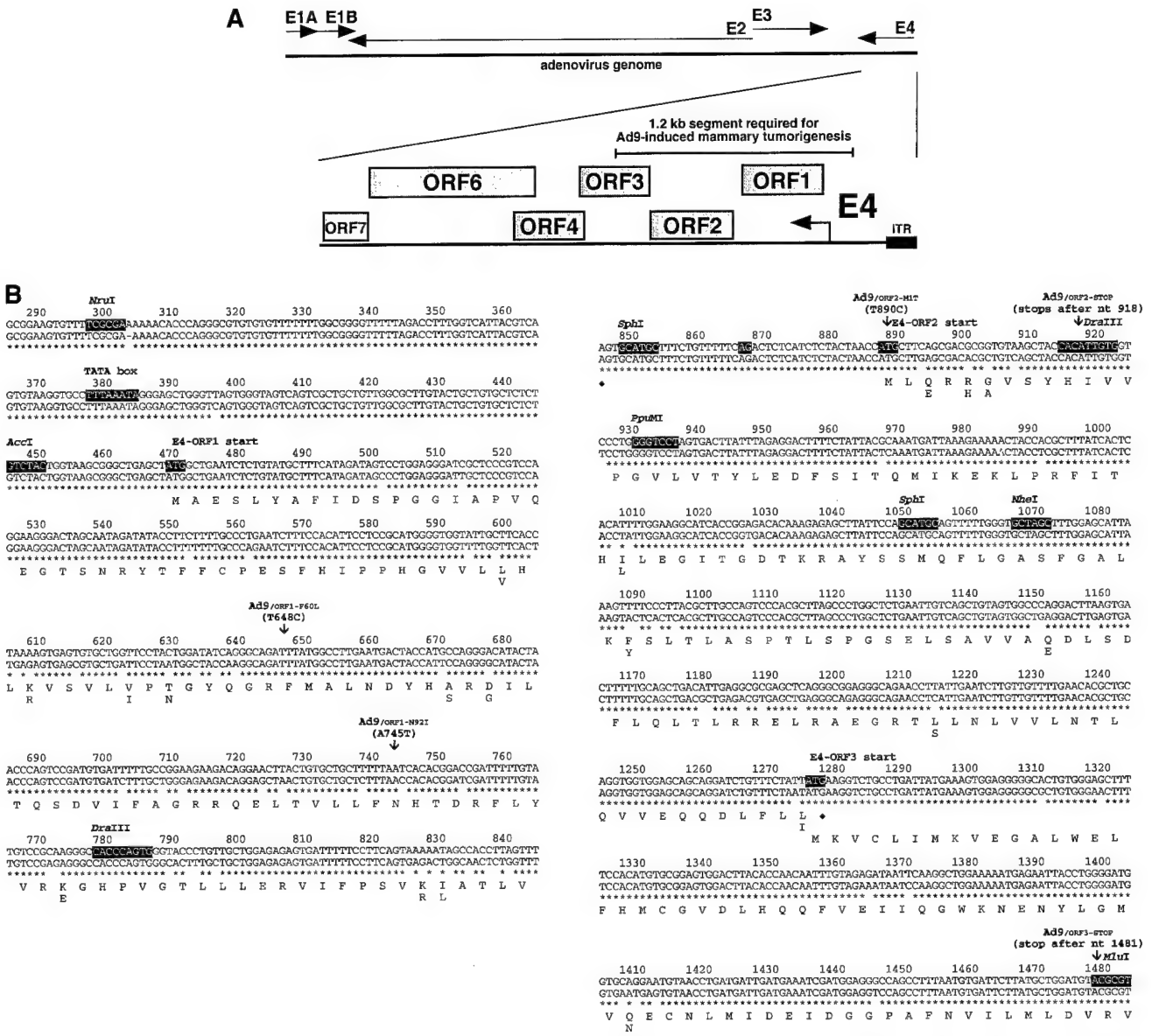

FIG. 1. (A) Illustration of the Ad9 E4 region showing the location of the 1.2-kb segment required for Ad9-induced mammary tumorigenesis. ITR, inverted terminal repeat. (B) Alignment of E4 region DNA sequences of Ad9 (top) and Ad26 (bottom) extending from nt 299 to 1481. Within the Ad9 DNA sequences, common restriction enzyme sites used to construct Ad9/Ad26 hybrid viruses, the E4 promoter TATA box, the initiator methionine codons of E4 proteins, and a putative splice acceptor site at nt 868 used to generate E4-ORF2 mRNAs are highlighted. Shown below the DNA sequences are the amino acid sequences of Ad9 E4 proteins, beneath which are indicated Ad26 amino acid residues differing from those of Ad9. The mutations of viruses shown in Table 1 are also described. Asterisks denote nucleotide identity between the Ad9 and Ad26 DNA sequences.

ORF1 genes of Ad9 and Ad26 may be solely responsible for the divergent tumorigenic phenotypes of these viruses.

We initially tested this idea by constructing the eight different Ad9/Ad26 hybrid viruses (group 1 hybrid viruses) shown in Fig. 2A. Seven of these viruses, 9/26-1 to 9/26-7, have an Ad26 genome in which specific blocks of the E4 region were replaced by equivalent Ad9 sequences, whereas virus 9/26-8 has an Ad9 genome in which the 5′ half of E4-ORF2 was replaced by equivalent Ad26 sequences. To determine the tumorigenic potentials of these viruses, we inoculated newborn rats subcutaneously with 7×10^7 PFU of each virus and then monitored the animals for the development of tumors for 8 months. In these assays, the hybrid viruses behaved identically to either the tumorigenic parental virus Ad9, which generates solely mammary tumors in 100% of infected female rats, or the nontumorigenic parental virus Ad26 (18).

Among the wild-type tumorigenic hybrid viruses shown in Fig. 2A, virus 9/26-4 contained the least amount of Ad9 E4 region DNA sequences, 622 bp, extending from the *Acc*I site at nt 447 to the *Nhe*I site at nt 1069 (Fig. 1B). This segment of the E4 region contains the entire E4-ORF1 gene, a 40-bp noncoding region between the E4-ORF1 and E4-ORF2 genes, and the

5′ half of the E4-ORF2 gene. For both Ad9 and Ad26, additional methionine codon-containing E4-ORFs having the capacity to code for peptides longer than 15 residues are absent in this segment, with the exception of nonconserved Ad9 E4-ORFa (nt 852 to 980, ORF1) which potentially expresses a 42-residue polypeptide (Fig. 2B). Whereas their 40-bp noncoding regions exhibit 100% sequence identity, Ad9 and Ad26 display 39 nucleotide differences in E4-ORF1 and 10 nucleotide differences in the defined portion of E4-ORF2, producing 9 amino acid differences in the E4-ORF1 protein and 4 amino acid differences in the E4-ORF2 protein, respectively (Fig. 1B). It was also noteworthy that hybrid viruses 9/26-6 and 9/26-5, containing only the corresponding Ad9 E4-ORF1 or Ad9 E4-ORF2 sequences of tumorigenic virus 9/26-4, respectively, were nontumorigenic in rats (Fig. 2A), as these results suggested that Ad9-induced tumorigenesis depends on two separate E4 region functions. Furthermore, viruses 9/26-4, 9/26-5, and 9/26-6 similarly expressed wild-type levels of the E4-ORF1 and E4-ORF2 proteins during lytic infections of human A549 cells (Fig. 3).

Because it was surprising to uncover a requirement for E4-ORF2 DNA sequences in tumorigenesis by Ad9, we performed a deletion mutation analysis of the 220-bp region immediately downstream of E4-ORF1, including the 40-bp noncoding region (nt 849 to 888) and the 5′ half of E4-ORF2 (nt 889 to 1069). For this purpose, we engineered three different Ad9 deletion mutant viruses (Ad9Δnt852-1055, Ad9Δnt856-917, and Ad9Δnt919-1070) (Fig. 4) which, consistent with their deletions, expressed approximately wild-type amounts of the E4-ORF1 protein in A549 cells yet did not express the E4-ORF2 protein (Fig. 5). The results of experiments examining the tumorigenic potentials of these mutant viruses showed that both Ad9Δnt852-1055 and Ad9Δnt856-917 failed to elicit tumors, whereas Ad9Δnt919-1070 exhibited a partially tumorigenic phenotype in that it generated mammary tumors in only 60% of infected females (Fig. 4). In contrast, wild-type Ad9 invariably promotes mammary tumors in 100% of infected females (Fig. 4) (17). Moreover, compared to wild-type Ad9-induced tumors, the tumors elicited by virus Ad9Δnt919-1070 showed an extended latency period (4 to 5 months versus 3 months) and were also typically smaller (data not shown). These results with mutant viruses provided further evidence indicating that a previously unrecognized oncogenic determinant for Ad9 is located within the 220-bp region immediately downstream of E4-ORF1.

The Ad9 E4-ORF1 protein, but not the E4-ORF2 or E4-ORF3 protein, is a critical oncogenic determinant for Ad9. As the results described thus far demonstrated a requirement for certain E4-ORF2 DNA sequences in Ad9-induced tumorigenesis, we were prompted to reevaluate a possible role for the E4-ORF2 protein in this process. For this purpose, we constructed two different Ad9 mutant viruses specifically unable to express a functional E4-ORF2 polypeptide. In the virus Ad9/$_{ORF2\text{-}MIT}$, the E4-ORF2 initiator methionine codon was changed to a threonine codon, whereas in virus Ad9/$_{ORF2\text{-}STOP}$, stop codons in all three reading frames were inserted after E4-ORF2 histidine codon 10 (Fig. 1B). It is also notable that the putative 42-amino-acid residue product of Ad9 E4-ORFa (Fig. 2B) was truncated to 22 residues in virus Ad9/$_{ORF2\text{-}STOP}$. As controls, we engineered three additional Ad9 mutant viruses, Ad9/$_{ORF1\text{-}N92I}$, Ad9/$_{ORF1\text{-}F60L}$, and Ad9/$_{ORF3\text{-}STOP}$. Ad9/$_{ORF1\text{-}N92I}$ carries the N92I mutant E4-ORF1 gene, which is transformation defective due to unstable protein expression, whereas Ad9/$_{ORF1\text{-}F60L}$ carries the F60L mutant E4-ORF1 gene, which expresses a transformation-proficient protein (Fig. 1B) (43). In addition, Ad9/$_{ORF3\text{-}STOP}$ has a 4-bp deletion within the *Mlu*I site at nt 1481, thereby truncating the 117-residue E4-ORF3 polypeptide to a 68-residue amino-terminal peptide (Fig. 1B). This mutation is identical to that of mutant hybrid virus *in*MluI reported previously (20).

The results of experiments assessing the tumorigenic potentials of these Ad9 mutant viruses are presented in Table 1. We found that despite their inability to express the E4-ORF2 protein (Fig. 5), viruses Ad9/$_{ORF2\text{-}MIT}$ and Ad9/$_{ORF2\text{-}STOP}$ displayed wild-type tumorigenic phenotypes in rats. Sequencing of E4-ORF2 genes PCR amplified from tumor DNAs confirmed that the tumors were caused by these mutant viruses and that their mutations had not reverted (data not shown). The findings with E4-ORF2 mutant viruses differed from those obtained with virus Ad9/$_{ORF1\text{-}N92I}$, in which a specific failure to express the E4-ORF1 protein (Fig. 5) led to a nontumorigenic phenotype. The latter result was specific because virus Ad9/$_{ORF1\text{-}F60L}$, which expressed wild-type levels of its transformation-proficient E4-ORF1 protein (Fig. 5), displayed wild-type tumorigenicity in animals. Though Ad9/$_{ORF3\text{-}STOP}$ was likewise tumorigenic in rats, mammary tumors promoted in females by this virus arose with a shortened latency period compared to tumors induced by wild-type Ad9 (2 months versus 3 months). Similar results have been reported for virus *in*MluI (20). Interestingly, Ad9/$_{ORF3\text{-}STOP}$ also generated mammary tumors in all of the male rats with a 5-month latency period. Introducing an identical E4-ORF3 mutation into Ad26, however, did not confer it with a tumorigenic phenotype (data not shown). While exhibiting substantially enhanced tumorigenicity in rats, virus Ad9/$_{ORF3\text{-}STOP}$ expressed wild-type rather than elevated levels of the E4-ORF1 protein in A549 cells (Fig. 5). These findings with Ad9 mutant viruses corroborated and extended our previous results indicating a requirement for the E4-ORF1 protein, but not for the E4-ORF2 and E4-ORF3 proteins, in tumorigenesis by Ad9 (20).

Evidence that an undefined regulatory element(s) represents a second E4 region oncogenic determinant for Ad9. As results with hybrid viruses showed that tumorigenesis by Ad9 depends in part on DNA sequences within the 5′ half of E4-ORF2 (Fig. 2A), we were interested in identifying the crucial nucleotide differences between Ad9 and Ad26 in this region. For this purpose, we constructed five different Ad9/Ad26 hybrid viruses (group 2 hybrid viruses) having a wild-type tumorigenic virus 9/26-4 genome (Fig. 2A) in which specific segments of the Ad9 E4-ORF2 sequences were replaced by equivalent Ad26 sequences (viruses 9/26-9 to 9/26-13) (Fig. 6). In A549 cells, two of these hybrid viruses (9/26-11 and 9/26-12) expressed wild-type levels of the E4-ORF1 and E4-ORF2 proteins, but the remaining three hybrid viruses (9/26-9, 9/26-10, and 9/26-13) expressed lower levels of both polypeptides (Fig. 3). Despite expressing reduced amounts of the E4-ORF1 and E4-ORF2 proteins, however, virus 9/26-9 showed wild-type tumorigenicity following inoculation into rats, whereas the remaining four hybrid viruses were found to be nontumorigenic (Fig. 6).

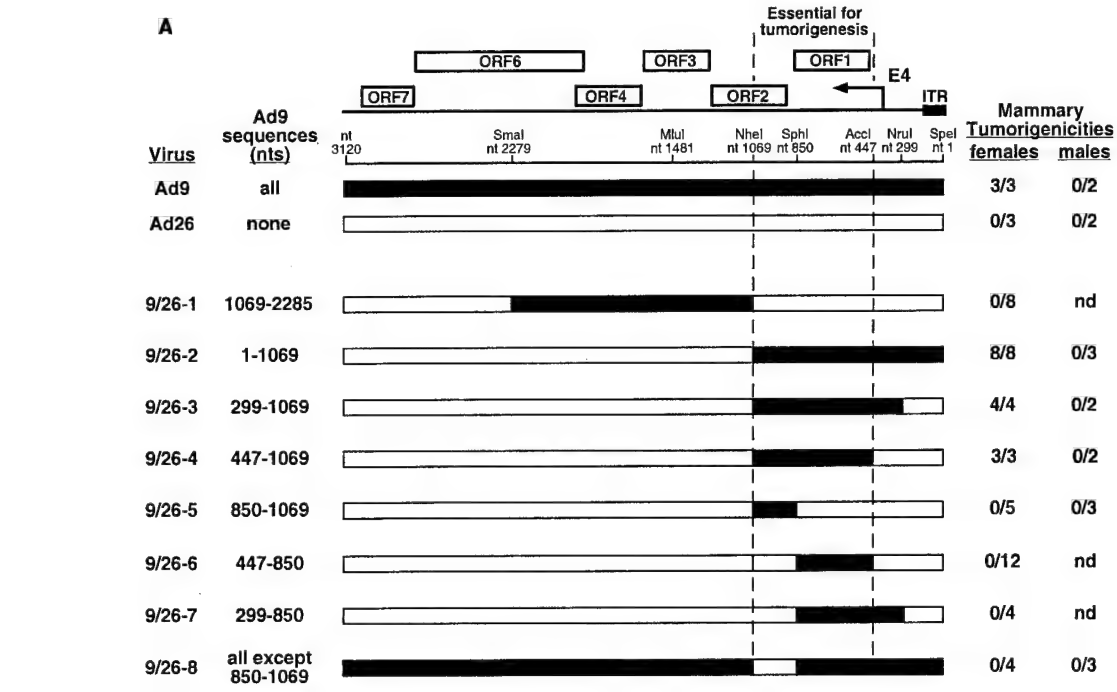

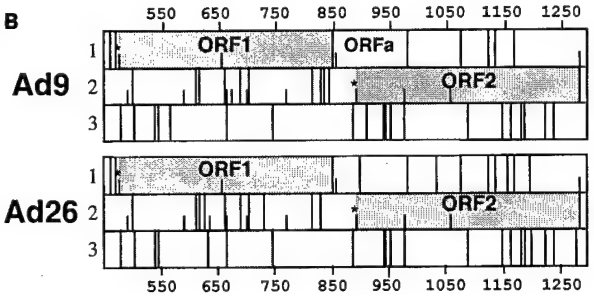

FIG. 2. (A) Genomic structures and tumorigenic potentials of group 1 Ad9/Ad26 hybrid viruses. Newborn rats were inoculated subcutaneously on each flank with a total of 7×10^7 PFU of the indicated virus, and the animals were monitored for tumor formation over an 8-month period. Filled and open genomic regions depict Ad9 and Ad26 DNA sequences, respectively; restriction enzyme sites used to construct these hybrid viruses are indicated. The two vertical dashed lines delimit the segment of the Ad9 E4 region shown by results with these hybrid viruses to be essential for tumorigenesis by Ad9. nd, not determined; ITR, inverted terminal repeat. (B) ORF maps spanning the E4-ORF1 and E4-ORF2 DNA sequences of Ad9 and Ad26. The three reading frames (1, 2, and 3) of the E4 region sense strand are shown. Darkly shaded regions highlight E4-ORF1 and E4-ORF2 coding sequences, whereas the lightly shaded region covers the 622-bp essential E4 region segment extending from nt 447 to 1069. Vertical lines segmenting each reading frame indicate stop codons, whereas shorter vertical ticks denote methionine codons. Asterisks mark the initiator methionine-codons of E4-ORF1 and E4-ORF2.

The results with these group 2 hybrid viruses implicated two separate E4-ORF2 segments, nt 850 to 916 and 932 to 993, in tumorigenesis by Ad9. An important role for the nt 850–916 segment was demonstrated by the fact that replacing these Ad9 sequences of tumorigenic virus 9/26-4 with equivalent Ad26 sequences resulted in nontumorigenic virus 9/26-12 (Fig. 6). In this 66-bp segment, Ad9 and Ad26 display four nucleotide and three amino acid differences at the amino terminus of the E4-ORF2 polypeptide (Fig. 1B). The nt 932–993 segment was likewise important because replacing these Ad9 sequences of tumorigenic viruses 9/26-4 and 9/26-9 with equivalent Ad26 sequences resulted in nontumorigenic viruses 9/26-13 and 9/26-10, respectively (Fig. 6). Significantly, in this 61-bp segment, Ad9 and Ad26 display two nucleotide differences (nt 969 and 993), both of which are silent with respect to the amino acid sequence of the E4-ORF2 polypeptide (Fig. 1B).

A similar strategy was used to identify crucial nucleotide differences between Ad9 and Ad26 within the essential E4-ORF1 sequences. In this case, we constructed five different Ad9/Ad26 hybrid viruses (group 3 hybrid viruses) having a wild-type tumorigenic virus 9/26-4 genome (Fig. 2A) in which specific segments of the Ad9 E4-ORF1 gene were replaced by equivalent Ad26 sequences (viruses 9/26-14 to 9/26-18) (Fig. 7). After inoculation into rats, these hybrid viruses manifested one of three distinct phenotypes, including wild-type tumorigenicity (virus 9/26-14), partial tumorigenicity (viruses 9/26-15 and 9/26-18), or nontumorigenicity (viruses 9/26-16 and 9/26-17) (Fig. 7). In addition, though possessing diminished tumorigenic potentials, the latter four viruses were found to express wild-type amounts of the E4-ORF1 protein in A549 cells (Fig. 3).

The results with these group 3 hybrid viruses revealed involvement of two separate E4-ORF1 segments, nt 596 to 780 and nt 780 to 850, in tumorigenesis by Ad9. The importance of the nt 596–780 segment was shown by the fact that replacing these Ad9 sequences of tumorigenic virus 9/26-14 with equivalent Ad26 sequences resulted in nontumorigenic virus 9/26-16 (Fig. 7). The partially tumorigenic phenotype of virus 9/26-15 further suggested that crucial nucleotide differences within E4-ORF1 are distributed both upstream and downstream of nt

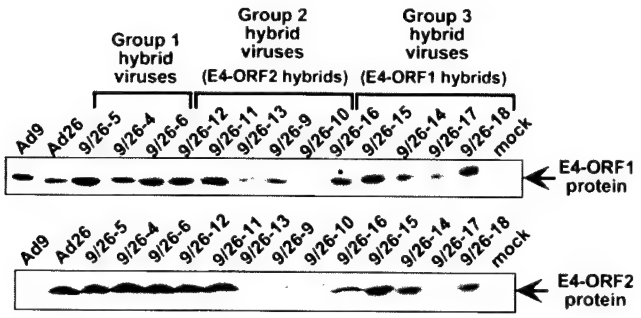

FIG. 3. Expression of E4-ORF1 and E4-ORF2 proteins by Ad9/Ad26 hybrid viruses. Cell extracts were prepared from human A549 cells mock infected or lytically infected with the indicated virus (10 PFU/cell, 24 h postinfection) and then subjected to immunoblot analyses with antisera raised against either an Ad9 E4-ORF1 or Ad9 E4-ORF2 fusion protein. The E4-ORF1 and E4-ORF2 proteins have molecular masses of 14 and 14.5 kDa, respectively.

672. In the defined 184-bp segment, Ad9 and Ad26 display 23 nucleotide and 7 amino acid differences in the middle of the E4-ORF1 polypeptide (Fig. 1B).

The nt 780–850 segment, on the other hand, was implicated by the fact that replacing these Ad9 sequences of tumorigenic virus 9/26-4 with equivalent Ad26 sequences resulted in nontumorigenic virus 9/26-17 (Fig. 7). In this 70-bp segment, Ad9 and Ad26 display 12 nucleotide differences, three of which produce two amino acid differences near the carboxyl terminus of the E4-ORF1 polypeptide (Fig. 1B). Virus 9/26-18 was constructed to distinguish whether the three amino acid-altering nucleotide differences (nt 829, 831, and 833) or the remaining nine silent nucleotide differences in this segment of E4-ORF1 were important. In this regard, virus 9/26-18 is identical to nontumorigenic virus 9/26-17 except that the three Ad26-derived amino acid-altering nucleotides of virus 9/26-17 are converted to the respective Ad9 nucleotides in virus 9/26-18. Conversely, virus 9/26-18 is likewise identical to wild-type tumorigenic virus 9/26-4 except that the nine Ad9-derived silent nucleotides of virus 9/26-4 are replaced with the respective Ad26 nucleotides in virus 9/26-18 (Fig. 1B and 7). Therefore, the fact that virus 9/26-18 exhibited a partially tumorigenic phenotype in rats (Fig. 7) suggested that both amino acid-altering and silent nucleotide differences in E4-ORF1 contribute to the divergent tumorigenic phenotypes of Ad9 and Ad26.

Collectively, our findings with group 2 and group 3 hybrid viruses revealed that amino acid-altering nucleotide differences in E4-ORF1, as well as silent nucleotide differences in both E4-ORF1 and E4-ORF2, are responsible for the divergent tumorigenic phenotypes of Ad9 and Ad26. The observed role for silent nucleotide differences, together with results demonstrating that the E4-ORF2 polypeptide is dispensable for tumorigenesis by Ad9 (Table 1), suggested that an undefined E4 region regulatory element(s), rather than a protein function, represents a second determinant for Ad9-induced tumorigenesis (see Discussion).

The E4-ORF1 oncoprotein is the major oncogenic determinant of Ad9. Compared with other oncogenic adenoviruses, Ad9 is unique both in targeting tumorigenesis to the mammary glands of animals and in having the E4-ORF1 protein as an oncogenic determinant (17, 18, 20). Considering these observations, we hypothesized that the strict propensity of Ad9 to promote mammary tumors may be largely due to unique activities associated with its E4-ORF1 oncoprotein. This question was addressed by examining whether an otherwise nontumorigenic subgroup C human adenovirus (Ad5) that is engineered to express the Ad9 E4-ORF1 oncoprotein would become tumorigenic and, if so, whether this virus would also

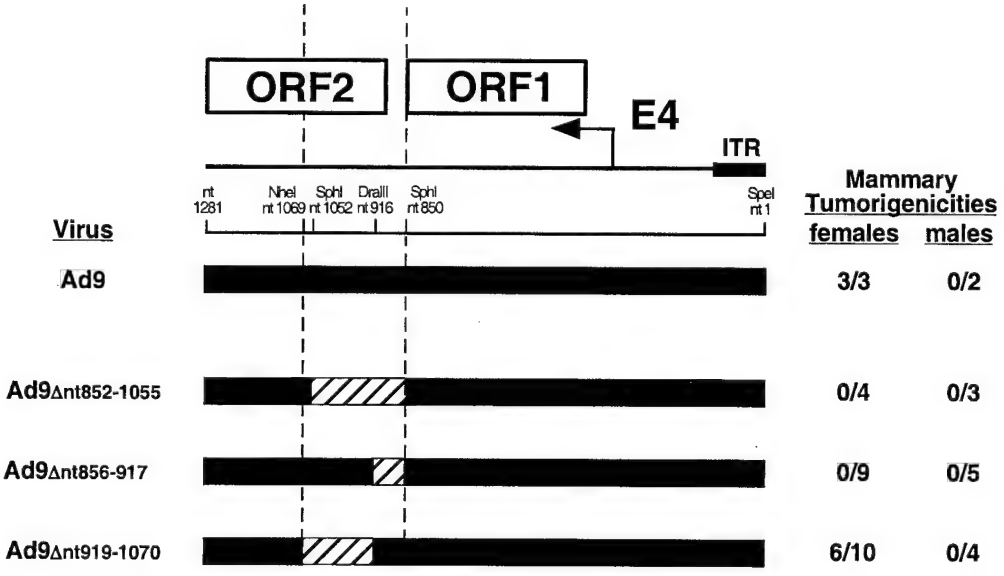

FIG. 4. Genomic structures and tumorigenic potentials of Ad9 deletion mutant viruses. Methods for determining the tumorigenicity of viruses are described in the legend to Fig. 2A. Filled and hatched genomic regions represent Ad9 and deleted DNA sequences, respectively; locations of restriction enzyme sites used to create these deletions are indicated. The two vertical dashed lines delimit the 220-bp region immediately downstream of E4-ORF1 implicated in Ad9-induced tumorigenesis by results with group 1 hybrid viruses (Fig. 2A). ITR, inverted terminal repeat.

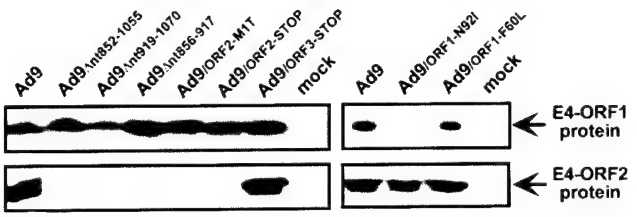

FIG. 5. Expression of E4-ORF1 and E4-ORF2 proteins by Ad9 mutant viruses. Immunoblot analyses used to detect E4-ORF1 and E4-ORF2 proteins in extracts of A549 cells mock infected or lytically infected with the indicated virus (10 PFU/cell, 24 h postinfection) were carried out as described in the legend to Fig. 3.

acquire the unique capacity to elicit exclusively mammary tumors in animals.

Because E1 region transforming functions of Ad9 are dispensable for its tumorigenic potential (41), we chose to utilize the Ad5 recombinant vector $dl327_{Bst}$β-gal, in which the Ad5 E1 region genes are deleted and replaced by a *lacZ* expression cassette (35). By replacing the *lacZ* cassette of this Ad5 vector with CMV promoter-driven Ad9 E4-ORF1 and Ad26 E4-ORF1 cassettes, we isolated viruses $dl327/_{9E4ORF1}$ and $dl327/_{26E4ORF1}$, respectively (Fig. 8A). Because our main interest was to investigate the E4-ORF1 protein determinant in these experiments, the expression cassettes contained only E4-ORF1 coding sequences and therefore lacked sequences downstream of this gene. Using our Ad9 E4-ORF1 antiserum, which reacts with subgroup D but not subgroup C adenovirus E4-ORF1 proteins (45), we detected heterologous E4-ORF1 protein expression by both $dl327/_{9E4ORF1}$ and $dl327/_{26E4ORF1}$ but not by $dl327_{Bst}$β-gal during lytic infections of human 293 cells (Fig. 8B), a cell line that complements the replication defects of such Ad5 vectors by stably expressing Ad5 E1 region gene products (14). Also noteworthy was that the E4-ORF1 protein levels observed for both $dl327/_{9E4ORF1}$ and $dl327/_{26E4ORF1}$ in these assays are substantially higher than those achieved by wild-type Ad9 after infection of 293 cells at the same multiplicity of infection (data not shown).

Following subcutaneous inoculation of newborn rats with 7×10^7 PFU of each Ad5 vector, we found that $dl327_{Bst}$β-gal and $dl327/_{26E4ORF1}$ failed to induce tumors, whereas $dl327/_{9E4ORF1}$ generated tumors in all of the females (3-month tumor latency) and in one male (5-month tumor latency) (Fig. 8A). As somewhat lower E4-ORF1 protein expression was observed for $dl327/_{26E4ORF1}$ than for $dl327/_{9E4ORF1}$ (Fig. 8B), we also demonstrated that rats inoculated with a 10-fold-higher dose of $dl327/_{26E4ORF1}$ likewise failed to develop tumors of any kind (Fig. 8A). More important, histological analyses of the $dl327/_{9E4ORF1}$-induced male and female tumors indicated that they were exclusively mammary fibroadenomas, identical to those generated by wild-type Ad9 (Fig. 9A) (17). Virus $dl327/_{9E4ORF1}$ rather than a wild-type Ad9 contaminant promoted these tumors because, using primers specific for the Ad9 E4-ORF1 cassette of $dl327/_{9E4ORF1}$, we succeeded in PCR amplifying the predicted 700-bp product from DNAs of $dl327/_{9E4ORF1}$-induced tumors but not from DNA of an Ad9-induced tumor or CREF cells (Fig. 9B). Additional results also showed that $dl327/_{9E4ORF1}$-induced tumors express the Ad9 E4-ORF1 protein at levels slightly above those seen in wild-type Ad9-induced tumors (data not shown). An inability to PCR amplify a 540-bp Ad5 E1 region product from these tumor DNAs also confirmed that the tumorigenic potential of $dl327/_{9E4ORF1}$ is not dependent on Ad5 E1 region functions (Fig. 9C). These findings are significant in demonstrating that an otherwise nontumorigenic E1 region-deficient Ad5 vector that heterologously expresses the Ad9 E4-ORF1 oncoprotein not only becomes tumorigenic but also promotes solely mammary tumors like those induced by wild-type Ad9.

DISCUSSION

The work presented in this paper was undertaken to precisely define the E4 region DNA sequences that determine mammary tumorigenesis by Ad9. Findings with Ad9/Ad26 hybrid viruses and Ad9 mutant viruses localized these essential DNA sequences to portions of both E4-ORF1 and E4-ORF2 (Fig. 2A and 4). We also showed that abrogating E4-ORF1 protein expression by introducing a single nucleotide substitution into the E4-ORF1 gene of Ad9 abolished its tumorigenic potential (virus $Ad9/_{ORF1\text{-}N92I}$) whereas, conversely, maintaining transformation-competent E4-ORF1 protein expression by introducing a different nucleotide substitution into the E4-ORF1 gene of Ad9 preserved its wild-type tumorigenic potential (virus $Ad9/_{ORF1\text{-}F60L}$) (Fig. 5; Table 1). These results demonstrate an absolute requirement for the Ad9 E4-ORF1 oncoprotein in tumorigenesis by Ad9. Results with Ad9/Ad26 hybrid viruses further suggested that certain amino acid differences between the E4-ORF1 polypeptides of Ad9 and Ad26 contribute to the dramatically divergent tumorigenic phenotypes of these viruses (Fig. 7). Because Ad9 and Ad26 E4-ORF1 expression plasmids display similar transforming potentials in CREF rat embryo fibroblasts in vitro (unpublished results) (18), we hypothesize that such amino acid differences cause the Ad26 E4-ORF1 protein to have stability or perhaps functional deficiencies specifically in cells of the rat mammary gland. Alternatively, similar to the Ad5 E1A protein (22), the Ad26 E4-ORF1 protein may provoke a strong inflammatory

TABLE 1. The E4-ORF1 oncoprotein but not the E4-ORF2 or E4-ORF3 protein is required for mammary tumorigenesis by Ad9[a]

Virus[b]	No. of rats that developed tumors/no. infected	
	Females	Males
Wild-type		
Ad9	3/3	0/2
E4-ORF1 mutants		
$Ad9/_{ORF1\text{-}N92I}$	0/5	0/4
$Ad9/_{ORF1\text{-}F60L}$	4/4	0/3
E4-ORF2 mutants		
$Ad9/_{ORF2\text{-}M1T}$	5/5	0/5
$Ad9/_{ORF2\text{-}STOP}$	13/13	0/3
E4-ORF3 mutant		
$Ad9/_{ORF3\text{-}STOP}$	3/3	3/3

[a] Methods for determining tumorigenicity are detailed in the legend to Fig. 2A.

[b] Mutations are described in Fig. 1B.

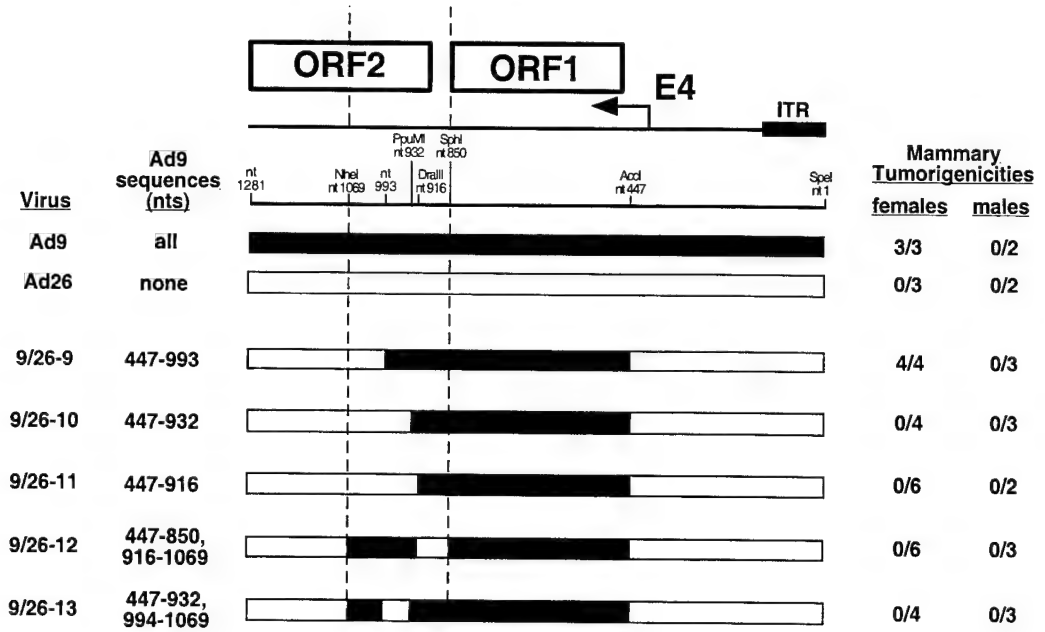

FIG. 6. Genomic structures and tumorigenic potentials of group 2 Ad9/Ad26 hybrid viruses. Methods for determining the tumorigenicity of viruses are described in the legend to Fig. 2A. Filled and open genomic regions represent Ad9 and Ad26 sequences, respectively; locations of restriction enzyme sites or PCR primers used to construct these hybrid viruses are indicated. The two vertical dashed lines delimit the 220-bp region immediately downstream of E4-ORF1 implicated in Ad9-induced tumorigenesis by results with group 1 hybrid viruses (Fig. 2A). ITR, inverted terminal repeat.

response, leading to clearance of infected cells. With respect to the essential Ad9 DNA sequences identified within E4-ORF2, however, results with mutant viruses indicated that the E4-ORF2 polypeptide is dispensable for Ad9-induced tumorigenesis (Table 1). Taken together, these findings argue that the tumorigenic potential of Ad9 depends on two separate E4 region determinants, only one of which represents a protein function.

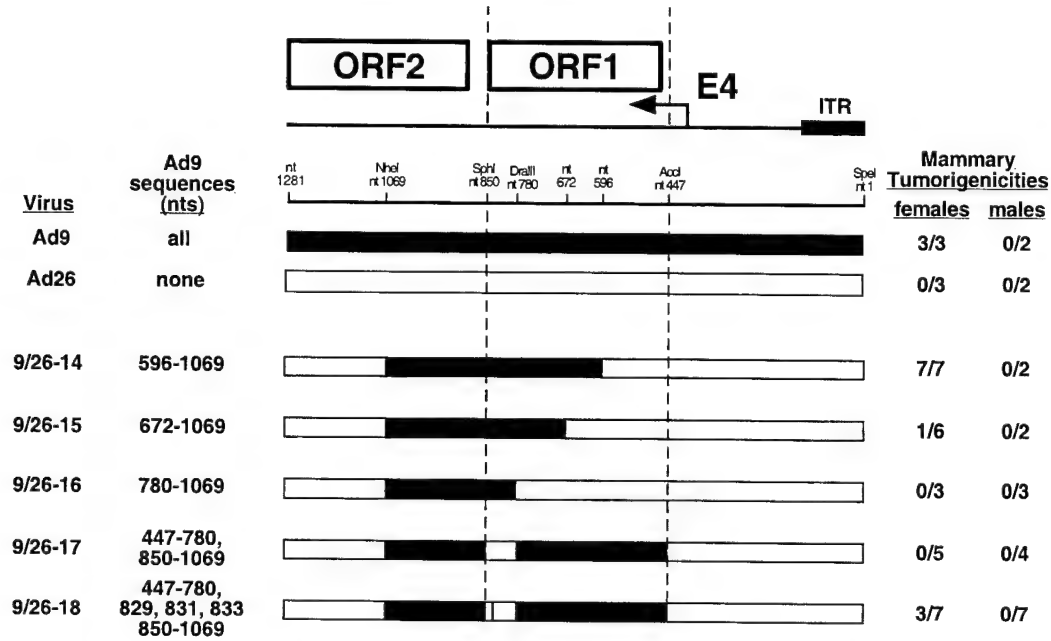

FIG. 7. Genomic structures and tumorigenic potentials of group 3 Ad9/Ad26 hybrid viruses. Methods for determining the tumorigenicity of viruses are described in the legend to Fig. 2A. Filled and open genomic regions represent Ad9 and Ad26 sequences, respectively; locations of restriction enzyme sites or PCR primers used to construct these hybrid viruses are indicated. The two vertical dashed lines delimit the 403-bp E4-ORF1 region implicated in Ad9-induced tumorigenesis by results with group 1 hybrid viruses (Fig. 2A). ITR, inverted terminal repeat.

Supporting the existence of a nonprotein oncogenic determinant in the Ad9 E4 region, results with Ad9/Ad26 hybrid viruses revealed that silent nucleotide differences with respect to the E4-ORF1 and E4-ORF2 polypeptides are also partly responsible for the divergent tumorigenic phenotypes of Ad9 and Ad26 (Fig. 6 and 7). With respect to other potentially important protein-encoding ORFs within the essential E4 region DNA sequences, Ad9 E4-ORFa is the only one, besides E4-ORF1 and E4-ORF2, capable of encoding a peptide larger than 15 residues (Fig. 2B). The fact that a stop codon interrupted Ad9 E4-ORFa in tumorigenic virus $Ad9/_{ORF2\text{-}STOP}$, however, argues against a role for this ORF in Ad9-induced tumorigenesis. Therefore, we postulate that the essential Ad9 sequences define a novel E4 region regulatory element(s) which, like the Ad9 E4-ORF1 oncoprotein, is also necessary for Ad9-induced tumorigenesis.

For tumorigenic virus 9/26-9, it was shown that only two silent substitutions, at nt 969 and 993, in E4-ORF2 are required to produce nontumorigenic virus 9/26-10 (Fig. 6). This finding indicates that these two nucleotides are critical for the function of the proposed E4 region regulatory element. Consequently, it was surprising that virus $Ad9_{\Delta nt919\text{-}1070}$, in which the segment extending from nt 919 to 1070 is deleted, displayed a partial tumorigenic rather than nontumorigenic phenotype (Fig. 4). The reason for this disparity is not known, but a possible explanation could be that for virus $Ad9_{\Delta nt919\text{-}1070}$, DNA sequences immediately downstream of the deleted region are able to partially complement the missing component of the regulatory element in a position-dependent manner, thereby endowing this mutant virus with weak but measurable tumorigenic potential.

A function for the proposed regulatory element(s) has not been established, but we presume that it would act at the level of transcription, mRNA stability, or splicing within the Ad9 E4 region transcription unit. It may be relevant, however, that the crucial, silent nucleotide differences within E4-ORF1 and E4-ORF2 flank both sides of a conserved 40-nt noncoding region containing the putative splice acceptor site at nt 868 used to generate E4-ORF2 mRNAs (Fig. 1B). Additionally, the regions affected by these silent nucleotide differences have sequences and locations reminiscent of splicing branch sites and exonic splicing enhancers, respectively (3). Recruitment of splicing factors to such elements in pre-mRNAs facilitates splicing through the formation of protein networks across introns and exons. Further considering that alternative splicing plays a central role in regulating gene expression by the adenovirus E4 region (36), we favor the idea that the proposed element(s) functions to modulate splicing of certain E4 region mRNAs. Perhaps related to this possibility, future studies will examine whether reduced E4-ORF2 splice acceptor site selection during production of E4 region mRNAs is responsible for the decreased E4-ORF2 protein expression observed for Ad9 compared to Ad26 in lytically infected A549 cells (Fig. 3).

While the proposed regulatory element(s) is expected to directly control the abundance of specific E4 region mRNAs in cells, this activity likely ultimately alters expression of one or more E4 proteins. Two different models in which the element either increases or decreases protein expression can be envisioned. In our first model, the abundance of E4 proteins that enhance tumorigenesis by Ad9 is increased. For example, an

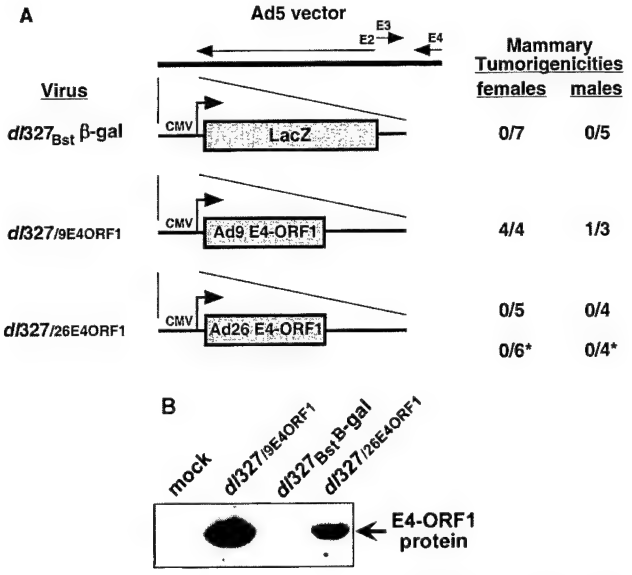

FIG. 8. (A) Genomic structures and tumorigenic potentials of E1 region-deficient Ad5 recombinant virus vectors that express the LacZ ($dl327_{Bst}$β-gal), Ad9 E4-ORF1 ($dl327/_{9E4ORF1}$), or Ad26 E4-ORF1 ($dl327/_{26E4ORF1}$) protein. Methods for determining the tumorigenicity of viruses are described in the legend to Fig. 2A. Asterisks indicate results obtained after inoculating rats with 7×10^8 PFU of virus, as opposed to the 7×10^7-PFU inoculum used with other rats in this experiment. (B) E4-ORF1 protein expression by Ad5 vectors. Immunoblot analyses used to detect heterologous E4-ORF1 protein in extracts of 293 cells mock infected or lytically infected with the indicated virus (10 PFU/cell, 24 h postinfection) were carried out as described in the legend to Fig. 3.

increase in E4-ORF1 protein levels might result if the element were to block conversion of the primary E4 region transcript, which expresses the E4-ORF1 protein (7), into spliced mRNA species coding for other E4 proteins. Although this idea is appealing because the element and E4-ORF1 share overlapping sequences, evidence for such an activity was not obtained in experiments examining E4-ORF1 protein levels in A549 cells infected with hybrid or mutant viruses (Fig. 3). It must be considered, however, that this postulated function for the element may be restricted to specific cell types, such as those of the rat mammary gland. Additionally, besides possibly increasing accumulation of the E4-ORF1 oncoprotein in cells, the proposed element could likewise potentially augment levels of other adenovirus E4 proteins known to possess transforming potential, including E4-ORF3 (30), E4-ORF6 (27, 29), and E4-ORF6/7 (47). In our second model, we imagine that the abundance of E4 proteins that suppress tumorigenesis by Ad9 is decreased by the proposed element. The E4-ORF4 protein, which triggers programmed cell death (26, 38), and the Ad9 E4-ORF3 protein, which antagonizes tumorigenesis by Ad9 (see below), represent plausible candidates for this scenario.

Although the Ad5 E4-ORF3 protein has been reported to possess transforming potential (30), our results with virus $Ad9/_{ORF3\text{-}STOP}$ indicate that the Ad9 E4-ORF3 gene product is dispensable for Ad9-induced tumorigenesis (Table 1). In fact, compared to wild-type Ad9, $Ad9/_{ORF3\text{-}STOP}$ displayed enhanced tumorigenicity in rats, as revealed by the shortened tumor latency period in females and by the occurrence of

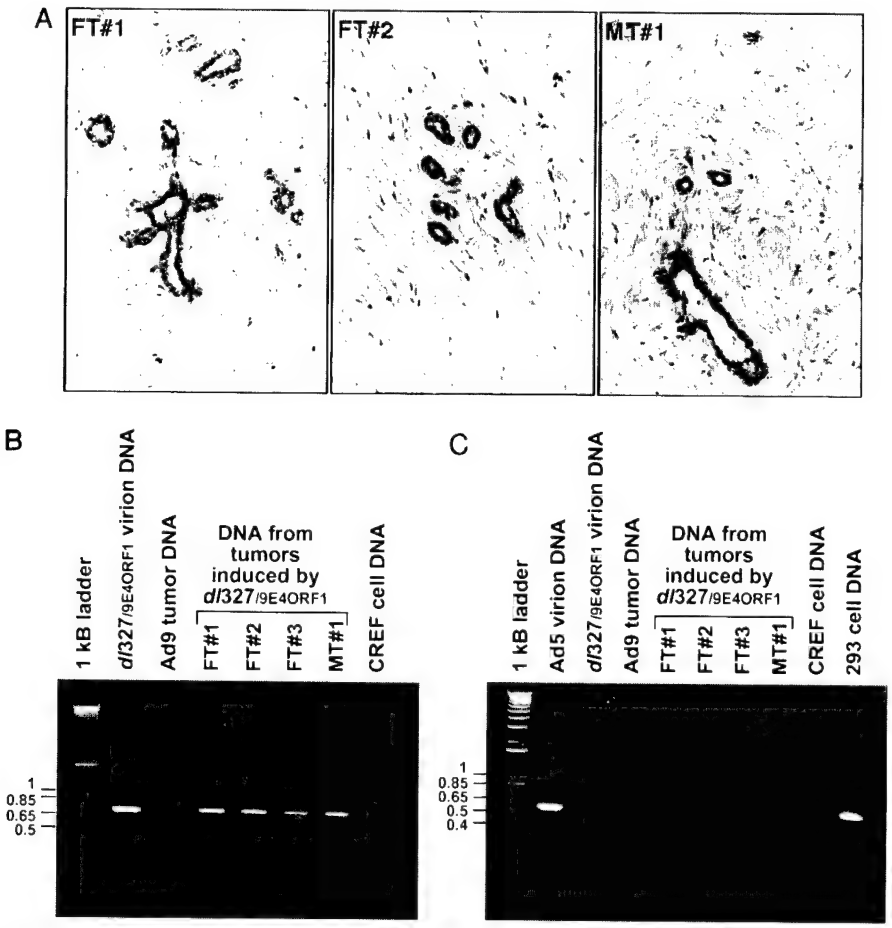

FIG. 9. (A) $dl327/_{9E4ORF1}$-induced tumors are histologically identical to mammary tumors generated by wild-type Ad9. Female tumor 1 (FT#1), female tumor 2 (FT#2), and male tumor 1 (MT#1) are fibroademomas. The stromal portion of MT#1, however, is more sclerotic, indicating higher collagen composition. (B) $dl327/_{9E4ORF1}$-induced mammary tumors contain Ad9 E4-ORF1 cassette DNA sequences (C) but not Ad5 E1 region DNA sequences. Tumor DNAs (2 μg) or virion DNAs (1 ng) were subjected to PCR amplification using primer pairs specific for either the Ad9 E4-ORF1 cassette of virus $dl327/_{9E4ORF1}$ or the Ad5 E1 region (see Materials and Methods). DNAs from three different $dl327/_{9E4ORF1}$-induced mammary tumors from females (FT#1, FT#2, and FT#3), as well as one from a male (MT#1), were examined. Water or DNA from Ad5 virions, CREF cells, 293 cells, or an Ad9-induced tumor served as controls. PCR products were separated by agarose gel electrophoresis and stained with ethidium bromide.

tumors in males. These results show that the Ad9 E4-ORF3 protein actually inhibits Ad9-induced tumorigenesis. Furthermore, the fact that $Ad9/_{ORF3\text{-}STOP}$ elicited mammary tumors in males with 100% frequency is particularly noteworthy because tumors induced by wild-type Ad9 are known to be absolutely dependent on estrogen for growth and maintenance (1, 17). Thus, our findings with $Ad9/_{ORF3\text{-}STOP}$ are significant in arguing that the Ad9 E4-ORF3 protein is responsible, in part, for the strict estrogen dependence of Ad9-induced mammary tumors. In this regard, one interesting possibility may be that the Ad9 E4-ORF3 protein possesses an activity that attenuates the response of estrogen receptor to its hormone ligand in mammary cells.

It is remarkable that the E1 region-deficient Ad5 vector $dl327/_{9E4ORF1}$, which heterologously expresses the Ad9 E4-ORF1 protein, not only was tumorigenic in rats but also generated exclusively mammary tumors identical to those induced by wild-type Ad9 (Fig. 8A and 9A). Expression of the Ad9 E4-ORF1 oncoprotein is specifically required for this effect because the Ad5 vector $dl327_{Bst}$β-gal or $dl327/_{26E4ORF1}$, which instead heterologously expresses the Ad26 E4-ORF1 protein, was nontumorigenic in rats. Additional work is needed to determine whether, in the context of the Ad5 vector, both silent and amino acid-altering nucleotide differences are responsible for the inability of Ad26 E4-ORF1 to promote mammary tumors. Considering that the E1 region codes for the major transforming functions of Ad5 (37), it is also notable that Ad5 E1 region genes were found to be dispensable for tumorigenesis by virus $dl327/_{9E4ORF1}$ (Fig. 9C). This observation is in agreement with our previous findings showing that the Ad9 E1 region is likewise unnecessary for mammary tumorigenesis by Ad9 (41). Nonetheless, because the Ad5 vector used in these studies possesses an intact E4 region, it is feasible that Ad5 E4 proteins contribute to the tumorigenic potential of $dl327/_{9E4ORF1}$. Regardless of this possibility, however, the fact that virus $dl327/_{9E4ORF1}$ and Ad9 display nearly identical oncogenic properties in rats provides a compelling argument that the major oncogenic determinant of Ad9 is its E4-ORF1 oncoprotein.

The reason that Ad9 generates only mammary tumors in rats has not been established. Its select tropism is unlikely due to restricted infection of mammary cells in animals because Ad9 binds to the same widely expressed cellular receptor used by Ad5 (33, 34). Additional findings also suggest that transcription from the Ad9 E4 region is neither enhanced in nor limited to estrogen receptor-expressing cells stimulated by hormone (unpublished results; 19). Thus, the finding that the Ad5 vector *dl*327/$_{9E4ORF1}$, like Ad9, caused exclusively mammary tumors in rats is significant because it indicates that certain activities associated with the Ad9 E4-ORF1 oncoprotein serve to promote tumorigenesis by Ad9 selectively in cells of the rat mammary gland. These observations lead us to hypothesize that in rats inoculated with Ad9, a wide variety of cell types become infected, yet only within certain mammary cells are the novel activities of the Ad9 E4-ORF1 oncoprotein sufficient to induce oncogenic transformation. With respect to this possibility, it may be found that cellular PDZ protein targets of the Ad9 E4-ORF1 oncoprotein are particularly important regulators of growth and proliferation in cells of the mammary gland in vivo.

In this study, we identified several different E4 region functions that represent key factors in determining the unique tumorigenic properties of Ad9, including the propensity to elicit only mammary tumors and the strict estrogen dependence of these neoplasms. Our results also suggest that Ad9-induced tumorigenesis is governed by a complex interplay between these E4 region functions, which act both positively and negatively to influence this process. This new information is expected to lead to a more complete understanding of the mechanisms responsible for tumorigenesis by Ad9.

ACKNOWLEDGMENTS

We thank Stephen Hoang and Ileana Silva for assistance in constructing plasmids and viruses. We also thank Siu Sylvia Lee, Britt Glaunsinger, Isabel Latorre, and Kris Frese for many helpful discussions.

D.L.T. was supported by National Research Service Award CA09197 from the National Cancer Institute and by the Federal Work-Study program of the U.S. Department of Education. This work was funded by grants from the National Cancer Institute (R01 CA/AI58541), American Cancer Society (RP6-97-068-01-VM), and Department of the Army (DAMD17-97-1-7082) to R.J. and from the National Institutes of Health (RO1 HL58344) to J.S.

REFERENCES

1. **Ankerst, J., and N. Jonsson.** 1989. Adenovirus type 9-induced tumorigenesis in the rat mammary gland related to sex hormonal state. J. Natl. Cancer Inst. **81:**294–298.
2. **Ankerst, J., N. Jonsson, L. Kjellen, E. Norrby, and H. O. Sjogren.** 1974. Induction of mammary fibroadenomas in rats by adenovirus type 9. Int. J. Cancer **13:**286–290.
3. **Blencowe, B. J.** 2000. Exonic splicing enhancers: mechanism of action, diversity and role in human genetic diseases. Trends Biochem. Sci. **25:**106–110.
4. **Bradford, M. M.** 1976. A rapid and sensitive method for the quantitation of microgram quantities of protein utilizing the principle of protein-dye binding. Anal. Biochem. **72:**248–254.
5. **Chinnadurai, G., S. Chinnadurai, and J. Brusca.** 1979. Physical mapping of a large-plaque mutation of adenovirus type 2. J. Virol. **32:**623–628.
6. **Craven, S. E., and D. S. Bredt.** 1998. PDZ proteins organize synaptic signaling pathways. Cell **93:**495–498.
7. **Dix, I., and K. N. Leppard.** 1993. Regulated splicing of adenovirus type 5 E4 transcripts and regulated cytoplasmic accumulation of E4 mRNA. J. Virol. **67:**3226–3231.
8. **Fanning, A. S., and J. M. Anderson.** 1999. PDZ domains: fundamental building blocks in the organization of protein complexes at the plasma membrane. J. Clin. Investig. **103:**767–772.
9. **Flint, S. J., L. W. Enquist, R. M. Krug, V. R. Racaniello, and A. M. Skalka.** 2000. Principles of virology: molecular biology, pathogenesis, and control, p. 552–593. ASM Press, Washington, D.C.
10. **Gardiol, D., C. Kuhne, B. Glaunsinger, S. S. Lee, R. Javier, and L. Banks.** 1999. Oncogenic human papillomavirus E6 proteins target the discs large tumour suppressor for proteasome-mediated degradation. Oncogene **18:** 5487–5496.
11. **Glaunsinger, B. A., S. S. Lee, M. Thomas, L. Banks, and R. Javier.** Interactions of the PDZ-protein MAGI-1 with adenovirus E4-ORF1 and high-risk papillomavirus E6 oncoproteins. Oncogene, in press.
12. **Gomez-Foix, A. M., W. S. Coats, S. Baque, T. Alam, and R. D. Gerard.** 1992. Adenovirus-mediated transfer of the muscle glycogen phosphorylase gene into hepatocytes confers altered regulation of glycogen metabolism. J. Biol. Chem. **267:**25129–25134.
13. **Graham, F.** 1984. Transformation by and oncogenicity of human adenoviruses, p. 339–398. *In* H. Ginsberg (ed.), The adenoviruses. Plenum Press, New York, N.Y.
14. **Graham, F. L., J. Smiley, W. C. Russell, and R. Nairn.** 1977. Characteristics of a human cell line transformed by DNA from human adenovirus type 5. J. Gen. Virol. **36:**59–72.
15. **Horwitz, M. S.** 1996. Adenoviruses, p. 2149–2171. *In* B. N. Fields, D. M. Knipe, and P. M. Howley (ed.), Fields virology, vol. 2. Lippincott-Raven, Philadelphia, Pa.
16. **Imreh, S., L. Szekely, K. G. Wiman, and G. Klein.** 1997. Oncogenes and signal transduction, p. 3–32. *In* G. Peters and K. H. Vousden (ed.), Oncogenes and tumour suppressors. Oxford University Press, New York, N.Y.
17. **Javier, R., K. Raska, Jr., G. J. Macdonald, and T. Shenk.** 1991. Human adenovirus type 9-induced rat mammary tumors. J. Virol. **65:**3192–3202.
18. **Javier, R., K. Raska, Jr., and T. Shenk.** 1992. Requirement for the adenovirus type 9 E4 region in production of mammary tumors. Science **257:**1267–1271.
19. **Javier, R., and T. Shenk.** 1996. Mammary tumors induced by human adenovirus type 9: a role for the viral early region 4 gene. Breast Cancer Res. Treat. **39:**57–67.
20. **Javier, R. T.** 1994. Adenovirus type 9 E4 open reading frame 1 encodes a transforming protein required for the production of mammary tumors in rats. J. Virol. **68:**3917–3924.
21. **Kiyono, T., A. Hiraiwa, M. Fujita, Y. Hayashi, T. Akiyama, and M. Ishibashi.** 1997. Binding of high-risk human papillomavirus E6 oncoproteins to the human homologue of the Drosophila discs large tumor suppressor protein. Proc. Natl. Acad. Sci. USA **94:**11612–11616.
22. **Krantz, C. K., B. A. Routes, M. P. Quinlan, and J. L. Cook.** 1996. E1A second exon requirements for induction of target cell susceptibility to lysis by natural killer cells: implications for the mechanism of action. Virology **217:** 23–32.
23. **Lee, S. S., B. Glaunsinger, F. Mantovani, L. Banks, and R. T. Javier.** 2000. Multi-PDZ domain protein MUPP1 is a cellular target for both adenovirus E4-ORF1 and high-risk papillomavirus type 18 E6 oncoproteins. J. Virol. **74:**9680–9693.
24. **Lee, S. S., R. S. Weiss, and R. T. Javier.** 1997. Binding of human virus oncoproteins to hDlg/SAP97, a mammalian homolog of the *Drosophila* discs large tumor suppressor protein. Proc. Natl. Acad. Sci. USA **94:**6670–6675.
25. **Lue, R. A., S. M. Marfatia, D. Branton, and A. H. Chishti.** 1994. Cloning and characterization of hdlg: the human homologue of the Drosophila discs large tumor suppressor binds to protein 4.1. Proc. Natl. Acad. Sci. USA **91:**9818–9822.
26. **Marcellus, R. C., J. N. Lavoie, D. Boivin, G. C. Shore, G. Ketner, and P. E. Branton.** 1998. The early region 4 orf4 protein of human adenovirus type 5 induces p53-independent cell death by apoptosis. J. Virol. **72:**7144–7153.
27. **Moore, M., N. Horikoshi, and T. Shenk.** 1996. Oncogenic potential of the adenovirus E4orf6 protein. Proc. Natl. Acad. Sci. USA **93:**11295–11301.
28. **Muller, B. M., U. Kistner, R. W. Veh, C. Cases-Langhoff, B. Becker, E. D. Gundelfinger, and C. C. Garner.** 1995. Molecular characterization and spatial distribution of SAP97, a novel presynaptic protein homologous to SAP90 and the Drosophila discs-large tumor suppressor protein. J. Neurosci. **15:** 2354–2366.
29. **Nevels, M., S. Rubenwolf, T. Spruss, H. Wolf, and T. Dobner.** 1997. The adenovirus E4orf6 protein can promote E1A/E1B-induced focus formation by interfering with p53 tumor suppressor function. Proc. Natl. Acad. Sci. USA **94:**1206–1211.
30. **Nevels, M., B. Tauber, E. Kremmer, T. Spruss, H. Wolf, and T. Dobner.** 1999. Transforming potential of the adenovirus type 5 E4orf3 protein. J. Virol. **73:**1591–1600.
31. **Nevins, J. R., and P. K. Vogt.** 1996. Cell transformation by viruses, p. 301–343. *In* B. N. Fields, D. M. Knipe, and P. M. Howley (ed.), Fields virology, 3rd ed, vol. 1. Lippincott-Raven, Philadelphia, Pa.
32. **Ranganathan, R., and E. M. Ross.** 1997. PDZ domain proteins: scaffolds for signaling complexes. Curr. Biol. **7:**R770–R773.
33. **Roelvink, P. W., I. Kovesdi, and T. J. Wickham.** 1996. Comparative analysis of adenovirus fiber-cell interaction: adenovirus type 2 (Ad2) and Ad9 utilize the same cellular fiber receptor but use different binding strategies for attachment. J. Virol. **70:**7614–7621.
34. **Roelvink, P. W., A. Lizonova, J. G. M. Lee, Y. Li, J. M. Bergelson, R. W. Finberg, D. E. Brough, I. Kovesdi, and T. J. Wickham.** 1998. The coxsack-

ievirus-adenovirus receptor protein can function as a cellular attachment protein for adenovirus serotypes from subgroups A, C, D, E, and F. J. Virol. **72:**7909–7915.

35. **Schaack, J., S. Langer, and X. Guo.** 1995. Efficient selection of recombinant adenoviruses by vectors that express β-galactosidase. J. Virol. **69:**3920–3923.
36. **Sharp, P. A.** 1984. Adenovirus transcription, p. 173–204. *In* H. Ginsberg (ed.), The adenoviruses. Plenum Press, New York, N.Y.
37. **Shenk, T.** 1996. Adenoviridae: the viruses and their replication, p. 2111–2148. *In* B. N. Fields, D. M. Knipe, and P. M. Howley (ed.), Fields virology, vol. 2. Lippincott-Raven, Philadelphia, Pa.
38. **Shtrichman, R., and T. Kleinberger.** 1998. Adenovirus type 5 E4 open reading frame 4 protein induces apoptosis in transformed cells. J. Virol. **72:**2975–2982.
39. **Smith, D. B., and L. M. Corcoran.** 1994. Expression and purification of glutathione-S-transferase fusion proteins, p. 16.7.1–16.7.7. *In* F. M. Ausubel, R. Brent, R. E. Kingston, D. D. Moore, J. G. Seidman, J. A. Smith, and K. Struhl (ed.), Current protocols in molecular biology. Greene Publishing Associates and Wiley-Interscience, New York, N.Y.
40. **Suzuki, T., Y. Ohsugi, M. Uchida-Toita, T. Akiyama, and M. Yoshida.** 1999. Tax oncoprotein of HTLV-1 binds to the human homologue of Drosophila discs large tumor suppressor protein, hDLG, and perturbs its function in cell growth control. Oncogene **18:**5967–5972.
41. **Thomas, D. L., S. Shin, B. H. Jiang, H. Vogel, M. A. Ross, M. Kaplitt, T. E. Shenk, and R. T. Javier.** 1999. Early region 1 transforming functions are dispensable for mammary tumorigenesis by human adenovirus type 9. J. Virol. **73:**3071–3079.
42. **Thomas, U., B. Phannavong, B. Muller, C. C. Garner, and E. D. Gundelfinger.** 1997. Functional expression of rat synapse-associated proteins SAP97 and SAP102 in Drosophila dlg-1 mutants: effects on tumor suppression and synaptic bouton structure. Mech. Dev. **62:**161–174.
43. **Weiss, R. S., M. O. Gold, H. Vogel, and R. T. Javier.** 1997. Mutant adenovirus type 9 E4 ORF1 genes define three protein regions required for transformation of CREF cells. J. Virol. **71:**4385–4394.
44. **Weiss, R. S., and R. T. Javier.** 1997. A carboxy-terminal region required by the adenovirus type 9 E4 ORF1 oncoprotein for transformation mediates direct binding to cellular polypeptides. J. Virol. **71:**7873–7880.
45. **Weiss, R. S., S. S. Lee, B. V. Prasad, and R. T. Javier.** 1997. Human adenovirus early region 4 open reading frame 1 genes encode growth-transforming proteins that may be distantly related to dUTP pyrophosphatase enzymes. J. Virol. **71:**1857–1870.
46. **Weiss, R. S., M. J. McArthur, and R. T. Javier.** 1996. Human adenovirus type 9 E4 open reading frame 1 encodes a cytoplasmic transforming protein capable of increasing the oncogenicity of CREF cells. J. Virol. **70:**862–872.
47. **Yamano, S., T. Tokino, M. Yasuda, M. Kaneuchi, M. Takahashi, Y. Niitsu, K. Fujinaga, and T. Yamashita.** 1999. Induction of transformation and p53-dependent apoptosis by adenovirus type 5 E4orf6/7 cDNA. J. Virol. **73:** 10095–10103.

(Submitted)

The Unique Transforming and Tumorigenic Properties of the Adenovirus Type 9 E4-ORF1 Oncoprotein Are Linked to a Select Interaction with the Candidate Tumor Suppressor Protein ZO-2

Britt A. Glaunsinger, Robert S. Weiss, Siu Sylvia Lee, and Ronald Javier

Department of Molecular Virology and Microbiology, Baylor College of Medicine, Houston, Texas 77030, USA

Running Title: Unique targeting of ZO-2 by Ad9 E4-ORF1

Keywords: ZO-2/PDZ/adenovirus/E4-ORF1/transformation

Corresponding author: Ronald T. Javier, Department of Molecular Virology and Microbiology, Baylor College of Medicine, Houston, TX, 77030, USA

Phone: (713) 798-3898

Fax: (713) 798-3586

E-mail: rjavier@bcm.tmc.edu

ABSTRACT

The study of DNA tumor viruses has considerably advanced our understanding of mechanisms responsible for the development of cancer. Adenovirus type 9 (Ad9) is distinct among human adenoviruses because this virus elicits solely mammary tumors in animals and its primary oncogenic determinant is the E4 region-encoded ORF1 (E4-ORF1) protein. Though the mechanism of action for Ad9 E4-ORF1 is not yet known, our previous findings indicate that transformation by this viral oncoprotein depends on its interactions with a specific group of cellular PDZ domain-containing proteins, including the multi-PDZ protein MUPP1 and the membrane-associated guanylate kinase-homology (MAGUK) proteins DLG and MAGI-1, which are predicted to function as adaptor proteins in cell signaling. Here we report identification of the cellular factor ZO-2, a MAGUK and candidate tumor suppressor protein, as the fourth Ad9 E4-ORF1-associated cellular PDZ protein. Whereas MUPP1, MAGI-1, and DLG likewise bind to non-tumorigenic wild-type E4-ORF1 proteins encoded by adenovirus types 5 and 12, ZO-2 was shown to represent an exclusive cellular target for tumorigenic Ad9 E4-ORF1. Complex formation was mediated by the carboxyl-terminal PDZ domain-binding motif of Ad9 E4-ORF1 and the first PDZ domain of ZO-2, and in cells this interaction resulted in aberrant sequestration of ZO-2 within the cytoplasm. In addition, transformation-defective Ad9 E4-ORF1 mutants exhibited impaired binding to and sequestration of ZO-2 in cells, and over-expression of wild-type ZO-2, but not mutant ZO-2 lacking the second and third PDZ domains, interfered with Ad9 E4-ORF1-induced focus formation. These results suggest that the select capacity to complex with the candidate tumor suppressor protein ZO-2 is key to defining the unique transforming and tumorigenic properties of the Ad9 E4-ORF1 oncoprotein.

INTRODUCTION

The 51 different serotypes of human adenovirus are distributed within six subgroups (A through F) based on physical and hemagglutinating properties of virions (48). In people, these agents are primarily associated with respiratory, gastrointestinal, and ocular infections (28). Under experimental conditions in rodents, however, viruses comprising subgroups A and B, as well as two viruses from subgroup D, are tumorigenic (48). Such viruses can be further subdivided into two categories based on the types of tumors they elicit in animals and the viral genes responsible for their oncogenic potential. Adenoviruses from subgroups A and B generate undifferentiated sarcomas, and the oncogenic determinants of these viruses are their *E1A* and *E1B* genes (22). In contrast, human adenovirus type 9 (Ad9) from subgroup D elicits only estrogen-dependent mammary tumors (1, 2, 32), and its oncogenic determinant is the E4 region-encoded ORF1 (*E4-ORF1*) gene (35, 53, 54). Whereas the oncogenic potentials of the E1A and E1B proteins largely stem from their capacities to inactivate the crucial cellular pRb and p53 tumor suppressors (48), respectively, the mechanisms underlying tumorigenesis by the Ad9 E4-ORF1 protein are still unknown.

The Ad9 *E4-ORF1* gene encodes a 125 amino-acid residue polypeptide which, following expression in rat CREF fibroblasts (16), induces a multitude of transformed properties, including morphological changes, focus formation, anchorage-independent growth, and increased saturation densities (59). With the exception of adenovirus types 40 and 41 comprising subgroup F, all human adenoviruses code for an E4-ORF1 protein (7, 25, 26, 34). Representative E4-ORF1 polypeptides from different viral subgroups display sequence similarities ranging from 45% to 51% identity and, in addition, these viral proteins share the ability to induce anchorage-independent growth in human TE85 cells (58), revealing a common

transforming activity *in vitro*. Nevertheless, among this family of viral proteins, only Ad9 E4-ORF1 possesses the capacities to promote tumors in animals and to transform CREF cells (35, 53, 58). An interesting possible explanation for the unique properties of Ad9 E4-ORF1 would be that it possesses an undetermined activity absent from other adenovirus E4-ORF1 proteins.

The results of mutational analyses demonstrate that transformation of CREF cells by Ad9 E4-ORF1 is dependent on three separate protein regions (56). One region located at the extreme carboxyl-terminus of Ad9 E4-ORF1 has been found to represent a PDZ domain-binding motif that mediates interactions with a specific group of cellular PDZ domain-containing proteins (38, 57). Three of these PDZ proteins were recently identified as the multi-PDZ protein MUPP1 and the membrane-associated guanylate kinase homology (MAGUK) proteins DLG and MAGI-1 (18, 37, 38). These interactions result from the ability of the Ad9 E4-ORF1 carboxyl-terminal motif to bind specific PDZ domains within each cellular factor. Also pertinent is that these three PDZ proteins represent common cellular targets for the subgroup C adenovirus type 5 (Ad5) and subgroup A adenovirus type 12 (Ad12) E4-ORF1 proteins, both of which fail to promote tumors in animals and to transform CREF cells (18, 37, 38). Thus, despite making predicted important contributions to the limited transforming potential common to all adenovirus E4-ORF1 proteins, interactions with MUPP1, MAGI-1, and DLG would not account for the additional, unique properties of Ad9 E4-ORF1.

It is noteworthy that the Tax oncoprotein of human T-cell leukemia virus type 1 (HTLV-1) and the E6 oncoproteins of high-risk human papillomaviruses (HPV) also have a PDZ domain-binding motif at their carboxyl-termini (38). The motifs of these viral proteins similarly mediate interactions with multiple cellular PDZ domain-containing proteins, including

DLG, lin-7, PSD-95, and β1-syntrophin for HTLV-1 Tax (38, 46) and MUPP1, MAGI-1, DLG, and scribble for high-risk HPV E6 proteins (18, 37, 38, 44). These findings may indicate that interactions with cellular PDZ proteins contribute to the tumorigenic potentials of several different human virus oncoproteins.

PDZ domains are protein-protein interaction modules present primarily within cellular factors that function in signal transduction (12). A distinguishing feature of these domains is that their recognition motifs are typically located at the extreme carboxyl-terminus of target proteins (51). Several different types of PDZ domain-binding motifs are known (14) and, at their carboxyl-termini, the adenovirus E4-ORF1, high-risk HPV E6, and HTLV-1 Tax proteins possess a type I motif having the consensus sequence -(S/T)-X-(V/I/L)-COOH (where X is any amino-acid residue). With respect to known functions for PDZ proteins, these cellular factors generally act as scaffolding proteins, which organize membrane receptors and cytosolic proteins into large signaling complexes and localize these large complexes to specialized membrane sites of cell-cell contact (12, 14).

While the precise signaling functions of the Ad9 E4-ORF1-associated PDZ proteins have not been determined, it seems pertinent that DLG is a mammalian homolog of the *Drosophila* discs large (dlg) tumor suppressor protein (40, 43). In addition, over-expression of DLG has been shown to block progression of NIH 3T3 fibroblasts from G0/G1 to S phase of the cell cycle (29), and HTLV-1 Tax is able to inhibit the anti-proliferative activity of this cellular protein (52). Such findings have led us to propose the two hypotheses that DLG, and perhaps other Ad9 E4-ORF1-associated PDZ proteins, function to suppress abnormal cellular proliferation and that the viral oncoproteins target these cellular factors for inactivation. Our results showing that Ad9 E4-ORF1 aberrantly sequesters MUPP1 and MAGI-1 in cells and that high-risk HPV E6

oncoproteins target these PDZ proteins, as well as DLG, for degradation in cells are consistent with these ideas (17, 18, 37).

We previously reported that, in addition to binding MUPP1, MAGI-1, and DLG, Ad9 E4-ORF1 likewise complexes with two unidentified cellular PDZ proteins designated p155 and p160 (57). Contrary to other Ad9 E4-ORF1-associated PDZ proteins, however, p160 fails to interact with non-tumorigenic Ad5 and Ad12 E4-ORF1 (57). The goal of the present study was to identify this uniquely Ad9 E4-ORF1-specific binding protein. We demonstrate here that p160 is the cellular MAGUK protein ZO-2 (4, 36), which was recently identified as a candidate tumor suppressor protein (8-10). Regarding the latter assertion, ZO-2 expression was either lost or significantly decreased in 80% (4/5) of examined breast cancer lines and in 83% (5/6) of examined primary breast adenocarcinomas, although this effect was rarely seen in colon cancers or prostate adenocarcinomas (9). Moreover, the *ZO-2* gene utilizes two alternate promoters, giving rise to two ZO-2 isoforms that differ at their amino-terminus by 23 amino-acid residues. Whereas both ZO-2 isoforms were detected in normal pancreatic-duct epithelial cells, the longer isoform was absent in 90% (9/10) of examined pancreatic-duct carcinoma lines and in 100% (4/4) of examined primary pancreatic adenocarcinomas (8, 10). In accordance with these observations, we show that the transforming potential of Ad9 E4-ORF1 in CREF cells is associated with its ability to bind and aberrantly sequester ZO-2 and that over-expression of ZO-2 in these cells inhibits Ad9 E4-ORF1-induced transformation. Additional results also confirm the expected failure of ZO-2 to bind non-tumorigenic adenovirus E4-ORF1 proteins. In light of these findings, we propose that the exclusive interaction between ZO-2 and Ad9 E4-ORF1 bestows distinct transforming and tumorigenic properties to this viral oncoprotein.

MATERIALS AND METHODS

Cells, transfections, and extracts. MDCK (ATCC# CCL-34), COS-7 (19), CREF (16), C127 (39), and TE85 (42) cell lines were maintained in culture medium [Dulbecco's Modified Eagle medium (DMEM) supplemented with 20 μg/ml gentamicin and 6% or 10% fetal calf serum (FCS)] in a 37°C humidified incubator under a 5% CO_2 atmosphere. CREF cells stably-expressing wild-type or mutant Ad9 E4-ORF1 proteins (56) or an influenza hemagglutinin (HA) epitope-tagged wild-type Ad9 E4-ORF1 protein (58) were maintained in culture medium supplemented with 100 μg/ml G418.

Transfections were carried out with either Fugene 6 (Roche Molecular Biochemicals), Lipofectamine, or Lipofectamine Plus (Life Technologies), as recommended by the manufacturer. Preparation of cell extracts was performed as described previously (18). Briefly, cells were washed twice with ice-cold phosphate-buffered saline (PBS) (4.3 mM Na_2HPO_4, 1.4 mM KH_2PO_4, 137 mM NaCl, 2.7 mM KCl) and lysed in either 1X sample buffer (SB) [0.15 M Tris-HCl pH 6.8, 2% (wt/vol) sodium dodecyl sulfate (SDS), 10% vol/vol glycerol, 1% (vol/vol) β-mercaptoethanol, 0.0015% bromophenol blue] or RIPA buffer [50 mM Tris-HCl pH 8.0, 150 mM NaCl, 1% (vol/vol) Nonidet P-40, 0.5% (wt/vol) sodium deoxycholate, 0.1% (wt/vol) SDS] supplemented with protease inhibitors (6 μg/ml each of aprotinin and leupeptin, 300 μg/ml phenylmethylsulfonyl fluoride) and phosphatase inhibitors (0.2 mM Na_3VO_4 and 50 mM NaF) for 10 min on ice. The resulting cell extracts were cleared by centrifugation (16,000 X *g*, 20 min). For cell fractionation experiments, the pellet recovered after centrifugation of cell extracts was suspended in a volume of 1X SB equivalent to the volume of RIPA buffer originally used for cell lysis (18). Protein concentrations were determined by the Bradford assay (6).

Plasmids. Ad9 E4-ORF1-expressing plasmids GW1-9ORF1wt, GW1-9ORF1IIIA, GW1-9ORF1IIIC, GW1-9ORF1IIID, and pJ4Ω-9ORF1 have been described previously (37, 56). Plasmids expressing RasV12 (pSG5-RasV12) and polyomavirus middle T oncoproteins (pPyMT1) (55) were kindly provided by Julian Downward (ICRF) and Janet Butel (Baylor College of Medicine), respectively. The RasV12 cDNA from pSG5-RasV12 was inserted between the *Bgl*II and *Eco*RI sites of CMV expression plasmid GW1 (British Biotechnology) to generate GW1-RasV12. Plasmid pBS-ZO-2, containing a wild-type canine ZO-2 cDNA (4), was generously provided by Bruce Stevenson (University of Alberta). The following three ZO-2 cDNA modifications were accomplished by PCR methods. An HA epitope tag (15) was placed at the amino-terminus of ZO-2, and this modified cDNA was inserted into the *Sma*I site of GW1 to generate GW1-HA-ZO-2. Plasmids GW1-HA-ZO-2ΔPDZ1 and GW1-HA-ZO-2ΔPDZ2+3 were derived from GW1-HA-ZO-2 by deleting the majority of ZO-2 PDZ1 [amino-acid residues (aa) 11-66] or a ZO-2 region containing both PDZ2 and PDZ3 (aa 288-531), respectively. ZO-2 DNA sequences coding for PDZ1 (aa 4-113), PDZ2 and PDZ3 (PDZ2+3) (aa 290-585), or unique sequences located between PDZ2 and PDZ3 (US2/3) (aa 394-495) were PCR amplified and inserted into the *Bam*HI and *Eco*RI sites of pGEX-2T in-frame with the glutathione *S*-transferase (GST) gene to generate plasmids pGEX-PDZ1, pGEX-PDZ2+3, and pGEX-US2/3, respectively. Plasmids pGEX-2TK-9ORF1, pGEX-2T-9ORF1, pGEX-2T-9ORF1IIIA, pGEX-2T-9ORF1IIIC, pGEX-2T-9ORF1IIID, pGEX-2T-5ORF1, and pGEX-2T-12ORF1 have been described previously (57). PCR reactions were carried out with either *deep vent* (New England Biolabs) or *pfu* (Stratagene) DNA polymerase. All plasmids were purified on CsCl density gradients and verified by restriction enzyme and limited sequence analyses.

Antisera and antibodies. Rabbit polyclonal antisera to Ad9 E4-ORF1 have been described previously (35). Rabbit polyclonal antisera to ZO-2 were raised against a purified, bacterially-expressed GST-US2/3 fusion protein by standard methods (23). IgG was purified from ZO-2 antisera or matched pre-immune sera using protein A-coated sepharose beads (Amersham Pharmacia Biotech). ZO-2 antibodies were affinity purified using the immunizing peptide coupled to an activated Affi-Gel 10 immunoaffinity support (Bio-Rad) (23). Commercially-available antibodies to the HA epitope (16B12; Covance), as well as normal rabbit IgG and peroxidase-conjugated goat anti-rabbit or goat anti-mouse IgG (Southern Biotechnology Associates), FITC-conjugated goat anti-rabbit IgG (Gibco BRL), and Texas red-conjugated goat anti-mouse IgG (Molecular Probe) were used.

GST-pulldown, immunoprecipitation, and immunoblot assays. GST-pulldown and immunoprecipitation assays were performed using cell extracts in RIPA buffer as described previously (38). That an equivalent amount of each GST fusion protein (5 μg) was utilized in GST-pulldown assays was verified by coomassie staining of protein gels. Immunoblot assays were carried out with primary antibodies to either Ad9 E4-ORF1 (1:5000), HA (1.2 μg/ml), or ZO-2 (1:5000) and with secondary antibodies to either horseradish peroxidase-conjugated goat anti-rabbit IgG or goat anti-mouse IgG (1:5000). Membranes were developed by enhanced chemiluminescence methods (Pierce).

Protein blotting assays. ZO-2 PDZ1 and PDZ2+3 were expressed as GST fusion proteins in bacteria, purified on glutathione sepharose beads (Pharmacia) (49), separated by SDS polyacrylamide gel electrophoresis (PAGE), and transferred to a nitrocellulose membrane. Methods for preparing [^{32}P]-labeled GST-Ad9 E4-ORF1 protein probes and performing protein-blotting assays have been described previously (38).

Immunofluorescence microscopy (IF) assays. IF assays were carried out by standard methods (23). Briefly, cells were grown on coverslips, fixed in 4% paraformaldehyde for 20 min, permeablized with 0.1% Triton X-100 for 15 min, incubated in IF blocking buffer [TBS (50 mM Tris-HCl pH 7.5, 200 mM NaCl) containing 10% goat serum (Sigma)] for 1 h at room temperature, and incubated with either affinity-purified ZO-2 antibodies (2.4 μg/ml) or normal rabbit IgG (2.4 μg/ml) for 12 h at 37°C. Cells were rinsed with TBS, incubated with IF blocking buffer for 1 h at RT and with FITC-conjugated goat anti-rabbit IgG antibodies (1:250) (Gibco BRL) for 1 h at 37°C, and washed extensively with TBS. For double-labeling IF assays, cells were incubated with a mixture of ZO-2 antibodies (2.4 μg/ml) and HA antibodies (50 μg/ml) and then with a mixture of FITC-conjugated goat anti-rabbit IgG (Gibco BRL) and Texas red-conjugated goat anti-mouse IgG (Molecular Probes) antibodies (1:250). Cells were stained with 4',6-diamidino-2-phenylindole (DAPI) (5 μg/ml) to visualize nuclei and examined with a Zeiss Axiophot fluorescent microscope.

Focus assays. 48 h post-transfection of 10^6 CREF cells, cells were passaged 1:3 and maintained in DMEM supplemented with 3% filtered FCS. At approximately three-weeks post-transfection, cells were fixed in methanol and stained with giemsa (VWR) to quantify numbers of transformed foci (35).

RESULTS

Ad9 E4-ORF1 uniquely complexes with ZO-2 in cells. Ad9 E4-ORF1 is set apart from other adenovirus E4-ORF1 polypeptides by its abilities to promote tumors in animals and to transform CREF cells. With respect to a specific Ad9 E4-ORF1 activity that may account for these unique properties, we previously detected an unidentified cellular factor, p160, which binds to tumorigenic Ad9 E4-ORF1 but not to non-tumorigenic Ad12 and Ad5 E4-ORF1 (57). Given that disruption of the PDZ domain-binding motif of Ad9 E4-ORF1 abolishes its interaction with p160 (57), we reasoned that p160 is a cellular PDZ domain-containing protein. A search for known 160-kDa cellular PDZ proteins led to ZO-2 (4), a cell junction-associated MAGUK protein related to the Ad9 E4-ORF1-associated proteins DLG and MAGI-1 (Fig. 1). In addition, recent reports indicate that ZO-2 is a candidate tumor suppressor protein (8-10). These observations prompted studies to assess whether p160 is ZO-2.

In GST pulldown assays, wild-type ZO-2 tagged at its amino-terminus with an HA epitope (HA-ZO-2) and expressed in COS-7 cells complexed with the wild-type Ad9 E4-ORF1 GST fusion protein but not with the GST protein control (Fig. 2A). This interaction is specific because, in similar assays, we have shown that Ad9 E4-ORF1 fails to bind other cellular PDZ proteins, including the closely-related MAGUK proteins ZO-1 and ZO-3, the multi-PDZ proteins FAP-1 and hINADL, and the Ras effector protein AF-6 (18). Transformation-defective Ad9 E4-ORF1 mutants having altered PDZ domain-binding motifs were also tested in the GST-pulldown assays. Mutant IIIA lacks a functional PDZ domain-binding motif and detectable transforming activity in CREF cells, whereas mutants IIIC and IIID have less disruptive PDZ domain-binding motif mutations and retain weak transforming activity in these cells (Table 1) (56). In pulldown assays, mutants IIIA and IIIC failed to interact with HA-ZO-2, while mutant IIID displayed some binding activity, albeit substantially less than

that of the wild-type viral protein (Fig. 2A). Moreover, the results of co-immunoprecipitation assays performed with COS-7 cells transiently co-expressing HA-ZO-2 and either wild-type or mutant Ad9 E4-ORF1 agreed with those of the GST pulldown assays (Fig. 2B). Particularly notable was the failure of Ad5 and Ad12 E4-ORF1 to complex with HA-ZO-2 in GST pulldown assays (Fig. 2C), despite the presence of a functional type I PDZ domain-binding motif at the carboxyl-termini of these viral proteins (Table 1) (18, 37, 38). We likewise did not detect binding of HA-ZO-2 to non-tumorigenic subgroup B adenovirus type 3 E4-ORF1, or the HTLV-1 Tax and high-risk HPV E6 oncoproteins (data not shown) (18). Therefore, binding of ZO-2 to Ad9 E4-ORF1 is highly selective and dependent on the PDZ domain-binding motif of this viral protein.

We were next interested in determining whether Ad9 E4-ORF1 also complexes with ZO-2 endogenously expressed in cells. For specific detection of ZO-2, we raised rabbit polyclonal antisera to a unique 100 amino-acid region between ZO-2 PDZ2 and PDZ3 (aa 394-495). The ZO-2 antisera, but not the matched pre-immmune sera (data not shown), recognized an expected 160-kDa polypeptide in CREF cells and several other cell lines, including canine MDCK cells, human 293 and TE85 cells, and murine 3T3 fibroblasts (Fig. 3A). The size of the detected protein in these lines was identical to that of authentic wild-type ZO-2 exogenously expressed in COS-7 cells. We also demonstrated that ZO-2 and Ad9 E4-ORF1-associated protein p160 co-migrate in a protein gel (Fig. 3B). This finding, coupled with results showing that these two proteins likewise display identical binding profiles to Ad9 E4-ORF1 mutants and fail to interact with Ad5 and Ad12 E4-ORF1 (see Fig. 2C) (57), strongly argue that ZO-2 and p160 are the same proteins.

To examine whether Ad9 E4-ORF1 also complexes with endogenous ZO-2 in CREF cells, we employed the ZO-2 antiserum in co-immunoprecipitation assays. The results, shown in Fig. 4, indicated that wild-type Ad9 E4-ORF1, but none of the Ad9 E4-ORF1 mutants, co-immunoprecipitates with endogenous ZO-2 from lysates of CREF cells stably expressing these viral proteins. These results in CREF cells differed slightly from those in COS-7 cells (see Figs. 2A and 2B), where viral mutant IIID showed substantially diminished yet detectable binding to over-expressed ZO-2. This discrepancy likely reflects enhanced detection of weak binding between mutant IIID and ZO-2 when high levels of this cellular protein are expressed in COS-7 cells. Nonetheless, these findings are important in suggesting that the interaction between ZO-2 and Ad9 E4-ORF1 is required for Ad9 E4-ORF1-induced transformation of CREF cells.

Ad9 E4-ORF1 binds ZO-2 PDZ1. To initially identify the ZO-2 PDZ domain(s) that mediates binding to Ad9 E4-ORF1, we blotted membrane-immobilized fragments of ZO-2 with a radiolabeled Ad9 E4-ORF1 protein probe. In these assays, Ad9 E4-ORF1 interacted with ZO-2 PDZ1 but not with a ZO-2 fragment containing both PDZ2 and PDZ3 (PDZ2+3) (Figs. 5A and 5B). This interaction required the Ad9 E4-ORF1 PDZ domain-binding motif because a mutant IIIA protein probe failed to react with either of these ZO-2 peptides (data not shown). Consistent with results of the protein blotting assays, wild-type ZO-2 and mutant ZO-2 missing both PDZ2 and PDZ3 (HA-ZO-2ΔPDZ2+3) co-immunoprecipitated with Ad9 E4-ORF1 from lysates of COS-7 cells, whereas mutant ZO-2 missing PDZ1 (HA-ZO-2ΔPDZ1) did not (Figs. 5A and 5C). Therefore, ZO-2 PDZ1 is both necessary and sufficient for mediating ZO-2 binding to Ad9 E4-ORF1 in cells.

Ad9 E4-ORF1 aberrantly sequesters ZO-2 in the cytoplasm of CREF cells. We have previously shown that association of Ad9 E4-ORF1 with the cellular PDZ proteins MUPP1 and MAGI-1 results in their aberrant sequestration within punctate bodies in the cytoplasm of CREF cells (18, 37). It was therefore of interest to examine whether ZO-2 is similarly affected by Ad9 E4-ORF1 in these cells. ZO-2 has been reported to localize primarily at tight junctions in polarized epithelial cells (36), or at adherens junctions in non-epithelial cells such as mouse 3T3 and rat 3Y1 fibroblasts that lack tight junctions (31). Consistent with these observations, IF assays performed with our antiserum to ZO-2 revealed prominent cell-cell contact staining for this cellular protein in MDCK epithelial cells (data not shown). In IF assays using affinity-purified ZO-2 antibodies with normal CREF fibroblasts, however, we found that ZO-2 was located primarily in the cytoplasm with a cytoskeleton-like staining pattern and, to a lesser extent, at the plasma membrane (Fig. 6A). In contrast, the majority of ZO-2 in CREF cells stably expressing wild-type Ad9 E4-ORF1 was instead aberrantly sequestered within cytoplasmic punctate bodies (Fig. 6A). Double-labeling IF assays further showed that ZO-2 and wild-type Ad9 E4-ORF1 co-localize in these structures (Fig. 6B). This effect is linked to Ad9 E4-ORF1-induced transformation in that transformation-defective mutants IIIA and IIIC failed, or mutant IIID showed a substantially reduced capacity, to aberrantly sequester ZO-2 in these cells (Fig. 6A).

The results of cell fractionation experiments confirmed the aberrant sequestration of ZO-2 by Ad9 E4-ORF1 in CREF cells. In these experiments, normal CREF cells or CREF cells stably expressing either wild-type or mutant Ad9 E4-ORF1 were lysed in RIPA buffer, and the cell extracts were separated by centrifugation into soluble (*S*) supernatant and insoluble (*I*) pellet fractions. Immunoblot analyses with ZO-2 antiserum were carried out to determine the relative

amount of ZO-2 present in each fraction. In normal CREF cells, ZO-2 was present primarily in the soluble fraction whereas conversely, in CREF cells stably expressing wild-type Ad9 E4-ORF1, the majority of ZO-2 was redistributed into the insoluble fraction (Fig. 6C). Concordant with results of IF assays (see Fig. 6A), we also found that ZO-2 from CREF lines expressing Ad9 E4-ORF1 mutants exhibited a fractionation profile similar to that of normal CREF cells (Fig. 6C). In addition, the ZO-2 protein present in the insoluble fraction of wild-type Ad9 E4-ORF1-expressing CREF cells displayed a reduced gel mobility compared to that of normal CREF cells or CREF cells expressing Ad9 E4-ORF1 mutants (Fig. 6C; see also Fig. 4A). This finding suggests that, in addition to aberrantly sequestering ZO-2, wild-type Ad9 E4-ORF1 also promotes an unknown post-translational modification(s) to this cellular factor.

ZO-2 blocks Ad9 E4-ORF1-mediated transformation of CREF cells. Recent reports showing that ZO-2 expression is lost or reduced in certain human cancers (9, 10) may indicate that ZO-2 suppresses the neoplastic growth of cells. This idea prompted experiments to determine whether over-expression of ZO-2 can inhibit transformation by Ad9 E4-ORF1. In accordance with our previous findings (59), transfection of a wild-type Ad9 E4-ORF1 expression plasmid into CREF cells resulted in numerous transformed foci (Fig. 7A). In similar assays, however, inclusion of a plasmid expressing either wild-type HA-ZO-2 or mutant HA-ZO-2ΔPDZ1 significantly decreased the number of Ad9 E4-ORF1-induced foci (2.9-fold and 2.5-fold reductions, respectively), whereas inclusion of a plasmid expressing mutant HA-ZO-2ΔPDZ2+3 did not (1.1-fold reduction) (Fig. 7A). The latter defect of HA-ZO-2ΔPDZ2+3 does not result from an expression deficiency, as this mutant achieved steady-state protein levels comparable to those of wild-type HA-ZO-2 in both COS-7 cells (see Fig. 5C) and CREF cells (data not shown). These findings are important in providing direct evidence that ZO-2 possesses a transformation-

repressive activity and in specifically localizing this activity to the protein sequences deleted from HA-ZO-2ΔPDZ2+3. Results with mutants HA-ZO-2ΔPDZ1 and HA-ZO-2ΔPDZ2+3 further indicated that binding of ZO-2 to Ad9 E4-ORF1 is neither necessary nor sufficient, respectively, to inhibit Ad9 E4-ORF1-induced focus formation. Precedence for this type of effect comes from a study showing that over-expression of a mutant p300 transcriptional co-activator, which is unable to bind the adenovirus E1A oncoprotein, retains the capacity to overcome E1A-mediated transcriptional repression of the SV40 promoter (13). We therefore predicted that ZO-2 would also be able to suppress transformation by other viral or cellular oncoproteins. Consistent with this idea, we showed that over-expression of HA-ZO-2 in CREF cells likewise significantly diminishes focus formation by the activated RasV12 and the polyomavirus middle T proteins (3.7-fold and 2.9-fold reductions, respectively) (Fig. 7B), which lack any recognizable PDZ domain-binding motifs.

DISCUSSION

Among human adenovirus E4-ORF1 proteins, Ad9 E4-ORF1 is unique in its abilities to promote tumors in animals and to transform CREF cells. One possible explanation for these striking distinctions would be that Ad9 E4-ORF1 possesses a crucial oncogenic activity lacking from non-tumorigenic adenovirus E4-ORF1 proteins. Consistent with this notion, we have previously detected a 160-kDa cellular polypeptide that complexes with Ad9 E4-ORF1, yet fails to interact with non-tumorigenic Ad5 and Ad12 E4-ORF1 (57). Here we identified this specific Ad9 E4-ORF1-associated 160-kDa polypeptide as the cellular MAGUK protein ZO-2. Additional results in CREF cells demonstrated that transformation-defective Ad9 E4-ORF1 mutants either failed or showed a substantially reduced capacity to bind ZO-2 and that over-expression of this cellular protein blocked Ad9 E4-ORF1-induced focus formation. These findings are significant in suggesting that this specific interaction with ZO-2 is essential for the Ad9 E4-ORF1 oncoprotein to transform CREF cells.

It is also important to note that Ad9 E4-ORF1 interacts with additional cellular PDZ proteins, including MUPP1, MAGI-1, and DLG, and that transformation-defective Ad9 E4-ORF1 mutants likewise display impaired binding to these cellular factors (18, 37, 38, 57). These three PDZ proteins also represent common cellular targets for Ad5 and Ad12 E4-ORF1 which, despite lacking tumorigenic potential, are similar to Ad9 E4-ORF1 in having the ability to transform anchorage-dependent human TE85 cells to grow in soft agar (18, 37, 38, 58). We therefore favor a model whereby the combined interactions of multiple cellular PDZ proteins with Ad9 E4-ORF1 are required for manifestation of its full transforming potential. Nevertheless, the fact that ZO-2 binds to tumorigenic Ad9 E4-ORF1, but not to non-tumorigenic Ad5 and Ad12 E4-ORF1, suggests that this particular interaction plays a central role in defining

the unique tumorigenic properties of Ad9 E4-ORF1. Moreover, whereas Ad9 E4-ORF1 efficiently transforms CREF cells, we have been unsuccessful in our attempts to transform CREF cells with Ad5 and Ad12 E4-ORF1 or to establish CREF lines stably expressing these proteins (58), even though they can be transiently expressed to levels comparable to those of Ad9 E4-ORF1 in these cells (SSL, unpublished results). The latter observations may indicate that the ZO-2 interaction also serves to broaden the range of cell types susceptible to transformation by Ad9 E4-ORF1. This idea is attractive as our findings argue that Ad9 E4-ORF1 plays an important role in targeting tumorigenesis by Ad9 exclusively to cells of the rat mammary gland (53).

As we propose in this paper that the tumorigenic deficiency of Ad5 and Ad12 E4-ORF1 is associated with an inability to complex with ZO-2, our results with subgroup D adenovirus type 26 (Ad26) E4-ORF1, a non-tumorigenic protein more closely related to Ad9 E4-ORF1 (33), also require discussion. Contrary to the non-transforming phenotypes of Ad5 and Ad12 E4-ORF1 in CREF cells, Ad26 E4-ORF1 displays potent transforming activity indistinguishable from that of Ad9 E4-ORF1 in these cells (53). Ad26 E4-ORF1 also binds ZO-2, as well as the other Ad9 E4-ORF1-associated cellular PDZ proteins (unpublished results). We therefore speculate that the tumorigenic deficiency of Ad26 E4-ORF1 is unrelated to that of Ad5 and Ad12 E4-ORF1. Consistent with this assertion, we have shown that silent nucleotide differences between Ad9 and Ad26 *E4-ORF1* are responsible in part for the divergent tumorigenic phenotypes of these viral genes (53), suggesting that Ad26 *E4-ORF1* has an unknown expression defect in relevant cells of the rat mammary gland.

The notion that the tumorigenic potential of a viral transforming protein may be controlled by a unique activity lacking in an otherwise equivalent, non-tumorigenic viral

transforming protein is not novel. A classic example of this concept comes from comparative studies with the tumorigenic Ad12 and non-tumorigenic Ad5 viruses (48). Although the *E1A* and *E1B* genes of Ad12 or Ad5 similarly cooperate to transform cultured cells, only those cells transformed by Ad12 *E1A* and *E1B* produce tumors in syngeneic, immunocompetent animals. The difference here stems from the fact that the Ad12 E1A protein, but not the Ad5 E1A protein, is capable of repressing transcription from the cellular MHC class I gene. Thus, cells transformed by Ad12 E1A avoid lysis by host cytotoxic T cells and, consequently, can form tumors in animals. Contrary to this unique Ad12 E1A activity permitting oncogenically transformed cells to evade host immunosurveillance, we instead favor the idea that the unique Ad9 E4-ORF1 activity to complex with ZO-2 functions directly in the process of oncogenic transformation, such as disregulation of novel pathways that control cell-cycle progression or programmed cell death.

ZO-2 was originally identified through its association with the closely-related MAGUK protein ZO-1 at tight junctions (36), specialized cell-cell contact sites forming a belt-like region that separates the apical from the lateral plasma membrane in polarized epithelial cells. ZO-2 has subsequently been found to associate with a number of other cellular proteins, including tight-junction transmembrane proteins occludin and claudins (30, 61), tight-junction submembranous proteins ZO-3 and cingulin (11, 24), adherens-junction protein α-catenin (31), actin-associated nonerythroid protein 4.1R (41), and F-actin (61). Therefore, it is believed that ZO-2 acts as a bridge linking transmembrane proteins with the actin cytoskeleton at specialized membrane regions of cell-cell contact, as well as a regulator of signals emanating from these sites (20). Such processes have a clear association with carcinogenesis because the hallmark properties of transformed cells, including morphological changes, anchorage-independent

growth, and loss of contact inhibition, are often traced both to deficiencies in processing signals transmitted from neighboring cells and to disruption of the cytoskeleton (5).

Although ZO-2 has been found to localize at adherens junction membrane sites in non-epithelial cells (31, 36), we found it present primarily in the cytoplasm of CREF fibroblasts, revealing both membrane and cytoplasmic forms of this cellular protein. β-catenin, a member of the Wnt/Wingless signaling pathway, is a notable example of a protein that exists in multiple functionally-distinct forms in cells. For instance, the membrane-associated form of β-catenin serves as a structural component of adherens junctions, whereas the cytoplasmic and nuclear forms of this protein function as latent and activated transcription factors, respectively (60). Similarly, ZO-1 accumulates at the plasma membrane of confluent cells yet, in subconfluent cells, this cellular protein is found in the nucleus (21) where it complexes with the Y-box transcription factor ZONAB to modulate cell-cycle progression (3). Because ZO-2 contains both putative nuclear localization and export signals and likewise accumulates in the nucleus of subconfluent cells (20), it seems probable that this cellular factor also performs distinct functions in several different cellular compartments.

Of particular significance to the present study is that ZO-2 has recently been identified as a candidate tumor suppressor protein. This observation suggests that ZO-2 functions to inhibit inappropriate cellular proliferation and, consequently, that it would be functionally inactivated by Ad9 E4-ORF1. Supporting both of these notions, we demonstrated in CREF cells that over-expression of ZO-2 blocks focus formation by Ad9 E4-ORF1 and other oncoproteins and that Ad9 E4-ORF1 sequesters ZO-2, perhaps post-translationally modified, within detergent-insoluble cytoplasmic complexes. Ad9 E4-ORF1 similarly sequesters and promotes an unknown post-translational modification of MUPP1 and MAGI-1 (18, 37), but not DLG (SL,

unpublished observations). We have suggested that Ad9 E4-ORF1-induced sequestration may functionally inactivate PDZ proteins by preventing their proper localization in cells and/or their interactions with critical cellular factors (18, 37).

Our results showing that over-expression of ZO-2 blocks Ad9 E4-ORF1-induced focus formation in CREF cells warrant further consideration. Because binding of over-expressed ZO-2 to Ad9 E4-ORF1 was neither necessary nor sufficient to produce this effect, the transformation-repressive activity of ZO-2 is not due to it titrating Ad9 E4-ORF1 away from other critical cellular targets. Our demonstration that over-expressed ZO-2 likewise interferes with transformation by unrelated oncoproteins is consistent with this conclusion. Instead, we propose that ZO-2 has an intrinsic transformation-repressive activity associated with a specific protein region that includes both PDZ2 and PDZ3. Based on this hypothesis and others discussed earlier, we have formulated a model whereby, in the context of normal cells expressing low physiologic levels of ZO-2, Ad9 E4-ORF1 is able to sequester the majority of this cellular factor in an inactive form, thereby neutralizing the transformation-repressive activity associated perhaps with PDZ2 and/or PDZ3. With respect to this model, it is interesting that ZO-2 PDZ2 has been shown to mediate binding to ZO-1, which also represents a candidate tumor suppressor protein. Supporting the latter claim, expression of ZO-1 was lost or significantly decreased in 78% (14/18) of examined human breast adenocarcinoma lines (50) and in 69% (33/48) of examined primary breast carcinomas (27). Loss of ZO-1 expression also correlates with increased *in vitro* invasiveness and decreased differentiation of cancer cells (50) and, in addition, the amino-terminal region of ZO-1 can transform epithelial cells to a mesenchymal morphology (45, 47). Thus, an intriguing possible scenario is that ZO-1 and ZO-2 form functional tumor-suppressor complexes, which can be targeted for inactivation by Ad9 E4-ORF1 through

its ability to bind and sequester ZO-2. While additional work is needed to determine whether this idea may be correct, we anticipate that future studies of the interaction between Ad9 E4-ORF1 and ZO-2 will aid in revealing molecular mechanisms whereby this candidate tumor suppressor inhibits malignant transformation of cells.

ACKNOWLEDGMENTS

We thank Andy Rice and Richard Sutton for comments on the manuscript and Darby Thomas, Isabel Latorre, and Kristopher Frese for helpful discussions.

BAG was the recipient of a predoctoral fellowship from the Molecular Virology Training Grant (T32 AI07471). RSW was the recipient of a predoctoral fellowship from the National Science Foundation. RSW and SSL were recipients of predoctoral fellowships from the U.S. Army Breast Cancer Training Grant (DAMD17-94-J4204). This work was supported by grants to RTJ from the National Institutes of Health (RO1 CA58541), the American Cancer Society (RPG-97-668-01-VM), and the US Army (DAMD17-97-1-7082).

REFERENCES

1. **Ankerst, J., and N. Jonsson.** 1989. Adenovirus type 9-induced tumorigenesis in the rat mammary gland related to sex hormonal state. J. Natl. Cancer Inst. **81:**294-298.
2. **Ankerst, J., N. Jonsson, L. Kjellen, E. Norrby, and H. O. Sjogren.** 1974. Induction of mammary fibroadenomas in rats by adenovirus type 9. Int. J. Cancer **13:**286-290.
3. **Balda, M. S., and K. Matter.** 2000. The tight junction protein ZO-1 and an interacting transcription factor regulate ErbB-2 expression. EMBO J. **19:**2024-2033.
4. **Beatch, M., L. A. Jesaitis, W. J. Gallin, D. A. Goodenough, and B. R. Stevenson.** 1996. The tight junction protein ZO-2 contains three PDZ (PSD-95/Discs-Large/ZO-1) domains and an alternatively spliced region. J. Biol. Chem. **271:**25723-25726.
5. **Ben-Ze'ev, A.** 1997. Cytoskeletal and adhesion proteins as tumor suppressors. Curr. Opin. Cell Biol. **9:**99-108.
6. **Bradford, M. M.** 1976. A rapid and sensitive method for the quantitation of microgram quantities of protein utilizing the principle of protein-dye binding. Anal. Biochem. **72:**248-254.
7. **Chen, M., and M. S. Horwitz.** 1990. Replication of an adenovirus type 34 mutant DNA containing tandem reiterations of the inverted terminal repeat. Virology **179:**567-575.
8. **Chlenski, A., K. V. Ketels, J. L. Engeriser, M. S. Talamonti, M. S. Tsao, H. Koutnikova, R. Oyasu, and D. G. Scarpelli.** 1999. ZO-2 gene alternative promoters in normal and neoplastic human pancreatic duct cells. Int. J. Cancer **83:**349-358.
9. **Chlenski, A., K. V. Ketels, G. I. Korovaitseva, M. S. Talamonti, R. Oyasu, and D. G. Scarpelli.** 2000. Organization and expression of the human ZO-2 gene (tjp-2) in normal and neoplastic tissues. Biochim. Biophys. Acta **1493:**319-324.

10. **Chlenski, A., K. V. Ketels, M. S. Tsao, M. S. Talamonti, M. R. Anderson, R. Oyasu, and D. G. Scarpelli.** 1999. Tight junction protein ZO-2 is differentially expressed in normal pancreatic ducts compared to human pancreatic adenocarcinoma. Int. J. Cancer **82:**137-144.

11. **Cordenonsi, M., F. D'Atri, E. Hammar, D. A. Parry, J. Kendrick-Jones, D. Shore, and S. Citi.** 1999. Cingulin contains globular and coiled-coil domains and interacts with ZO-1, ZO-2, ZO-3, and myosin. J. Cell Biol. **147:**1569-1582.

12. **Craven, S. E., and D. S. Bredt.** 1998. PDZ proteins organize synaptic signaling pathways. Cell **93:**495-498.

13. **Eckner, R., M. E. Ewen, D. Newsome, M. Gerdes, J. A. DeCaprio, J. B. Lawrence, and D. M. Livingston.** 1994. Molecular cloning and functional analysis of the adenovirus E1A-associated 300-kD protein (p300) reveals a protein with properties of a transcriptional adaptor. Genes Dev. **8:**869-884.

14. **Fanning, A. S., and J. M. Anderson.** 1999. PDZ domains: fundamental building blocks in the organization of protein complexes at the plasma membrane. J. Clin. Invest. **103:**767-772.

15. **Field, J., J. Nikawa, D. Broek, B. MacDonald, L. Rodgers, I. A. Wilson, R. A. Lerner, and M. Wigler.** 1988. Purification of a RAS-responsive adenylyl cyclase complex from Saccharomyces cerevisiae by use of an epitope addition method. Mol. Cell. Biol. **8:**2159-2165.

16. **Fisher, P. B., L. E. Babiss, I. B. Weinstein, and H. S. Ginsberg.** 1982. Analysis of type 5 adenovirus transformation with a cloned rat embryo cell line (CREF). Proc. Natl. Acad. Sci. USA **79:**3527-3531.

17. **Gardiol, D., C. Kuhne, B. Glaunsinger, S. Lee, R. Javier, and L. Banks.** 1999. Oncogenic papillomavirus E6 proteins target the discs large tumour suppressor for proteasome-mediated degradation. Oncogene **18:**5487-5496.

18. **Glaunsinger, B. A., S. S. Lee, M. Thomas, L. Banks, and R. Javier.** 2000. Interactions of the PDZ-protein MAGI-1 with adenovirus E4-ORF1 and high-risk papillomavirus E6 oncoproteins. Oncogene **19:**5270-5280.

19. **Gluzman, Y.** 1981. SV40-transformed simian cells support the replication of early SV40 mutants. Cell **23:**175-182.

20. **Gonzalez-Mariscal, L., A. Betanzos, and A. Avila-Flores.** 2000. MAGUK proteins: structure and role in the tight junction. Semin. Cell. Dev. Biol. **11:**315-324.

21. **Gottardi, C. J., M. Arpin, A. S. Fanning, and D. Louvard.** 1996. The junction-associated protein, zonula occludens-1, localizes to the nucleus before the maturation and during the remodeling of cell-cell contacts. Proc. Natl. Acad. Sci. USA **93:**10779-10784.

22. **Graham, F. L.** 1984. Transformation by and oncogenicity of human adenoviruses, p. 339-398. *In* H. S. Ginsberg (ed.), The adenoviruses. Plenum Press, New York.

23. **Harlow, E., and D. Lane** 1988. Antibodies: a laboratory manual. Cold Spring Harbor Laboratory, Cold Spring Harbor, N.Y.

24. **Haskins, J., L. Gu, E. S. Wittchen, J. Hibbard, and B. R. Stevenson.** 1998. ZO-3, a novel member of the MAGUK protein family found at the tight junction, interacts with ZO-1 and occludin. J. Cell Biol. **141:**199-208.

25. **Herisse, J., M. Rigolet, S. D. de Dinechin, and F. Galibert.** 1981. Nucleotide sequence of adenovirus 2 DNA fragment encoding for the carboxylic region of the fiber protein and the entire E4 region. Nucleic Acids Res. **9:**4023-4042.

26. **Hogenkamp, T., and H. Esche.** 1990. Nucleotide sequence of the right 10% of adenovirus type 12 DNA encoding the entire region E4. Nucleic Acids Res. **18:**3065-3066.

27. **Hoover, K. B., S. Y. Liao, and P. J. Bryant.** 1998. Loss of the tight junction MAGUK ZO-1 in breast cancer: relationship to glandular differentiation and loss of heterozygosity. Am. J. Pathol. **153:**1767-1773.

28. **Horwitz, M. S.** 1996. Adenoviruses, p. 2149-2171. *In* B. N. Fields, D. M. Knipe, and P. M. Howley (eds), Fields Virology, vol. 2. Lippincott-Raven Publishers, Philadelphia.

29. **Ishidate, T., A. Matsumine, K. Toyoshima, and T. Akiyama.** 2000. The APC-hDLG complex negatively regulates cell cycle progression from the G0/G1 to S phase. Oncogene **19:**365-372.

30. **Itoh, M., M. Furuse, K. Morita, K. Kubota, M. Saitou, and S. Tsukita.** 1999. Direct binding of three tight junction-associated MAGUKs, ZO-1, ZO-2, and ZO-3, with the COOH termini of claudins. J. Cell Biol. **147:**1351-63.

31. **Itoh, M., K. Morita, and S. Tsukita.** 1999. Characterization of ZO-2 as a MAGUK family member associated with tight as well as adherens junctions with a binding affinity to occludin and alpha catenin. J. Biol. Chem. **274:**5981-5986.

32. **Javier, R., K. Raska, Jr., G. J. Macdonald, and T. Shenk.** 1991. Human adenovirus type 9-induced rat mammary tumors. J. Virol. **65:**3192-3202.

33. **Javier, R., K. Raska, Jr., and T. Shenk.** 1992. Requirement for the adenovirus type 9 E4 region in production of mammary tumors. Science **257:**1267-1271.

34. **Javier, R., and T. Shenk.** 1996. Mammary tumors induced by human adenovirus type 9: a role for the viral early region 4 gene. Breast Cancer Res. Treat. **39:**57-67.

35. **Javier, R. T.** 1994. Adenovirus type 9 E4 open reading frame 1 encodes a transforming protein required for the production of mammary tumors in rats. J. Virol. **68:**3917-3924.

36. **Jesaitis, L. A., and D. A. Goodenough.** 1994. Molecular characterization and tissue distribution of ZO-2, a tight junction protein homologous to ZO-1 and the Drosophila discs-large tumor suppressor protein. J. Cell Biol. **124:**949-961.

37. **Lee, S. S., B. Glaunsinger, F. Mantovani, L. Banks, and R. T. Javier.** 2000. Multi-PDZ domain protein MUPP1 is a cellular target for both adenovirus E4-ORF1 and high-risk papillomavirus type 18 E6 oncoproteins. J. Virol. **74:**9680-9693.

38. **Lee, S. S., R. S. Weiss, and R. T. Javier.** 1997. Binding of human virus oncoproteins to hDlg/SAP97, a mammalian homolog of the Drosophila discs large tumor suppressor protein. Proc. Natl. Acad. Sci. USA **94:**6670-6675.

39. **Lowy, D. R., E. Rands, and E. M. Scolnick.** 1978. Helper-independent transformation by unintegrated Harvey sarcoma virus DNA. J. Virol. **26:**291-298.

40. **Lue, R. A., S. M. Marfatia, D. Branton, and A. H. Chishti.** 1994. Cloning and charcterization of hdlg: the human homologue of the Drosophila discs large tumor suppressor binds to protein 4.1. Proc. Natl. Acad. Sci. USA **91:**9818-9822.

41. **Mattagajasingh, S. N., S. C. Huang, J. S. Hartenstein, and E. J. Benz.** 2000. Characterization of the interaction between protein 4.1R and ZO-2. A possible link between the tight junction and the actin cytoskeleton. J. Biol. Chem. **275:**30573-30585.

42. **McAllister, R. M., J. E. Filbert, M. O. Nicolson, R. W. Rongey, M. B. Gardner, R. V. Gilden, and R. J. Huebner.** 1971. Transformation and productive infection of human osteosarcoma cells by a feline sarcoma virus. Nat. New Biol. **230:**279-282.

43. **Muller, B. M., U. Kistner, R. W. Veh, C. Cases-Langhoff, B. Becker, E. D. Gundelfinger, and C. C. Garner.** 1995. Molecular characterization and spatial distribution of SAP97, a novel presynaptic protein homologous to SAP90 and the Drosophila discs-large tumor suppressor protein. J. Neurosci. **15:**2354-2366.

44. **Nakagawa, S., and J. M. Huibregtse.** 2000. Human scribble (Vartul) is targeted for ubiquitin-mediated degradation by the high-risk papillomavirus E6 proteins and the E6AP ubiquitin-protein ligase. Mol. Cell. Biol. **20:**8244-8253.

45. **Reichert, M., T. Muller, and W. Hunziker.** 2000. The PDZ domains of zonula occludens-1 induce an epithelial to mesenchymal transition of Madin-Darby canine kidney I cells. Evidence for a role of beta-catenin/Tcf/Lef signaling. J. Biol. Chem. **275:**9492-9500.

46. **Rousset, R., S. Fabre, C. Desbois, F. Bantignies, and P. Jalinot.** 1998. The C-terminus of the HTLV-1 Tax oncoprotein mediates interaction with the PDZ domain of cellular proteins. Oncogene **16:**643-654.

47. **Ryeom, S. W., D. Paul, and D. A. Goodenough.** 2000. Truncation mutants of the tight junction protein ZO-1 disrupt corneal epithelial cell morphology. Mol. Biol. Cell. **11:**1687-1696.

48. **Shenk, T.** 1996. Adenoviridae: the viruses and their replication, p. 2111-2148. *In* B. N. Fields, D. M. Knipe, and P. M. Howley (eds), Fields Virology, vol. 2. Lippincott-Raven Publishers, Philadelphia.

49. **Smith, D. B., and L. M. Corcoran** 1994. Expression and purification of glutathione-*S*-transferase fusion proteins, p. 16.7.1-16.7.7. *In* F. M. Ausubel, R. Brent, R. E. Kingston, D. D. Moore, J. G. Seidman, J. A. Smith, and K. Struhl (eds), Current Protocols in Molecular Biology, vol. 2. John Wiley & Sons, Inc., New York.

50. **Sommers, C. L., S. W. Byers, E. W. Thompson, J. A. Torri, and E. P. Gelmann.** 1994. Differentiation state and invasiveness of human breast cancer cell lines. Breast Cancer Res. Treat. **31:**325-335.

51. **Songyang, Z., A. S. Fanning, C. Fu, J. Xu, S. M. Marfatia, A. H. Chishti, A. Crompton, A. C. Chan, J. M. Anderson, and L. C. Cantley.** 1997. Recognition of unique carboxyl-terminal motifs by distinct PDZ domains. Science **275:**73-77.

52. **Suzuki, T., Y. Ohsugi, M. Uchida-Toita, T. Akiyama, and M. Yoshida.** 1999. Tax oncoprotein of HTLV-1 binds to the human homologue of Drosophila discs large tumor suppressor protein, hDLG, and perturbs its function in cell growth control. Oncogene **18:**5967-5972.

53. **Thomas, D. L., J. Schaack, H. Vogel, and R. T. Javier.** 2001. Several E4 region functions influence mammary tumorigenesis by human adenovirus type 9. J. Virol. **75:**557-568.

54. **Thomas, D. L., S. Shin, B. H. Jiang, H. Vogel, M. A. Ross, M. Kaplitt, T. E. Shenk, and R. T. Javier.** 1999. Early region 1 transforming functions are dispensable for mammary tumorigenesis by human adenovirus type 9. J. Virol. **73:**3071-3079.

55. **Treisman, R., U. Novak, J. Favaloro, and R. Kamen.** 1981. Transformation of rat cells by an altered polyoma virus genome expressing only the middle-T protein. Nature **292:**595-600.

56. **Weiss, R. S., M. O. Gold, H. Vogel, and R. T. Javier.** 1997. Mutant adenovirus type 9 E4 ORF1 genes define three protein regions required for transformation of CREF cells. J. Virol. **71:**4385-4394.

57. **Weiss, R. S., and R. T. Javier.** 1997. A carboxy-terminal region required by the adenovirus type 9 E4 ORF1 oncoprotein for transformation mediates direct binding to cellular polypeptides. J. Virol. **71:**7873-7880.

58. **Weiss, R. S., S. S. Lee, B. V. V. Prasad, and R. T. Javier.** 1997. Human adenovirus early region 4 open reading frame 1 genes encode growth-transforming proteins that may be distantly related to dUTP pyrophosphatase enzymes. J. Virol. **71:**1857-1870.

59. **Weiss, R. S., M. J. McArthur, and R. T. Javier.** 1996. Human adenovirus type 9 E4 open reading frame 1 encodes a cytoplasmic transforming protein capable of increasing the oncogenicity of CREF cells. J. Virol. **70:**862-872.

60. **Willert, K., and R. Nusse.** 1998. Beta-catenin: a key mediator of Wnt signaling. Curr. Opin. Genet. Dev. **8:**95-102.

61. **Wittchen, E. S., J. Haskins, and B. R. Stevenson.** 1999. Protein interactions at the tight junction. Actin has multiple binding partners, and ZO-1 forms independent complexes with ZO-2 and ZO-3. J. Biol. Chem. **274:**35179-35185.

Table 1. Carboxyl-terminal sequence, transforming potential in CREF cells, and ZO-2-binding capacity of wild-type and mutant adenovirus E4-ORF1 proteins

	Carboxyl-terminal four amino-acid residues* (Consensus type I PDZ domain-binding motif)				Transforming potential in	Binding to
Protein	X	(S/T)	X	(V/I/L)-COOH	CREF cells**	ZO-2***
wt Ad9 E4-ORF1	A	T	L	V	+++++	+++++
mutant IIIA	A	**P**			-	-
mutant IIIC	**D**	T	L	V	+	-
mutant IIID	A	T	**P**	V	+	+/-
wt Ad5 E4-ORF1	A	S	N	V	-	-
wt Ad12 E4-ORF1	A	S	L	I	-	-

*Bolded amino-acid residues depict substitution mutations.

**Scores for transforming potential are based on focus formation, soft agar growth, and tumor growth assays with Ad9 E4-ORF1 proteins or on focus formation assays with Ad5 and Ad12 E4-ORF1 proteins (58, 59). Additionally, unlike the Ad9 E4-ORF1 protein, the Ad5 and Ad12 E4-ORF1 proteins do not serve as oncogenic determinants for their respective viruses (48). +++++, wild-type activity; +, weak activity; +/-, very weak activity; -, no detectable activity.

***Results presented in this study, as well as similar findings with p160 (57).

FIGURE LEGENDS

Figure 1. Domain structures of the cellular MAGUK proteins ZO-2, MAGI-1, and DLG. PDZ, PDZ domain; SH3, src-homology 3 domain; GuK, guanylate kinase-homology domain; -, acidic domain; β, alternatively spliced region; pro-rich, proline-rich region; WW, WW motif; NLS, consensus nuclear localization signal; NES, consensus nuclear export signal. Scale at top indicates polypeptide length in number of amino-acid residues.

Figure 2. Binding of wild-type but not mutant Ad9 E4-ORF1 to ZO-2 in GST pulldown assays. (A) ZO-2 binds to wild-type Ad9 E4-ORF1 in GST-pulldown assays. 100 μg of protein from RIPA buffer-lysed COS-7 cells transfected with 5 μg of either empty GW1 plasmid or GW1 plasmid expressing HA-ZO-2 was subjected to GST pulldown assays with the indicated fusion protein. Recovered proteins were separated by SDS-PAGE and immunoblotted with anti-HA antibodies. As a control, one-tenth the amount of protein used in GST pulldown assays was directly immunoblotted with the same antibodies. **(B)** Wild-type Ad9 E4-ORF1 co-immunoprecipitates with HA-ZO-2. 150 μg of protein from RIPA buffer-lysed COS-7 cells co-transfected with 5 μg of GW1 plasmid expressing HA-ZO-2 and 5 μg of either empty GW1 plasmid or GW1 plasmid expressing wild-type or the indicated mutant Ad9 E4-ORF1 was immunoprecipitated with Ad9 E4-ORF1 antibodies. Recovered proteins were separated by SDS-PAGE and immunoblotted with either anti-HA or anti-Ad9 E4-ORF1 antibodies. As a control, one-tenth the amount of protein used in the immunoprecipitation reactions was directly immunoblotted with the same antibodies. **(C)** Binding of ZO-2 to Ad9 E4-ORF1 but not to Ad5 and Ad12 E4-ORF1 in GST-pulldown assays. Experiments were performed as described above in (*A*).

Figure 3. Co-migration of ZO-2 and Ad9 E4-ORF1-associated protein p160. (A) Gel mobilities of ZO-2 proteins expressed in various cell lines. 100 μg of protein from the indicated RIPA buffer-lysed cells was separated by SDS-PAGE and immunoblotted with ZO-2 antibodies. As controls, 2.5 μg of protein from RIPA buffer-lysed COS-7 cells transfected with 4 μg of either empty GW1 plasmid or GW1 plasmid expressing wild-type ZO-2 was run on the same protein gel. **(B)** Ad9 E4-ORF1-associated cellular protein p160 co-migrates with endogenous ZO-2 of CREF cells. 50 μg of protein from RIPA buffer-lysed normal CREF cells was separated by SDS-PAGE and then immunoblotted with ZO-2 antibodies (*left panel*). Alternatively, 4 mg of protein from RIPA buffer-lysed normal CREF cells was subjected to GST pulldown assays with the indicated fusion proteins. Recovered proteins were separated by SDS-PAGE and blotted with a radiolabeled Ad9 E4-ORF1 protein probe (*right panel*). Samples in both panels were run on the same gel to allow comparison of protein mobilities.

Figure 4. Binding of wild-type but not mutant Ad9 E4-ORF1 to endogenous ZO-2 of CREF cells. 1 mg of protein from RIPA buffer-lysed normal CREF cells or CREF cells stably expressing wild-type or mutant Ad9 E4-ORF1 were immunoprecipitated with ZO-2 antiserum or the matched pre-immune serum (pre). Recovered proteins were separated by SDS-PAGE and immunoblotted with either ZO-2 or Ad9 E4-ORF1 antiserum (*top panel*). As a control, 100 μg of protein from RIPA buffer-lysed normal CREF cells was also directly immunoblotted with the same antisera (*bottom panel*). Sample 1 of the *top panel* was not analyzed in the *bottom panel.*

Figure 5. ZO-2 PDZ1 mediates binding of ZO-2 to Ad9 E4-ORF1. (A) Illustration of ZO-2 protein fragments and ZO-2 deletion mutants. **(B)** Specific binding of Ad9 E4-ORF1 to ZO-2 PDZ1 in protein blotting assays. Approximately 5 μg of the indicated ZO-2 GST fusion protein,

separated by SDS-PAGE and immobilized on a membrane, was either stained with coomassie brilliant blue dye to verify the presence of equivalent amounts of protein (*left panel*) or probed with a radiolabeled wild-type Ad9 E4-ORF1 protein probe (*right panel*). **(C)** Requirement of ZO-2 PDZ1 for ZO-2 to co-immunoprecipitate with Ad9 E4-ORF1 from cell extracts. 400 μg of protein from RIPA buffer-lysed COS-7 cells co-transfected with 5 μg of either empty GW1 plasmid or GW1 plasmid expressing Ad9 E4-ORF1 and 5 μg of GW1 plasmid expressing wild-type HA-ZO-2 or mutant HA-ZO-2 lacking either PDZ1 (HA-ZO-2ΔPDZ1) or both PDZ2 and PDZ3 (HA-ZO-2ΔPDZ2+3) were immunoprecipitated with Ad9 E4-ORF1 antibodies. Recovered proteins were separated by SDS-PAGE and immunoblotted with anti-HA or anti-Ad9 E4-ORF1 antibodies. As a control, one-fifteenth the amount of protein used in the immunoprecipitation reactions was also directly immunoblotted with the same antibodies.

Figure 6. Ad9 E4-ORF1 aberrantly sequesters ZO-2 in the cytoplasm of CREF cells. (A) Distribution of ZO-2 in normal CREF cells or CREF cells stably expressing either wild-type or the indicated mutant Ad9 E4-ORF1. Indirect immunofluorescence (IF) assays were performed with either affinity-purified ZO-2 antibodies (*panels a, c-f*) or normal rabbit IgG (*panel b*) and visualized by fluorescence microscopy. **(B)** ZO-2 and Ad9 E4-ORF1 co-localize within cytoplasmic punctate bodies in CREF cells. Double-label IF assays were performed using both affinity-purified ZO-2 and anti-HA antibodies in CREF cells stably expressing HA-Ad9 E4-ORF1. Each of the three panels represents the same field of five cells stained for ZO-2 (*left panel*), HA-Ad9 E4-ORF1 (*center panel*), or the merged images (*right panel*). **(C)** Ad9 E4-ORF1 aberrantly sequesters ZO-2 within detergent-insoluble complexes in CREF cells. Normal CREF cells or CREF cells stably expressing either wild-type or the indicated mutant Ad9 E4-ORF1 were lysed in RIPA buffer, and extracts were centrifuged to produce RIPA

buffer-soluble (*S*) supernatant and RIPA buffer-insoluble (*I*) pellet fractions. 100 μg of protein from *S* fractions or an equivalent amount from *I* fractions (see *Materials and Methods*) was separated by SDS-PAGE and immunoblotted with either ZO-2 or Ad9 E4-ORF1 antiserum.

Figure 7. ZO-2 inhibits oncogene-induced focus formation in CREF cells. (A) ZO-2 interferes with Ad9 E4-ORF1-induced focus formation. CREF cells were transfected either alone with 8 μg of empty GW1 plasmid or GW1 plasmid expressing the indicated wild-type or mutant HA-ZO-2 protein (lanes 1-4) or together with 2 μg of pJ4Ω plasmid expressing wild-type Ad9 E4-ORF1 (lanes 5-8). At three weeks post-transfection, transformed foci were counted. Numbers of transformed foci are presented as percent relative to the Ad9 E4-ORF1 plasmid alone (control), which was normalized to 100 percent. Data are compiled from three independent assays, each performed in duplicate. **(B)** ZO-2 also blocks focus formation by the RasV12 and polyomavirus middle T oncoproteins. CREF cells were transfected either alone with 9 μg of empty GW1 plasmid or GW1 plasmid expressing wild-type HA-ZO-2 protein (lanes 1-2) or together with 3 μg of either pJ4Ω plasmid expressing wild-type Ad9 E4-ORF1 (lanes 3-4), GW1 plasmid expressing RasV12 (lanes 5-6), or pPyMT1 plasmid expressing polyomavirus middle T (PyMT) (lanes 7-8). Assays were scored as indicated above in (*A*). Numbers of transformed foci are presented as percent relative to the respective Ad9 E4-ORF1, RasV12, or PyMT plasmid alone (control), each of which was normalized to 100 percent. Data are compiled from two independent assays, each performed in duplicate.

Fig. 1

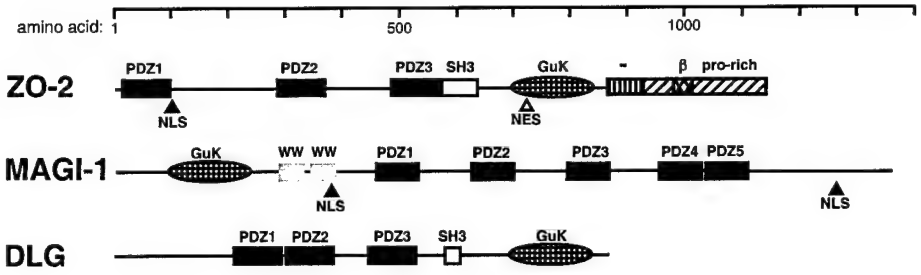
amino acid: 1
500
1000
ZO-2
PDZ1
PDZ2
PDZ3
SH3
GuK
β
pro-rich
NLS
NES
MAGI-1
GuK
WW
WW
PDZ1
PDZ2
PDZ3
PDZ4
PDZ5
NLS
NLS
DLG
PDZ1
PDZ2
PDZ3
SH3
GuK

Fig. 2

A

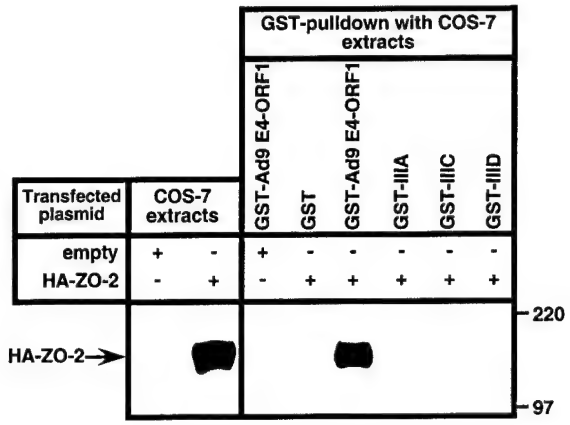
GST-pulldown with COS-7 extracts
GST-Ad9 E4-ORF1
GST
GST-Ad9 E4-ORF1
GST-IIIA
GST-IIIC
GST-IIID
Transfected plasmid
COS-7 extracts
empty + - + - - - - -
HA-ZO-2 - + - + + + + +
HA-ZO-2
220
97

B

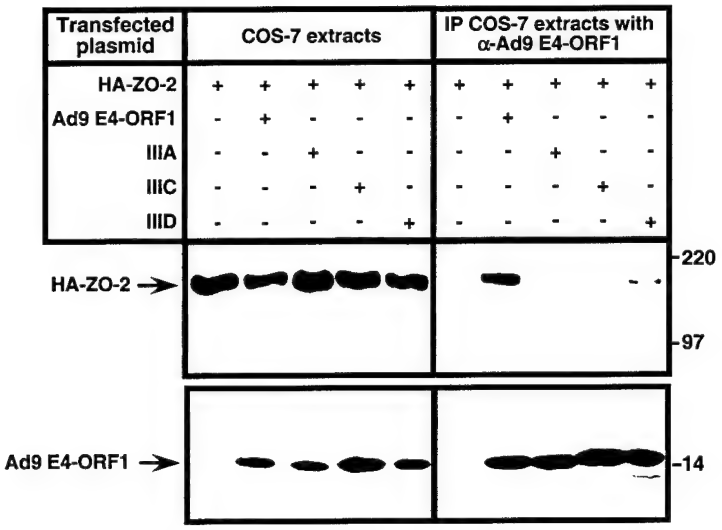
Transfected plasmid
COS-7 extracts
IP COS-7 extracts with α-Ad9 E4-ORF1
HA-ZO-2 + + + + + + + + + +
Ad9 E4-ORF1 - + - - - - + - - -
IIIA - - + - - - - + - -
IIIC - - - + - - - - + -
IIID - - - - + - - - - +
HA-ZO-2
220
97
Ad9 E4-ORF1
14

C

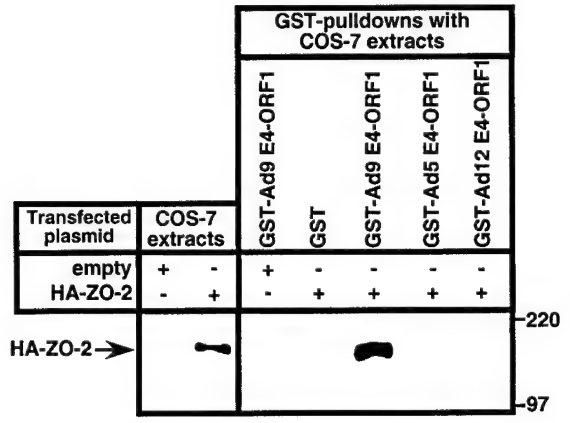
GST-pulldowns with COS-7 extracts
GST-Ad9 E4-ORF1
GST
GST-Ad9 E4-ORF1
GST-Ad5 E4-ORF1
GST-Ad12 E4-ORF1
Transfected plasmid
COS-7 extracts
empty + - + - - - -
HA-ZO-2 - + - + + + +
HA-ZO-2
220
97

Fig. 3

A.

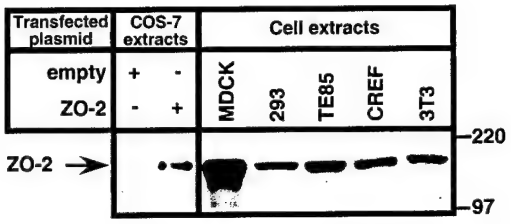
Transfected plasmid
COS-7 extracts
Cell extracts
empty
ZO-2
+
-
-
+
MDCK
293
TE85
CREF
3T3
ZO-2
220
97

B.

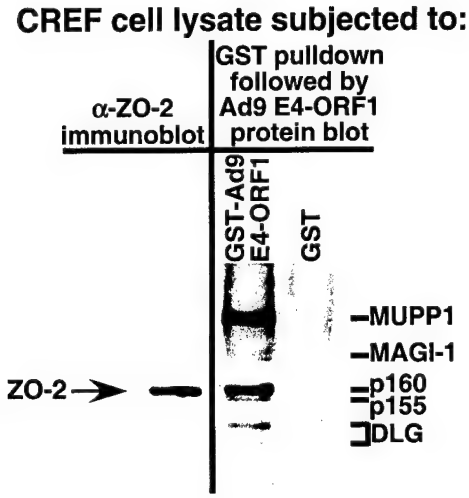
CREF cell lysate subjected to:
α-ZO-2 immunoblot
GST pulldown followed by Ad9 E4-ORF1 protein blot
GST-Ad9 E4-ORF1
GST
ZO-2
MUPP1
MAGI-1
p160
p155
DLG

Fig. 4

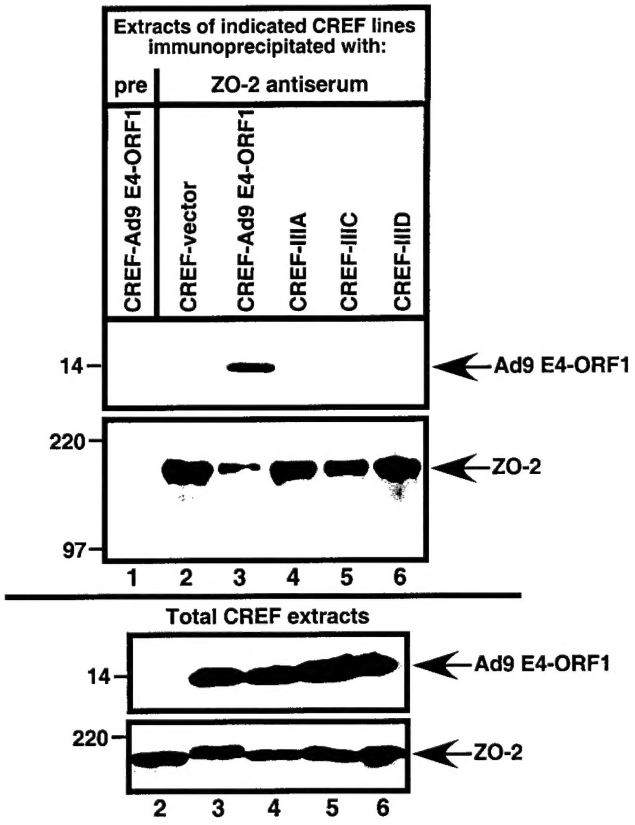
Extracts of indicated CREF lines immunoprecipitated with:
pre
ZO-2 antiserum
CREF-Ad9 E4-ORF1
CREF-vector
CREF-Ad9 E4-ORF1
CREF-IIIA
CREF-IIIC
CREF-IIID
14
Ad9 E4-ORF1
220
ZO-2
97
1 2 3 4 5 6
Total CREF extracts
14
Ad9 E4-ORF1
220
ZO-2
2 3 4 5 6

Fig. 5

A.

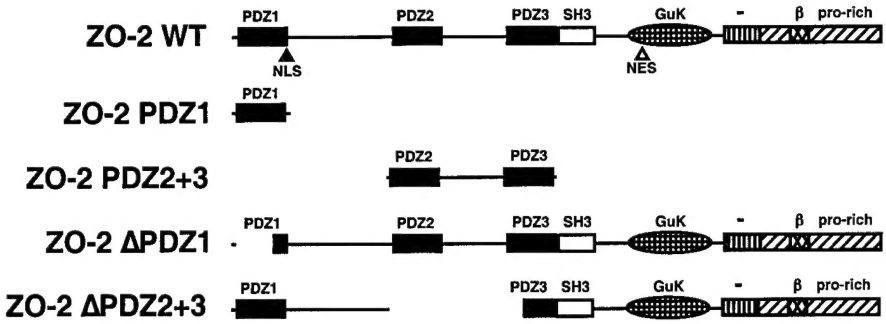
ZO-2 WT
PDZ1
PDZ2
PDZ3
SH3
GuK
β
pro-rich
NLS
NES
ZO-2 PDZ1
ZO-2 PDZ2+3
ZO-2 ΔPDZ1
ZO-2 ΔPDZ2+3

B

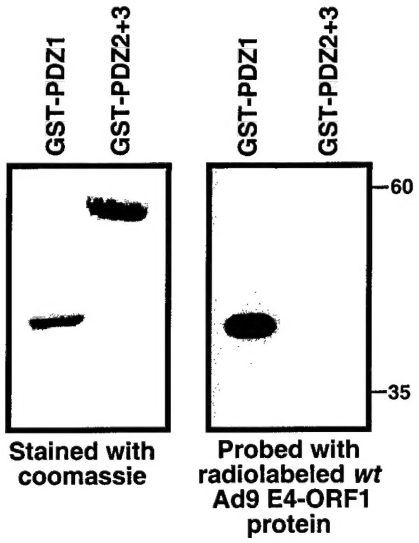
GST-PDZ1
GST-PDZ2+3
GST-PDZ1
GST-PDZ2+3
60
35
Stained with coomassie
Probed with radiolabeled *wt* Ad9 E4-ORF1 protein

C

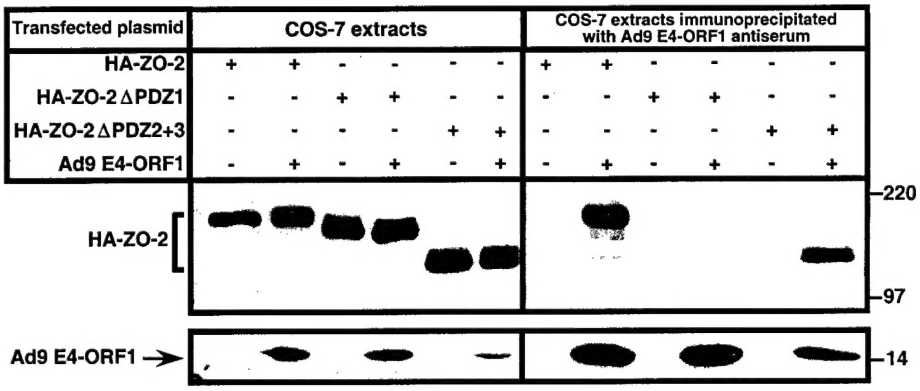
Transfected plasmid
COS-7 extracts
COS-7 extracts immunoprecipitated with Ad9 E4-ORF1 antiserum
HA-ZO-2
HA-ZO-2 ΔPDZ1
HA-ZO-2 ΔPDZ2+3
Ad9 E4-ORF1
HA-ZO-2
Ad9 E4-ORF1
220
97
14

Fig. 6

A

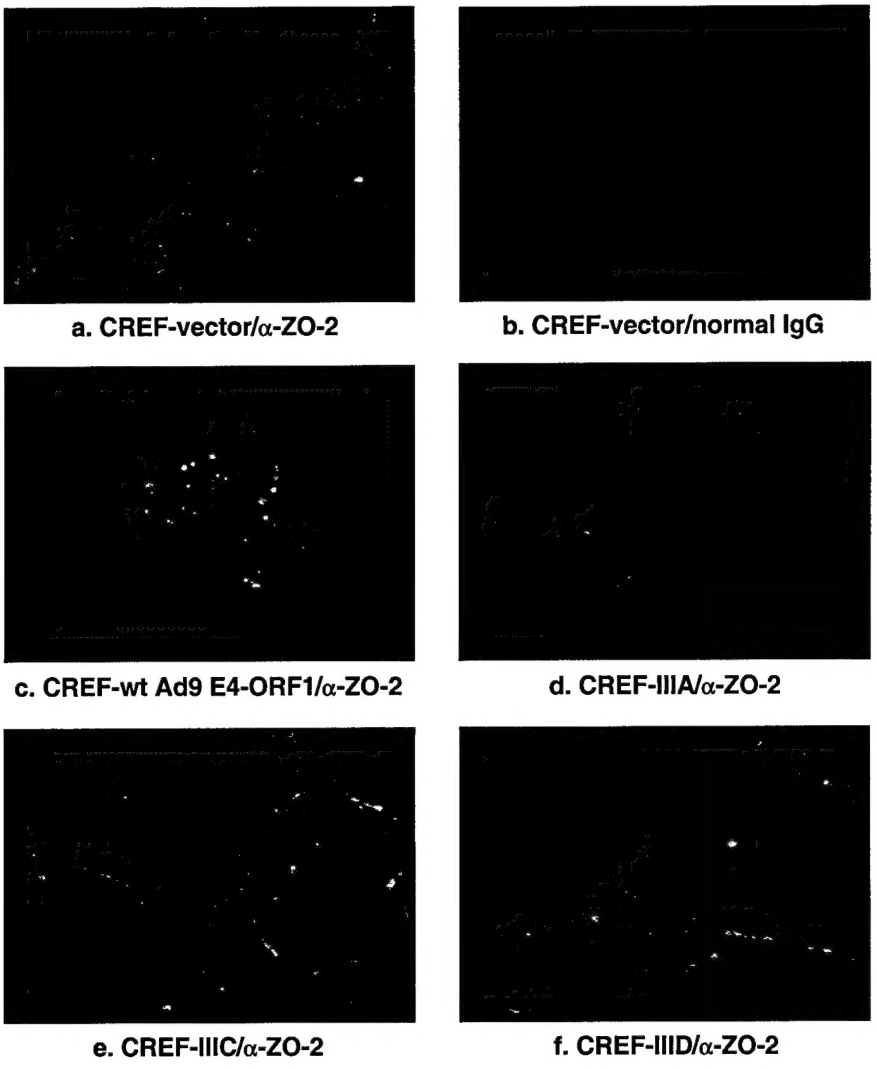
a. CREF-vector/α-ZO-2
b. CREF-vector/normal IgG
c. CREF-wt Ad9 E4-ORF1/α-ZO-2
d. CREF-IIIA/α-ZO-2
e. CREF-IIIC/α-ZO-2
f. CREF-IIID/α-ZO-2

B

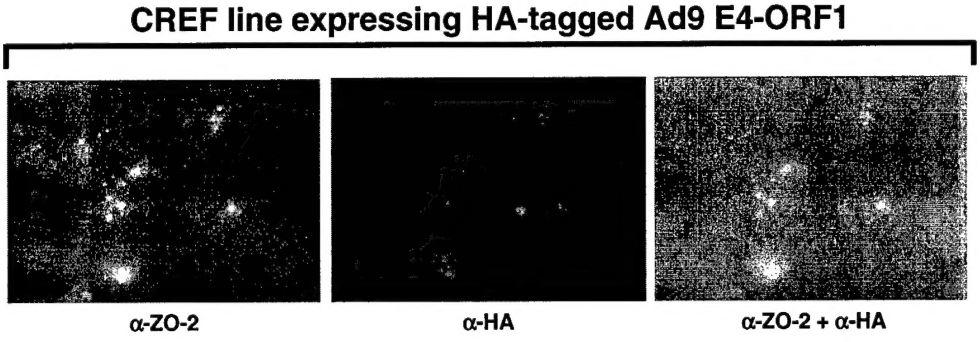
CREF line expressing HA-tagged Ad9 E4-ORF1
α-ZO-2
α-HA
α-ZO-2 + α-HA

C.

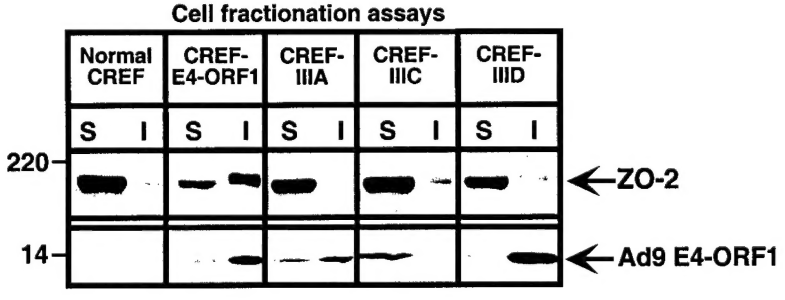
Cell fractionation assays
Normal CREF
CREF-E4-ORF1
CREF-IIIA
CREF-IIIC
CREF-IIID
S I
220
14
ZO-2
Ad9 E4-ORF1

Fig. 7

A.

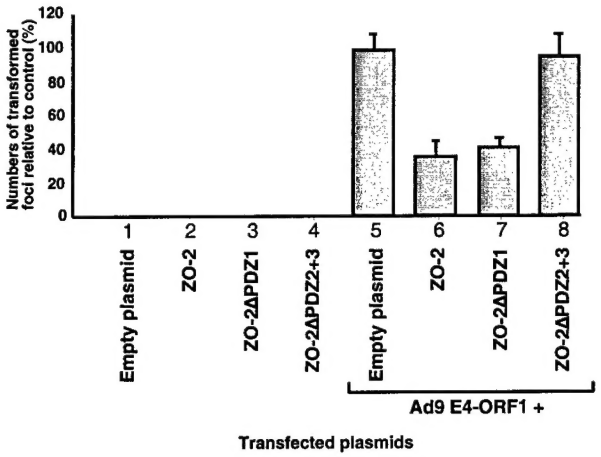
Numbers of transformed foci relative to control (%)
120
100
80
60
40
20
0
1 2 3 4 5 6 7 8
Empty plasmid
ZO-2
ZO-2ΔPDZ1
ZO-2ΔPDZ2+3
Empty plasmid
ZO-2
ZO-2ΔPDZ1
ZO-2ΔPDZ2+3
Ad9 E4-ORF1 +
Transfected plasmids

B.

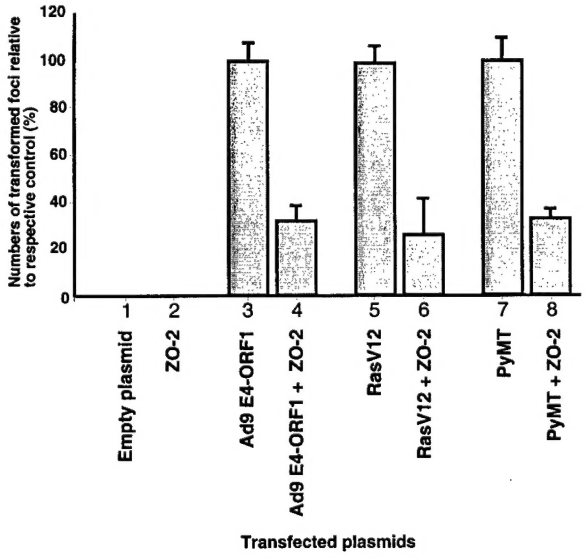
Numbers of transformed foci relative to respective control (%)
120
100
80
60
40
20
0
1 2 3 4 5 6 7 8
Empty plasmid
ZO-2
Ad9 E4-ORF1
Ad9 E4-ORF1 + ZO-2
RasV12
RasV12 + ZO-2
PyMT
PyMT + ZO-2
Transfected plasmids